University of Cyprus

DEPARTMENT OF BIOLOGICAL SCIENCES

THE ROLE OF N-ALPHA TERMINAL ACETYLTRANSFERASE *NAT4* IN THE REGULATION OF GENE EXPRESSION IN *SACCHAROMYCES CEREVISIAE*

DOCTOR OF PHILIOSOPY DISSERTATION

VASSILIKI SCHIZA

2015

University of Cyprus

DEPARTMENT OF BIOLOGICAL SCIENCES

THE ROLE OF N-ALPHA TERMINAL ACETYLTRANSFERASE *NAT4* IN THE REGULATION OF GENE EXPRESSION IN *SACCHAROMYCES CEREVISIAE*

VASSILIKI SCHIZA

A Dissertation Submitted to the University of Cyprus in Partial Fulfillment of the Requirements for the Degree of Doctor of Philosophy

November 2015

VALIDATION PAGE

Doctoral Candidate: Vassiliki Schiza

Doctoral Thesis Title: The role of N-alpha terminal acetyltransferase *NAT4* in the regulation of gene expression in *Saccharomyces cerevisiae*

The present Doctoral Dissertation was submitted in partial fulfillment of the requirements for the Degree of Doctor of Philosophy at the ***Department of Biological Sciences*** *and was approved on the 12/11/2015 by the members of the* ***Examination Committee****.*

Examination Committee:

Research Supervisor:

Antonis Kirmizis, Assistant Professor _____

Committee Member:

Yiorgos Apidianakis, Assistant Professor _____

Committee Member:

Chrysoula Pitsouli, Assistant Professor _____

Committee Member:

Thomas Arnesen, Associate Professor _____

Committee Member:

Popi Syntichaki, Assistant Professor _____

DECLARATION OF DOCTORAL CANDIDATE

The present doctoral dissertation was submitted in partial fulfillment of the requirements for the degree of Doctor of Philosophy of the University of Cyprus. It is a product of original work of my own, unless otherwise mentioned through references, notes, or any other statements.

_____

_____

Acknowledgements

First and foremost I want to thank my supervisor Antonis Kirmizis for his continous support, guidance and training as well as for giving me the opportunity to realize one of my biggest goals. It has been an honor to be his Ph.D student. The passion he has for research was motivational for me during tough times along this journey. I have been lucky to have as a mentor such an enthousiastic hard-working and excellent scientist. I want to thank him for giving me the opportunity to work on a very interesting and challenging project and to work with a group of people that from each one of them I feel I have learnt a lot.

The members of the Kirmizis lab have been a source of good friendship as well as good advice and collaboration. I am especially thankful to Dr Diego Molina Serrano for sharing his scientific knowledge as well as his patience in answering all of my questions. I am grateful for his help, his proofreading and for providing me with valuable insights and advice throughout the Ph.D. I know that I learnt a lot from Diego, especially during the period we worked together for our publication. Special thanks also go to Dr Manolis Stavrou for his support and help whenever I needed it. Heartfelt thanks go to my lab-buddies Demetria and Dimitris for all the moments we shared in and out of the lab, moments of excitement as well as disappointment. We were next to each other from the very beginning and I know that I could not make it without you. My thanks also go to Christis Demosthenous for managing the lab, making our Ph.D life easier by preparing all those media and for keeping everyone entertained during those long days. Chris you rock. I also thank past and present group members that I have had the pleasure to work with.

I gratefully acknowledge the funding source ERC that made my Ph.D. work possible and our collaborators starting from Dr Jan Oppelt for bioinformatics analysis, Dr Weiwei Dang, Dr Helmut Bergler and Dr Scott Pletcher. Furthermore, my special thanks go to the members of my oral defense committee Dr Thomas Arnesen, Dr Popi Syntichaki, Dr Yiorgos Apidianakis and Dr Chrysoula Pitsouli for their time and insightful questions.

Lastly, I would like to thank my dear friends who have supported me over the last five years and my family for all their love and encouragement. For my parents who raised me with a love for science and supported me in all my pursuits as well as my brother and sister who believed in me, and always reminded me that I am almost at the end. Finally, I would like to thank Michalis, who stood by me through the entire Ph.D journey and for pushing me to keep on working hard.

This work is dedicated

to the memory of my beloved grandmother Vassoula, who gave me the finest example I could have of strength, kindness and love.

to my parents Louis and Maria, the reason for what I became today and who taught me to work hard for the things I aspire to achieve. I hope that this PhD will complete the dream you had for me all these years when you chose to give me the best education you could.

to my fiance Michalis, for being a constant source of support, tolerance and encouragement. I am truly thankful for having you in my life.

Περίληψη

Η Ν-άλφα-τελική ακετυλίωση είναι μια από τις πιο κοινές συντηρημένες τροποποιήσεις πρωτεϊνών σε ευκαρυωτικά κύτταρα, η οποία εμφανίζεται επίσης και σε ιστόνες. Διακρίνεται από τις υπόλοιπες τροποποιήσεις καθώς εντοπίζεται στην Ν-άλφα-αμινομάδα του πρώτου υπολείμματος αντί στην πλευρική αλυσίδα των αμινοξέων. Η Ν-αλφα-τελική ακετυλίωση της ιστόνης (N-acH4) καταλύεται από την Ν-τελική ακετυλοτρανσφεράση (Nat4). Παρά το γεγονός ότι, έχουν ήδη εξακριβωθεί βιολογικοί ρόλοι της Nat4 στο ζυμομύκητα (*Saccharomyces cerevisiae*) καθώς και στον άνθρωπο, η μοριακή λειτουργία του N-acH4 δεν έχει προηγουμένως μελετηθεί. Στην παρούσα μελέτη αποδεικνύουμε ότι η N-acH4 είναι ένας νέος ρυθμιστής της μεθυλίωσης της αργινίνης 3 στην ιστόνη 4 H4 καθώς και της αποσιώπησης της χρωματίνης στο ζυμομύκητα. Η σημαντικότητα των αποτελεσμάτων μας επιβεβαιώνεται από το γεγονός ότι δείχνουμε για πρώτη φορά ότι η συνεργιστική επικοινωνία μεταξύ N-acH4 και της εσωτερικής ακετυλίωσης ιστόνης σε λυσίνες 5, 8 και 12 ενισχύει έντονα την εναπόθεση της ασύμμετρης διμεθυλίωσης της αργινίνης (H4R3me2a) καθώς και την αποσιώπηση του ριβοσωμικού DNA (rDNA). Ως εκ τούτου μειώνεται σημαντικά η ανάπτυξη του ζυμομύκητα, η οποία μπορεί να διασωθεί μεταλλάσσοντας την αργινίνη 3 προς λυσίνη (H4R3K), γεγονός το οποίο καταδεικνύει ότι η ανώμαλη εναπόθεση μιας ενιαίας τροποποίησης ιστόνης μπορεί να έχει επίδραση στην κυτταρική ανάπτυξη. Ακολούθως, αποδείξαμε ότι η επικοινωνία μεταξύ N-acH4 και H4R3me2a στη ρύθμιση της αποσιώπησης του rDNA προκαλείται υπό συνθήκες θερμιδικού περιορισμού (CR). Προκειμένου να προσδιοριστεί αν η Nat4 ρυθμίζει την έκφραση του γονιδίων εκτός από το ριβοσωμικό DNA πραγματοποιήσαμε RNA-αλληλούχιση, και εντοπίσαμε μια ομάδα γονιδίων που η έκφραση τους είναι σημαντικά αυξανόμενη όταν η δραστηριότητα της Nat4 χάνεται. Είναι ενδιαφέρον ότι, κάποια από αυτά τα γονίδια συμβάλουν στον μεταβολισμό, και κάποια γονίδια συσχετίζονται με συνθήκες στρες που επάγονται ισχυρά υπό συνθήκες CR. Το αποτέλεσμα αυτό υποδεικνύει ότι η έλλειψη Nat4 μιμείται συνθήκες CR. Βασιζόμενοι σε μελέτες γήρανσης, γνωρίζουμε ότι σε συνθήκες CR η διάρκεια ζωής του ζυμομύκητα αυξάνεται. Επομένως, θέλαμε να προσδιορίσουμε αν η απουσία της Nat4 επίσης αυξάνει τη μακροζωία (RLS) του ζυμομύκητα. Τα αποτελέσματα μας υποστηρίζουν ότι η απώλεια της Nat4 επεκτείνει την μακροζωία σε παρόμοια επίπεδα με την CR και η διαγραφή της Nat4 σε συνδυασμό με CR δεν έχει καμία πρόσθετη επίδραση στη μακροζωία, υπονοώντας μια επιστατική επίδραση. Επιπλέον, η επέκταση της διάρκειας ζωής κατά την διαγραφή της Nat4 διαμεσολαβείται από την απώλεια της H4 Ν-τελικής ακετυλίωσης, καθώς η απώλεια αυτής

της τροποποίησης μεταλλάσσοντας την σερίνη 1 στην ιστόνη H4 σε ασπαρτικό οξύ (H4S1D) οδηγεί σε παράταση της μακροζωίας. Σύμφωνοι με αυτό, δείχνουμε ότι η αργινίνη 3 επί ιστόνης H4 (H4R3) απαιτείται για την επέκταση της μακροζωίας στον ζυμομύκητα καθώς επίσης και για την Nat4 μεσολαβούμενη ρύθμιση της γονιδιακής έκφρασης. Είναι αξιοσημείωτο ότι τα αποτελέσματα από την παρούσα μελέτη αποκάλυψαν ένα νέο ρόλο της Nat4 στη ρύθμιση τόσο της ετεροχρωματινικής όσο και της ευχρωματινικής έκφρασης γονιδίων στο γονιδίωμα του ζυμομύκητα.

Abstract

N-alpha-terminal acetylation is one of the most common and conserved post-translational modifications in eukaryotes, occurring on 60-70% of proteins. This modification also exists on histone proteins but is distinct from the numerous other histone modifications identified so far because it is deposited on the N-alpha amino group of the first residue instead of the side-chain of amino acids. The enzyme catalyzing histone N-alpha terminal acetylation was first identified in yeast and was named N-terminal acetyltransferase 4 (Nat4). Although other groups have provided insight about the biological role of yeast Nat4 and its human ortholog (Naa40), the molecular function of histone N-terminal acetylation has not been studied before. Our results suggest that N-terminal acetylation of histone H4 (N-acH4) is a novel regulator of histone arginine methylation and chromatin silencing in *Saccharomyces cerevisiae*. Importantly, we show that synergistic communication between N-acH4 and internal histone acetylation at lysines 5, 8 and 12 strongly enhances the deposition of asymmetric arginine dimethylation (H4R3me2a) and ribosomal DNA silencing. This leads to a severe growth defect that is remarkably rescued by mutating arginine 3 to lysine (H4R3K), pointing out that abnormal deposition of a single histone modification can have an effect on cell growth. Notably, we reveal that the cross-talk between N-acH4 and H4R3me2a in regulating rDNA silencing is induced under calorie restriction (CR) conditions. In order to determine whether Nat4 regulates gene expression beyond the ribosomal DNA locus, we performed RNA-sequencing (RNA-seq) and have identified a group of genes that are significantly upregulated when Nat4 activity is lost. Interestingly, these are metabolic and stress response genes that are highly induced under CR conditions. This result suggests that lack of Nat4 mimics CR and consistent with this we found that loss of Nat4 extends replicative lifespan (RLS) in yeast to similar levels as CR. Additionally, deletion of Nat4 in combination with CR does not have an additive effect on longevity implying an epistatic relationship between Nat4 and CR. This is further indicated by the fact that Nat4 expression and its activity are strongly repressed under CR. Accordingly, the extension in longevity upon Nat4 deletion is mediated by loss of H4 N-terminal acetylation since loss of this modification by mutating histone H4 serine 1 to aspartate (H4S1D) results in an extension in lifespan. Furthermore, we show that arginine 3 on histone H4 (H4R3) is required for the extension of RLS as well as for the Nat4-mediated regulation of gene expression. Collectively, the findings within this study reveal a novel role of Nat4 in regulating both heterochromatic and euchromatic gene expression in the yeast genome.

List of Contents

List of Figures and Tables

Figures

Tables

List of Abbreviations

3-AT	3-Amino-1,2,4-triazole
5-FOA	5-Fluoroorotic Acid
Ac-CoA	Acetyl-Coenzyme
ATG	Autophagy
bp	base pair
BSA	Bovin Serum Albumin
ChIP	Chromatin Immunoprecipitation
CLS	Chronological Lifespan
CR	Calorie Restriction
DTT	Dithiothreitol
ERC	Extrachromosomal rDNA circle
ETS	External Transcribed Spacer
Fob	Fork Block Protein
Gcn4	General Control Nonderepressible 4
GLC3	Glycogen branching gene 3
GNAT	GCN5-Related N-acetyltransferases
GPH1	Glycogen Phosphorylase 1
GPS	Global Proteomic Screen
GSY1	Glycogen Synthase 1
H4K5,K8,K12ac	Histone H4 lysine 5,8,12 acetylation
H4R3me1	Histone H4 arginine 3 monomethylation
H4R3me2a	Histone H4 arginine 3 asymmetric dimethylation
H4R3me2s	Histone H4 arginine 3 symmetric dimethylation
H3K4me3	Histone H3 lysine 4 trimethylation
H3K9me2	Histone H3 lysine 9 dimethylation
H3K27me3	Histone H3 lysine 27 trimethylation
H3R2me2a	Histone H3 arginine 2 asymmetric dimethylation
HML	Homothallic mating left

HMR	Homothallic mating right
Hmt1	Histone methyltransferase 1
HXK1	Hexokinase 1
IP	Immunoprecipitation
ITS	Internal Transcribed Spacer
KATs	Lysine acetyltransferases
KDAs	Lysine deacetylases
KMTs	Lysine methyltransferases
MEP	Mother Enrichment Program
MS	Mass Spectrometry
Msn	Multicopy Suppressor of Snf1 mutation
N-acH4	N terminal acetylation of histone H4
NAT	N-terminal acetyltranferase
NCR	Non-Caloric Restriction Conditions
ncRNA	Non-coding RNA
NTH1	Neutral Trehalase
NTS	Non-transcribed Spacer
OD	Optical Density
ORF	Open Reading Frame
PBS	Phosphate-Buffered-Saline
PEV	Position Effect Variegation
PKA	Protein Kinase A
Pnc1	Pyrazinamidase Nicotinamidase 1
PRMTs	Protein Arginine Methyltrasnsferase
PTM	Post-translational Modification
qRT-PCR	quantitative RT-PCR
rARs	rDNA origin of replication
rDNA	ribosomal rDNA
RFB	Replication fork barrier
RLS	Replicative Lifespan

RNA-seq	RNA sequencing
RP	Ribosomal protein
RPKM	Reads Per Kilobase of transcript per Million mapped reads
Rpm	Rounds Per Minute
RPP0	Ribosomal Protein P0
rRNA	ribosomal RNA
SAM	S-Adenosyl-Methionine
SC	Synthetic Complete
SD	Synthetic Defined
SDS	Sodium Dodecyl Sulfate
Sir	Silencing Regulator
TAF10	TATA-binding protein-Associated Factor
TIR1	Tip1-related
Tor	Target of Rapamycin
TPE	Telomere Position Effect
TPS2	Trehalose-6-phosphatase
WT	Wild Type
YPD	Yeast Extract Peptone Dextrose

CHAPTER 1
INTRODUCTION

Chapter 1.Introduction

1.1Epigenetics

The genomic DNA of eukaryotes was once thought to be the ultimate template of inheritance. This view was challenged in the early 1950s when Conrad Waddington introduced the term "epigenetics" and defined it as*" the branch of biology which studies the causal interactions between genes and their products which bring the phenotype into being''* (Holliday, 1987, Dupont et al., 2009). Over the following years, the meaning of the word changed and today the field of epigenetics is defined and accepted as *''the study of changes in gene function that are mitotically and/or meiotically heritable and that do not entail a change in DNA sequence"* (Wu et al., 2001). Within the immense field of epigenetics, we are looking into different processes of epigenetic modifications and into the underlying mechanisms of how they work together to regulate gene expression.

Epigenetic processes are characterized by DNA methylation, post-translational histone modifications and non-coding RNAs (ncRNAs) (Peschansky and Wahlestedt, 2014). Such epigenetic mechanisms can govern the regulation of DNA-based processes such as transcription, DNA repair and replication as well as cell growth and disease development (Berger et al., 2007; Suganuma and Workman, 2008, Lee et al., 2010). The first epigenetic mechanism to be identified was DNA methylation (Holliday, and Pugh, 1975), which involves the addition of a methyl group (-CH3) to the cytosine DNA nucleotides, occuring mostly at CpG islands. In mammals, DNA methyltransferases (DNMT) are responsible for ensuring the mitotic inheritance of methylated DNA bases (DNMT1), as well as the de novo methylation of unmethylated sites (DNMT3A and DNMT3B) (Okano et al., 1999). The importance of the role of DNA methylation has been established and is considered to be one of the key steps in epigenetic regulation during normal development (Plongthongkum et al., 2014)

Besides DNA methylation, histone post-translational modification (PTM) is another epigenetic mechanism, which has been implicated in the organization of chromatin structure as well as the regulation of gene transcription. Histone modifications involve the addition or removal of various chemical groups such as methyl or acetyl groups on several amino-acid residues on the main histones H1, H2A, H2B, H3 and H4 (see section 1.3) as well as on their variants (Berger et al., 2007; Kouzarides, 2007; Suganuma and Workman, 2008, Lee et al., 2010). Unlike DNA methylation, which is primarily linked to gene

silencing, histone modifications can direct gene expression towards activation or repression.

Prior to the sequencing of the human genome, a major part of non-protein coding DNA was considered to be junk DNA. Ongoing research has led researchers to reveal that part of this non-protein coding genome is transcribed and produces RNA without any coding potential. These RNA molecules are reffered to in general as noncoding RNAs (ncRNAs). Increasing emphasis has been placed on the ability of ncRNAs to modulate gene expression and on their role as epigenetic modifiers, since they interact with histone modifying complexes and DNA methyltransferases (Peschansky and Wahlestedt, 2014). In recent years, it has become apparent that epigenetic modifications do not function alone, but work together in various combinations, and cross- regulate each other in a manner that diversifies their functional states (Suganuma and Workman, 2008; Lee et al., 2010; Bannister and Kouzarides, 2011; Molina et al., 2013; Zhang et al., 2015). Moreover, patterns of epigenetic modifications act as markers for certain gene activities and occur at different sites in the genome attaining regulatory roles (Liu et al., 2015). Epigenetic modifications control gene expression by establishing and maintaining different chromatin states (Lee et al., 2010).

1.2 Chromatin

Chromatin is a complex higher-order macromolecular structure, whose basic architecture is formed by the nucleosome. The nucleosome is comprised of 147 base pairs of DNA wrapped in 1.7 superhelical turns around an octamer of histone proteins, which contains two copies of each of the four core histones H2A, H2B, H3 and H4 (Figure 1.1). The packaging of chromatin involves a series of steps illustrated in Figure 1.2. The first level of chromatin organization involves the wrapping of DNA around the histone octamer to form a “beads-on-a-string” fibre with a diameter of 11-nm in width. Further condensation of nucleosomes into a chromatin fiber is achieved through the locking of linker histone H1 at the nucleosome base near the DNA entry and exit sites (Woodcock and Ghosh, 2010). Nucleosome arrays are then organized into a more condensed 30-nm chromatin fibre, which packs the nucleosomes more closely together. During interphase, “scaffold” proteins fold the 30 nm fibers into a more condensed structure in order to fit into the nucleus and chromatin is packed to form the chromosome (Figure 1.2) (Felsenfeld and Groudine, 2003, Li and Reinberg, 2011).

Eukaryotic genomes can be divided into two structurally and functionally geographically different environments (Bannister and Kouzarides, 2011). The first is a relaxed environment, characterized by a loosely packed and 'open' state of chromatin, which is less condensed, gene-rich, transcriptionally active or inactive; known as euchromatin. The second is a more condensed environment, characterized by a 'compact' state, gene-poor known as heterochromatin, which contains mostly inactive genes (Figure 1.1, 1.3). Chromatin shows a dynamic modulation between the transcriptionally active and inactive states in order to regulate gene expression (Lee et al., 2010). Additionally, the two environments of chromatin can be distinguished in a cytological manner. Under the microscope, euchromatin resembles light colored bands while heterochromatin is dark colored (Figure 1.3). A key role in chromatin regulation in eukaryotes is played by histones, which undergo a variety of post-translational modifications (PTMs) (Suganuma and Workman, 2008; Lee et al., 2010; Bannister and Kouzarides, 2011; Molina et al., 2013; Rothbart and Strahl, 2014; Huang et al., 2014; Zhang et al., 2015).

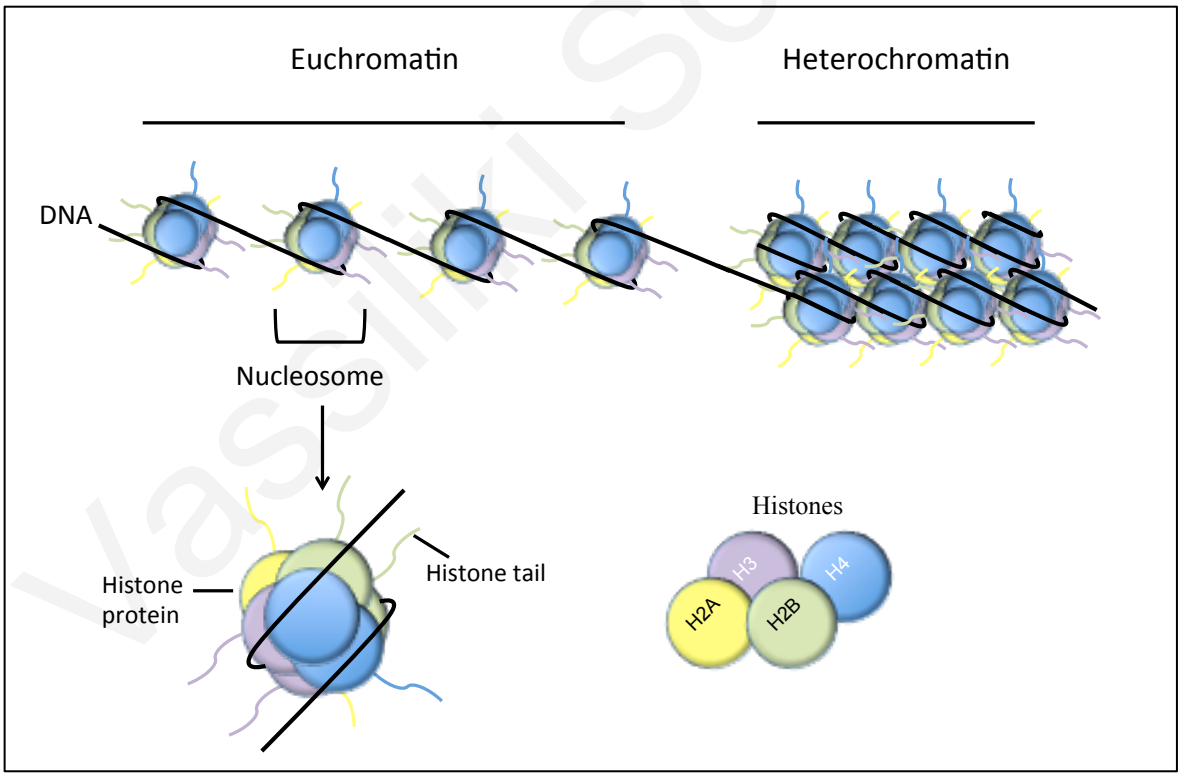

Figure 1.1. Chromatin environments and the nucleosome. Euchromatin is characterized by a loosely packed and open state of chromatin that is transcriptional active, whereas heterochromatin is a more condensed environment containing mostly inactive genes. The nucleosome is the building block of chromatin that encompasses two copies of histones H2, H2B, H3 and H4. The tails of the histones protrude from the nucleosome and their residues are modified by different chemical modifications.

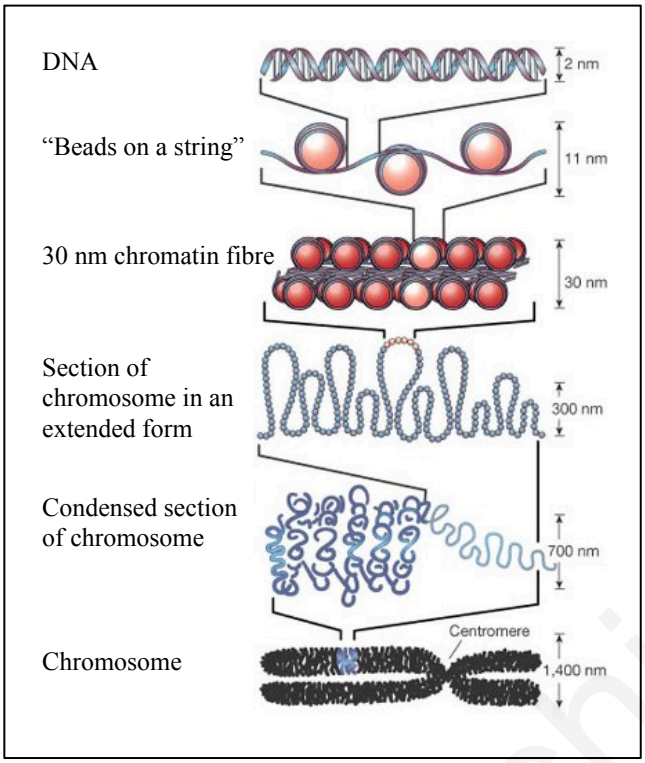

Figure 1.2. Chromatin organization. The nucleosome is the first step in which DNA wraps around a histooctamer. Nucleosomes are connected to one another by short stretches of linker DNA forming a "beads on a string" fibre. At the next level, the string of nucleosomes is folded into a 30 nm chromatin fibre and these fibres are then further folded into higher-order structures (adapted from Feisenfeld and Groudine, 2003).

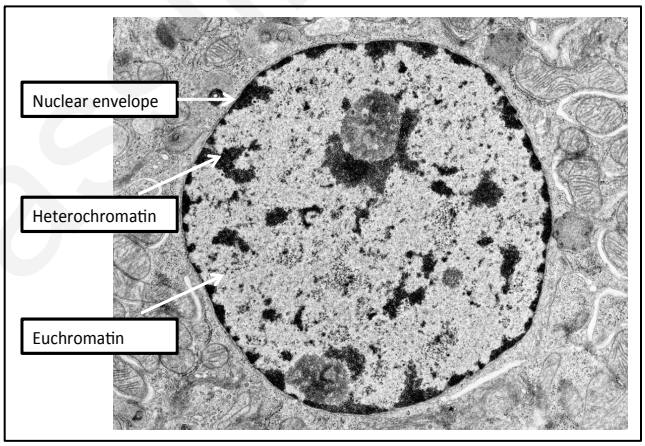

Figure 1.3. Histology of heterochromatin and euchromatin. Heterochromatin appears as dark- stained irregular particles spread throughout the nucleus or close to the nuclear envelope abundant mostly in cells that are less or not at all active in the transcription of many their genes. Euchromatin is dispersed and not stainable and is mostly predominant in cells that are active in the transcription of many of their genes (adapted from http://medcell.med.yale.edu/histology/cell_lab/euchromatin_and_heterochromatin.php).

1.3 Histone Post-Translational Modifications

Post-translational modifications (PTMs), which decorate several amino-acid residues on histones, are key regulators of chromatin structure and function (Murr, 2010). Located mostly on the terminal tails of histones, and to a lesser extent within their core domain, PTMs are covalent modifications that can dictate chromatin dynamics, orchestrate recruitment of enzyme complexes onto DNA and regulate gene transcription (Kouzarides, 2007). The study of PTMs goes back to 1964, when histone acetylation was the first to be discovered (Allfrey et al., 1964). Different types of PTMs have been identified since then, including methylation of lysines (K) and arginines (R), citrullination of arginines (R), phosphorylation of serines (S), threonines (T), tyrosines (Y) and histidines (H) (Lee et al., 2010; Rothbart and Strahl, 2014, Huang et al., 2014; Zhang et al., 2015). Over the last ten years, advances in technology have established mass spectrometry (MS) as a powerful tool for discovering histone modification sites and studying the interplay among them (Soldi et al., 2013). Numerous studies have used MS technology and focused on providing maps of PTMs for the core histones H3 and H4 due to their perceived importance in controlling gene expression and their involvement in cancer (Wang et al., 2010).

How do PTMs work towards chromatin dynamics? First, they can disrupt contacts between histones and DNA or between nearby nucleosomes by changing the overall charge of histones. One example is histone lysine acetylation which neutralizes the positive charge of lysine and weakens the affinity between histone and DNA, thus creating an 'open', transcriptionally permissive chromatin structure. Second, a single PTM or a combination of PTMs may work together to recruit effector proteins or protein complexes that can "read" the PTMs and convert them into functional chromatin states (Suganuma and Workman, 2008; Lee et al., 2010; Izzo and Schneider, 2011; Bannister and Kouzarides, 2011; Molina et al., 2013). For example in yeast, asymmetric dimethylation of arginine 2 on histone H3 (H3R2me2a) contributes to transcriptional repression by inhibiting the deposition of trimethylation of lysine 4 on histone H3 (H3K4me3) (see section 1.3.1.2) (Kirmizis et al., 2007; Kirmizis et al., 2009).

Histone modifications are established through a dynamic interplay between "writers", "erasers" and "readers", and are associated with distinct transcriptional states. Depending on the residue that is modified and the enzyme that adds ("writers") or removes ("erasers") the modification, different complexes can recognize the modification ("readers") and lead to a certain outcome (Suganuma and Workman, 2008; Izzo and Schneider, 2011; Lee et al., 2010; Bannister and Kouzarides, 2011; Molina et al., 2013;

Zhang et al., 2015). For example, K can be acetylated by lysine acetyltransferases (KATs) or deacetylated by histone deacetylases (KDAs). In addition, K and R can also be methylated by the lysine methyltansferases (KMTs) and protein arginine methyltransferases (PRMTs) respectively.

Notably, histone modifications can be read by various complexes. Lysine modfiications can be read by bromodomains/PHD/Gcn5p and SWI/SNF complexes (Bannister and Kouzarides, 2011), whereas Tudor domains are the "primary" readers of methylarginine marks (Gayatri and Bedford, 2015). The recognition of PTMs by readers recruits a number of components of the nuclear signaling network to chromatin, mediating processes such as gene transcription, DNA replication and chromatin remodeling. Chromatin-associating complexes may contain several readers within one or numerous subunits that show specificities for distinct PTMs. Importantly the coordinated binding to several PTMs can offer a lock-and- key–type mechanism for targeting specific sites and ensuring certain biological outcomes. Reader-PTM interactions have attracted a lot of scientific research interest due to the finding that misregulation of epigenetic pathways has been implicated in many diseases such as cancer and mental disorders (Musselman et al., 2012).

1.3.1 Histone Arginine Methylation

One histone modification that is of great scientific research is histone arginine methylation. This is mainly due to the identification of the family of enzymes that target arginine and lay down this modification as well as their involvement in cellular processes and various diseases (Bedford and Richard, 2005). Arginine has the longest side chain of the 20 amino acids and bears a positive charge at the end of the side chain, making it a good anchor for protein-protein interactions. It has a guanidine group that has five hydrogen bond donors, used to stabilize interactions with DNA, RNA and proteins (Bedford and Calrke, 2009). Arginine methylation emerges when nitrogens of arginine are post translationally modified by methyl groups (Figure 1.4). Such methylation may change the shape of the molecule but does not change the charge. However, it removes hydrogen bond donors, which would potentially inhibit possible interactions (Bedford et al., 2000). Three distinct types of methylated arginine residues occur in mammalian cells (Figure 1.4). The most abundant type is asymmetric omega-N^G, N^G-dimethylarginine. This PTM involves the addition of two methyl groups, on one of the two guanidino groups of arginine

residues resulting in an asymmetrically dimethylated state (Rme2a). The other two methylation states occur at levels less than 50% of Rme2a. These include the symmetrically dimethylated arginine, where one methyl group is placed on each of the terminal guanidine nitrogens *(*omega-N^G*,* N^G-dimethylarginine*;* referred to as Rme2s) and the monomethylated derivative with a single methyl group on the terminal nitrogen atom (omega-N^G-monomethylarginine; commonly referred to as Rme1) (Molina et al., 2013, Gayatri and Bedford 2014). These three methylation states of arginine methylation, are catalyzed by a family of nine AdoMet-dependent enzymes called the protein arginine methyltransferases (PRMTs) (Figure 1.4). Whether a demethylase exists that can remove this modification from arginine residues is still unknown. An earlier report identified the JmjC-domain-containing protein JMJD6 as an arginine demethylase (Chang et al., 2007; Liu et al., 2013), but more recently this enzyme was shown to be a hydroxylase (Webby et al, 2009).

The histone tails as well as the histone core contain arginine residues that are methylated. Many sites have been characterized, however their existence still needs to be confirmed by *in vitro* methylation assays and by specific antibodies (Gayatri and Bedford 2014). Notably, the dynamic interplay between the different types of arginine methylation is revealed by type-specific antibodies and amino acid analysis, showing that when the levels of a certain state of arginine methylation changes, this leads to major changes in the levels of the other two methylation states (Dhar et al., 2013). The importance of this competition for the different arginine methylation states on the same substrates is highlighted, because control of one type of arginine methylation by protein arginine methyltransferase (PRMT) knockouts, small molecule inhibition or overexpression, may affect the presence of other types of arginine methylation (Kirmizis et al., 2009; Dhar et al., 2013, Gayatri and Bedford 2014). In addition, arginine methylation is a master regulator of protein function as it regulates a number of cellular processes including RNA processing, signal transduction, transcriptional regulation and DNA repair (Bedford and Richard, 2005).

1.3.1.1 Protein Arginine Methyltransferases

Histone arginine methylation, is catalyzed by the family of protein arginine methyltransferases (PRMTs) (Figure 1.4). Classification of PRMTs is based on the type of the methylation state they can catalyze. Types I, II and III are able to deposit one methyl group to the guanidino groups of arginine residues resulting in the monomethylated (Rme1) state. Type I enzymes (PRMT1, PRMT2, PRMT3, PRMT4/CARM1, PRMT6, and PRMT8) can also perform a second methylation step and form the asymmetrically dimethylated mark (Rme2a). Type II enzyme (PRMT5) produces the symmetrically dimethylated (Rme2s) state while type III enzyme (PRMT7) generates only a monomethylated mark (Gayatri and Beford, 2014). Histone arginine methylation is related to both active and repressed chromatin states depending on the residue involved and the state of methylation (Kirmizis et al., 2007; Kirmizis et al., 2009; Molina-Serrano et al., 2013). Arginine 3 on histone 4 (H4R3) is one of the residues that can exist in any one of the three methylation states. Specifically, the asymmetrically dimethylated mark (H4Rme2a), catalyzed by PRMT1 is related with active transcription in mammals (Strahl et al., 2001;Wang et al., 2001). The yeast homolog of PRMT1, known as Hmt1, catalyzes H4R3me2a *in vitro* (Lacoste et al., 2002) and is related to transcriptional repression. Additionally, Hmt1 and H4R3me2a play a role in the establishment of silent chromatin at yeast heterochromatin-like loci, including the rDNA repeat region (Yu et al., 2006).

Moreover, PRMTs are involved in a number of biological processes such as regulation of chromatin structure through transcriptional repression or activation as well as cell cycle and DNA repair (Jahan and Davie, 2015). Finally, aberrant expression of PRMTs is involved in several diseases in addition to their involvement in the proliferation and differentiation of various cancer cell lines. This makes these proteins promising candidates for cancer therapeutic targets (Cha and Jho, 2012).

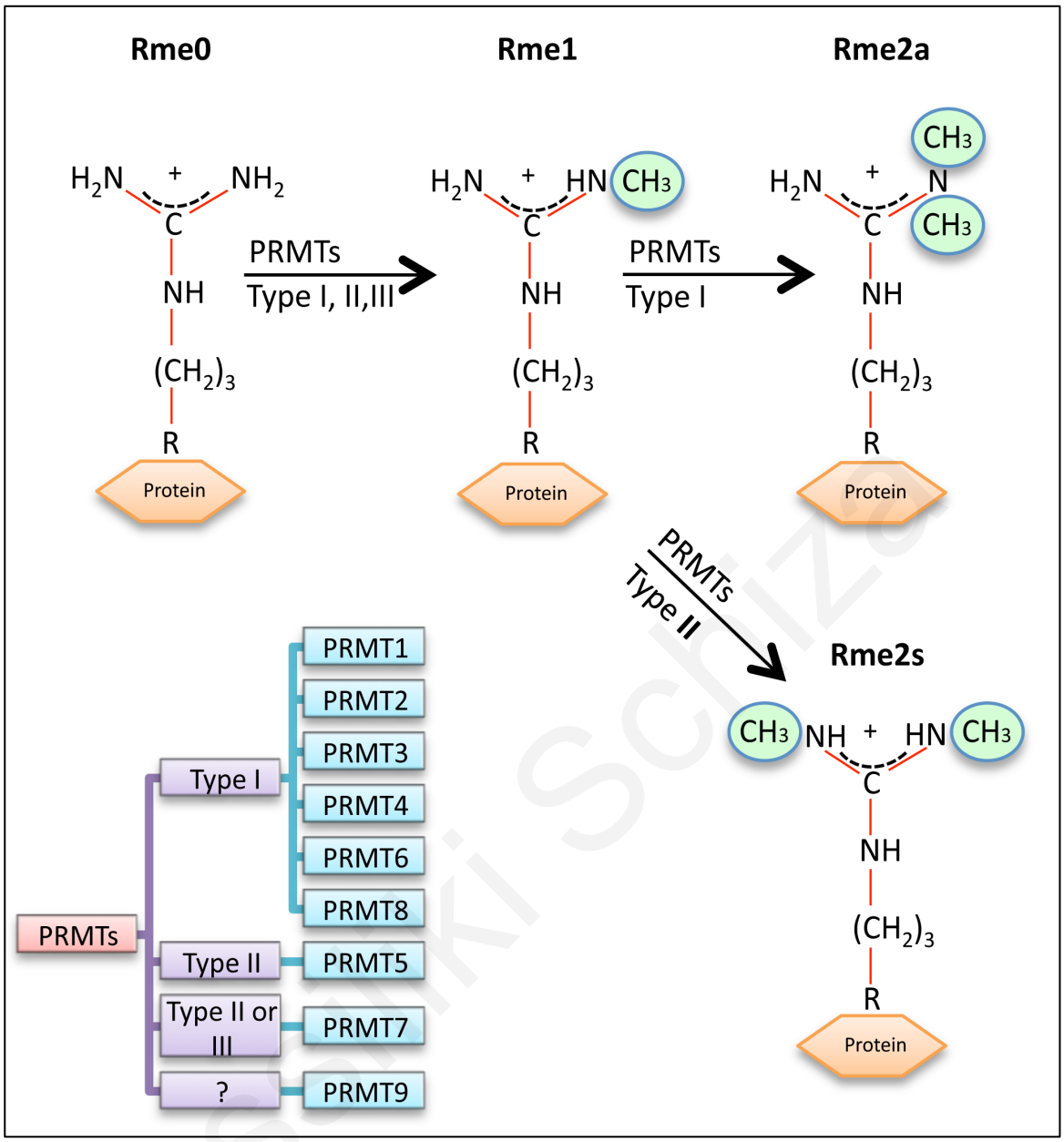

Figure 1.4. Protein arginine methylation is catalyzed by protein arginine methyltransferases (PRMTs). The three types (I, II and III) of mammalian PRMTs are shown, each consisting of different members. Type I, II and III can monomethylate Rme0 on one of the terminal guanidino nitrogen atoms (Rme1). Type I PRMTs generate asymmetric Rme2a, while type II PRMTs generate symmetric Rme2s (Molina-Serrano et al., 2013).

1.3.1.2 Crosstalk between Histone Arginine Methylation and other Epigenetic Modifications

A number of histone modifications have being identified to communicate among themselves by influencing the presence of each other or by collaborating to bring about a functional outcome. These communications, known as cross-talks, happen in a context-dependent manner (Lee et al., 2010, Molina et al., 2013). Cross-talks can occur on the same histone (*cis*) or between different histones (*trans*), and it has been proposed that *trans* mechanisms could even involve more than one nucleosome (Lee et al., 2010, Musselman et al., 2012). The study of these cross-talks has received great attention because the combinatorial reading of these modifications influences gene expression (Murr, 2010; Molina-Serrano et al., 2013; Zhang et al., 2015), and misinterpretation of these cross-talks by readers may trigger various diseases, including cancer (Dawson et al., 2012, Sharma et al., 2012, Yang et al., 2013).

Cross-talks between modifications can take place through different mechanisms. These mechanisms can be divided into two major categories, each comprising of two subcategories. The first category includes histone modifications that take part in a sequential cross-talk, during which one modification either promotes (sequential positive) or inhibits (sequential negative) the deposition of another modification (Figure 1.5A and Figure 1.5B respectively). The second category of mechanisms comprises modifications that function in a combinatorial manner during which two or more modifications existing simultaneously regulate together the binding of effector molecules. These epigenetic modifications can work synergistically, for example by recruiting together a specific reader (Figure 1.5C), or antagonistically, where one modification blocks the binding of a reader to the other modification (Figure 1.5D). These two general mechanisms appear to apply for all modification cross-talks regardless of whether they occur within the same histone (cis) or between histones (trans) (Molina-Serrano et al., 2013).

Histone arginine methylation is involved in a number of cross-talks. One of the most studied cross-talks is between H3R2me2a and H3K4me3. H3R2me2a regulates the activity of the methyltransferase Set1 by modulating the binding of the COMPASS subunit Spp1. Spp1 regulates H3K4me3 through its PHD (plant homeodomain) only when H3R2me2a is absent in order to stimulate H3K4me3 by Set1 (Kirmizis et al., 2007; Kirmizis et al., 2009). Another example comes from *in vitro* and *in vivo* studies that have shown that H4R3me2a by PRMT1 facilitates p300-mediated histone H4 acetylation, leading to nuclear-receptor-dependent transcription (Strahl et al., 2001; Wang et al., 2001).

Further validation of this cross-talk came from another study that showed that recruitment of PRMT1, p300 and PRMT4 by the tumour-suppressor gene p53 activates transcription in a stepwise manner. During this p53- mediated activation, H4R3me2a is initially deposited and then stimulates the acetylase activity of p300 towards K residues on H4 (K5, K8, K12) (An et al., 2004). Moreover, studies have also shown that H4R3me2a is also involved in arginine methylation trans-histone cross-talk. Loss of H4R3me2a by PRMT1 knockdown leads to localized induction of H3K9me2 and global increase of H3K27me3 over the β-globin locus. (Huang et al., 2005). H4R3 methylation also communicates with DNA methylation. One study showed that PRMT7-mediated deposition of H4R3me2s at the ICR (imprinting control region) of the *Igf2*/*H19* locus was necessary for subsequent DNA methylation (Jelinic et al., 2006).

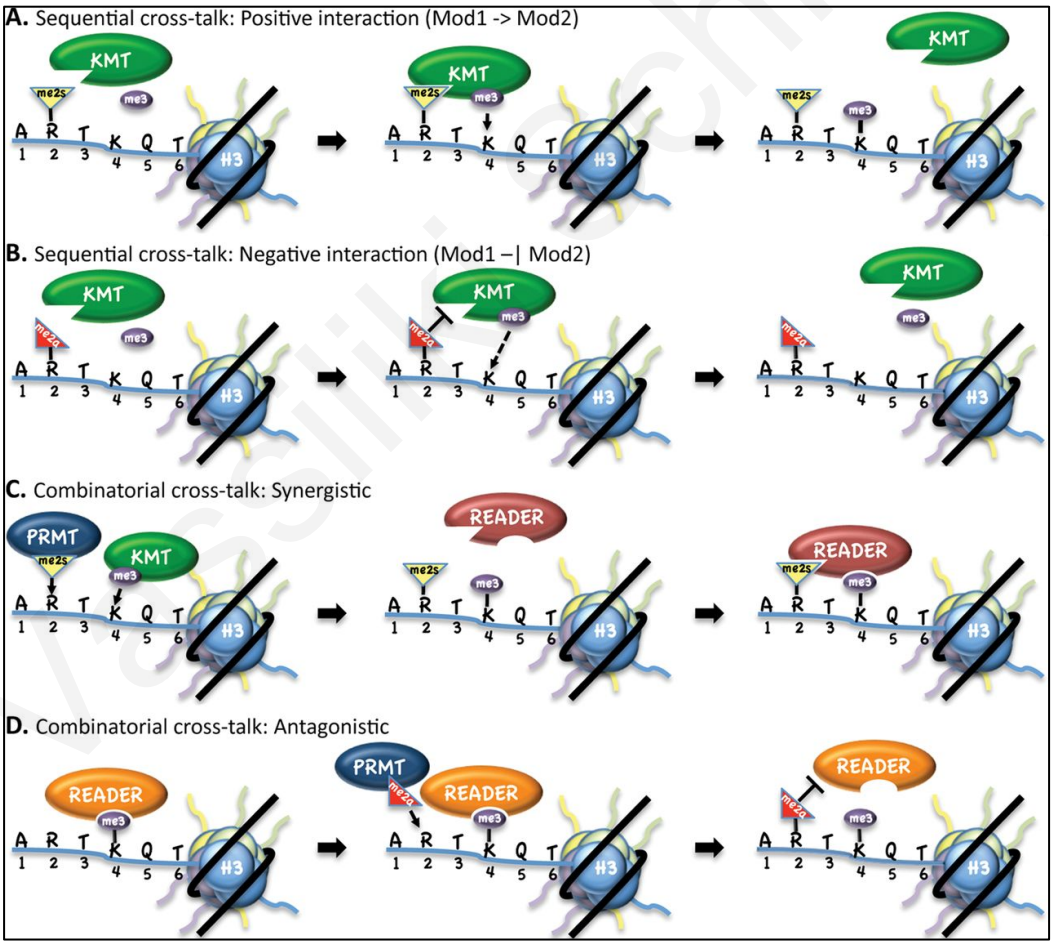

Figure 1.5. Mechanisms of cross-talk involving arginine methylation (**A**) A sequential positive interaction, where a lysine methyltransferase (KMT) binds the histone tail through recognition of the Rme2s mark, and deposits a second PTM (Kme3). (**B**) A sequential negative interaction, where the same KMT cannot bind to the histone tail because of the Rme2a mark, thus blocking downstream PTM deposition. (**C**) A combinatorial synergistic cross-talk, where after the deposition of both PTMs by their respective enzymes, a reader can bind to the histone tail to exert its function. (**D**) A combinatorial antagonistic mechanism where a reader can recognize one PTM on the histone tail, but the deposition of a second mark (Rme2a) impairs this recognition (Molina et al., 2013).

1.3.2 Protein N^{α} terminal Acetylation

N-alpha-terminal acetylation (N^{α}-terminal acetylation) of proteins is an enzymatic process that is characterized by the transfer of an acetyl moiety (Ac) from acetyl coenzyme (Ac-CoA) to the α-amino group of the first amino acid residue of a protein (Figure 1.6). The enzymes that are involved in the catalysis of N^{α}-terminal acetylation are known as N-terminal acetyltransferases (NATs) and are members of the GNAT family protein (GCN5-related N-acetyltransferase). So far six different NATs have been identified denoted as NatA-NatE. N^{α}-terminal acetylation is considered to be an irreversible process, as no N-terminal deacetylase has been identified to date (Arnesen, 2011; Starheim et al., 2012, Varland et al., 2015).

N^{α}-terminal acetylation is an abundant protein modification that is present in all kingdoms of life. It has a high level of evolutionary conservation as the same system of N^{α}-terminal acetylation may operate in all species, such as in *Saccharomyces cerevisiae*, *Caenorhabditis elegans, Drosophila melanogaster, Arabidopsis thaliana, Xenopus laevis*, *Mus musculus,* and *Homo sapiens* (Polevoda and Sherman 2003; Starheim et al., 2012). It is present in 84% of mammalian cytosolic proteins and 57% of yeast proteins, reflecting small differences in enzymatic properties and alterations in sequence distribution between the two species (Brown et al., 1976; Arnesen et al., 2009). In bacteria, however, a small number of proteins are known to be N^{α}-terminal acetylated (Polevoda and Sherman, 2003) while in archaea 15% of proteins are N^{α}-terminal acetylated (Falb et al., 2006).

For quite some time, the functional role N^{α}-terminal acetylation remained a mystery. Over the past five years, astonishing progress has been made in the research field of N^{α}-terminal acetylation regarding the understanding of the existence of this modification, as well as the mechanisms involved. This is due to the development of powerful proteomic tools for studying *in vivo* global N^{α}-terminal acetylation (Starheim et al., 2012). N^{α}-terminal acetylation functions in various fundamental cellular processes like protein degradation, regulation of cell survival pathways, endoplasmic rediculum translocation and cellular metabolism (Starheim et al., 2012).

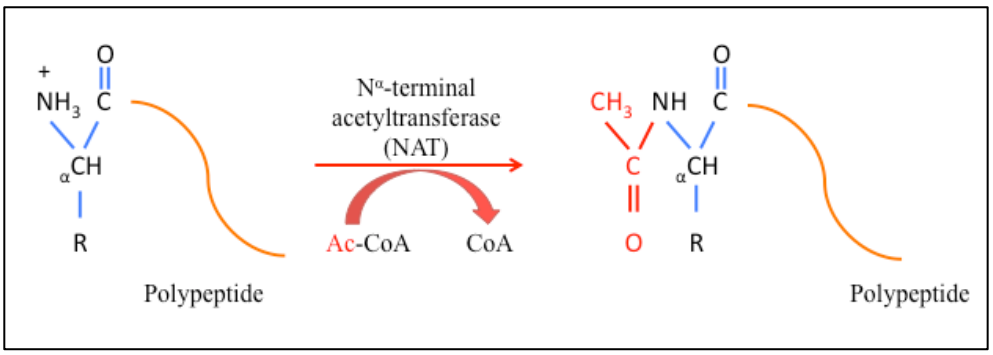

Figure 1.6. N$^{\alpha}$-terminal acetylation. NAT transfers an acetyl group from Ac-CoA to the α-amino group of the first amino acid residue of a polypeptide. The positive charge of the N-terminal amino group is removed by the acetylation, changing in this way the chemical properties of the N-terminus of the polypeptide

1.3.2.1 N-alpha Terminal Acetyltransferases (NATs)

The eukaryotic NAT-machinery involves a group of NATs that perform most N$^{\alpha}$-terminal acetylation. These NATs differ between them not only in subunit composition but also in substrate specificity. They acetylate subsets of proteins according to their N-terminal amino acid sequence and each enzyme consists of one or more different subunits (Polevoda and Sherman, 2003; Starheim et al., 2012). Proteins with methionine, alanine or serine are the ones that are mostly acetylated, with the latter two being acetylated in more than 74% of all N$^{\alpha}$-acetylated proteins in *Saccharomyces cerevisiae* (Polevoda and Sherman 2003).

The NatA-E enzymes and their substrate specificities are conserved from yeast to humans whereas NatF is mostly found in higher eukaryotes (Table 1) (VanDamme et al., 2011). Insight into the function of N$^{\alpha}$-terminal acetylation comes from studies done on NATs in *S.cerevisiae.* NatA accounts for acetylation of the majority of N$^{\alpha}$-acetylated proteins in humans and yeast, and acetylates proteins with alanine or serine, and occasionally with glycine, threonine, valine or cysteine N-termini (Mullen et al., 1989; Polevoda et al., 1999; Starheim et al., 2012; Varland et al., 2015). NatA is composed of the catalytic subunit Naa10 (Ard1) and the auxiliary subunit Naa15 (Nat1). In the absence of Naa15, the substrate specificity profile of Naa10 changes and acetylates proteins with aspartic acid and glutamic acid N termini (Van Damme et al., 2011;Varland et al., 2015) (Table 1). In yeast, deletion of either Ard1 and Nat1 subunits generates phenotypes of reduced sporulation, failure to enter G_o phase under certain conditions, decreased survival after heat shock and sensitivity to various chemical stressors (Polevoda et al., 2003). The NatB complex is composed of the catalytic Naa20 (Nat3) and the auxiliary subunit Naa25

(Mdm20) and acts on the N-terminal methionine when the second residue is glutamic acid, aspartate, asparagine or glutamine (Van Damme et al., 2012). Deletion mutants of the subunits in yeast leads to slow growh, defects in vacuolar and mitochondrial inheritance and inability to form functional actin cables (Polevoda et al., 2003). The NatC complex consists of the catalytic Naa30 (Mak3) and the auxiliary subunits Naa38 (Mak10) and Naa35 (Mak31); and acetylates substrates starting with methionine and are followed by isoleucine, leucine, tryptophan or phenylalanine (Polevoda and Sherman 2003; Varland et al., 2015). Mutations of NatC complex subunits gives similar phenotypes to NatA and NatB deletions (Starheim et al., 2012). NatD, also known as Nat4 consists only a catalytic unit (Naa40) and the only two substrates known to date in both yeast and humans are histones H2A and H4 (Song et al., 2003; Hole et al., 2011). Nat4 is described further in the next section. Moreover, NatE is composed of catalytic Naa50 (Nat5) as well as the NatA subunits Naa10 and Naa15; and acetylates methionine-starting N-termini. Depletion of Naa50 in human studies showed that it increases regrowth of microtubules (Chu et al., 2001) whereas in yeast, no phenotype has been observed in the absence of Naa50 (Gautschi et al., 2003; Starheim et al., 2012). NatF is defined by Naa60 and is found only in higher eukaryotes. NatF acetylates substrates starting with methionine and are followed by leucine, phenylalanine, isoleucine and tryptophan (Van Damme et al., 2011). The only NATs, whose structures and biochemical activitites have been characterized, are NatA, NatE (Liszczak et al., 2011; 2013) and just recently, Nat4 (Magin et al., 2015). All in all, the different NATs differ in subunit composition, substrate specificity (Table 1) and phenotypes (Varland et al., 2015).

Yeast NAT (subunit composition)	**Human NAT ortholog (subunit composition)**	**Substrate Specificity**
NatA (Ard1^{cat}, Nat1^{aux})	NatA (Naa10^{cat,} Naa15^{aux})	Met-Asp-, Met-Glu-Ala-,Cys-, Gly-Ser-,Thr-, Val-, Asp-, Glu-
NatB (Nat3^{cat}, Mdm20^{aux})	NatB (Naa20^{cat}, Naa25^{aux})	Met-Asn-, Met-Asp, Met-Gln-, Met-Glu-
NatC (Mak3^{cat}, Mak10^{aux}, Mak31^{aux})	NatC (Naa30^{cat}, Naa35^{aux}Naa38^{aux})	Met-Ile-, Met-Leu-, Met-PhE-, Met-Trp-
NatD (Nat4^{cat})	NatD (Naa40^{cat})	Ser-Gly-Arg-Gly-, Ser-Gly-Gly-Lys
NatE (Nat5^{cat})	NatE (Naa50^{cat})	Met-Ala-,Met-Leu-, Met-Lys-, Met-Phe-, Met-Ser-, Met-Thr-, Met-Tyr-, Met-Val-
-	NatF (Naa60^{cat})	Met-Ala-, Met-Gln-, Met-Gly-, Met-Ile-, Met-Leu-, Met-Lys-, Met-Met-, Met-Ser-, Met-Thr-, Met-Tyr-, Met-Val-

Table 1. NATs in yeast along with their human ortholog and substrate specificity.

The biological significance of N^{α}-terminal acetylation has been studied in different organisms and the lack of N^{α}-terminal acetylation as well as abnormal acetylation can result in various defects and can prevent normal protein function (Starheim et al., 2012; Van Damme et al., 2012). Moreover, N^{α}-terminal acetylation has been implicated in the pathophysiology of the Ogden syndrome known to be caused by a Ser37Pro in *NAA10* resulting in diminished enzymatic activity and NatA complex formation (Van Damme et al., 2014; Myklebust et al., 2015; Varland et al., 2015). Furthermore, whole-exome sequencing studies identified de novo missense variants in the *NAA10* gene suggesting a genotype-phenotype correlation in two cases of global developmental delay (Popp et al., 2015). Several studies have also connected the aberrant activity of NATs, particularly NatA, making them attractive targets for drug development (Kalvik and Arnesen, 2013).

1.3.2.2 Nat4 and Histone N-terminal Acetylation

As mentioned above, N^{α}-terminal acetylation is also present on histones H2A and H4 and the only known enzyme responsible for this is N-alpha terminal acetyltransferase 4 (Nat4 also known as NatD or yNaa40), originally identified in *Saccharomyces cerevisiae* (Song et al., 2003), and in humans is known as hNaa40 (Patt1, hNatD or Nat11) (Liu et al., 2009; Hole et al., 2011). Both human and yeast Nat4 are associated with ribosomal fractions from whole cell lysates. In addition, hNaa40 localizes to both the nucleus and the cytoplasm, suggesting that it may act both post and co-translationally (Polevoda et al., 2009; Hole et al., 2011). Recently, Magin *et al*, reported the crystal structure of Nat4 which explains its high substrate selectivity. The authors observed unique structural requirements for the first four residues of its substrate, emphasizing the importance of Ser-Gly-Arg-Gly recognition sequence for histone-specific acetylation (Magin et al., 2015).

Earlier studies have provided some insight into the physiological role of human and yeast Nat4. In yeast, a strain deletion of *NAT4* has shown growth sensitivity to-aminotriazole (3- AT), an inhibitor of transcription. This growth sensitivity was stronger in a yeast strain that contains a *NAT4* deletion combined with mutations in histone H4 where lysines 5, 8 and 12 have been replaced by arginines (K5,K8,K12R) (Polevoda et al., 2009). In humans, hNaa40 is highly expressed in the liver and is downregulated in hepatocellular carcinoma. In addition, overexpression of hNaa40 in hepatoma cells drives them towards apoptosis (Liu et al., 2009). Moreover, hNaa40 liver specific knock out (LKO) mice are protected from age associated hepatic steatosis, suggesting a role for hNaa40 in hepatic

lipid metabolism and age-dependent associated disseases (Liu et al., 2012). These studies have identified phenotypes that provide clues on the physiological role of yeast and human Nat4. They have not, however, explored the underlying molecular mechanisms and especially, the function of Nat4-mediated histone N-terminal acetylation.

1.4 *Saccharomyces cerevisiae* as a Model Organism

Numerous studies have used the budding yeast *S. cerevisiae* as a model organism in order to uncover a number of histone PTMs involved in the control of gene expression and silencing. Such studies have been crucial to our current understanding of epigenetic regulation. *S. cerevisiae* is a single-cell eukaryotic organism with a genome size of about 14 megabases pairs of genomic DNA divided among 16 chromosomes ranging in size from 200 to 2200 kb. There are approximately 6000 genes in the yeast genome, packed along chromosomal arms with less than 2 kb spacing between them (Grunstein and Gasser, 2013). Budding yeast has a generation time of approximately 90 minutes, with colonies being produced after two days of growth (Sherman, 2002). Moreover, budding yeast allows the alteration of any chosen chromosomal sequence through the highly efficient system of homologous recombination (Grunstein and Gasser, 2013). As a model organism, yeast has a key advantage in the genetic analysis of histones. In contrast to mammalian cells, which contain around 60-70 copies of the core histone coding genes (H2A, H2B, H3, and H4), yeast has only two copies of each of these genes. Due to the fact that the two copies are functionally redundant, it has enabled researchers to produce yeast strains that contain single histone gene copies. The ease of creating mutations or deletions of certain residues on histones has uncovered their role in heterochromatin and other cellular functions. Furthermore, the power of yeast genetics makes it easier to connect genotype to phenotype. Thus, systematic mutagenesis of most amino acids on the core histones has led to the identification of proteins that interact with the histone residues being mutated (Huang et al., 2009).

S.cerevisiae grows through mitotic division in either a haploid or diploid state, by producing a bud that expands and eventually separates from the mother cell (Figure 1.8). Haploid yeast cells have two mating types; mating type a, (Mat a) and mating type α (Mat α), each producing a distinct pheromone that attracts the cells of the opposite mating type: α cells produce a 13 amino acid peptide (α factor) that binds to the α-factor receptor on the surface of the a cells and a cells produce a peptide of 12 amino acids (a factor), which

binds to a membrane spanning a-factor receptor on the surface of an α cell. These interactions result in the arrest of the cells in mid to late G phase of the cell cycle. Arrested cells can efficiently fuse at their tips to form an **a/α** diploid. This diploid cell contains the 16 chromosomes of each of the original haploid cell. Thus it has two copies of each gene and is unable to mate with either a or α haploid cells, but can either divide by mitotic division or under nutritional starvation conditions (carbon and nitrogen limitation) can undergo meiosis to result in the formation of an ascus containing four spores, two of each mating type. Given sufficient nutrients, germination occurs and the wall of the ascus breaks allowing the release of the four spores which can grow into cells capable of mating, starting the life cycle over again (Figure 1.8) (Herskowitz, 1988; Grunstein and Gasser, 2013).

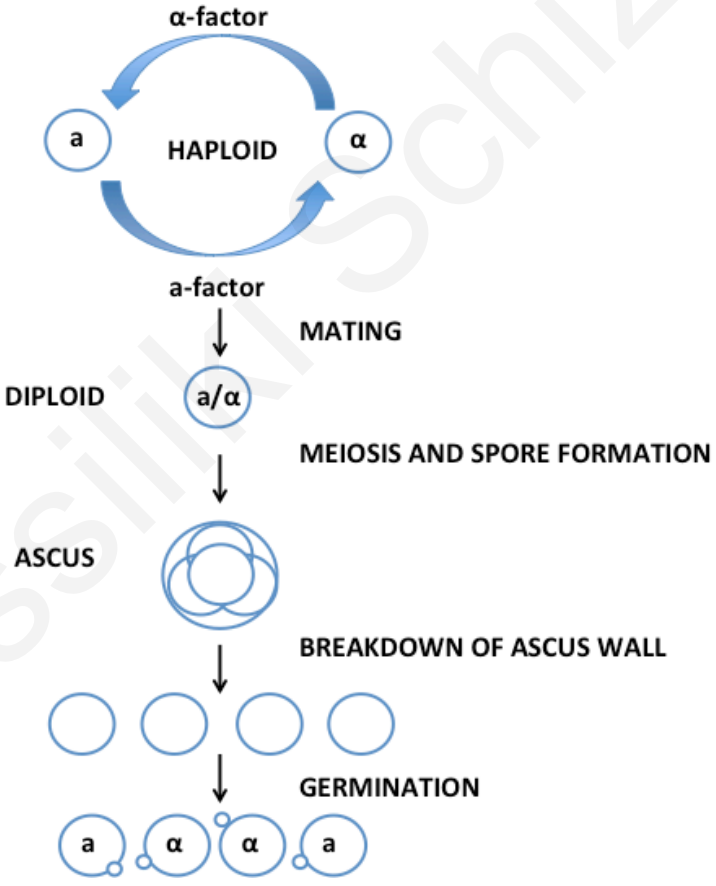

Figure 1.7. The life cycle of budding yeast. Haploid yeast cells mate and yield a diploid and meiosis of a diploid yields haploid cells. Sporulation is induced in a diploid by starvation, whereas mating occurs spontaneously by pheromone secretion when haploids of opposite mating type are close to each other. Haploid a/a cells produce an ascus, which contains four spores. These spores through the process of germination grow on nutrient media (Modified from Herskowitz, 1988).

1.4.1 Sllencing in *S.cerevisiae*

The budding yeast provides a well-studied and ideal model for heritable silent chromatin. Similar to higher eukaryotic organisms silent chromatin in *S.cerevisiae* shares features such as inaccessibility of DNA, hypoacetylation of nucleosomes and late replication (Loo and Rine 1994; Lustig 1998). In yeast, there are distinct heterochromatin-like regions adjacent to all 32 telomeres, the two silent mating type loci on chromosome III (*HML* and *HMR*) as well as the ribosomal DNA locus. Transcriptional silencing at the rDNA locus, telomeres and the *HML*, *HMR* can spread into adjacent DNA, essential for maintaining a mating state (Grunstein and Gasser, 2013). In *S.cerevisiae*, at the end of all yeast chromosomes, there are $C_{1-3}A/TG_{1-3}$ repeats. A phenomenon called telomere position effect (TPE) occurs adjacent to these repeats and is similar to the Position Effect Variegation (PEV) studied in *Drosophila melanogaster*, when the white gene is used to screen for mutations that suppress or increase white variegation (Elgin and Reuter, 2013). TPE involves a phenomenon in which the addition of a gene near a telomere causes repression of transcription. Genes under the influence of TPE, switch between an inactive repressed state to a transcrptionally active state (Sandell et al., 1994). An assay that has been widely used for the study of TPE involves the *URA3* reporter genes (2.13). In addition to genetic approaches, yeast are also involved in various biochemical and molecular techniques such as Chromatin Immunoprecipitation (ChIP), transcriptomics as well as proteomic approaches to map protein networks.

1.4.1.1 The ribosomal DNA Locus

Protein synthesis is carried out by ribosomes, which are large ribonucleoprotein particles in a eukaryotic cell, present in large numbers. Ribosomal proteins account for 50% of the total protein and ribosomal RNA (rRNA) represents approximately 80% of the total RNA in the cell (Warner, 1999; Kobayashi, 2011). In order to meet the biosynthetic demand, eukaryotic cells contain more than 100 copies of rRNA organized in clusters of ribosomal deoxyribonucleic acid (rDNA) (Kobayashi et al., 2011).

In the nucleolus, the ribosomal rRNA genes of *S.cerevisiae* are organized as an rDNA cluster, making up about two-thirds of chromosome XII. The rDNA is organized in a single tandem array consisting of approximately 150 copies of a 9.1-kilobase repeating unit (Warner, 1999; Venema and Tollervey, 1999; Woolford and Basega, 2013). The

repeating unit is arranged as shown in Figure 1.8. Each repeat encodes a 5S rRNA, transcribed by polymerase III and a 35S precursor RNA transcribed by RNA polymerase I that is subsequently processed to form the 18S, which is found in the 40S ribosomal subunit and the 5.8S and 25S RNAs, which are found in the 60S subunit (Warner, 1999; Venema and Tollervey, 1999; Woolford and Basega, 2013). The 35S coding regions are separated by nontranscribed spacers, NTS1 and NTS2 (Smith and Boeke 1997, Venema and Tollervey, 1999; Woolford and Basega, 2013). The internal transcribed spacers are found on either side of the *RDN58* gene and are described as ITS1 and ITS2 (Woolford and Basega, 2013). Notably, around half of the rDNA repeats are active at a given time point, whereas the other half are transcriptionally silent (Warner 1999).

The repetitive nature of the rDNA region makes it very recombinogenic and susceptible to loss of copies after deleterious recombination events among the repeats (Kobayashi, 2011). Budding yeast has a well-studied gene amplification system that responds to the recombination-mediated loss of rDNA copies. During the S phase of the cell cycle, replication is inititated at replication origin (rARS) and is inhibited at the replication fork barrier (RFB) (Figure 1.8) by the function of the fork blocking protein Fob1 inducing amplifcation for copy number recovery (Kobayashi, 2003). Amplification is regulated by a bidirectional promoter, E-pro, which is located beside RFB within the NTS1 region. In situations where the copy number is normal, rDNA silencing is mediated by histone deacetylase Sir2, which keeps the E-pro off and the copy number remains stable. When the rDNA copy number is reduced, Sir2 is repressed and E-pro starts transcription to activate the rDNA amplifation system. When it reaches physiological copy numbers, Sir2 levels are increased and repress E-pro (Kobayashi, 2011).

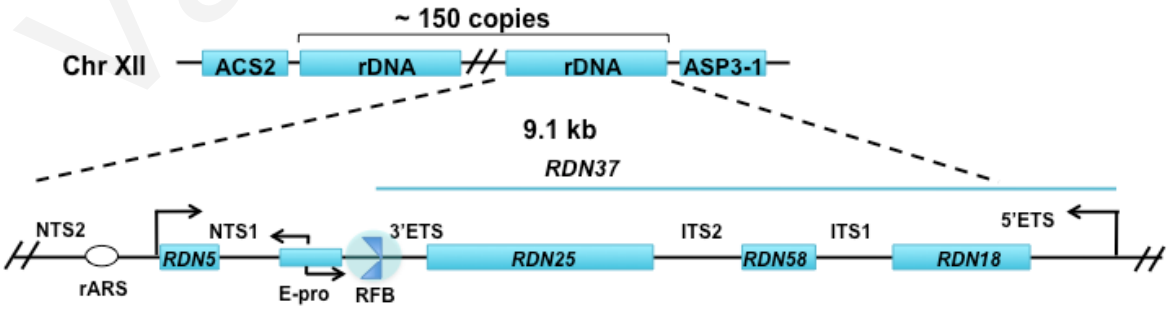

Figure 1.8. Schematic representation of the rDNA locus on chromosome XII in *Saccharomyces cerevisiae.* The yeast rDNA unit consists of the *RDN5* gene, which encodes for the 5S rRNA and the *RDN37* gene, which encodes for 35S rRNA. Between the two genes there are two nontranscribed spacers, NTS1 and NTS2. The rDNA origin of replication (rARS) lies within the NTS2 region. Within the NTS1 region, there is a bidirectional noncoding promoter, E-pro as well as the replication fork binding site (RFB). The 35S pre-rRNA precursor contains the 18S, 5.8S and 25S rRNAs, separated by two internal transcribed spacers ITS1 and ITS2, and flanked at either end by two external transcribed spacers, ETS1 and ETS2.

1.4.2 Ageing in *S.cerevisiae*

In addition to its use in silencing studies, budding yeast is also one of the most important model organisms to be used in ageing research with immense contributions to the understanding of longevity in mammalian and invertebrate models (Longo et al., 2012) Ageing is a complex process accompanied by damaging changes that eventually lead to death (Choi et al., 2011). The main advantage of budding yeast over other systems in studying ageing is the ease and speed with which longevity can be quantified (Kaebrerlein, 2010). In addition, yeast has a short lifespan as a unicellular organism with metabolic and regulatory mechanisms being conserved in higher eukaryotes (Kaeberlein, 2010). Ageing in the budding yeast is accompanied by morphological changes including an increase in cell size, sterility by expression of the mating type (*HM)* loci and enrlargement and fragmentation of the nucleolus (Sinclair et al., 1997). In addition genetic alterations resulting in a decrease in lifespan have been identified; such as deletion of *SGS1* (a RecQ-like DNA helicase) which is the yeast homolog of the human *WRN* gene (Sinclair et al., 1997). In humans, defects in *WRN* cause Werner syndrome, a premature-ageing disease (Yu et al., 1997). Thus, yeast is also used as a model to unravel ageing-related human diseases. Furthermore, apart from changes in the nucleus, age-associated changes occur in the cell organelles such as the mitochondria, vacuoles, endoplasmic rediculum and cytoplasm (Lippuner et al., 2014).

1.4.2.1 Replicative and Chronological Lifespan

The two well-known ageing models that exist in yeast are replicative and chronological lifespan (Figure 1.9). Firstly, replicative lifespan (RLS) relies on the mitotic division that yields distinct mother and daughter cells and is defined by the number of daughter cells that are produced by a particular mother cell prior to senescence (Mortimer and Johnston, 1959; Steffen et al., 2009). The "gold standard" method to study RLS, which is also the method used in this project, is the separation of mother and daughter cells by manual microdissection after every division (see section 2.21). This technique, however, is tedious and constrained by the small number of cells it can analyze, making it difficult to be used for high-throughput studies (Lippuner et al., 2014).

Recently, advances in the development of techniques to study RLS have emerged. One technique is the Mother Enrichment Program (MEP), which involves the use of strains

that enable the genetic selection against newborn daughter cells, thus preventing them to divide (Lindstrom and Gottschling, 2009). This allows mother cells to achieve a normal RLS and leads to a linear dilution of mothers in a population of arrested daughters (Lippuner et al., 2014). Therefore, MEP cultures permit the comparison of RLS between different yeast strains and since they are not subject to nutrient limitation, single-step affinity purification of aged cells can be achieved at any point during their life span (Lindstrom and Gottschling, 2009). Another recent technique to study RLS is the use of microfluidic devices (Lee et al., 2012; Xie et al., 2012; Jo et al, 2015). This technique involves continuous and high-resolution microscopic time-lapsed imaging of the entire lifespan of yeast cells. A microfluidic chamber retains mother cells, while daughter cells are flushed away throughout the lifespan of the mother cells. This technique allows the simultaneous study of lifespan, cell division dynamics and morphological cell and organelle changes in a large number of individual cells; as well as the characterization of cellular and molecular phenotypes of ageing cells.

Secondly, chronological lifespan (CLS) involves the length of time that a mother yeast cell can survive in a non-dividing, quiescence-like state (Kaeberlein, 2006; Fabrizio and Longo, 2007) and acts as a model for post-mitotic cells (Kaeberlein, 2010). CLS is measured by growing cells in liquid media, in which cells enter a non-dividing state when the carbon source in the media is exhausted. The ability of cells to resume mitotic growth is then measured by viability over time (Nagarajan et al., 2014). RLS is considered to be similar to ageing phenomena observed in stem cells in humans, while CLS is akin to the ageing of non-dividing cells such as neurons (Longo et al., 2012). Both RLS and CLS make budding yeast a powerful system to study ageing as the two models can be measured independently allowing comparisons to be made between the gene regulating lifespan in dividing and non dividing cells (Smith et al., 2006).

Importantly, changes in ageing and development of age-associated diseases are due to certain damages that occur in cells. In the RLS model, age-associated damage is inherited from the mother to the daughter cells. In the CLS model, however, damage develops over time within a non-dividing cell reaching a point at which the cell can no longer enter the cell cycle (Kaeberlein et al. 2010). Despite these differences, it is evident that nutrient availability plays a role in both ageing models. When cells undergo starvation during prolonged periods as in CLS, then RLS is reduced when they re-enter the cell cycle (Ashrafi et al., 1999).

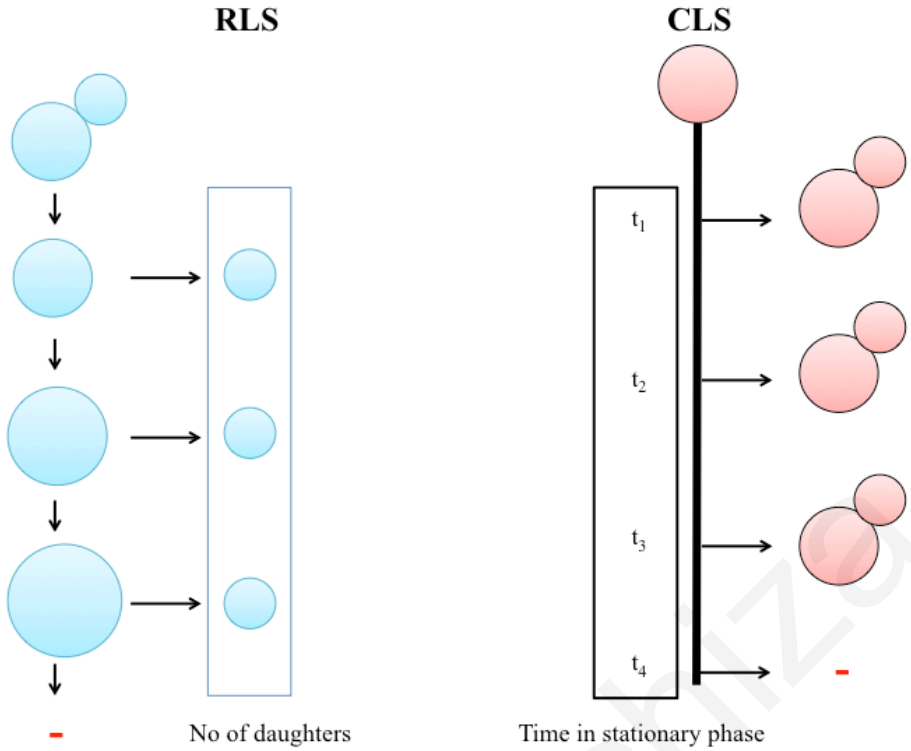

Figure 1.9. Schematic diagram for Replicative lifespan (RLS) and Chronological Lifespan (CLS). RLS accounts for the number of daughter cells produced by a mother cell before senescence (-). CLS is defined by the survival time of a cell in a non-dividing state in a stationary phase culture.

1.4.2.2 Calorie Restriction

Environmental cues can play a vital role in longevity determination. One of the most important laboratory tools for studying the effects of energy intake is the intervention by limiting the nutrient availability, known as calorie restriction (CR). Throughout eukaryotic evolution, a conserved survival strategy has developed. This is to adjust metabolism in low-nutrient conditions in order to enable a more efficient use of the energy available (Vaquero and Reinberg, 2009). As already mentioned, yeast has proven to be a valuable research model due to its shorter lifespan than most other models. In *S. cerevisiae,* CR can be modeled by reducing the levels of carbon source such as glucose in growth media from 2% to 0.5% or below. Recent studies demonstrate that yeast cells grown under CR show many hallmarks associated with yeast grown to stationary phase, such as the accumulation of reserve carbohydrates (Boender et al., 2011).

1.4.2.3 Reserve Carbohydrates

In a natural habitat, *S. cerevisiae* copes with variations in environmental conditions, by adapting its metabolism to such conditions, with cell division being coordinated at the G1 phase of the cell cycle (Thomas and Hall, 1997). When yeast cells are grown in rich media containing glucose as the carbon source, they metabolize glucose through glycolysis, releasing ethanol in the medium. As soon as glucose is diminished, cells exit the mitotic cycle and enter a diauxic shift that involves slower growth rate and a switch from glycolysis to aerobic utilization of ethanol, preparing for survival in stationary phase (Galdieri et al., 2010; Li et al., 2013). Stationary phase is defined as a component of the culture cycle of organisms when there is no further net increase in cell number (Werner-Washburne et al., 1999). During this phase, a reduction of the glycolytic flux occurs (Lillie and Prignle, 1980) and stationary phase cells undergo changes that resemble those occuring in cells that stimulate a stress response. Such alterations involve induction of the expression of heat shock and stress proteins (Parrou et al., 1999) as well as accumulation of glycogen and treahalose in the cytoplasm (Gray et al., 2004) and an induction of autophagy (Noda and Ohsumi, 1998). Although glycogen accumulation occurs before glucose is exhausted completely, trehalose accumulates just after the diauxic shift (Lilie and Pringle, 1980) and protects cells against stress.

Accumulation of glycogen and trehalose, also known as “reserve carbohydrates” or storage carbohydrates, occurs in cells during a transition period from the end of the exponential phase of growth to the entrance into the diauxic shift (Lillie and Pringle, 1980; Parrou et al., 1999), when one of the essential nutrients is limited (Parrou et al., 1997). Initially, reserve carbohydrates were believed to act as storage factors but during the last decade it is evident that they are also implicated in other roles such as stress protectants (Sillje et al., 1999; Hazelwood et al. 2009). A schematic view of the biosynthesis and degradation of reserve carbohydrates is shown in Figure 1.10.

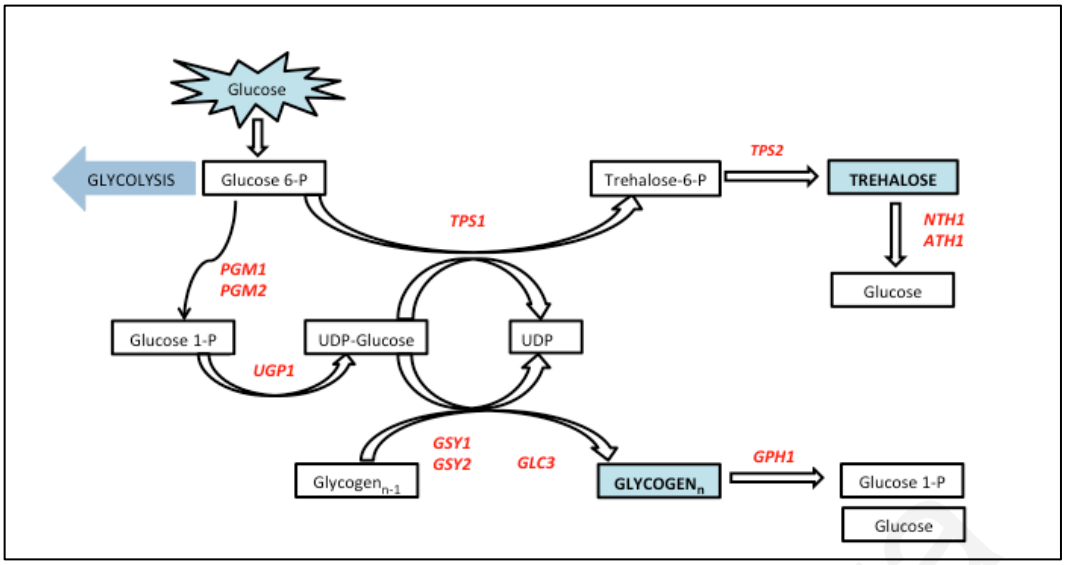

Figure 1.10. Schematic representation of the biosynthesis and degradation of reserve carbohydrate genes, glycogen and trehalose. Key genes involved in the accumulation of glycogen and trehalose are shown in red. For their biosynthesis two compounds participate, glucose-6-P and UDP-glucose. UDP glucose is formed from glucose-1-P and UTP through the action of UDP-glucose pyrophosphorylase (UGPase); encoded by *UGP1*. During biosynthesis of glycogen, glycogen synthase genes (*GSY1, GSY2*) and the glycogen branching gene (*GLC3*) are needed for maximum accumulation of glycogen (Thon et al., 1992). Glycogen phosphorylase (*GPH1*) and a debranching enzyme are responsible for degradation of glycogen to glucose-1-P. Moreover, trehalose is synthesized in yeast from UDP-glucose and glucose-6-P via trehalose-6-P. The enzymes that catalyze the reaction are encoded by the genes trehalose-6-P synthase (*TPS1*) and trehlaose-6-phosphatase (*TPS2*). Hydrolysis of trehalose to glucose is carried out by trehalase *NTH1*.

1.4.3 Calorie Restriction and Longevity

As a response to diminishing glucose levels, yeast has shown an increase in both RLS and CLS (Tahara et al., 2013). In 1935 McCay and colleagues published the first paper showing that CR without malnutrition extends lifespan in rats (McCay et al., 1935). Our understanding of how CR extends lifespan is far from complete, possibly because it affects different features of the ageing process in parallel. During the last decades, CR has been reported to extend the lifespan of a broad range of organisms, including yeast, worms, flies, rats and monkeys (Huberts et al., 2014). This evolutionary conserved effect of CR led to intense research of the underlying molecular mechanisms. CR can mediate cellular adaptation to changes in metabolism through the control of gene expression (up-regulation of certain genes and down-regulation of others) (Vaquero and Reinberg, 2009). In addition to CR, there are certain mutations that mimic low nutrient availability and extend lifespan. Such mutations include deletion of hexokinase 2 (*HXK2),* which catalyzes the entry of glucose into the glycolytic pathway (Lin et al., 2000) as well as deletion of nutrient-sensing kinases (*tor1Δ, tPK1/2/3Δ* and *Sch9Δ*) (Toda et al., 1988; Lin et al., 2000; Fabrizio et al., 2001; Kaebelein et al., 2005; Powers et al., 2006).

1.4.3.1 The Role of rDNA in Calorie Restriction-Induced Replicative Lifespan

In replicative lifespan, the most characterized type of damage that emerges and results in nucleolar fragments in old yeast cells (Sinclair and Guarente, 1997) is the accumulation of self-replicating extra-chromosomal ribosomal DNA circles (ERCs). As mentioned earlier (1.4.1.3) the yeast rDNA consists of 100 to 150 copies containing information to code for rRNA. Due to the highly repetitive nature, rDNA array is unstable and fragile, thus an easy target for homologous recombination (Ha and Huh, 2011). A primary cause of ageing in yeast is homologous recombination between rDNA repeats, which leads to the formation of ERCs that accumulate in toxic levels in mother yeast cells and can be quantified in a sorted population of ageing cells (Sinclair and Guarente, 1997).

Under normal conditions, rDNA repeats remain stable as rDNA recombination is negatively regulated through rDNA silencing (Ha and Huh, 2011). An important player in this process is silent information regulator 2 (Sir2), whose role is to repress E-pro in order to obtain a wild-type rDNA copy number; and forestall the appearance of the first rDNA circle that accumulates in mother cells by creating a silenced chromatin (Kobayashi and Gangley, 2005). Deletion of *SIR2* increases rDNA recombination and ERC formation (Kaeberlein et al., 1999) and shortens lifespan by approximately 50% (Kennedy et al., 1995). In addition, artificial introduction of ERCs into young cells decreases replicative lifespan while reducing their generation leads to an extension in lifespan (Sinclair & Guarente, 1997; Defossez et al., 1999; Lin et al., 2000; Lin et al., 2002)

Furthermore, the idea that an extension in RLS is a result of a reduction in ERC formation is also supported by a recent study that suggests that under nitrogen starvation and rapamycin treatment, inhibition of a nutrient-responsive phosphatidylinositol kinase (Tor1) occurs and this stabilizes rDNA locus by increasing association of Sir2 with the rDNA repeats. This leads to increased transcriptional silencing at the rDNA locus, which represses ERC formation by inhibiting rDNA recombination and leads to RLS extension (Ha and Huh, 2010). These studies support that CR may promote longevity, through Sir2-dependent silencing at the rDNA locus.

The idea, however, that Sir2 solely modulates RLS in yeast by repressing ERC formation is not well supported as evidenced by the incomplete suppression of lifespan in *sir2Δ* when the rDNA replication fork barrier protein Fob1 is also deleted (*sir2Δ fob1Δ*) (Defossez et al. 1999). Moreover, the model proposed above has been questioned by others, who showed that CR and Sir2 act in different genetic pathways to promote

longevity (Kaeberlein et al., 2004). In addition, combining CR and *SIR2* overexpression results in an additive lifespan extension, implying their action in parallel pathways. Furthermore, the ability of CR to extend longevity in a *sir2Δ* strain demonstrates the existence of a Sir2-independent ageing pathway in response to CR (Kaeberlein et al., 2004). In addition, an increase in lifespan was observed in *fob1Δ* under CR conditions (Kaeberlein et al., 2005). These results suggest that CR may function through a pathway parallel to Sir2 and Fob1 to regulate longevity.

1.4.3.2 The Role of TOR in Calorie Restriction- Induced Replicative Lifespan

The target of rapamycin (TOR) is a nutrient-responsive phosphatidylinositol kinase that is conserved in eukaryotes (Ha and Huh, 2011). In budding yeast, TOR kinases are encoded by *TOR1* and *TOR2* and exist in two complexes, TORC1 and TORC2. Both kinases control cell growth by regulating transcription, ribosome biogenesis, nutrient transport and autophagy (Martin and Hall, 2005). In yeast inhibition of TOR signalling by the drug rapamycin leads to a change in the activity of hexose transporters, which lead to a conversion from fermentation to respiration (Hardwick et al., 1999). Although the mechanisms by which TOR is activated are different from one species to another, what is common is that in all species TOR responds to nutrient levels (McCormick et al., 2011). Studies in *S. cerevisiae, Caenorhabditis elegans and Drosophila melanogaster* have shown that inhibition of TOR signalling leads to an extension in lifespan (Vellai et al., 2003; Kaeberlein et al., 2005; Kapahi et al., 2004) similar to an extension induced by CR (Wei et al., 2008).

A remaining question is how inhibition of TORC1 signalling extends lifespan. The mechanism involved is still poorly understood but it has been proposed by several studies using different models that it may involve changes in ribosome assembly, translation and response to stress (Kaeberlein et al., 2005; Syntichaki et al., 2006; Medredik et al., 2007; Dang et al., 2014). A random screen of 565 yeast strains, each lacking a single non-essential gene, identified TOR as a regulator of lifespan (Kaeberlein et al., 2005). Yeast strains with deleted genes involved in the TOR signalling pathway, such as deletions of *TOR1* and *SCH9,* were identified to be long-lived as well as strains with ribosomal protein (RP) deletions *RPL31A* and *RPL6B* (Kaeberlein et al., 2005). This observation suggested that CR might slow RLS by a decrease in RP production through downregulation of TOR and Sch9 activity. In *C.elegans*, knockdown of a number of 40S and 60S subunit RP genes

have also been reported to extend lifespan (Chen et al., 2007; Curran and Ruvkun, 2007; Hansen et al., 2007). Moreover, epistasis experiments in yeast showed that a decrease of 60S ribosomal subunits leads to enhanced Gcn4 translation, proposing that an extension of lifespan is a result of a decrease in ribosome biogenesis (Steffen et al., 2008; Dang et al., 2014). Moreover, rapamycin specifically inhibits TORC1 and leads to a rapid decrease in the expression of rRNAs, including 35S rRNA, ribosomal proteins and 5S rRNA (Zaragoza et al., 1998; Powers and Walter, 1999).

A study has shown that deletion of TOR1 extends lifespan but it has no effect on Sir2 activity (Kaeberlein et al., 2005). On the contrary, other studies proposed that TORC1 inhibition by rapamycin increases the Sir2 activity and stabilizes the rDNA locus (Medvedik et al., 2007; Ha and Huh, 2011). Medvedik *et al* have shown that TOR inhibition by rapamycin extends lifespan by the same mechanism as CR, by promoting Sir2 activity and stabilizing the rDNA. In addition the same group observed a relocalisation of transcription factors Msn2 and Msn4 from the cytoplasm to the nucleus, where they trigger expression of the longevity gene pyrazinamidase / nicotinamidase 1 *PNC1,* which stimulates Sir2 (Medvedik et al., 2007; Anderson et al., 2003). Furthermore, another study proposed that TORC1 signalling inhibition supports transcriptional silencing at the rDNA and reduces homologous recombination between rDNA repeats (Ha and Huh, 2011). In addition, TORC1 inhibition stimulates deacetylation of histones at rDNA, and Pnc1 and Net1 are required for enhancement of association of Sir2 with rDNA. Thus, the above results propose a model in which TORC1 inhibition stabilizes the rDNA locus by enhancing Sir2 binding to rDNA and thus extends lifespan in yeast (Ha and Huh, 2011).

1.4.3.3 Collective model of Calorie Restriction-Induced Replicative Lifespan

Studies mentioned above led to a collective model, which links different pathways that extend RLS in CR conditions. One pathway is the Sir2-mediated longevity pathway, which under conditions of nutrient deficiency, Sir2 is activated to silence rDNA associated chromatin in order to prevent recombination events and the generation of ERCs (Kennedy et al., 1995; Kaeberlein et al., 1999; Kaeberlein et al., 2004). The nutrient responsive pathway mediated by kinases Tor1, Sch9 and PKA is inhibited under nutrient deprivation conditions or under the presence of the drug rapamycin. Tor signalling is known to promote a stress response as well as the synthesis of ribosomal proteins. Thus, when it is inhibited, ribosome biogenesis is downregulated, inducing Gcn4 activity and leading to an

extension in lifespan (Steffen et al., 2008; Dang et al., 2014). In addition, in the absence of stress, Msn2/4 exist in the cytoplasm and are inactivated by protein kinase A (PKA) (Beck and Hall, 1999). However, following yeast exposure to CR, these proteins translocate to the nucleus where they promote the transcription of stress induced genes such as the induction of *PNC1* nicotinamidase, enhancing the activity of Sir2 to inhibit formation of ERCs and thus extend lifespan (Medvedik et al., 2007).

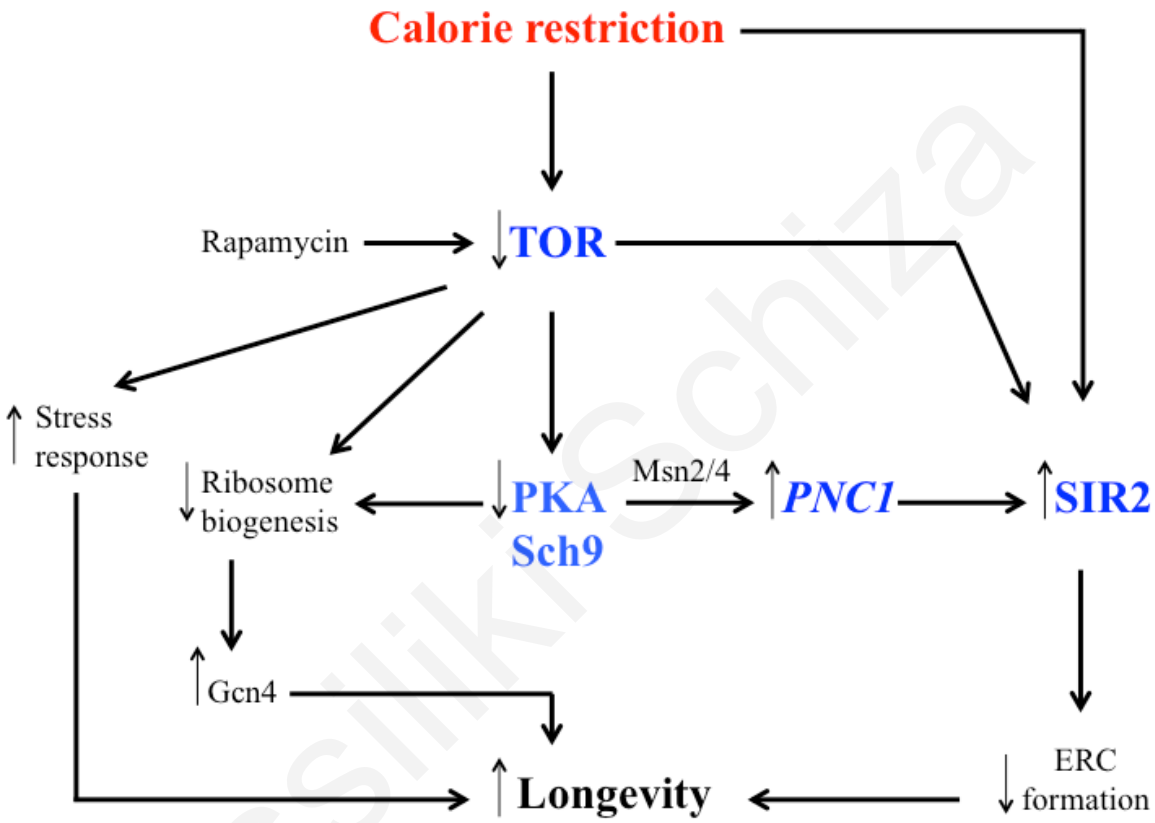

Figure 1.11. Yeast replicative lifespan regulation by CR. CR inhibits the TOR signaling pathway, which can also be inhibited by the drug rapamycin. When TOR is inhibited, a stess response is induced and this leads to an extension in longevity. In addition, ribosomal proteins are formed, blocking ribosome biogenesis, increasing Gcn4 activity and leading to an increase in longevity. CR and TOR signaling regulate the nuclear localization of transcription factors Msn2/Msn4 and promote the transcription of the nicotinamidase *PNC1*. *PNC1* increases the activity of Sir2 and prevents accumulation of ERCs, increasing longevity. CR has also been proposed to extend longevity independently of the TOR pathway, by activating the Sir2-mediated pathway through rDNA stability and preventing the formation of ERCs.

1.5 Scientific Hypothesis and Aims

For the purpose of this project, we hypothesized that the N^{α}-terminal acetyltransferase Nat4 and its associated histone modification would have a regulatory role within the cell and specifically be involved in the control of gene expression. This hypothesis is supported by the following facts:

a) Nat4 acetylates specifically histones H2A and H4, and histone modifications in general are involved in gene regulation.

b) A Global Proteomic Screen analysis (GPS) showed that Nat4 is a regulator of H4R3me2a, which is a modification implicated in gene repression.

c) Nat4 deletion shows sensitivity to 3-AT, which is an inhibitor of transcription.

d) Transcriptomic analysis shows deregulation of several metabolic and stress-induced genes in the absence of Nat4.

To examine the above hypothesis, we investigated the following two specific aims.

Specific aim 1: Investigate the role of Nat4 in H4R3me2a regulation and heterochromatin silencing

H4R3me2a was previously shown to be involved in the formation of silent chromatin at yeast heterochromatin-like loci (rDNA, *HML, HMR* and telomeres*)* (Yu et al., 2006). Hmt1 catalyzes H4R3me2a *in vitro* and relates to transcriptional repression (Lacoste et al., 2002). During a global proteomic screen we identified Nat4 as a regulator of H4R3me2a and hence we hypothesize that histone N-alpha-terminal acetylation by Nat4 would be involved in a mechanism with H4R3me2a to regulate silencing at these genomic loci.

Specific aim 2: Investigate the role of Nat4 in regulating the expression of euchromatic genes

Preliminary results from a transcriptome analysis using RNA-sequencing showed that deletion of Nat4 significantly deregulates the expression of several euchromatic genes. We hypothesize that Nat4 and histone N-terminal acetylation would regulate the expression of these genes to control specific cellular processes.

CHAPTER 2
METHODOLOGY

Chapter 2.Methodology

2. 1 Growth of yeast strains

Glycerol stocks of *Saccharomyces cerevisiae* strains (Table 2) were taken from -80°C and with a loop, cells were streaked on solid media (plates) and were left for 2-3 days in 30°C incubators. Yeast can be grown either in a liquid medium or on the surface of a solid agar plate. For their growth, either rich or minimal media is used. Yeast cells grow normally in rich medium of yeast extract, peptone and dextrose (YPD). YPD is a liquid medium and with the addition of agar, a solid medium (plates) is made (YPAD). It provides an excess of amino acids, vitamins and metabolites needed for optimal cell growth and within these conditions, yeast cells divide approximately every 90 minutes (Sherman, 2002).

Minimal media, known as synthetic defined (SD) or synthetic complete (SC) allows growing of yeast on synthetic defined medium containing the minimal amount of nutritional supplements necessary for yeast division. It consists of a mixture of salts, vitamins and yeast nitrogen base and dextrose. SD/SC medium supports the growth of *S.cerevisiae* strains with a doubling time of approximately 140 minutes. Minimal media is mostly used to select for plasmids carrying TRP or URA auxotrophic markers (SC-TRP, SC-URA), by not adding these amino acids to the media used for the selection. In addition, minimal media is used when yeast is grown under specific nutritional conditions such as calorie restriction (SD). Notably, depending on the composition of the strain, the amino acids that the strain lacks must be added in the medium in order for yeast to grow. For sterilization of yeast media, autoclaving is necessary. Temperature sensitive compounds such as 5-FOA and antibiotics are added to the autoclaved medium after it has cooled to ~50 ^{o}C from a sterile, filtered stock solution. All the media used for this project are shown in table 2.

Table 2. Composition of Media

Liquid Media	
Media	**Materials**
YPAD	10 g Yeast Extract20 g Peptone 0.1 g Adenine Hemisulphate ddH_20 up to final volume of 900ml Autoclave for 25 min 100 ml 20% Glucose (prior to use) Stored at RT
SD	1.7g Yeast Nitrogen base w/o a.a and ammonium sulfate 5g Ammonium sulfate 2ml 10mg/ml Histidine 6ml 10mg/ml Leucine 1ml 20mg/ml Methionine 20ml 0.2% Uracil Make up to 900ml with ddH_2O Autoclave for 25 min 100 ml 20% Glucose prior to use
SC	1.7g Yeast Nitrogen base w/o a.a and ammonium sulfate 5g Ammonium sulfate 0.6g Amino Acid mix 2ml 10mg/ml Histidine 6ml 10mg/ml Leucine 2ml 10mg/ml Tryptophan 2ml 10mg/ml Lysine 10ml 0.4% Adenine Sulfate 20ml 0.2% Uracil Make up to 900ml with ddH_2O Autoclave for 25 min 100 ml 20% Glucose prior to use
Solid Media (plates)	
YPAD	900 ml YPAD media 20 g agar 100 ml 20% Glucose Stored at 4 ^{0}C
YPAD+ G418	Same as YPAD 200mg/ml G418
SC	Same as liquid SC Add 20g Bacto Agar
SC-TRP	Same as SC No addition of TRP
SC -URA	Same as SC No addition of URA
SC+FOA	Same as SC 1g/L FOA

2.1.1 Measurement of cell density

From the streaked plates, a single colony was added into 5ml liquid media and the culture was placed in 30°C shakers at 200 rpm for overnight growth. The next day, the approximate number of cells in the culture was determined with a spectrophotometer (Nanodrop 2000, Thermo scientific) by measuring the optical density (OD) at 600 nm. Cultures were diluted such that the reading (OD_{600}) for the overnight culture was <0.1 ($3x10^7$ cells/ml). Early log phase of yeast growth is the period in which cell densities are < 10^7 cells/ml, mid-log phase involves densities between 1-$5x10^7$ cells/ml and late log phase occurs when cell densities are between $5x10^7$ and $2x10^8$ cells/ml (Sherman, 1991). For experiments performed within this project, overnight cultures were diluted to OD 0.1 and were left to grow to mid-logarithmic phase (OD 0.8). Cells were then centrifuged at 3000 rpm for 3 minutes, the pellet was collected and either processed immediately in downstream applications or stored at -20°C for future use.

2.2 Plasmid transformation and construction of yeast strains

Point mutations in H4 (pMR206) and H2A (pJD150) were generated in plasmids pMR206 (Kirmizis et al., 2007) and pJD150 (Harvey et al., 2005) respectively, by PCR mutagenesis using the QuickChange (Stratagene) site directed mutagenesis kit. The mutation was introduced in a single PCR with one pair of complementary 50mer primers containing the mutations of interest. For oligo design, http://bioinformatics.org/primerx was used and a T_m of at least 78 ^oC was chosen with the mutation centered in the middle. The mix included: 0.5 ul forward primer (2.5 pmoles/ul), 0.5 ul reverse primer (2.5 pmoles/ul), 0.25 ul 40 um dNTP mix (10 mM each), 1.25 ul 10x PfuUltra buffer (contains Mg^{++}), 1 ul template DNA (2 ng/ul), 0.25 ul PfuUltra Hotstart (Stratagene) and 8.75 ul sterile H20 (12.5 ul total). The PCR program included 5 minutes at 95 ^OC and then 18 cycles of: 50 seconds at 95 ^OC, 50 seconds at 60 ^OC and 1 min +1 min/1 kb template at 68 ^OC, followed by 7 minutes at 68 ^OC. 2.5 ul of the reaction was then loaded on an agarose gel and a band was observed corresponding to the amplification product. 0.25 ul DpnI (20 U/ul, New England BioLabs) was then added to the reaction to digest the product and then incubated at 37 ^OC for 1 hour. The final product was then transformed into competent bacteria (1 ul into 50 ul of XL-10 Gold). Finally, a colony was picked and miniprep was performed to isolate the corresponding plasmid. The plasmid was sent for sequencing to verify the mutation of interest and to ensure that no other PCR errors were introduced. H4 mutant strains were constructed as follows: the pMR206 (TRP1-HHT2-HHF2) plasmid bearing the appropriate point mutations on histone H4 (HHF2) was used to transform the

NAT4 and *nat4*Δ JHY6 strains. Initial selection was performed on SC-Trp plates, so that the transformed cells can keep the pMS333 (URA3-HHT2-HHF2) plasmid encoding wild-type H4 in order to minimize the appearance of suppressing mutations. Then, the pMS333 plasmid was shuffled out by counterselection on SC-Trp plates containing 5-fluoroorotic acid. The counterselection step was repeated twice and the final strains were tested on YPAD, SC-Ura, SC-Trp and SC+FOA. Using a similar methodology, we constructed the strains AK224 and AK226 from the parental strain UCC1188. *NAT4* catalytic mutants were generated as follows: the entire *NAT4* ORF and the first 200bp of its 3'-UTR were cloned into pCR2.1 TOPO plasmid (Invitrogen), and a C-terminal HA-tag was introduced by PCR on this template. HA-tagged *NAT4* was then used as template to introduce point mutations by PCR in motif A (*nat4cmA-HA*), motif B (*nat4cmB-HA*), both (*nat4cmAB-HA*) or nat4E186A. To integrate the *NAT4-HA* wild-type or point-mutant versions to the genome, a PCR fragment containing 40bp of the *NAT4* 5'-UTR, *NAT4-HA* ORF, 200 bp of the *NAT4* 3'-UTR and the first 40 nucleotides of the KanMX cassette, was transformed in the wild-type JHY6 yeast strain together with another PCR fragment containing the full KanMX4 cassette and 40 bp of the *NAT4* 3'-UTR. The mutants were selected on YPAD+G418 plates and confirmed by sequencing. The following mutations were generated as needed: arginine 194 to histidine, glycine 199 to valine, asparagine 233 to serine, tyrosine 240 to tryptophan and glutamic acid 186 to alanine. The Y7092 yeast strain was transformed with the MORF-HMT1 plasmid (Gelperin et al., 2005) to obtain the strain AK267 that was used for overexpression of the Hmt1-6His-Ha-ZZ protein. All strains used in this study are listed in Table 3.

Table 3. List of yeast strains

Name	Genotype	Reference
BY4741	*MAT**a**, ura3Δ0, leu2Δ0, his3Δ1, met15Δ0*	Euroscarf
AK312	Same as BY4741, with *set5::KanMX4, nat4::NatMX4*	This work
JHY6	*MAT**a***, *ura3-52*, *lys2-801*, *ade2-101*, *trp*1-289, *his3*Δ*1*, *leu2-*3,112, *Δhhf2-hht2*, Δ*hhf1-hht1*, pMS333*[URA3-HHT2-HHF2]*	Kirmizis *et al*. (2007) Nature 449:928-932
AK236	Same as JHY6, except *nat4::KanMX4*	This work
AK244	Same as JHY6, except *nat4::NAT4-HA-KanMX4*	This work
AK245	Same as JHY6, except *nat4::nat4cmA-HA-KanMX4*	This work
AK246	Same as JHY6, except *nat4::nat4cmB-HA-KanMX4*	This work
AK247	Same as JHY6, except *nat4::nat4cmAB-HA-KanMX4*	This work
AK237	*MAT**a**, ura3-52, lys2-801, ade2-101, trp1-289, his3Δ1, leu2-3,112, Δhhf2-hht2, Δhhf1-hht1*, pMR206[*TRP1-HHT2-HHF2*]	Kirmizis *et al*. (2007) Nature 449:928-932
AK222	Same as AK237, except pAK25[pMR206 *HHF2 S1A*]	This work
AK238	Same as AK237, except *nat4::KanMX4*	This work
AK239	Same as AK237, except pAK110[pMR206 *HHF2 K5,8,12R*]	This work
AK240	Same as AK237, except pAK110[pMR206 *HHF2 K5,8,12R*], *nat4::KanMX4*	This work
AK326	Same as AK237, except pAK127[pMR206 *HHF2 R3K, K5,8,12R*], *nat4::KanMX4*	This work
AK327	Same as AK237, except pAK128[pMR206 *HHF2 S1A, K5,8,12R*]	This work
FY406	*MAT**a**, (hta1-htb1)Δ::LEU2, (hta2-htb2)Δ::TRP1, ura3-52,1, leu2Δ1, lys2Δ1, lys2-128Δ, his3Δ200, trp1Δ63*, pAB6[*HTA1-HTB1, URA3*]	Harvey *et al*. (2005) Genetics 170:543-553
FHY2	Same as FY406, except pJD150[*HTA1-HTB1, HIS3*]	Harvey *et al*. (2005) Genetics 170:543-553
AK234	Same as FHY2, except pAK27[pJD150 *HTA1 S1A*]	This work
YSC5106 WT	*MAT**a**, his3Δ200, leu2Δ0, lys2Δ0, trp1Δ63, ura3Δ0, met15Δ0, can1::MFA1pr-HIS3, hht1-hhf1::NatMX4, hht2-hhf2::*[*HHTS-HHFS*]*-*URA3*	Open biosystems
AK315	Same as YSC5106, except *nat4::KanMX4*	This work
YSC5106 H4R3K	Same as YSC5106, except *hht2-hhf2::*[*HHTS-HHFS R3K*]*-*URA3*	Open biosystems
AK318	Same as H4R3K, except *nat4:NatMX4*	This work
AK566	*Same as YSC5106, except hht2-hhf2::[HHTS-HHFS S1D*]*-URA3*	Open biosystems
Y10000 pBEVY-U	*MAT**α**, his3Δ1; leu2Δ0; lys2Δ0; ura3Δ0* pBEVY-U	Hole *et al*. (2011) PLoS One 6:e24713
Y16202 pBEVY-U	Same as Y10000 pBEVY-U, except *nat4::kanMX4*	Hole *et al*. (2011) PLoS One 6:e24713
Y16202 pBEVY-U-h*NAA40*	Same as Y16202 pBEVY-U, except pBEVY-U-h*NAA40*	Hole *et al*. (2011) PLoS One 6:e24713
UCC1188	*MAT**α**, leu2Δ1, lys2-801, trp1, ura3, hhf1-hht1::LEU2 hhf2-hht2::HIS3 RDN1::URA3,* pMP9[*LYS2 CEN ARS*]*-HHF2-HHT2*	Van Leeuwen *et al*. (2002)

		Cell 109:745-756
AK208	Same as UCC1188, except *nat4::NatMX4*	This work
AK224	Same as UCC1188, except pMR206[*TRP1-HHT2-HHF2*]	This work
AK226	Same as UCC1188, except pAK25[pMR206 *HHF2 S1A*]	This work
UCC1369	*MAT**a**, ade2Δ::hisG, his3Δ200, leu2Δ0, lys2Δ0, met15Δ0, trp1Δ63, ura3Δ0, adh4::URA3-TEL(VII-L), ADE2-TEL(V-R), Δhhf2-hht2::MET15, Δhhf1-hht1::LEU2,* pMP9[*LYS2 CEN ARS*]-*HHF2-HHT2*	Van Leeuwen *et al*. (2002) Cell 109:745-756
AK210	Same as UCC1369, except *nat4::NatMX4*	This work
UCC7262	*MAT**a**, ade2 his3 leu2 lys2 ura3 ADE2-TEL(V-R) hmra::URA3, hhf2-hht2::MET15, hhf1-hht1::LEU2,* pMP9[*LYS2 CEN ARS*]-*HHF2-HHT2*	Van Leeuwen *et al*. (2002) Cell 109:745-756
AK207	Same as UCC7262, except *nat4::NatMX4*	This work
UCC7266	*MAT**a**, ade2 his3 leu2 lys2 ura3 ADE2-TEL(V-R) hmlα::URA3, hhf2-hht2::MET15, hhf1-hht1::LEU2,* pMP9[*LYS2 CEN ARS*]-*HHF2-HHT2*	Van Leeuwen *et al*. (2002) Cell 109:745-756
AK209	Same as UCC7266, except *nat4::NatMX4*	This work
AK410	Same as AK237, except pAK130[pMR206 *HHF2 S1P*]	This work
AK267	*MAT**α**, can1Δ::STE2pr-Sp-his5, lyp1Δ, his3Δ1, leu2Δ0, ura3Δ0, met15Δ0,* pMORF[*HMT1-6xHis-HA-ZZ*]	This work
AK490	Same as BY4741 *nat4::NatMX/pnc1::KanMX4*	This work
BY4742	*MATα his3Δ1 leu2Δ lys2Δ ura3Δ*	Thermo Fisher
AK447	Same as BY4742, *nat4::NatmX4*	This work
DH461	Same as BY4742, *tor1Δ::URA3*	(Steffen et al., 2008)
AK478	Same as BY4742, *nat4::NatMX/tor1::KanMX4*	This work
AK500	Same as BY4741, *fob1::KanMX*	This work
AK562	Same as BY4741, except *nat4::NAT4-HA-KanMX4*	This work
AK563	Same as BY4741, except *nat4::nat4E186A-HA-KanMX4*	This work

2.3 RNA preparation

2.3.1 Isolation of total RNA

Total RNA from yeast cells was extracted using the hot phenol method (Schmidtt et al., 1990). Cell pellets were thawed and resuspended in 600 ul hot acidic phenol (Sigma Aldrich #P4682) (previously heated to 70 °C) and transferred to a tube that contained 400 ul RNA extraction buffer (50 Mm NaOAc, 10 mM EDTA) and 50 ul 10% SDS. Samples were placed on a preheated thermomixer at 65 °C for 5 minutes and then immediately mixed vigorously using Vortex genie (Scientific industries) for 2 minutes, placed on ice for 2 minutes, vortex again for 2 minutes and left on ice for 5 minutes. The samples were then centrifuged at maximum speed for 15 min at RT to separate the aqueous and inorganic

phases. The upper aqueous layer was taken out carefully and was transferred to a tube that contained 600 ul of hot phenol. The phenol extraction and centrifugation was repeated. The upper aqueous layer was transferred to a tube that contained 600 ul chloroform/isoamyl alcohol 24:1 (Sigma Aldrich #C0549) and was mixed and centrifuged as above. The upper aqueous layer was collected and transferred to a new tube. RNA was precipitated by addition of 1 volume of isopropanol and let stand overnight at -20 °C. The precipitate was centrifuged at RT at 14000 rpm for 15 minutes. The supernatant was discarded and the pellet was washed with 75% EtOH (prepared with RNAse-free water) followed by a centrifugation at RT at 10000rpm for 5 min. The resulting pellet was air-dried and dissolved in 20 µl DNase RNAse free water (Invitrogen #10977). Total RNA was stored at -80°C. The integrity of total RNA was examined by SDS-electrophoresis on 1.5 % agarose gel. RNA concentration was determined using the nanodrop 2000 (Thermo scientific) by measuring the absorbance at 260 nm (A260).

2.3.2 Measurement of quantity and quality of total RNA

RNA concentration was determined using the nanodrop 2000 (Thermo scientific) by measuring absorbance at 260 nm (A260) and 280 nm (A280). The ratio of absorbance values at 260 nm and 280 nm (A260/A280) gives an indication of the RNA purity. RNA samples with an A260/A280 ratio ~2 were considered to be sufficiently pure for further experiments. As a secondary measure of RNA purity, the 260/230 ratio was also observed, with a ratio expected to be in the range of 2.0-2.2. If the ratio was lower than expected, the presence of contaminants, which absorb at 230 nm was indicated. The 260/230 value for "pure" RNA were higher than the corresponding 260/280 value. The integrity of total RNA was examined by agarose electrophoresis on a 1.5 % agarose gel (section 2.14)

2.3.3 DNAse treatment of total RNA

Contaminating genomic DNA was removed from the RNA samples using the TURBO DNA-free kit according to the manufacturer's directions (Ambion #AM1907) for rigorous DNase treatment. To 10 ug of total RNA, 5 ul of 10X TURBO DNAse buffer was added, 2 ul of TURBO DNase(2U/µl) and nuclease-free water to a final volume of 50 ul. The mixture was incubated at 37°C for 1 hour followed by addition of 5 ul of DNase inactivation reagent and mixing well. Mixture was incubated for 2 minutes at RT and then

was centrifuged at 14000 rpm for 1.5 minutes. The supernatant, which contained the RNA was transferred into a fresh tube. RNA quantity and quality were measured.

2.4 Gene expression analysis

For reverse transcription, the PrimeScript RT reagent kit (TAKARA, # RR820A) was used. Isolated RNA (0.5 μg) of each sample was mixed with 2 ul 5x PrimeScript Buffer, that contained dNTP mixture and Mg^{2+}, 0.5 ul of oligo dT primer (50 μM), 0.5 ul random hexamers (100 μM) and 0.5 ul of PrimeScript RT Enzyme Mix I. The mixture was incubated for 15 min at 37 °C, for 5 sec at 85°C and then at 4 °C. A negative control reaction was carried out without the RT enzyme. 70 ul of DNase RNAse-free water was added to the final cDNA and was stored at -20°C. The cDNA synthesis was verified by real time PCR with primers shown in table 4.

2.5 Quantitative Real-Time PCR

SYBR Green (KAPA SYBR Fast qPCR KitMaster Mix # KK4602) was used to quantify the level of expression of each sample. Relative quantification was measured using the housekeeping genes *RPP0* and *TAF10* for normalization. Real-time PCR 10 ul reactions included 1 ul of DNA, 0.2 ul of forward primer (50 μM), 0.2 ul of reverse primer (50 μM), 5 ul of SYBR Green and 3.6 ul DNase RNase free water (Invitrogen #10977). Reactions were incubated in a Biorad CFX96 Real-Time PCR system in non-skirted 96-well plates (4titude, # 4ti-0750), sealed by adhesive seal sheets (4titude, #0565) using specific primers (Table 4). A standard curve was prepared and was added for each primer set to assess the reaction efficiency. The qPCR reaction was run under the following thermal cycling parameters: enzyme activation at 95°C for 2 min, followed by denaturation and annealing in 40 cycles of 95°C for 2 sec; 60°C for 20 sec and 72 °C for 5 sec, with fluorescence read at the end of each cycle. All standards and unknown samples were run in duplicates.

2.6 Primer Design for RT-PCR

Gene sequences were found from the UCSC Genome Browser (https://genome.ucsc.edu/). The sequence was copied into an online tool for design of primers "Primer3" software (http://bioinfo.ut.ee/primer3-0.4.0/). Primers parameters included a primer length of 18-22 base pairs, primer melting temperatures (T_m) in the range 59-61 °C and a product size of 50-100 bp. Primer sequences were provided by Integrated DNA Technologies (IDT).

Table 4. List of primers

Primers	Forward (5'- 3')	Reverse (5'- 3')
A	GCACCTGTCACTTTGGAAAAA	TCGCCGAGAAAAACTTCAAT
B	CCGTTATTGGTAGGAGTGTGG	TAACATCCCAATGCGGACTA
C (RDN5)	TGGTAAGAGCCTGACCGAGT	GATTGCAGCACCTGAGTTTC
D	TACACCCTCGTTTAGTTGCTTCT	CGGTATGCGGAGTTGTAAGA
E	AGAACGCGGTGATTTCTTTG	GGACGCCTTATTCGTATCCA
F	GGTGATTTCTTTGCTCCACA	TGCTAGCCTGCTATGGTTCA
G	GACCCGAAAGATGGTGAACT	CCAGAGTTTCCTCTGGCTTC
H	TGCGAGTGTTTGGGTGTAAA	ATCCGAAGACATCAGGATCG
I (RDN25)	TTGACTTACGTCGCAGTCCTCAGT	AGGACGTCATAGAGGGTGAGAATC
J (RDN58)	AACGGATCTCTTGGTTCTCG	TGTGCGTTCAAAGATTCGAT
K	CTGGGCAAGAAGACAAGAGA	CACCGTTTGGAATAGCAAGA
L (RDN18)	TCAGAGCGGAGAATTTGGAC	GGTTCACCTACGGAAACCTT
M	CTGGTTGATCCTGCCAGTAG	TAATGAGCCATTCGCAGTTT
N (RDN37)	CAAGAGGGAATAGGTGGGAAAA	GACAAGCATATGACTACTGGCA
RPP0	AACGGTCAAGTGTTCCCATC	AGCGGAAACGAAGTGAGAAA
TAF10	CCTATCATTCCCGATGCAGT	CCTTGCAATAGCTGCCTAGC
ACT1	AGATTCAGAGCCCCAGAAGC	TACCGGCAGATTCCAAACCC
TIR1	TTAGCAGCACCGTTTTCAGTT	AATCCAAGCTACCAAGGCTGT
YGR079W	TGTGCTGTTGGTGAAGGAAG	TCGAAAGTACGCTCGGCTAT
GPH1	TACCACGGCGATTATTACCTG	TTGATTGTGGAACTCCTGGTC
GLC3	TGCTTCTAAAAACGTCGAGGA	CACCCCTACCGGAGCTTATAG
HXK1	GCCGACTCTTTGAAGGACTTT	GGTGTCCTTGGTGTTTAGCA
TPS2	ATCCTGTCACTGTGGGATCTG	TTGCTGAGGATCGGTTAAATG
GSY1	AACAAACGTTTCTGGGTTCG	TGCTCGACAGATTCATCAGG
PNC1	GACCACTGTCCTGCTGGATT	TTGTGGGCCTTCAACTCTTC
NTH1	GAGTCGGGGTTTTTCTTTGAC	CGGATTCGTATGACGTTCTGT
NAT4	TATATGAGGCGCTTGGGTTC	GTGACGAATTGTGGGTGATG

2.7 Ribosomal DNA copy Number

DNA was extracted by standard methods and diluted 10-fold before real time PCR. Relative ribosomal copy number was estimated by normalizing to an intergenic region in chromosome V as discussed in Dang *et al*., 2014.

2.8 RNA sequencing

Total RNA was extracted from mid-logarithmic grown cells grown under different conditions as in 2.3.1 and was treated as in 2.3.3. Each extraction experiment was performed in independent triplicates. For the purpose of this research there were two service providers for strand-specific RNA sequencing, BGI and EMBL.

BGI: Paired-end cDNA libraries were prepared from 10 μg of total RNA using the Illumina mRNA-Seq-Sample Prep Kit according to manufacturer's instructions. cDNA fragments of ~400 bp were purified from each library and confirmed for quality by Agilent

2100 Bioanalyzer. High-throughput sequencing was done on an Illumina HiSeq2000 plaform, according to the manufacturer's instructions (Illumina). RNA-sequencing data was analyzed by assembling the genes against the *Saccharomyces cerevisiae* genome. Assembled transcripts were annotated to the most recent Ensembl transcript annotation (Ensembl37.60) and estimated RPKM (Reads Per Kilobase of transcript per Million mapped reads. Library construction, sequencing and data analysis was performed by BGI.

EMBL: Quality of the sequence data was checked by FastQC *0.11.1* (http://www.bioinformatics.bbsrc.ac.uk/projects/fastqc/). The sequence reads were mapped to the reference yeast genome sequence (UCSC Apr2011 [sacCer3] assembly (http://hgdownload-test.cse., http://genome.ucsc.edu/cite), using GSNAP *2014-09-30* (Wu and Nacu, 2010). (Settings used: *gsnap -N 1 -n 1 -O -A sam --merge-distant-samechr -s splicesites_sacCer3_)*. Only uniquely mapped reads were considered for further analysis. which were post-processed using SAMtools *0.1.16 (http://www.ncbi.nlm.nih.gov/).* Gene abundance was quantified using HTSeq-count *0.6.1* (http://www-huber.embl.de/HTSeq) (Settings used: *htseq-count -f bam -r pos -s reverse -m union -a 10 -t exon -i gene_id*) with the Ensemble gene annotation (release 78 http://www.ensembl.org/, ftp://ftp.ensembl.org/pub/, and http://www.ensembl.org/info/). Gene annotation was used to evaluate gene expression and to guide the mapping software, taking into account the strand-specific sequencing protocol. Gene expression analysis was performed using edgeR R/Bioconductor package *3.8.2* (http://www.ncbi.nlm.nih.gov/, https://stat.ethz.ch/, https://www.r-project.org/). Differential gene expression was calculated using information from two biological replicates for each condition using generalized linear model (McCarthy et al., 2012) with tagwise dispersion and FDR correction according to the edgeR vignette. Expression levels were normalized using TMM (Robinson and Oschlack, 2010). Genes were considered as differentially expressed if abs(logFC) >= 1 and FDR <= 0,0001.

2.9 Gene Ontology

Gene ontology was calculated using the Database for Annotation Visualization and Integrated Discovery (DAVID 6.7 (https://david.ncifcrf.gov/). This tool allowed the condensation of a list of genes shown to be upregulated or downregulatd by RNA-seq into organized classes of related genes. This organization was accomplished by grouping genes based on the biological process they are implicated in, their molecular function and cellular

component. This resulted into a number of clusters for efficient interpretation of gene lists. For evaluation of the GO clusters, the EASE score was used (http://david.abcc.ncifcrf.gov/helps/functional_annotation.html#fisher) with an enrichment score for each cluster given as a mean of $-\log_{10}p$ of member GO categories with $p<0.05$.

2.10 Venn diagrams

Venn diagrams were generated using online tool Venny 2.0 (www.cmbi.ru.nl/cdd/biovenn/index.php) to help with the analysis and visualization of differential gene expression data from RNA-seq experiments. The signifance of overlap was evaluated by gmp R package 0.5-12 (http://CRAN.R-project.org/) using hypergeometric p-value (http://stackoverflow.com/).

2.11 Chromatin Immunopreciptation.

The method used is described in Meluh and Broach (1999). Translation of that protocol with some extra detail is shown below. For culture preparation, yeast cells were grown to mid-logarithmic phase in 150 ml conical flasks with 200 rpm shaking at 30˚C. Crosslinking: For cell fixation, formaldehyde 37% (Sigma Aldrich catalogue # 252549) was added to a final concentration of 1% in mid-logarithmic cells with gentle shaking at room temperature for 2 hours. 30 ml from the culture was poured into four 50 ml conical polypropylene Falcon (BD # 352070) and was centrifuged at 3000xg for 3 minutes. 15 ml of cold 1X PBS buffer (10x Phosphate Buffered Saline pH 7.2 (Invitrogen # 70013), was added in each falcon tube to allow washing and was followed by 3 min of centrifugation at 3000xg (twice). The crosslinked yeast pellet was added in a 2 ml Eppendorf tube.Cell lysis: Crosslinked cells were resuspended in 250 ul of SDS lysis buffer (1% SDS, 10mM EDTA, 50mM TrisHCl (pH 8.0), adjusted to a final volume of 500 ul dH_2O) twice, supplemented with complete protease inhibitor cocktail tablet (Roche # 11697498001). Cell disruption occured by adding 0.5 mm glass beads (Thistle Scientific catalogue # 11079105), vortex for 1 min and rest for 1 min (twice). A hot 25G x 5/8 needle (Terumo Neolus # NN-2516R) was used and the eppie was nested in a 15 ml polystyrene conical Falcon (BD # 352099) and centrifuged at 500 rpm for 2 min. Sonication: The sonicator (Diagenode, Bioruptor USD-200) was set at high power for 17.5 min (three times), keeping water cool in the water bath by adding ice (50% ice, 50% cool water). Each

sonicated tube was transferred to 1 eppendorf tube and centrifuged at full speed at 4 ^{0}C for 10 minutes. The supernatant was removed and transferred to a 15 ml falcon tube.

Chromatin pre-clearing: 10 ml of cold IP buffer (0.1% SDS, 1.1% Trition X-100, 1.2 mM EDTA, 16.7 mM TrisHCl (pH 8.0), 167 mM NaCl, adjusted to a final volume of 500 ul dH_2O) was mixed with a complete protease inhibitor cocktail tablet and was added to the supernatant. Protein A sepharose 4 fast flow beads (GE # 17-5280-01) were prepared as a 50% slurry in IP buffer and were blocked by salmon sperm DNA (SSD) (1 ug/ul) and bovine serum albumin (BSA) (10 mg/ml) to prevent non-specific binding to protein or DNA. For the pre-clearing of chromatin, 200 ul of the slurry was added to the 10 ml chromatin tube and was left to mix on the rotator for 1 hour at 4˚C.

Immunoprecipitation: 1ml of chromatin was aliquoted in microfuge tubes and 1 ug of antibody (see list of antibodies, section 2.12) was added to each reaction and incubated on a rotator for 1 hour at 4 ˚C. 40 ul of blocked protein A sepharose beads were then added to each reaction and were left overnight at 4 ˚C to mix. 200 ul of chromatin was added in a tube (Input) and was processed as a control (no antibody and no beads) left overnight at 4˚C to mix.

Washing/Elution: Overnight tubes were centrifuged and supernatant was discarded. Beads were washed sequentially with 950 ul of the following buffers: TSE-150 (1% Triton X-100, 0.1% SDS, 2mM EDTA, 20 mM TrisHCl (pH 8.0), 150 mM NaCl, adjusted to a final volume of 500 ul dH_2O), TSE-500 (1% Triton X-100, 0.1% SDS, 2mM EDTA, 20 mM TrisHCl (pH 8.0), 5000 mM NaCl, adjusted to a final volume of 500 ul dH_2O), Li/DOC (250 mM LiCl, 1% NP-40, 1% Deoxycholate, 1mM EDTA, 10 Mm TrisHCl (pH8.0), adjusted to a final volume of 500 ul dH_2O) and TE (1 mM TrisHCl (pH8.0), 1 mM EDTA), incubating for 3 minutes with gentle mixing, followed by centrifugation for 30 seconds at 14000 rpm. Immuno-complexes were eluted from the protein A sepharose beads by adding 100 µl elution buffer (1% SDS, 100 mM $NaHCO_3$, adjusted to a final volume of 100 ul dH_2O) and incubating the samples for 15 minutes at RT on the thermomixer (25˚C, 1400 rpm) (twice). The 100 ul eluated was transferred to clean tubes.

Reverse crosslinking: Eluted samples as well as input samples underwent reverse-crosslinking. Heating can reverse the formaldehyde crosslinking so all samples were incubated at 65 ˚C for 5 hours at 1100 rpm. Prior to heating, 8 ul NaCl (5 M, Sigma # 050M0135V) and 10 ul RNase-Dnase free from bovine pancreas (50 ug/ml) (Roche # 11119915001) were added to the samples. For the diluted input, 10 ul is taken from the 200 ul sample, and is added to 190 ul Elution buffer together with 8 ul NaCl and 10 ul RNAse. If an input is needed to make a standard curve or to run it on a gel, 20 ul NaCL

and 20 ul Rnase are added to the remaining ~180 ul input. Samples are mixed well and incubated at 65^0C for at -5 hours at 1100 rpm.

DNA Purification: Purification followed using the QIAquick PCR purification kit (QIAGEN # 28104) according to the instructions of QIAGEN. 1 ml of buffer PB (5 M Gu-HCl, 30% isopropanol) was added to 200 ul of sample. A QIAquick spin column was labelled and placed in a 2 ml collection tube. First, 600 ul of the sample was applied to the QIAquick column and was centrifuged for 30–60 seconds at high speed in order for DNA to bind. Flow-through was discarded and QIAquick column was placed back into the same tube. The procedure was repeated with the other 600 ul of the sample. In order to wash the column, 0.75 ml Buffer PE (10 mM Tris-HCl pH 7.5, 80% ethanol) was added to the QIAquick column and was centrifuged for 30–60 seconds. Flow-through was discarded and was placed back in the same tube. The column was centrifuged for an additional 1 min. The QIAquick column was placed in a clean 1.5 ml microcentrifuge tube. For elution of DNA, 50 µl (for IPs) or 30 ul (for input samples only) of water (pH 7.0–8.5) was added to the center of the QIAquick membrane and the column was centrifuged for 1 min. Samples were ready to be used for RT-PCR or stored at -20 ˚C.

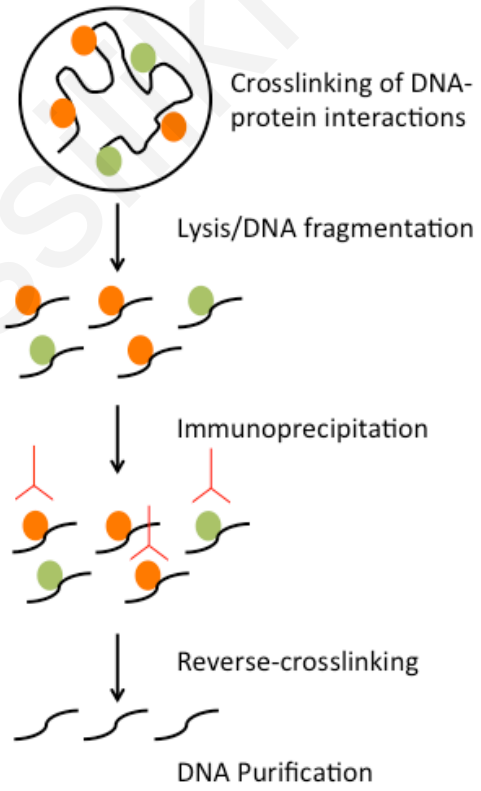

Figure 2.1. Outline of ChIP assay. The process begins with formaldehyde crosslinking of DNA-protein interactions, followed by cell lysis and sonication for DNA fragmentation, overnight immunoprecipitation with specific antibodies, reverse crosslinking and then finally DNA purification.

2.12 Antibodies

Rabbit polyclonal antibodies were raised against H4R3me2a and N-acH4 in collaboration with Eurogentec (Belgium). For the generation of H4R3me2a the animal was immunized with the keyhole limpet hemocyanin (KLH) conjugated synthetic peptide H2N-SGR (AsymDimethyl) GKG GKG LGK C-CONH2. Serum was affinity-purified by the manufacturer in a two-step procedure. Antibodies specific to the modification were captured on the AF-Amino TOYOPEARL 650 M matrix together with the immunization peptide. After elution with 100 mM glycine (pH 2.5), the antibodies recognizing the peptide in the absence of modification were eliminated with a matrix coupled with the unmodified peptide H2N- SGR GKG GKG LGK C- CONH2. After the purification, antibody specificity was determined by enzyme-linked immunosorbent assay (ELISA) using the specific and non-specific peptides as antigens. The purity of the H4R3me2a antibody was >89% as determined by high pressure-liquid chromatography. The procedure described above was repeated for the generation of the N-acH4 antibody using the KLH-conjugated peptide AcNH-SGR GKG GKG LGK GGA C-CONH2 and the unmodified peptide H2N-SGR GKG GKG LGK GGA C-CONH2. Specificity of the antibody was tested by ELISA and the purity of the N-acH4 antibody was >99.4%. Other antibodies used were: H4K5ac (ab51997; Abcam), H4K12ac (ab46983; Abcam), H4K8ac (ab15823; Abcam), H4R3me1 (ab17339; Abcam), H4R3me2s (ab5823; Abcam), H3 (ab1791; Abcam), H4 (62-141-13; Millipore), Naa40 (ab106408; Abcam), b-Actin (ab8226; Abcam) and His-tag (2365; Cell Signalling).

2.13 Growth and silencing assays

Overnight cultures were diluted to OD ~0.1 and grown to mid-log phase. Approximately 1.2×10^4cells were serially diluted 10-fold, and spotted onto the right media plates (YPAD, SC or SC+5′-Fluoroorotic acid). The plates were incubated at 30°C or 37°C for 2 days. Doubling time of cell growth was measured as indicated on http://www.doubling-time.com/compute.php. Silencing assays were performed to measure the ability of strains carrying a copy of the *URA3* gene, to grow on plates carrying 5-Fluoroorotic acid (5-FOA). The URA3 reporter was integrated at the rDNA, telomere-VIIL, *HMR* or *HML* (*RDN1::URA3, adh4::URA3-TelVII-L*, *hmr::URA3*, or *hml::URA3*). *URA3* encodes for an enzyme (orotidine 5-phosphate decarboxylase), involved in the uracil pathway. This enzyme also metabolizes the chemical 5-Fluoroorotic acid (5-FOA) into 5-fluorouracil, which is a toxic metabolite (Boeke et al., 1984). The ability of the cell to survive in the

presence of 5'-FOA depends on the expression levels of the *URA3* gene in the heterochromatin-like regions where it is inserted. Loss of silencing activates expression of *URA3*, preventing growth on 5-FOA, while stronger silencing leads to more cell growth.

2.14 Gel Electrophoresis

Agarose gel electrophoresis was performed in order to obtain the quality of the RNA samples and to check DNA fragmentation during the sonication optimization for ChIP. Gel electrophoresis was performed using 1% agarose gel. 0.3g dry agarose powder (Biorad, #AC003522500) suspended in 30ml 1X TAE buffer (40mM Tris, 20mM glacial acetic acid, 1mM EDTA pH 8.0 and ddH_2O) and heated to dissolve. 0.8µl of Ethidium Bromide (Sigma Aldrich, #030M8710) was added. Solution was then poured into a plastic casting tray for 30 minutes to solidify. 1X TAE buffer was poured to cover the agarose gel. Before the loading, samples were mixed with 2µl of 5x Loading buffer (Invitrogen, #10816-015) and 7µl of ddH_2O. 4µl of 1Kb DNA ladder (Invitrogen, #10488-072) was used as a molecular weight standard. The electrophoresis was performed in 1x TAE buffer at 100 V/cm. for 20 minutes. Bands were visualized under UVP bioimaging system.

2.15 SDS- PAGE gele electrophoresis and Western blotting

Yeast cells were grown to mid-exponential phase in a 30°C shaker. Total yeast extracts were prepared by first resuspending cell pellets in a tenfold volume of SDS loading buffer (50 mM Tris-HCl pH 6.8, 2% SDS, 10% glycerol, 1% β-mercaptoethanol, 12.5 mM EDTA and 0.02% bromophenol blue). The samples were then alternately boiled at 95°C for 5 min, vortex and chilled three times in ice to rupture cell membranes. Protein samples were loaded and separated on 10, 12,5 or 15% SDS-PAGE gel (Laemmli 1970) at 200 V for 1 h. The proteins were wet transferred into a nitrocellulose membrane (GE Healthcare life sciences) with transfer buffer (20% Methanol, 25 mM Tris, 192 mM glycine, pH 8.3), at 100 V for 1 h. After bathing in blocking buffer (5% BSA, 0.1% Tween-20 TBS buffer (25 mM Tris, 150 mM NaCl, 2 mM KCl, pH 8)) for 1 h at RT to reduce unspecific binding, the membrane was incubated with a primary antibody of interest, diluted in blocking buffer for 2h on the shaker at low speed at RT. Next, the membranes were washed with TBS-Tween (0.5%) (three times with 10 min incubation) and incubated with Horseradish peroxidase–conjugated secondary antibody diluted in blocking buffer for 1 h at RT. The membranes were washed three times with 5 min incubation on the shaker at RT. Protein bands were

detected by the enhanced chemiluminescent system using the Luminol reagent (GE Healthcare, Amersham,ECLWestern Blotting Detection Reagent, # RPN2209) according to the manufacturer's protocol and analyzed using the UVP Bioimaging system.

2.16 Northern blot

RNA samples were extracted as described in section 2.3.1 Precipitation was carried out by adding 8M of LiCl (final concentration ≥2.5M). Samples were left overnight at -20^{0}C and then centrifuged for 15 minutes at full speed. The supernantant was discarded, and the pellet was washed with 70% ethanol, centrifuged for 5 minutes at full speed, air dried and resuspended in 30 ul RNAse DNAse free H_2O. The concentration and purity of RNA was measured as described in section 2.3.2. 30 ug of RNA was mixed with loading buffer (10µl deionized Formamide + 3.5µl 37% Formaldehyde + 2µl 5x Formaldehyde buffer (5x Formaldehyde buffer: 0.1M MOPS pH7,0, 40mM Sodium acetate, 5mM EDTA pH8.0)) to a final volume of 50ul, heated at 70 ^{o}C for 10 minutes and loaded onto a 1% RNA-formaldehyde agarose gel (1% agarose + 75ml H2O (heat to dissolve), cool shortly + 20ml 5xFormaldehyde buffer + 5,4ml 37% Formaldehyde). The samples were run in 1x formaldehyde buffer (5x Formaldehyde buffer: 0.1M MOPS pH7,0, 40mM Sodium acetate, 5mM EDTA pH8,0.) for 30 minutes at 100 V. Gel was then stained with ethidium bromide (0,75 ug/ml in water), equilibrated by 10x SSC buffer (150 mM NaCl and 15 mM sodium citrate, pH7) and transferred by capillarity overnight with 20X SSC onto a to hybond nylon membrane (Amersham Hybond-N+ GE Healthcare). The membrane and the RNA were UV-cross linked with (700 Joules/cm2). The membrane was then equilibrated with 10 ml of hybridization buffer (50% formamide, 5X SSC, 0.1% Ficoll, 0.1% PVP, 1% SDS, 0.01% salmon sperm DNA) at 52^{o}C for 1 hour. The buffer was discarded and 10 ml of fresh hybridization buffer containing the probe (100 ng/ml final concentration) of interest was added and incubated at 52^{0}C overnight. The probe was prepared into 150ul of hybridization buffer heating at 98 ^{0}C for 90s, cooling in ice for 5 minutes and then adding it to the final 10 ml of hybridization buffer. The biotinylated probes were ordered from IDT using the sequences annotaded in table 5. The next morning, washes were performed as indicated: 3 x 10' with SSC (x2), 0.1% SDS at room temperature and 1 x 15' with SSC (x 0.1), 0.1% SDS at 52 ºC. The membrane was exposed using Chemiluminescent Nucleic Acid Detection Module (Thermo # 89880) using the UVP Bioimaging system.

Table 5: Probe Sequences

Probe	Sequence
E-Pro-25S side	5- AGT TCC AGA GAG GCA GCG TAA AAG GAT GAG GCT ACT GGG AAG AAG AAA GAG GAA AAG TGC AAG ATG AAT AGC CAG TGC AAT ATA TAC ATG /3Bio/ -3
E-Pro-5S side	5- CAT TAT GCT CAT TGG GTT GCT ACT ACT TGA TAT GTA CAA ACA ATA TTC TCC TCC GAT ATT CCT ACA AAA AAA AAA AAA AAA ACA CTC CGG /3Bio/ -3
ACT1	5- GGG CAA CTC TCA ATT CGT TGT AGA AGG TAT GAT GCC AGA TCT TTT CCA TAT CGT CCC AGT TGG TGA CAA TAC CGT GTT CAA TTG GGT AAC /3Bio/ -3

2.17 Dot blot analysis

Synthesized peptides with at least 90% purity (Cambridge Peptides, UK) were dissolved in water. Polyvinylidine difluoride (PVDF) membranes were used. Having the membrane ready for use, a grid was drawn by pencil to indicate the region to be blotted. Using a narrow-mouth pipette tip, 250, 50, and 10 pmol were deposited onto the membrane at the center of each possition on the grid. The membrane was left to air-dry for 1 hour. The membrane was then submerged in 100% Methanol for 1 minute, water for another minute and then stained with Ponceau S or blocked by soaking in TBS-T blocking buffer 5% BSA 0.1% Tween-20 TBS (25 mM Tris, 150 mM NaCl, 2 mM KCl, pH 8). Incubation followed with appropriate antibody and dissolved in BSA/TBS-T for 2 hours on the shaker at low speed at RT. Next, the membranes were washed with TBS-T (three times with 10 min incubation). Incubation with appropriate secondary antibody followed, diluted in blocking buffer for 1h at RT. Membranes were washed three times with TBS-T (three times with 10 min incubation). Incubation with ECL detection reagent (GE Healthcare, Amersham # RPN2209) followed for 1 min and membrane was exposed.

2.18 Yeast Protein Purification

The AK267 strain was incubated overnight in SC-Ura + 2% Glucose at 30ºC, and then diluted to O.D ~0.2 in 1L SC-Ura containing 2% Ethanol and 3% Glycerol. At OD ~0.8, Galactose was added (2% final) and the culture was grown for 4.5 hours. Cells were first

collected and washed with 10 ml of cold lysis buffer (25 mM Tris-HCl pH 8, 300 mM NaCl, 5% Glycerol, 1mM EDTA pH8 containing complete protease inhibitors obtained from Roche), and then resuspended in lysis buffer (1ml/6gr of pellet). Cells were frozen in liquid nitrogen and then were ground with dry ice powder in a coffee bean grinder. The sample was stored at -20ºC overnight for the dry ice to sublime. All the following steps were performed at 4ºC. The proteins in the yeast powder were solubilized by incubating for 15min in 1ml Binding Buffer A (20 mM Tris-HCl pH8, 600mM NaCl, 5% Glycerol, 10 mM Imidazol and protease inhibitors), and then centrifuged at 14000 rpm for 5 minutes. The supernatant was kept, and the lysing procedure was repeated with the remaining pellet using 0.5ml of Binding Buffer. The supernatants were pooled and diluted with an equal volume of Binding buffer B (20 mM Tris-HCl pH8, 5% Glycerol, 10 mM Imidazol and protease inhibitors) before addition of 200ml Nickel-NTA beads (Qiagen). The samples were incubated at 4ºC for 2h. The beads were recovered by centrifugation at 2000 rpm for 2 minutes and washed 2x3min in 2ml Binding Buffer C (20 mM Tris-HCl pH 8, 300mM NaCl, 5% Glycerol, 10-20 mM Imidazol and protease inhibitors). The Hmt1-6His-HA-ZZ protein was eluted in 50-100 µl fresh Elution Buffer (20 mM Tris-HCl pH 8, 50mM NaCl, 5% Glycerol, 250 mM Imidazol and protease inhibitors) with vigorous shaking at 25ºC for 5min. The eluate was separated from the beads by centrifugation and was stored at -20ºC until further analysis by SDS-PAGE, western blotting and *in vitro* methyltransferase assays.

2.19 *In vitro* methyltransferase assay

For the *in vitro* methyltransferase assays, histone H4 peptides of size 20-22 amino acids were synthesized by Cambrige peptides (UK) and were Biotin conjucated on C-terminus, 10kD. The enzyme involved was yeast recombinant arginine methyltransferase (Hmt1), overexpressed under GAL promoter (MORF plasmid, multicopy), C-terminally tagged (His-HA-ZZ), isolated in native contitions, used on Ni-NTA beads or eluted (Storage Bfr: 20mM Tris pH 8, 50mM NaCl, 5% Glycerol, 20mM (on beads) or 300mM Imidazol (eluted), protease inhibitors (tablet-Roche)). First, fresh 100 ml reaction buffer was made: 20mM Tris-Hcl pH 8, 50mM NaCl, 1mM EDTA pH 8, 5% Glycerol, 1mM DTT, 2mM non-radioactive S-adenosylmethyonine (SAM) (NEB #B9003S) and protease inhibitors. The right consentration of DTT and EDTA was added in the reaction buffer in order to have 1mM of each in the final volume of the reaction. A master mix of the enzyme was

then made with 3-5ug of enzyme per reaction. The enzyme can be eluted or bound on beads (e.g. Nickel-NTA beads).

For the reaction, in a 1.5ml eppie the following were added: 3-5 ug enzyme,1-2 ul biotinilated peptide (15 ug/ul), 6 ul fresh SAM (32mM), 20-80 ul MyOne Dynal Streptavidine beads T1 (Invitrogen #65601) and reaction buffer up to 100 ul (final volume). For every peptide tested, one reaction is performed. For 10-40 ul beads 1ul peptide was used and for 40-80ul beads 2ul of peptide were used The reaction was then centrifuged at 2000 rpm for 2 minutes, followed by vortex at 1400-1800 rpm for 10 seconds and then overnight incubation (16-20 hours) at 550 rpm on thermomixer at 30 ˚C. The next day, vortex the tubes at 1400-1800 rom for 10 seconds and spindown at 2000 rpm for 2 minutes. Eppies were placed on a magnet so that the streptavidine beads are bound. The supernatant was transferred in a new eppie at -20 C. The superanatant can be re-used to isolate peptides that have been methylated and were not bound on the streptavidine beads. These peptides can be isolatd by adding streptavidine beads in the supernatant and rotating at 20rpm at room temerature for 1-2 hours. Spindown follows at 2000 rpm for 1 minute. The eppies were then placed on the magnet and the rest of the liquid was removed from the bottom of the tube. 1X SDS-Loading Buffer (2% SDS+mercaptoethanol) is added as much as the volume of the beads (e.g. 40ul beads + 40ul SDS-loading buffer 1X). Spindown at 1300 rpm for 1 min and then elution of the peptides took place by alternately boiling at 95ºC, cooling on ice and vortexing the beads (x3). The volume of the sample was removed by evaporating the distilled H2O using the heating speedvac to a volume suitable for loading in PAGE wells. The volume of each sample was loaded on 12% SDS-PAGE gel and the gel was run at 100volts for 1hour and 35 minutes. For Western blot, samples were run for 1h at 100volts and were blocked for 1h in 5%BSA-TBS-T at room temperature. Ponceau staining was used as a loading control. Washes, blocking and the then the antibody (anti-H4R3me2a) was added. The controls included a no-peptide (no substrate) reaction (negative control for the methyltranserase) as well as reactions with subtrates but using a catalytic mutant enzyme or BSA or another protein that cannot methylate the peptides. All control proteins and enzymes carried the same Tag (His-HA-ZZ) as the wild-type Hmt1 enzyme for proper comparison among the various reactions

2.20 Polysome analysis

Polysome analysis was carried out by collaborator as described previously (MacKay et al., 2004).

2.21 Replicative Life Span assay

To determine yeast longevity, replicative life span assays (RLS) were performed as described previously (Kennedy et al. 1994; Kaeberlein et al., 1999, Steffen et al, 2009). RLS studies the number of daughter cells a yeast mother cell produces prior to senescence. Mother and daughter cells were differentiated using a tetrad dissector microscope (SporePlay, Singer SP0-001). Physical separation of daughter cells from mother cells was achieved using a manual micromanipulator equipped with a fiber-optic needle. For the purpose of this protocol, solid YPAD plates (1% yeast extract, 2% bacto-peptone, 2% agar, 2% glucose) were prepared and were used for culturing yeast cells and for the replicative life span analysis. Plates were prepared at least two days before the life span experiment and were allowed to dry at room temperature. Yeast strains were streaked onto the YPAD plates and were incubated at 30ºC for two consecutive days. Plates were removed from the incubator and from one single colony, cells were streaked onto a fresh YPAD plate. Two patches from two different colonies were generated for each strain, incubated at 30 ˚C for two days. Cells were collected from each patch and individual cells were placed near the initial patch. These daughter cells were then separated and from each strain, 20 cells were patched along a vertical line on the left side of a fresh YPAD plate (experimental plates) that was used for replicative life span analysis. A hole was made by forcing the needle on the agar in order to act as a marker to orient the researcher on the plate during dissection and daughter cell removal. Above the hole, individual yeast cells were aligned vertically into 20 positions with 1-3 needle diameter between each cell position. Once cells were arrayed for each patch, parafilm was placed around the plate and was incubated at 30˚C for 2 hours. Virgin daughter cells were then isolated as buds from mother cells by gently placing the needle on top of the attached cells. The detached daughter cells were placed in the vertical line on the plate, replacing the mother cell and any additional daughter cells, moving them aside (Figure 2.2). All of the mother and extra daughter cells were collected and were transferred back to the area near the patches. Parafilm was placed around the plate and was incubated at 30ºC for 2 hours. In order to measure the replicative capacity of individual yeast cells, replicative life span data sheets were necessary, which include a grid where each row corresponds to an individual mother cell and each column represents an age point (Steffen et al., 2009). Data were used to generate a survival growth curve and calculate mean lifespan.

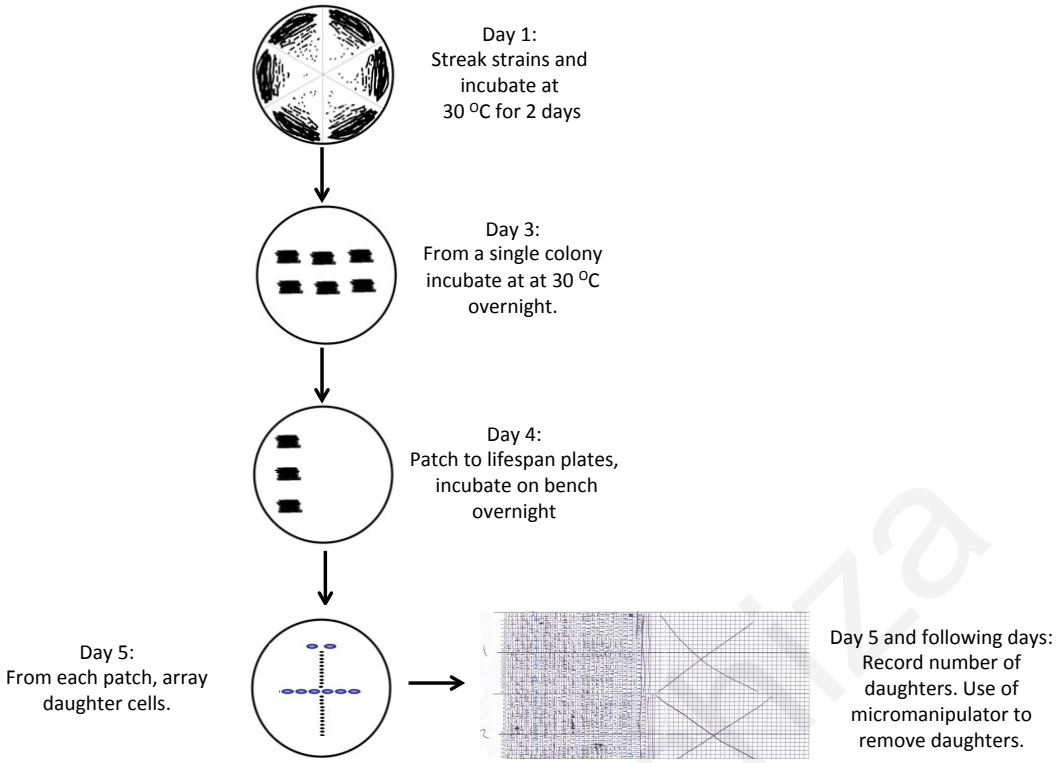

Figure 2.2. Schematic of a replicative lifespan plate. Strains are patched onto the suface of a YPD plate vertically in one side of the plate. Following growth overnight, around 30 individual cells from each strain are arrayed vertically into a line containing 20 positions. Daughter cells are obtained from these mother cells and lifespan analysis begins. Unwanted daughters are placed with the help of a microdissector away from the experimental cells (modified from Stephen et al., 2009).

2.22 Statistical Analysis

All statistics calculated for RNA-sequencing data analysis was done by - R statistical package, version 3.1.1 and Bioconductor, version 2.26.0 (Gentleman et al., 2004, https://www.r-project.org/). For ChIP experiments and gene expresssion assays, triplicate independent experiments were performed with dublicates of each sample in each experiment. Statistical significance between samples was evaluated by standard error of mean, was identified for each sample and was represented by an error bar. For lifespan assays, statistical significance was determined by a Wilcoxon rank sum test and average lifespan was considered significantly different when $P < 0.05$.

CHAPTER 3

RESULTS OF AIM 1

Chapter 3. The role of Nat4 in the expression of heterochromatin-like regions

Asymmetric dimethylation of histone H4 arginine 3 (H4R3me2a) was previously shown to be involved in the formation of silent chromatin at yeast heterochromatin-like loci (rDNA, *HML, HMR* and telomeres) (Yu et al., 2006). The histone methyltransferase Hmt1, which is the yeast functional homolog of PRMT1, catalyzes *in vitro* H4R3me2a and this is linked to transcriptional repression (Lacoste et al., 2002). The regulation of H4R3me2a *in vivo,* however, remains elusive. Therefore, we sought to identify proteins that regulate the deposition of H4R3me2a on chromatin within cells. A proteomic approach known as Global Proteomic Screen (GPS) has been previously used to identify regulators of histone modifications (Schneider et al., 2004). A GPS screen involves testing extracts of yeast gene deletion mutants by Western blotting, using as a probe an antibody specific to the histone modification of interest. For the purpose of this research, in collaboration with Eurogentec, we developed and characterized an antibody that recognizes specifically histone H4 arginine 3 (Figure 3.1.1A, B) when it is asymmetrically dimethylated (Figure 3.1.1C) and performed a global proteomic screen (GPS) using the yeast gene deletion collection. In this screen we identified a robust increase of H4R3me2a levels when the N-terminal acetyltransferase *NAT4* was deleted (Figure 3.1.2A). This led us to hypothesize that Nat4 might be a regulator of H4R3me2a. Since H4R3me2a is involved in the formation of silent chromatin in yeast (Yu et al, 2006), we initially determined the role of Nat4 in the control of heterochromatin transcription. Next, we explored the molecular mechanism underlying Nat4-mediated regulation and investigated the cellular conditions during which this mechanism is functional.

3.1 Nat4 is a novel regulator of H4R3me2a

Through the GPS screen, we found by western blotting that deletion of N-alpha acetyltransferase 4 (*nat4Δ*) results in robust induction of H4R3me2a levels (Figure 3.1.2A, lane 6). In order to confirm that the above result was not due to specificity issues of the antibody, we performed dot blot analysis to check whether the H4R3me2a antibody showed any preference for peptides that were N-terminally unacetylated. Notably, the increase of H4R3me2a in Nat4 deficient cells was not due to epitope preference of the H4R3me2a antibody as it recognizes equally well H4R3me2a peptides that are either N-terminally acetylated or unacetylated (Figure 3.1.1C, compare rows 5 and 6).

As previously mentioned, apart from the asymmetrically dimethylated state of arginine 3 (H4R3me2a), other methylation states exist for H4R3 (see Figure 1.4). Thus, we wanted to examine whether the effect we saw was specific to the asymmetrically dimethylated form at H4R3. We performed western blotting by using specific antibodies (Figure 3.1.1C) towards monomethylated H4R3me1 and symmetrically dimethylated H4R3me2s states. Interestingly, we detected similar levels for these marks between wild-type *NAT4* and *nat4Δ* strains (Figure 3.1.2B), concluding that the absence of *NAT4* affects only the silencing mark H4R3me2a.

Nat4 is the only NAT known to date to acetylate histones H4 and H2A (Song et al., 2003; Polevoda et al, 2009). It has a catalytic domain comprised of motif A and motif B (Song et al., 2003) that refers to the acetyl-CoA binding motif that is characteristic of members of the GNAT superfamily (Neuwald and Landsman 1997). In order to determine whether Nat4 regulation towards H4R3me2a was dependent on the catalytic activity of Nat4, we constructed catalytic mutant strains, in which the N-terminal acetyltransferase activity of Nat4 was compromised (Figure 3.1.3). In the strain containing mutations within motifA (*natcmA*), H4R3me2a levels are not affected, whereas in the strain that carries mutations within motif B (*natcmB*) the H4R3me2a levels are slightly increased (Figure 3.1.4, compare lanes 3, 4 and 5). However, mutation of the four highly conserved residues found within the two motifs of the acetyltransferase domain resulted in increased signal of H4R3me2a mimicking *nat4Δ* (Figure 3.1.4, compare lane 2 and lane 6).

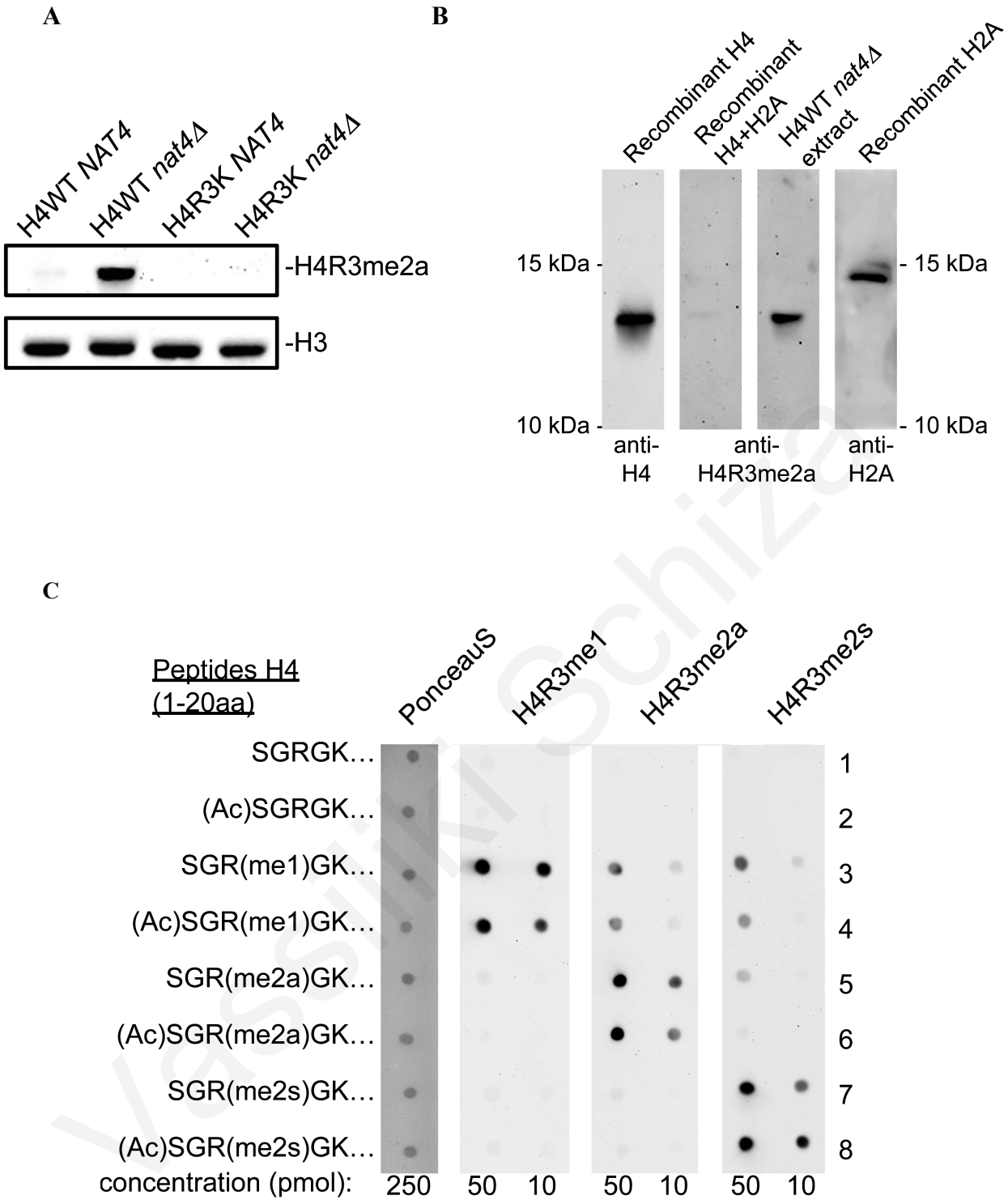

Figure 3.1.1. Specificity of the H4R3me antibodies. (A) Whole cell extracts from the indicated wild-type and mutant strains were analyzed by western blotting using an antibody against H4R3me2a. Equal loading was monitored with an H3 antibody. (B) Western blot analysis of whole yeast cell extract or recombinant histones H4 and H2A expressed and purified from bacteria. The samples were analyzed with antibodies against H4R3me2a, H4 and H2A. The H4R3me2a antibody recognizes a band in yeast extract that is equivalent to the size of histone H4. (C) Dot-blot analysis using synthetic peptides representing the first 20 amino acids of histone H4 and possessing various combinations of R3 methylation and S1 N-alpha-amine acetylation. The peptides were spotted on a PVDF membrane at the indicated concentrations and then probed with antibodies against H4R3me1, H4R3me2a and H4R3me2s. Equal loading of peptides was monitored by Ponceau staining (left panel).

A

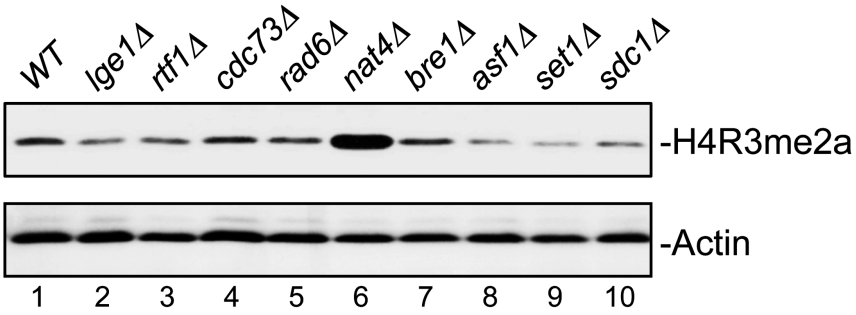

B

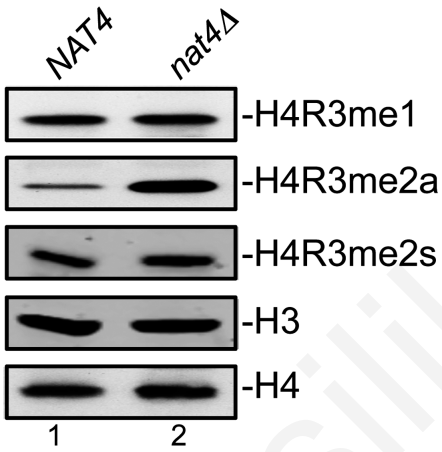

Figure 3.1.2. Deletion of *NAT4* increases the levels of H4R3me2a. (A) Whole cell extracts from the indicated deletion strains were analyzed by western blotting with an antibody against H4R3me2a (top panel). Equal loading was monitored using an antibody against actin (bottom panel). (B) Whole cell extracts from a wild-type strain (*NAT4*, lane1) and another strain carrying a *NAT4* deletion (*nat4Δ*, lane 2) were analyzed using antibodies against H4R3 methylation states (H4R3me1, H4R3me2a, H4R3me2s). Equal loading was monitored with H3 and H4 antibodies.

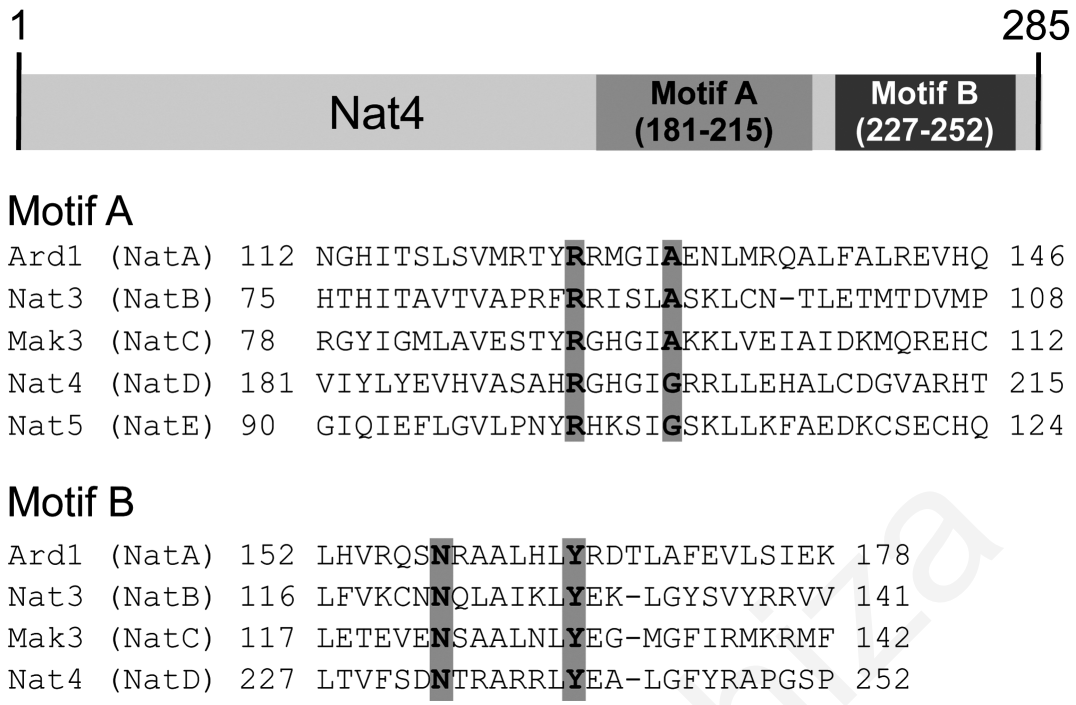

Figure 3.1.3. Sequence alignment of the catalytic motifs A and B of the five NATs present in *S. cerevisiae*. Mutated residues within each motif to generate the Nat4 catalytic mutants are highlighted in grey. Mutations generated were: arginine 194 to histidine, glycine 199 to valine, asparagine 233 to serine and tyrosine 240 to tryptophan.

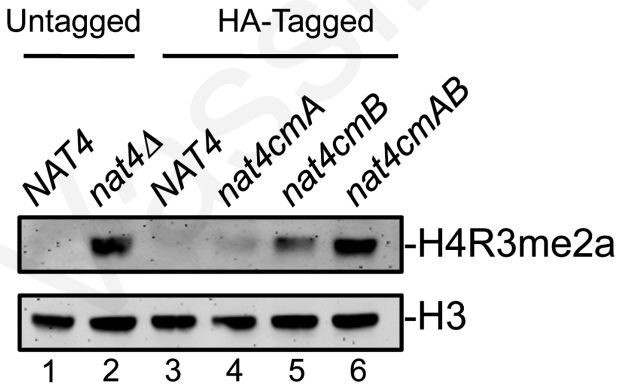

Figure 3.1.4. Inactivation of *NAT4* catalytic activity increases the levels of H4R3me2a. Whole cell extracts from wild-type *NAT4* (lanes 1 and 3) and different *NAT4* mutants (lanes 2, 4, 5 and 6) were analyzed by western blotting using antibodies against H4R3me2a (top panel) and H3 (bottom panel). The strain in lane 2 represents a Nat4 deletion strain. All catalytic mutant strains (lanes 4–6) have a C-terminal hemaglutinin (HA) tag. The strain containing the mutations within motif A is designated as *nat4cmA* (lane 4), the one with mutations in motif B is *nat4cmB* (lane 5) and the one with mutations in both motifs is noted as *nat4cmAB* (lane 6). Their equivalent wild-type strain contains only the C-terminal HA-tag (lane 3).

3.2 Loss of Nat4 activity enhances rDNA silencing and H4R3me2a deposition

As mentioned earlier, Yu *et al*. have shown that H4R3me2a is a silencing mark in yeast for the heterochromatin-like regions (rDNA, *HML, HMR* and telomeres) (Yu et al., 2006). Hence, we first sought to determine whether the loss of Nat4 activity affects silencing at these loci by performing FOA-sensitivity assays. A *URA3* reporter gene was integrated at the telomere-VIIL, *HMR* and *HML* and rDNA loci. *URA3* enzyme metabolizes 5′-Fluoroorotic acid (FOA) into a toxic compound, and the ability of the cell to survive in the presence of FOA depends on the degree of silencing in the different regions, such that stronger silencing coincides with more cell growth. We found that deletion of *NAT4* strongly increases silencing at the rDNA locus but does not affect telomeric, *HMR* or *HML* silencing (Figure 3.2.1). Recent papers, however, have shown that the widely used *URA3*-VII-L assay does not necessarily represent changes in natural silencing (Rossman et al., 2011; Takashi et al., 2011), but rather reflects metabolic changes due to an imbalance in ribonucleotide reductase (RNR) levels induced by 5-FOA (Rossman et al., 2011). Thus, we validated the silencing assays result by testing the expression of the endogenous rDNA transcripts (Figure 3.2.2). By quantitative real-time PCR we examined the levels of the different ribosomal RNAs (5S, 25S, 5.8S, 18S and the precursor 35S) and confirmed the result of the silencing assays. Deletion of *NAT4* significantly reduced the expression levels of all rRNAs (Figure 3.2.2). Due to the fact that the 35S primary transcript is quickly processed (Kos and Tollervey, 2010; Veinot et al., 1988), the observed changes in the levels of rRNAs are most likely caused by a decrease in transcription. Notably, deletion of *NAT4* does not affect the mRNA levels of ribosomal protein *RPP0*, which acts as a control in the gene expression assays (Figure 3.2.2, rightmost panel).

According to these results, we predicted that reduced expression of all rRNAs would correlate with increased deposition of H4R3me2a at the rDNA genes. Thus, we performed ChIP assays and using primers along the rDNA region we tested by qRT-PCR the deposition of H4R3me2a. The rDNA region represents an array consisting of ~150 tandem copies of a 9.1 kb repeating unit. Each repeat contains the genes *RDN5* and *RDN37* (encodes the 35S primary transcript) as well as two non-transcribed spacers (*NTS1*, *NTS2*), two external transcribed spacers (*ETS1*, *ETS2*) and two internal transcribed spacers (*ITS1*, *ITS2*). Higher nucleosomal deposition of H4R3me2a was detected across the entire rDNA locus in the absence of Nat4 by ChIP analysis (Figure 3.2.3 top panel).

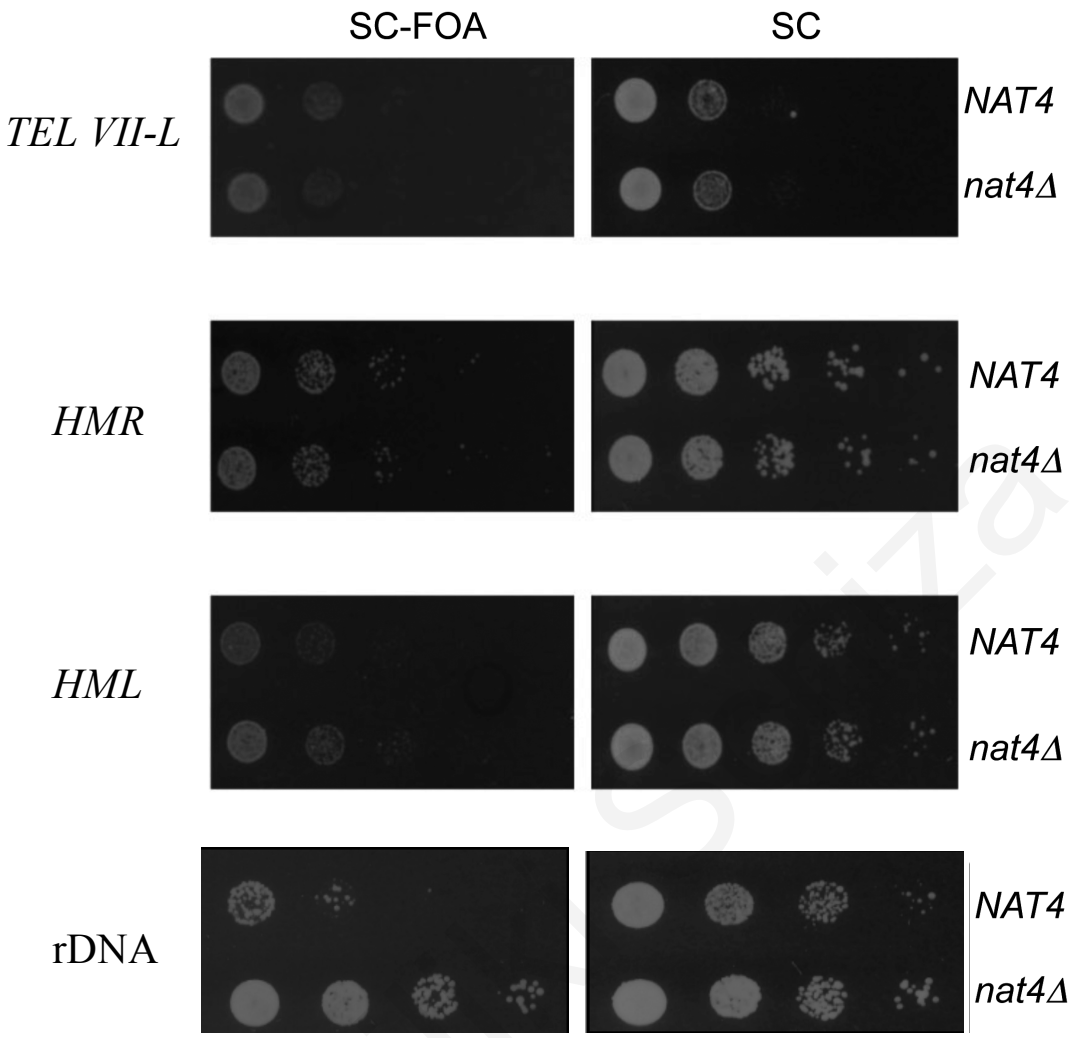

Figure 3.2.1. Deletion of *NAT4* enhances rDNA silencing but does not affect telomeric, *HMR* or *HML* silencing. Silencing assays for the rDNA, *TEL VII-L, HMR* and *HML* region were performed with wild-type (*NAT4*) or *nat4Δ* strains (row 2). Both strains (*NAT4* and *nat4Δ*) carry a copy of the *URA3* gene, that encodes for an essential enzyme in the Uracil metabolic pathway, integrated at telomere-VIIL, *HMR*, *HML* OR RDNA (*adh4::URA3-TelVII-L*, *hmr::URA3*, or *hml::URA3, RDN1::URA3*). The cells were spotted in 10-fold dilutions on SC medium (right panel) or SC+5′-Fluoroorotic acid (left panel) and then grown for 48 h at 30°C.

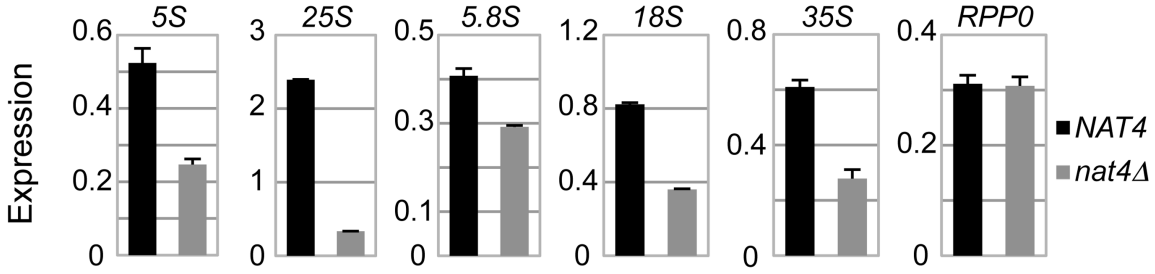

Figure 3.2.2. Deletion of *NAT4* enhances silencing across the rDNA locus. Expression levels of rRNAs 5S, 25S, 5.8S, 18S, 35S and the *RPP0* gene were analyzed by qRT-PCR using total RNA extracted from *NAT4* and *nat4Δ* strains. Error bars indicate s.e.m for duplicate experiments.

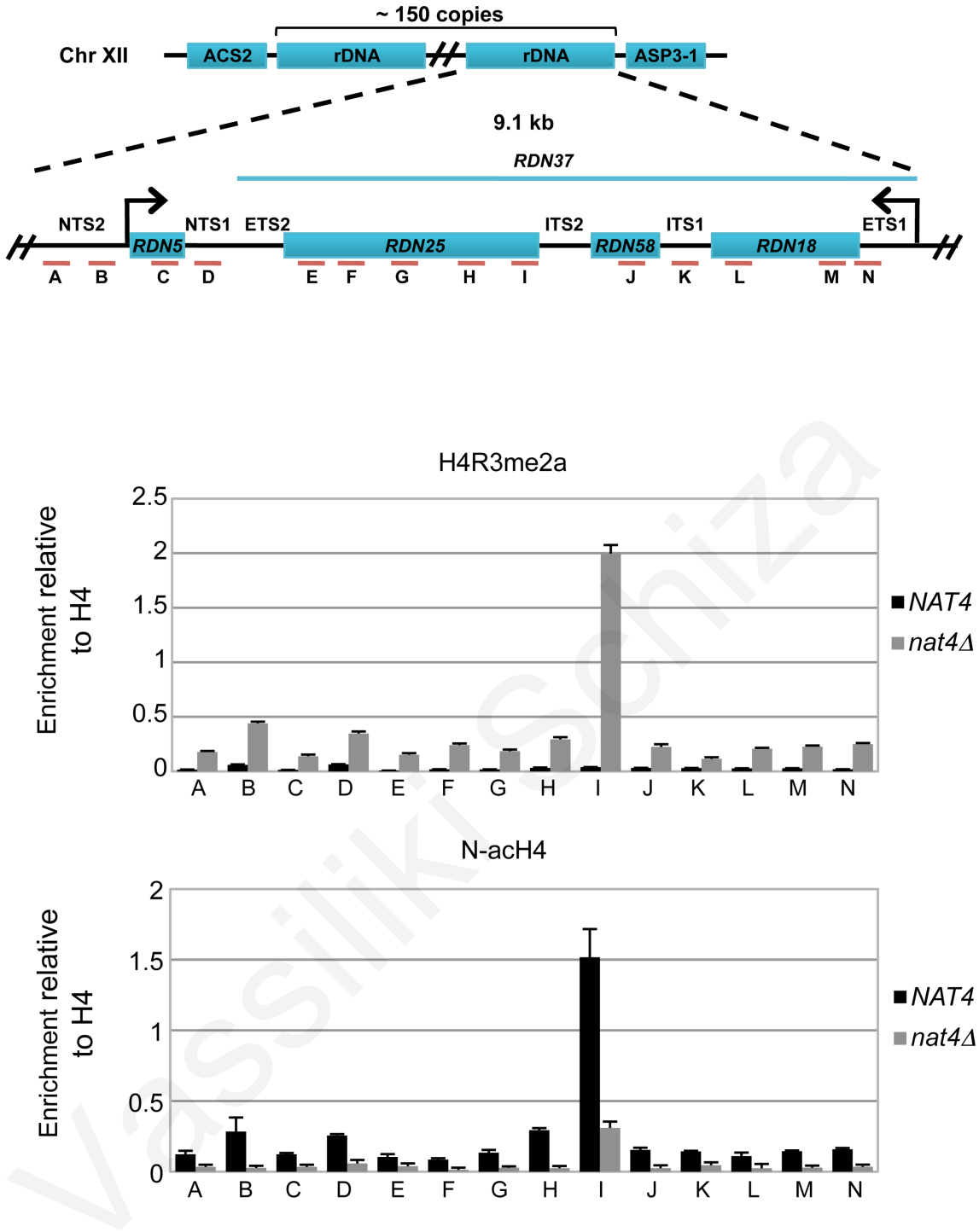

Figure 3.2.3. Deletion of *NAT4* enhances H4R3me2a deposition across the rDNA locus. Schematic of the budding yeast rDNA locus on chromosome XII. Primers were designed along the rDNA locus as indicated by the red lines and letters A–N (Table 1). ChIP experiments were performed in the *NAT4* and *nat4Δ* strains using antibodies against H4R3me2a (top panel) and N-acH4 (bottom panel). The immunoprecipitated chromatin was analyzed by qRT-PCR using the primers A–N. (see chapter 2.6 Table 4 for their sequence). The enrichment from each antibody was normalized to the levels of histone H4. Error bars indicate s.e.m for duplicate experiments.

In order to further examine whether the decrease in rDNA expression is dependent on the catalytic acetyltransferase activity of Nat4, we examined the levels of 25S in the Nat4 catalytic mutant strain (*nat4cmAB-HA*). We observed a decrease in the expression levels of 25S rRNA in the *nat4cmAB-HA* compared to wild-type levels (Figure 3.2.4A) which was similar to the decrease we detected in *nat4Δ* (Figure 3.2.2). This confirmed that rDNA expression is dependent on the Nat4 acetyltransferase activity (Figure 3.2.4A).

Consistent with this result, an increase in H4R3me2a deposition was also observed by ChIP assays at *RDN25* in the catalytic mutant strain (*nat4cmAB-HA*) (Figure 3.2.4B). As expected, based on the results in Figure 3.2.4B, we did not observe changes in the occupancy of H4R3me1 at *RDN25* in the *nat4Δ* strain (Figure 3.2.4 C). Notably, the absence of N-terminal acetyltransferase activity in the *nat4Δ* and Nat4 catalytic mutant strains was confirmed by using an antibody against N-terminally acetylated H4 (N-acH4) showing that N-acH4 levels decreased throughout the rDNA locus (Figure 3.2.3, bottom panel and Figures 3.2.4 B, C).

Taking into consideration the existence of other N-terminal acetyltransferases (NATs), we wanted to examine the possibility of another NAT affecting H4R3me2a levels and subsequently rRNA expression. We performed western blotting and observed that none of the other four NAT enzymes known in yeast (NatA, NatB, NatC or NatE) showed an effect on H4R3me2a when they were deleted (Figure 3.2.5A). The above results verify the importance of the enzymatic activity of Nat4 towards rDNA silencing and increase of H4R3me2a deposition. Consistent with this, we did not observe changes in *RDN25* expression when Ard1, the catalytic component of NatA, was deleted (Figure 3.2.5B).

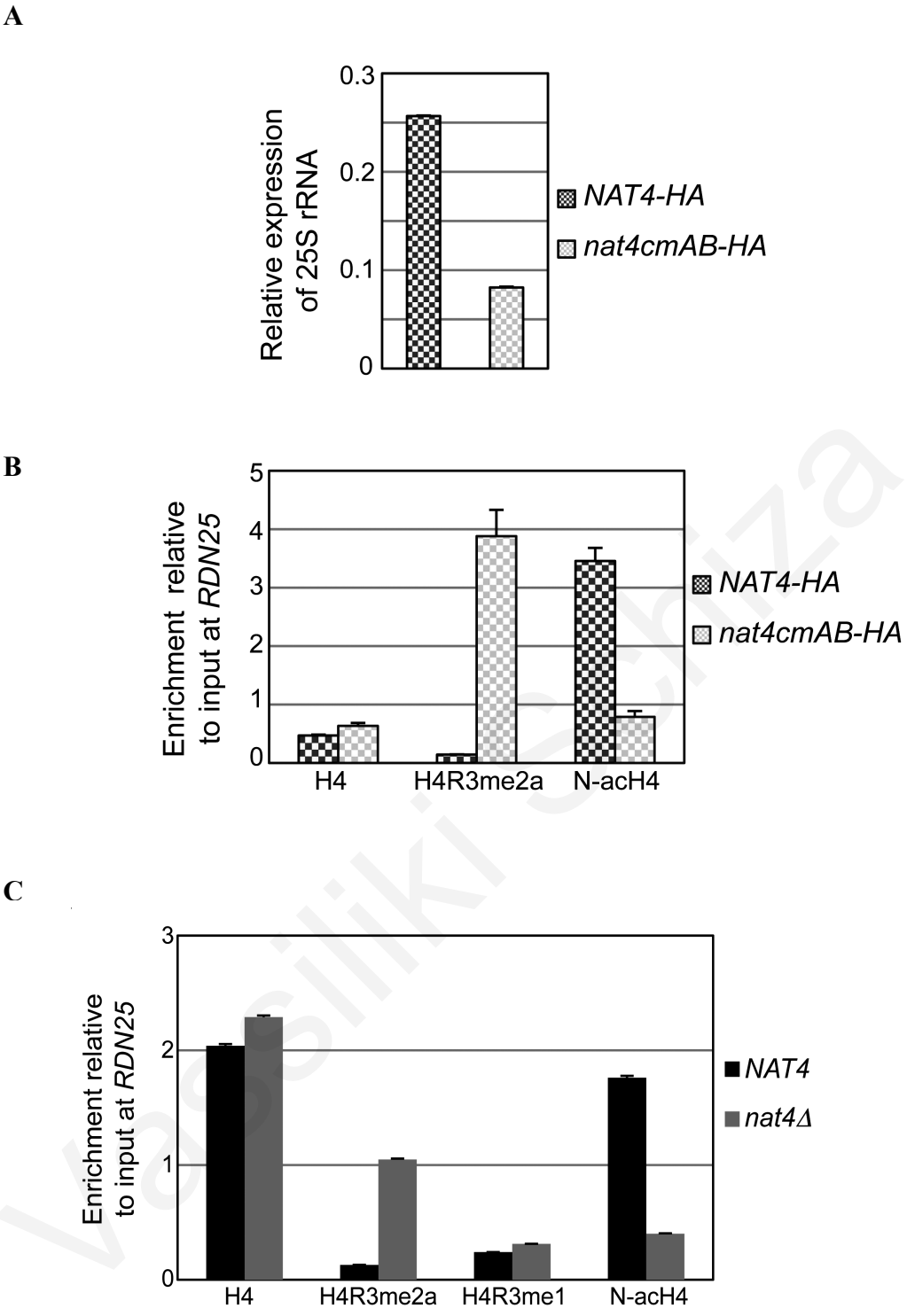

Figure 3.2.4. The catalytic activity of Nat4 is required to control *RDN25* silencing and H4R3me2a deposition. (A) The expression levels of 25S rRNA were analyzed by qRT-PCR using total RNA that was extracted from *NAT4-HA* and *nat4cmAB-HA*. The expression levels of 25S were normalized to the levels of *RPP0.* Error bars indicate s.e.m for duplicate experiments. (B) ChIP experiments were performed in *NAT4-HA* and *nat4cmAB-HA* strains using antibodies against H4, H4R3me2a and N-acH4. The immunoprecipitated chromatin was analyzed by qRT-PCR using primers for *RDN25S.* (primer I, Table 1). The enrichment from each antibody was normalized to the levels of histone H4. (C) ChIP experiments performed in *NAT4* and *nat4Δ* strains using H4R3me2a, H4R3me1 and N-acH4 antibodies and analyzed as in (3.2.4B). Error bars in (A), (B) and (C) indicate s.e.m for duplicate experiments.

A

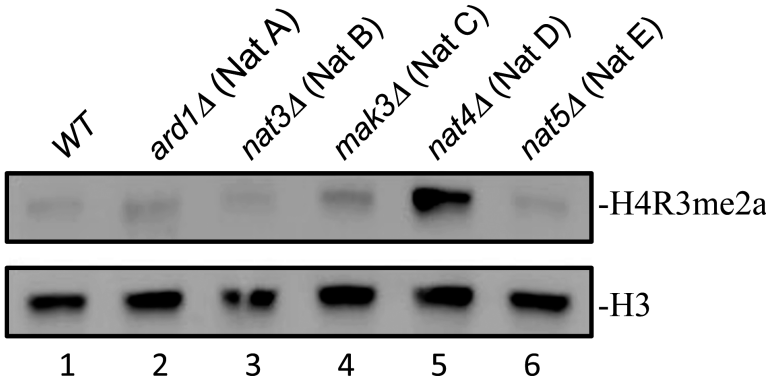

B

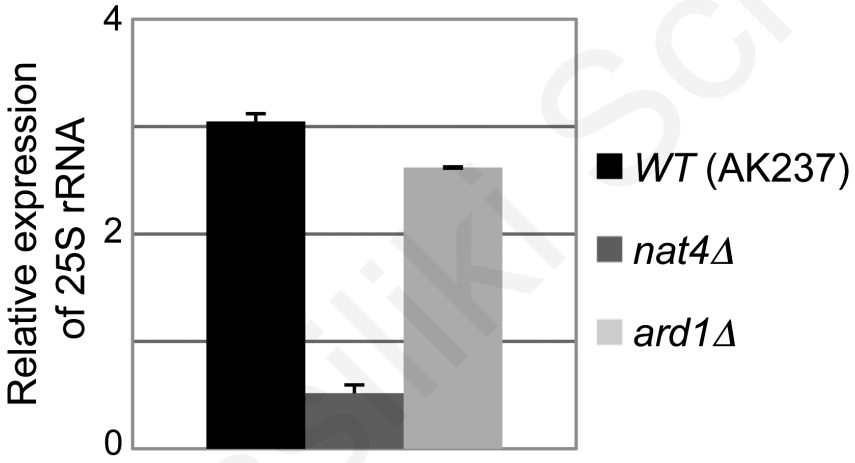

Figure 3.2.5. The yeast N-acetyltransferases A, B, C or E do not regulate H4R3me2a and do not affect expression levels of 25S rRNA (A) Whole cell extracts prepared from the indicated wild-type and single deletion (*ard1Δ*, *nat3Δ*, *mak3Δ*, *nat4Δ*, *nat5Δ*) strains were analyzed by western blotting using an antibody against H4R3me2a (top panel). The H3 antibody was used as a loading control (bottom panel). (B) 25S rRNA expression level analysis was performed with wild-type and the indicated deletion (*nat4Δ* or *ard1Δ*) strains. The expression levels of 25S were normalized to the levels of *RPP0*. Error bars indicate s.e.m for duplicate experiments.

3.3 Nat4 controls rDNA silencing and H4R3me2a through N-alpha acetylation of H4

Previous studies have demonstrated that Nat4 has only two substrates, histones H4 and H2A and suggested that the first 30 amino acids of both H2A and H4 are required for efficient acetylation by Nat4 (Song et al., 2003; Liu et al., 2009; Magin et al., 2015). Recent evidence, provided by Magin *et al* confirms the high susbstrate selectivity of Nat4 compared to other NAT enzymes because its active site is tailored for the sequence Ser-Gly-Arg-Gly and Ser-Gly-Gly-Lys, which is found in the beginning of the H4 and H2A N termini respectively. Although our data so far demonstrated that Nat4 reduces rDNA silencing and prevents H4R3me2a deposition, they do not show which one of its two targets, H2A or H4 are implicated in this regulation. Hence, it was important to examine whether Nat4 regulation of H4R3me2a is mediated through N-terminal acetylation of histone H4 or H2A. To accomplish this objective, we generated yeast strains in which either H2A or H4 were compromised for N terminal acetylation. Endogenous H4 or H2A were expressed with an alanine as the first residue instead of a serine (H4S1A or H2AS1A). By western blotting, H4S1A shows induced H4R3me2a levels compared to wild type (H4WT) (Figure 3.3A compare lanes 1 and 2) while H2AS1A has no effect on this methylation (compare lanes 3 and 4) (Figure 3.3A). ChIP assays also show an increase in H4R3me2a deposition at the *RDN25* gene compared to an isogenic wild type (H4WT) strain. The H2AS1A mutant strain did not show significant difference in H4R3me2a levels at the *RDN25* locus compared to the H2AWT strain (Figure 3.3B). These results indicated that Nat4 regulation of H4R3me2a is mediated through H4 and not H2A. Importantly, results for the H4S1A haploid mutant strain are not affected by the fact that that H4S1 can also be phosphorylated because phosphorylation of serine 1 on H4 is only induced under sporulation conditions in diploid, and not haploid cells (Krishnamoorthy et al., 2006).

To confirm that Nat4 regulates of rDNA silencing through H4, we then examined the expression of this locus in the H4S1A strain (Figure 3.3C and 3.3D). In agreement with the increased H4R3me2a levels shown in Figure 3.3B, expression analysis of 25S rRNAs and silencing spot assays validated that H4S1A reduces transcription at this locus similarly to *nat4Δ* (Figure 3.3C and 3.3D). However, the repression in H4S1A was not as strong as in *nat4Δ* possibly because H4S1A is partly acetylated by other NATs. H2AS1A, on the other hand, does not show any change in the levels of 25S rRNA (Figure 3.3C). Moreover, to provide further evidence that rDNA silencing is mediated through N-terminal acetylation of H4, we constructed another mutant strain, in which serine was substituted by a proline at position 1 expressing a H4S1P mutant. The presence of proline at position 1

blocks N-terminal acetylation completely as shown by mass-spectrometry analysis of proteins extracted from yeast, *Drosophila melanogaster* and human cells (Arnesen et al., 2009; Goetze et al., 2009). A significant decrease was observed in the 25S rRNA levels in the H4S1P mutant strain, similar to the effect shown in the *nat4Δ* strain (Figure 3.3E).

Furthermore, expression of the human ortholog of Nat4 (hNaa40) in yeast has been previously shown to result in N-terminal acetylation of H4 and not of H2A (Hole et al., 2011). Hence, we examined H4R3me2a levels in a *nat4Δ* strain that expresses ectopically hNaa40. By western blotting, we found that expression of hNaa40 in a *nat4Δ* strain reduces H4R3me2a to wild-type levels (Figure 3.3F) and ChIP analysis showed that the N-acH4 levels are restored at *RDN25* in a *nat4Δ* strain (3.3.G). This finding confirmed that histone H4 is the main substrate through which Nat4 regulates H4R3me2a. Hence, all in all, the above results suggest that Nat4 regulates rDNA silencing and H4R3me2a deposition via H4 N-terminal acetylation, but not through N-acH2A.

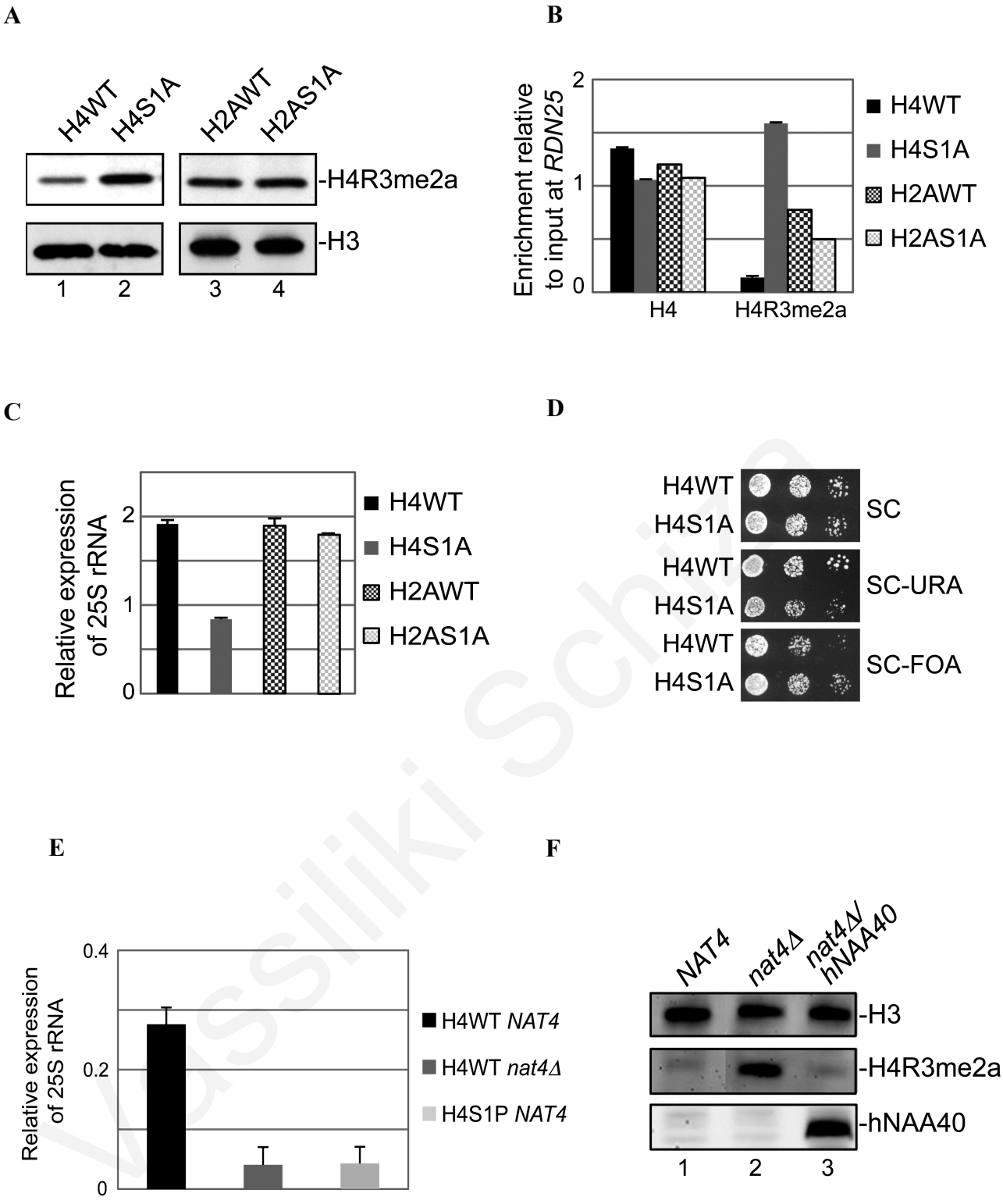

G

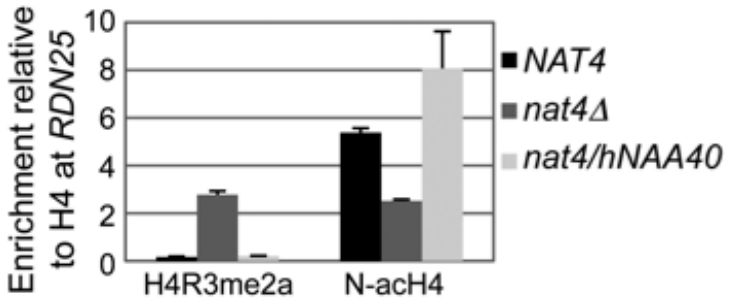

Figure 3.3. Nat4 inhibits rDNA silencing and H4R3me2a through N-terminal acetylation of H4. (A) Whole cell extracts prepared from the wild-type strains (H4WT and H2AWT) and their correspondent Serine-to-Alanine mutants in position 1 (H4S1A and H2AS1A) were analyzed by western blotting using antibodies against H4R3me2a (top panel) and H3 as control (bottom panel). (B) ChIP experiments were performed in the same strains as in (A) using the H4 and H4R3me2a antibodies. The immunoprecipitated chromatin was analyzed by qRT-PCR using primer I specific to the RDN25 gene. The enrichment from each antibody was normalized to 1% of the total input DNA. (C) Gene expression analysis of 25S rRNA performed using the same strains as in (A). The expression levels of the 25S rRNA were normalized to the levels of *RPP0*. (D) Silencing assays for the rDNA locus were performed with a wild-type (H4WT) or a H4S1A mutant strain as described in 3.2.1. (E) Gene expression analysis of the 25S rRNA was performed in wild-type (H4WT NAT4) and in mutant strains containing a *NAT4* deletion (H4WT *nat4Δ*) or a serine to proline substitution at position 1 of H4 (H4S1P *NAT4*). The expression levels of 25S were normalized to the levels of RPP0. Error bars indicate s.e.m for duplicate experiments. (F) Whole yeast cell extracts prepared from the wild-type strains *NAT4* (lane 1), and the mutant strains *nat4Δ* (lane 2) and *nat4Δ/hNAA40* (that carries a *NAT4* deletion and a plasmid that expresses ectopically *hNAA40,* lane 3) were analyzed by western blotting using the indicated antibodies. (G) ChIP assays performed in the indicated strains as in (F) using antibodies against H4R3me2a and N-acH4. The enrichment of each antibody was normalized to the levels of H4 occupancy. Error bars in (B), (C). (E) and (G) indicate s.e.m for duplicate experiments.

3.4 N-acH4 inhibits the Hmt1 methyltransferase activity towards H4R3

Taking into consideration the above results, we decided to explore further the mechanism by which N-acH4 regulates H4R3me2a. Arginine 3 on histone 4 (H4R3) was previously shown to be an *in vitro* target for methyltransferase Hmt1 (Lacoste et al., 2002). Thus, we thought that N-acH4 might inhibit H4R3 methylation by Hmt1 and decided to perform *in vitro* methyltransferase assays and western blot analysis to test the H4R3me2a levels. We first purified Hmt1 from yeast cells (Figure 3.4A) and synthesized peptides corresponding to the first twenty amino acids of H4 that were conjucated to Biotin on the C-terminus (Cambridge peptides, UK). Next, we performed *in vitro* methylation assays using purified Hmt1, the biotinilated peptides and fresh S-adenosylmethyonine (SAM). After the methylation assay the H4 peptides were isolated using streptavidin beads and subjected to western anlsysis. Figure 3.4B shows that Hmt1 dimethylates much more efficiently H4R3me1 peptides that are not N-terminally acetylated as opposed to those that possess N-acH4 (compare lanes 13 and 14). This suggests that N-acH4 represses H4R3me2a deposition by blocking the activity of the associated arginine methyltransferase towards arginine 3.

A

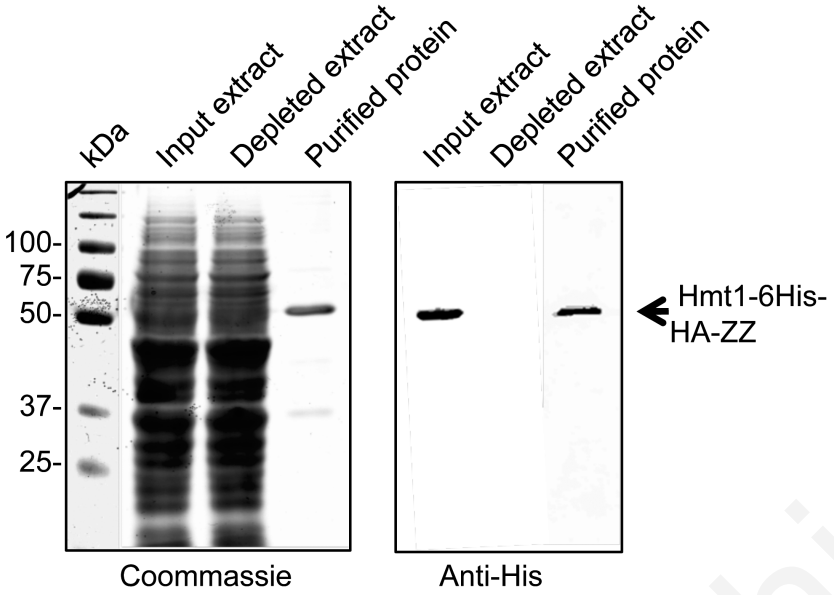

B

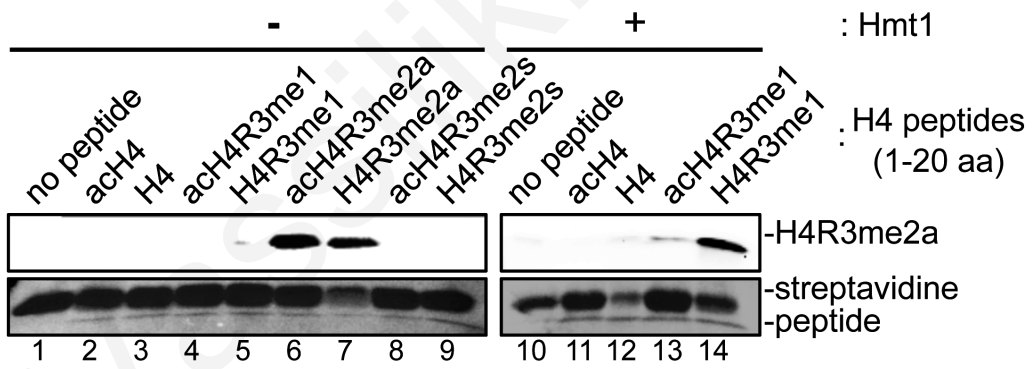

Figure 3.4. N-acH4 inhibits the Hmt1 methyltransferase activity towards H4R3. (A) Purification of yeast Hmt1. Immunoblot analysis of purified Hmt1-6His-Ha-ZZ protein using an antibody against the His-tag (right panel). Crude extract (input) prepared from the strain expressing Hmt1-6His-Ha-ZZ was used as a positive control and post-purification extract (depleted) were used to examine the efficiency of the protein purification. Coomassie staining (left panel) was used to monitor protein loading. (B) *In vitro* methylation assays were performed with synthetic biotinylated peptides representing the first 20 amino acids of histone H4 in the absence (lanes 1 to 9) or presence (lanes 10 to 14) of purified yeast Hmt1. The methyltransferase activity was monitored by western blotting using an antibody against H4R3me2a. Peptide loading was controlled by ponceau staining. Controls included no peptide reaction (negative control for the methyltranserase) as well as all the reactions-peptides with the catalytic mutant enzyme or BSA or other protein that can not methylate this substrate and has the same Tag as the enzyme that is checked (negative control for the methylation of substrates).

3.5 H4R3 is required for the regulation of rDNA silencing by Nat4 and N-acH4

The above findings show that in the absence of Nat4, the deposition of H4R3me2a increases and this is linked to enhanced rDNA silencing. However, the results do not show whether methylation at H4R3 is necessary and sufficient for the effect of Nat4 towards rDNA expression. In order to study this, we constructed a mutant in which arginine 3 was mutated to lysine (H4R3K) in order to prevent its methylation (Figure 3.5A) as well as a strain in which *NAT4* was deleted together with the H4R3K mutation. We first performed ChIP analysis at *RDN25* to check the deposition of H4R3me2a and N-acH4. As expected, H4R3me2a is increased in the *nat4Δ* strain and due to the mutation, this modification is undetected in the H4R3K and H4R3K *nat4Δ* strains (Figure 3.5A). We also observed a significant loss of N-acH4 in the H4R3K *nat4Δ* mutant strain, similar to the loss in *nat4Δ* (Figure 3.5A) and thus decided to investigate the effect of H4R3K *nat4Δ* on 25S rRNA expression. When we performed gene expression assays in these strains along with a wild-type (H4WT) and *nat4Δ* strain, the levels of 25S rRNA in the H4R3K *nat4Δ* were similar to wild type levels (H4WT) and were not reduced compared to the *nat4Δ* only strain (Figure 3.5B). This finding indicates that H4R3 and most likely its methylation are absolutely required for the control of rDNA silencing by Nat4 and N-acH4.

A

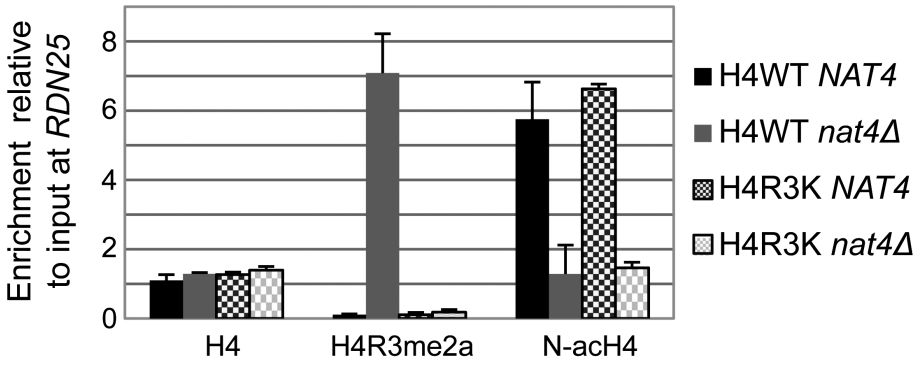

B

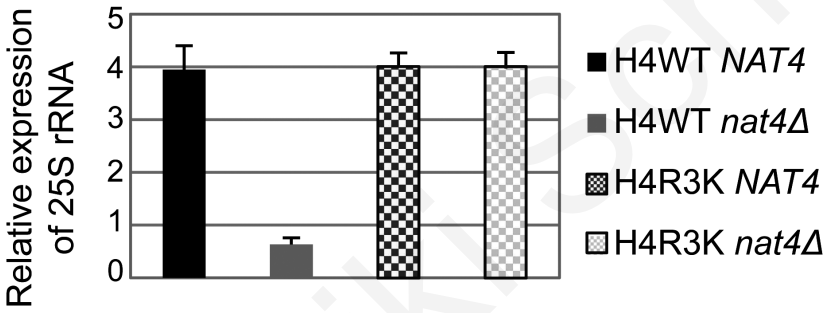

Figure 3.5. H4R3 is required for the regulation of rDNA silencing by Nat4 and N-acH4. (A) ChIP experiments were performed in the wild-type (H4WT *NAT4*) and the mutant strains carrying a *NAT4* deletion (H4WT *nat4Δ*), an H4 Arginine-to-Lysine mutation in position 3 (H4R3K *NAT4*) or both (H4R3K *nat4Δ*), using antibodies against H4, H4R3me2a and N-acH4. The enrichment at *RDN25* was analyzed as in (3.3B). (B) 25S rRNA expression level analysis was performed in the same strains as in (A). The qRT-PCR analysis was performed as in (3.3C). The expression levels of 25S were normalized to the levels of *RPP0*. Error bars in (A) and (B) indicate s.e.m for duplicate experiments.

3.6 N-acH4 cooperates with H4K5, -K8, -K12 acetylation to control H4R3me2a, rDNA silencing and cell growth

Previous studies prompted us to examine whether N-acH4 cooperates with acetylation of H4K5, H4K8 and H4K12 in order to control H4R3me2a deposition. One study showed that H4R3me2a mediated by PRMT1 is inhibited *in vitro* by acetylation of lysines K5, K8 and K12 of H4 (Feng et al., 2011). Another study demonstrated a synthetic defect in yeast containing *nat4Δ* and a triple lysine to arginine mutant (H4K5, 8, 12R) (Polevoda et al., 2009). In order to explore whether N-acH4 cooperates with acetylation of H4K5, H4K8 and H4K12 to control H4R3me2a deposition, we constructed a strain in which *NAT4* was deleted in the same strain with H4K5, 8, 12R mutant (H4K5, 8, 12R *nat4Δ*). This triple mutation at lysines 5, 8 and 12 was done because deletion of the histone acetyltansferase Esa1 that acetylates these three lysines is inviable (Clarke et al., 1999). Interestingly, when we performed western blotting we found that simultaneous loss of N-acH4 acetylation together with loss of acetylation of H4K5, 8, 12 (H4K5, 8, 12R *nat4Δ*) strongly increased H4R3me2a levels compared to *nat4Δ* alone (Figure 3.6.1A, compare lanes 2 and 4). We examined the possibility that this finding might be due to an antibody artifact but we confirmed that it is not, as the H4R3me2a antibody recognizes slightly better methylated peptides in which positions 5, 8, and 12 are lysines than when these residues are arginines (Figure 3.6.2, compare rows 2 and 3). Notably, in the absence of Nat4, internal lysine acetylation at K5, K8 and K12 remains unaffected (Figure 3.6.1B) suggesting that N-aH4 and internal lysine acetylations regulate H4R3me2a independently. However N-terminal acetylation is the dominant modification in the crosstalk because Nat4 deletion increases the levels of H4R3me2a at a greater extent than the K5, K8, K12 to R triple mutation (Figure 3.6.1A, compare lanes 2 and 3).

For further validation of the above, we decided to examine the result of combining *nat4Δ* with H4K5,8,12R on the nucleosomal deposition of H4R3me2a. In agreement with our findings above, we detected a significant enrichment in H4R3me2a at the *RDN25* gene when *NAT4* is deleted together with the H4K5,8,12R mutant as opposed to the *nat4Δ* single mutant (Figure 3.6.1 C). Recently, a study reported that the methyltransferase Set5 methylates H4K5, K8 and K12 (Green et al., 2012). Therefore, we examined whether methylation of these lysines could also act synergistically with N-acH4 to control H4R3me2a. We constructed the double mutant *nat4Δset5Δ* and performed western blotting to test the H4Rme2a levels. Based on our findings, *nat4Δset5Δ* did not further increase the H4R3me2a levels compared to the *nat4Δ* single mutant (Figure 3.6.3, compare lanes 2 and

4), indicating that it is acetylation, and not methylation of H4K5, 8, 12 that collaborates with N-acH4 to control H4R3me2a.

Additionally, the higher presence of H4R3me2a in the H4K5, 8, 12R *nat4Δ* double mutant strain results in further reduction of 25S rRNA levels when compared to the single *nat4Δ* (Figure 3.6.4A). Altogether, the above results reveal that, both N-acH4 (Figure 3.6.1C) and internal lysine acetylation (Feng et al., 2011) can impede the methylase activity that targets H4R3, but according to our findings N-acH4 is the main regulator of H4R3me2a and rDNA silencing (Figure 3.6.1A, 3.6.1C, 3.6.2A). Taking into consideration that the double mutant of *nat4Δ* with H4K5,8,12R results in strong reduction of 25S rRNA levels (Figure 3.6.4A), we then examined the growth rate of this strain using serial dilution spotting assays (Figure 3.6.4B) and by measuring its doubling time (Figure 3.6.4C). We observed that the double mutant strain (H4K5,8,12R *nat4Δ*) shows a severe growth defect in comparison to the corresponding single mutants (Figures 3.6.4B and 3.6.4C left panels). This growth defect becomes lethal when cells are stressed by growing them at a higher (37°C) temperature (Figures 3.6.4B and 3.6.4C, right panels). Furthermore, the combination of a H4K5,8,12R mutant with a H4S1A mutant also leads to a growth defect, although less severe (Figures 3.6.4B and 3.6.4C, left panels), consistent with the milder deregulation of H4R3me2a and rDNA expression in the H4S1A mutant as opposed to *nat4Δ* (compare Figures 3.2.3 and 3.3). This synthetic defect supports the synergistic effect between N-acH4 and internal H4 lysine acetylation in controlling rDNA expression and H4R3me2a.

Because previous experiments showed that arginine 3 is necessary and sufficient for rDNA regulation by Nat4 (Figure 3.5), we studied whether H4R3K can rescue the growth defect caused by the combination of *nat4Δ* and the H4K5,8,12R mutant. Notably, H4R3K rescues entirely the growth defect of the double H4K5,8,12R *nat4Δ* mutant grown at 30˚C or even at a higher (37˚C) temperature (Figures 3.6.4B and 3.6.4C). In addition, H4R3K restores rRNA expression levels (almost near wild-type expression levels) in the double H4K5,8,12R-*nat4Δ* mutant strain (Figure 3.6.4A). Overall, the results in figure 3.6.4 show that excessive H4R3 asymmetric dimethylation caused by lack of N-acH4 and internal H4 lysine acetylation impedes cell growth.

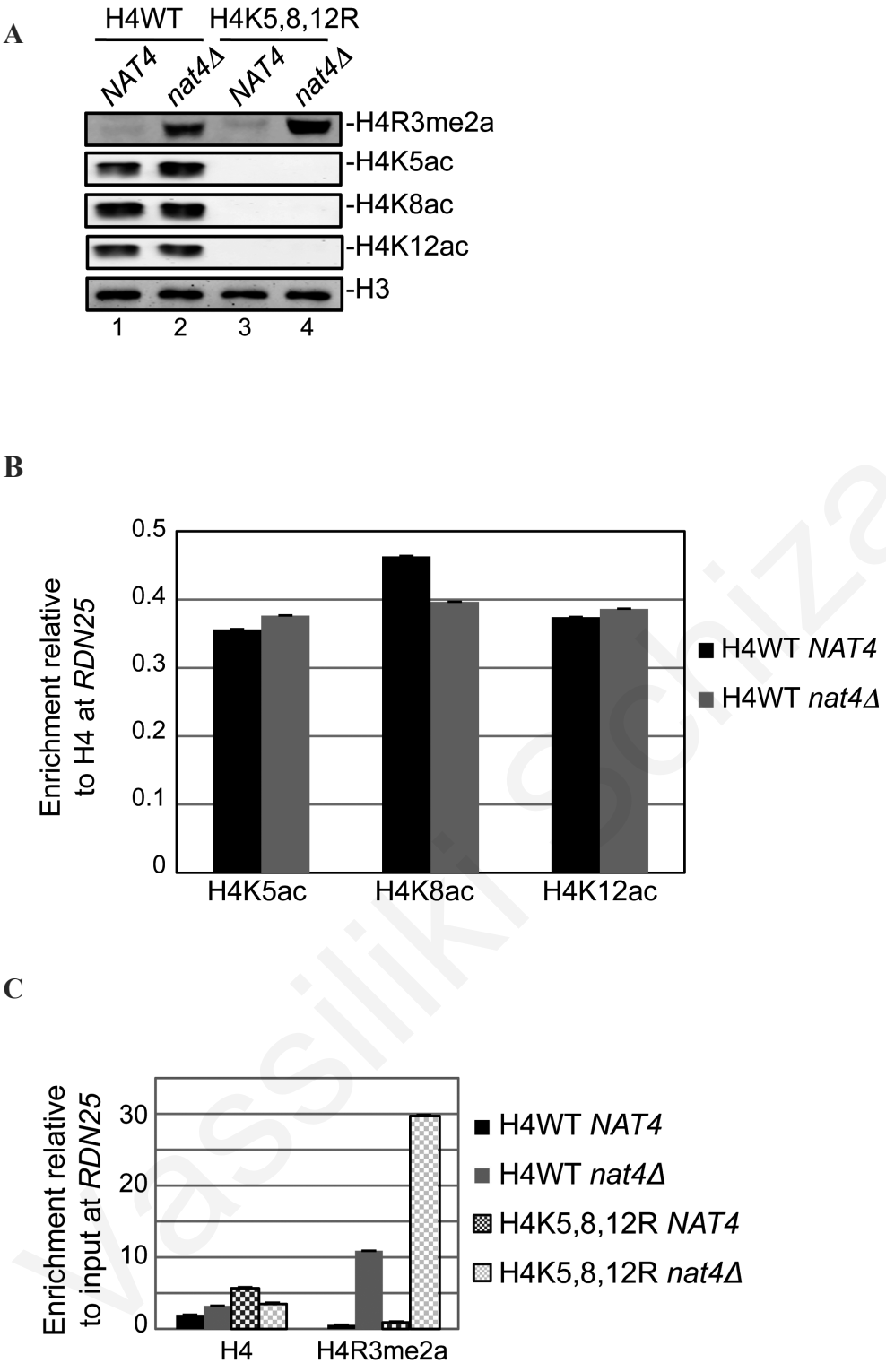

Figure 3.6.1. N-acH4 cooperates with H4K5, -K8, -K12 acetylation to control H4R3me2a. (A) Whole yeast cell extracts were prepared from the wild-type (H4WT *NAT4*) and the mutant strains carrying a *NAT4* deletion (H4WT *nat4Δ*), a triple Lysine-to-Arginine mutation in H4 in positions 5, 8 and 12 (H4K5,8,12R *NAT4*) or both (H4K5,8,12R *nat4Δ*) and then analyzed by western blotting using the H4 modification antibodies shown. Equal loading was monitored with an H3 antibody (bottom panel). (B) Deletion of *NAT4* does not affect the levels of H4K5, 8 or 12 acetylation. ChIP experiments were performed in the indicated strains using antibodies against H4K5ac, H4K8ac and H4K12ac. The immunoprecipitated chromatin was analyzed by quantitative RT-PCR using primers specific to the *RDN25* gene. The enrichment from each antibody was normalized to the occupancy of H4 (C) ChIP experiments were performed in the same strains as in (A) using the antibodies against H4 and H4R3me2a. The immunoprecipitated chromatin was analyzed by qRT-PCR using primer I specific to the *RDN25* gene. The enrichment from each antibody was normalized to 1% of the total input DNA

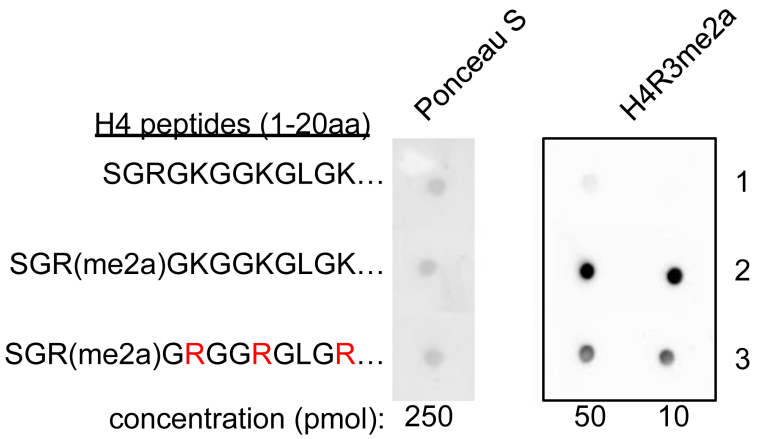

Figure 3.6.2. The H4K5,8,12R mutation does not enhance recognition by the H4R3me2a antibody. Dot-blot analysis using the indicated synthetic peptides containing the first 20 amino acids of histone H4. The peptides were spotted on a PVDF membrane at the indicated concentrations, and then probed with a H4R3m2a antibody (right panel). Equal loading of peptides was monitored with Ponceau S staining (left panel).

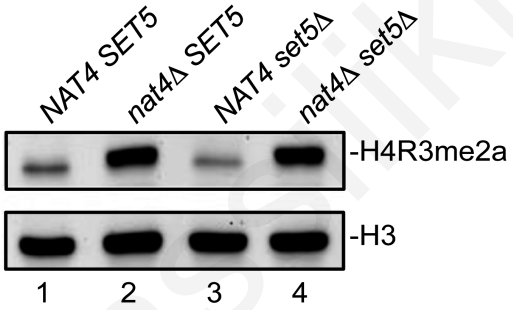

Figure 3.6.3. Methylation of H4K5, K8 and K12 by *SET5* does not act synergistically with N-acH4 in regulating H4R3me2a. Whole cell extracts prepared from the wild-type (*NAT4 SET5*) and the mutant strains carrying a *NAT4* deletion (*nat4Δ SET5*), a *SET5* deletion (*NAT4 set5Δ*) or both (*nat4Δ set5Δ*) were analyzed by western blotting. Equal loading was monitored by an H3 antibody.

A

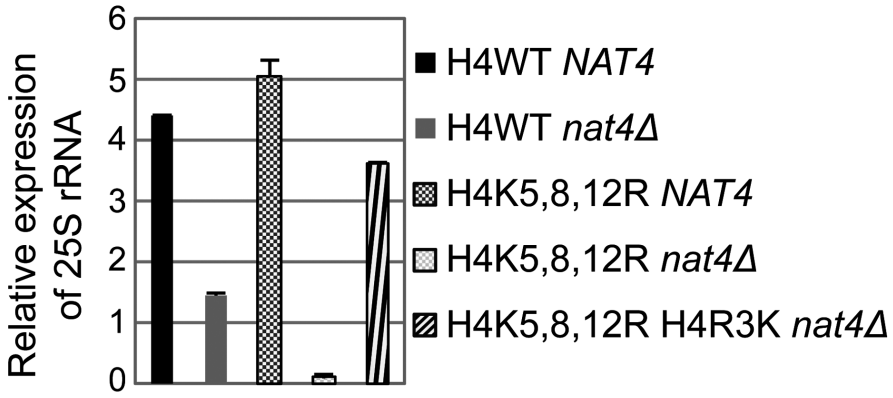

B

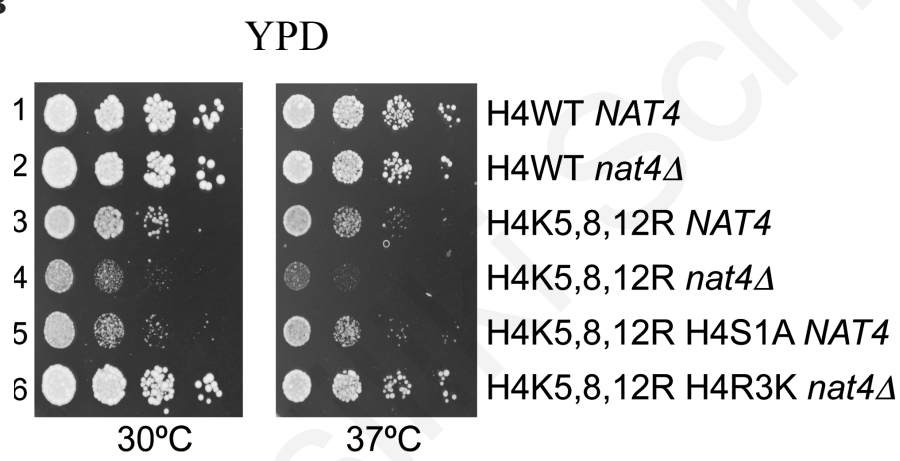

C

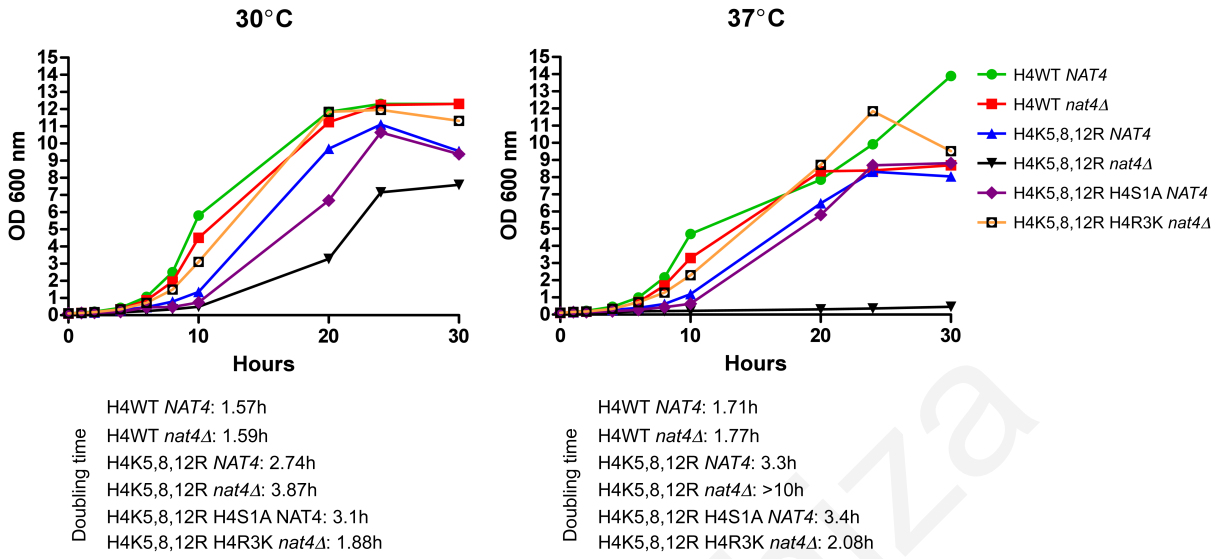

Figure 3.6.4. A+B N-acH4 acts synergistically with H4K5, 8, 12 to control rDNA silencing and cell growth. (A) 25S rRNA expression level analysis was performed in the wild-type (H4WT *NAT4*) and the mutant strains carrying a *NAT4* deletion (H4WT *nat4Δ*), a triple H4 Lysine-to-Arginine mutation in positions 5, 8 and 12 (H4K5,8,12R *NAT4*) both (H4K5,8,12R *nat4Δ*), and a multiple H4 mutant with a triple Lysine-to-Arginine substitution in positions 5, 8 and 12, an Arginine-to-Lysine mutation in position 3, and a *NAT4* deletion (*H4K5,8,12R H4R3K nat4Δ*). The expression levels of 25S rRNA were normalized to the levels of *RPP0*. Error bars in (A) indicate s.e.m for duplicate experiments. (B) Growth assay of the same yeast strains as in (A) plus a multiple H4 mutant with a triple Lysine-to-Arginine substitution in positions 5, 8 and 12, and Serine-to-Alanine mutation in position 1 (H4K5,8,12R H4S1A *NAT4*). Cells were spotted in 10-fold dilutions on YPAD medium plates. Cell growth was examined at 30°C (left panel) or 37°C (right panel) (C) Cell growth analysis was performed at 30 and 37°C. The strains used are described in 3.6.3B. The OD at 600 nm was measured at 0, 1, 2, 4, 6, 8, 10, 20, 24 and 30 h after inoculation of the culture.

3.7 Calorie restriction increases rDNA silencing and the ratio of H4R3me2a to N-acH4

In order to investigate under what physiological conditions the above regulatory mechanism becomes functional, we considered various environmental and intracellular stress conditions during which rRNA expression is altered. One such condition is calorie restriction in which reduction of glucose from 2% to 0.5% increases rDNA silencing (Lamming et al., 2005; Lin et al., 2002). In agreement with previous studies, we found that by limiting glucose availability the levels of 25S rRNA are reduced, and this reduction is greater under severe (0.05% glucose) calorie restriction (Figure 3.7A). Therefore, we sought to determine whether the crosstalk of N-acH4 and H4R3me2a is induced under these conditions in a wild-type yeast strain. Interestingly, the decrease in 25S rRNA is accompanied with an increase in the H4R3me2a:N-acH4 enrichment ratio at the *RDN25* locus (Figure 3.7B). These results suggest that the crosstalk of N-acH4 and H4R3me2a controls rDNA silencing in response to environmental stimuli such as calorie restriction.

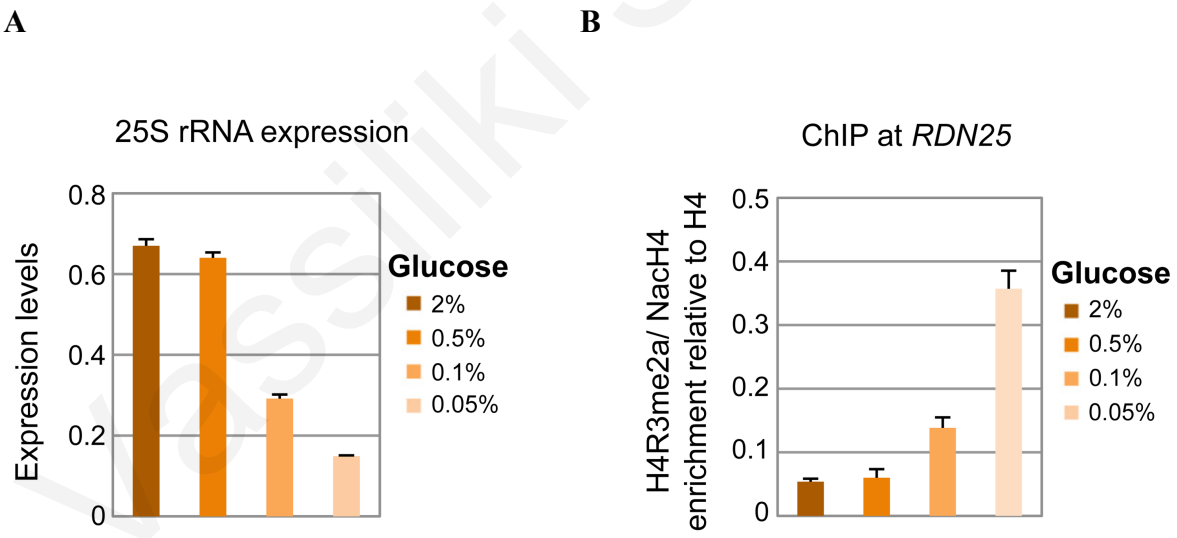

Figure 3.7. Calorie restriction increases *RDN25* silencing and the H4R3me2a: NacH4 enrichment ratio. (A) The levels of 25S rRNA were analyzed by qRT-PCR using total RNA extracted from a wild-type strain (BY4741) grown in minimal media containing different glucose concentrations (2%, 0.5%, 0.1% and 0.05%). The expression levels of 25S were normalized to the levels of *TAF10.* Error bars indicate s.e.m for duplicate experiments. (B) ChIP experiments were performed in a wild-type BY4741 strain grown in the same conditions as in (A), using antibodies against H4R3me2a and N-acH4. Their enrichment is normalized to histone H4 and represented as ratio of H4R3me2a to N-acH4. Error bars in (A) and (B indicate s.e.m for duplicate experiments.

CHAPTER 4

RESULTS OF AIM 2

Chapter 4. The role of Nat4 in regulating the expression of euchromatic genes

After establishing the role of Nat4 in regulating the heterochromatin-like locus rDNA, we were interested in investigating whether Nat4 has also a role in regulating gene induction at euchromatic regions. A transcriptome analysis using RNA-sequencing was performed in order to study global gene expression changes in the yeast lacking Nat4 (*nat4Δ*). Notably, we observed that deletion of Nat4 significantly deregulates the expression of several euchromatic genes (Figure 4.1). We therefore hypothesized that Nat4 may be involved in a mechanism to regulate the expression of these genes in addition to the rDNA locus.

4.1 Loss of Nat4 induces the expression of metabolic and stress response genes

We sought to identify whether Nat4 regulates other genes in the yeast genome apart from the rDNA locus. To do this, we performed RNA-sequencing using RNA isolated from wild type cells and cells that carry the *NAT4* deletion that were grown in rich YPAD media. Interestingly, transcriptome data revealed the deregulation of 194 genes in the absence of Nat4 (*nat4Δ*) when using 2-fold differential expression and False discovery rate (FDR) < 0.001 as the cut-off. As graphically illustrated in the scatter plot in Figure 4.1, 138 genes were upregulated (green points) and 56 genes were downregulated (red points) in *nat4Δ* compared to wild type *NAT4*. In order to determine if the dereguated genes belong to specific functional functions, we performed gene ontology analysis. We examined the differentially expressed genes based on biological process, cellular component and molecular function. Our results indicated a significant enrichment for genes belonging to metabolic processes like glycolysis/gluconeogenesis and stress response genes (Figure 4.2A).

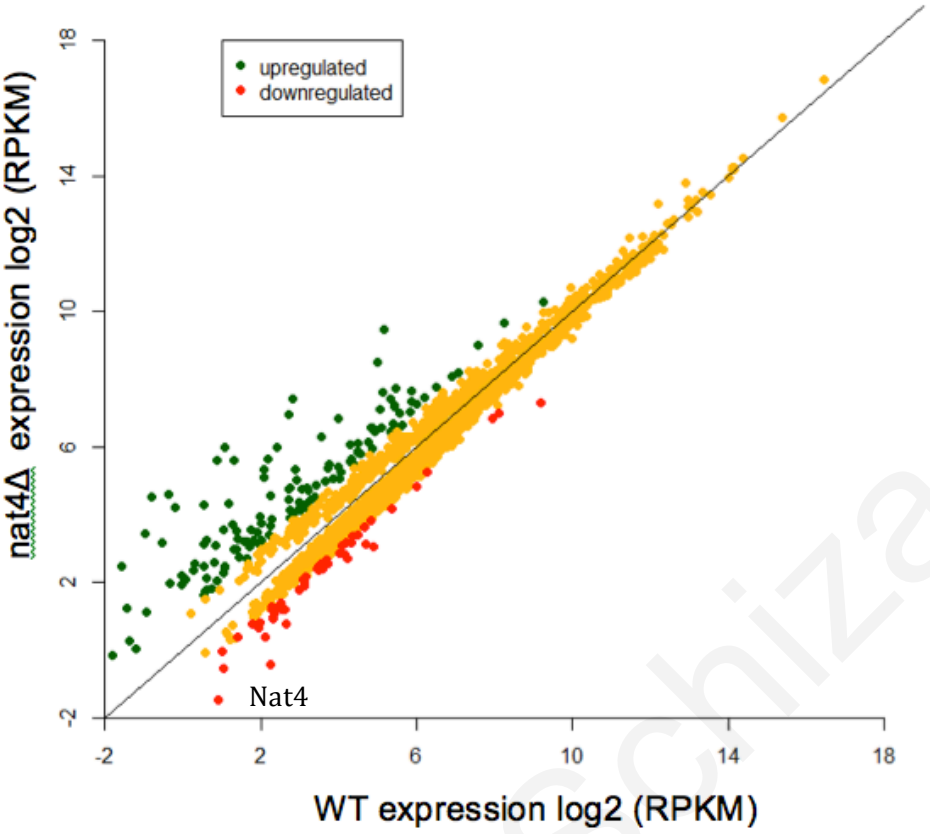

Figure 4.1. Deletion of *NAT4* exhibits gene expression changes in a number of eukaryotic genes. Scatter plot comparing log-scale RPKM expression values in libraries derived from wild type *NAT4* (x-axis) and *nat4Δ* (y-axis) yeast cells. Each dot represents the RPKM value of a specific gene. Points displayed in green are genes that are 2-fold upregulated in *nat4Δ*. Points in red are genes that are 2-fold-downregulated in *nat4Δ*. The yellow points represent genes where no significant difference in expression was observed between *NAT4* and *nat4Δ*. Nat4 is the most downregulated gene. A threshold for false discovery rate (FDR) of < 0.001 and an absolute value of log2 ratio>1 were used to determine significant differences in gene expression. RPKM: Reads per kilobase transcript per million reads. The plot is on a log2 transformed scale.

4.2 Deletion of *NAT4* exhibits gene expression changes that mimic those occurring during calorie restriction

Previous studies have shown that cells which are grown in nutrient deficient conditions such as calorie restriction (CR) induce the expression of metabolic and stress-response genes (Lee et al., 2008; Sharma et al., 2011; Steffen et al., 2008; Wang et al., 2010; Dang et al., 2014). This raised the hypothesis that deletion of Nat4 *(nat4Δ)* might mimic CR effects. In order to obtain a better understanding of the changes that occur in CR and compare it to those that occur in *nat4Δ,* we performed a second RNA-sequencing (RNA-seq), looking at differential gene expression between cells grown in media containing 2% glucose (Non Caloric Restriction condition = NCR) and cells grown in media containing 0.1% glucose (Calorie Restriction = CR). As we expected, the expression of a vast number of genes changed in CR. Data analysis was performed using a 2-fold change (log>1) and FDR<0.001 again as the threshold and we found 914 genes that were upregulated and 990 downregulated in CR compared to NCR. We then performed gene ontology analysis to determine the functional groups of the differentially expressed genes. GO clustering analysis of upregulated and downregulated genes due to CR (Figure 4.2A) enriched various biological processes/pathways that were consistent with those reported in a previous study (Dang et al., 2014), thus validating our methodology.

Importantly, as shown in Figure 4.2, most of the gene ontology terms that were enriched in *nat4Δ* were also enriched in CR (shown in bold). The most noticeable overlap was that for the GO term response abiotic stimulus, which largely encompasses stress-response genes and was the most significantly enriched functional group among the upregulated genes in *nat4Δ* (Figure 4.2A). As expected, response to abiotic stimulus, was among the top three upregulated groups in GO clustering analysis of CR cells (Figure 4.2B). Apart from abiotic stimulus other groups that were enriched in both *nat4Δ* and CR deregulated genes included vacuolar protein catabolic process, carbohydrate transport, generation of metabolites and energy, hexose metabolic process, transmembrane transporter activity, phoshphorylation and ribonucleoprotein complex biogenesis (compare Figure 4.2A and Figure 4.2B).

Although many enriched GO clusters were common between CR and *nat4Δ* (Figure 4.2A) it was still possible that there was not significant overlap in the individual genes that were differentially expressed between the two experimental conditions. Therefore, we then compared the lists of genes present in the functional clusters from the

two data sets (*nat4Δ* and CR). From the 138 genes that were upregulated in *nat4Δ,* 83 were also upregulated in CR conditions (Figure 4.2B) resulting in a statistically significant overalp (p-value<4 $x10^{13}$). These data suggested that *nat4Δ* partially mimics CR-treated cells at the trasncriptome level. Additionally, there was an overlap of 6 genes between those downregulated in *nat4Δ* (56 genes) and those in CR treated cells (991 genes) (Figure 4.2B, right). Although this was not a significant overlap, these 6 genes belong to the three GO terms (cell cycle, RNA processing and ribonucleoprotein complex biogenesis) that were enriched in the GO clustering analysis for *nat4Δ* (Figure 4.2A).

Since we observed a significant overlap among the genes that were differentially expressed in *nat4Δ* and CR we were wondering whether these two conditions would have a synergistic effect on the deregulation of these genes. Hence, we selected genes among the most deregulated ones in both *nat4Δ* and CR cells and examined by qRT-PCR using total RNA extracted from wild-type and *nat4Δ* cells grown in normal 2% glucose conditions and from wild-type and *nat4Δ* cells grown in CR (0.1% glucose). Consistent with the RNA-seq data, we observed a significant increase in the expression of seven examined stress induced genes (*GPH1, GLC3, HXK1, TPS2, GSY1, PNC1, NTH1)* in both CR and *nat4Δ* (albeit to a lesser extent) as well as downregulation of the examined genes *YGR079W and TIR1* (Figure 4.2D). Importantly, deletion of Nat4 in combination with CR (*nat4Δ* CR) does not have an additive effect on gene expression changes, implying a possible epistatic effect between *nat4Δ* and CR (Figure 4.2C). Overall, these findings show that Nat4 regulates a group of stress induced genes and that deletion of Nat4 exhibits gene expression changes that mimic those of cells growing under calorie restriction.

Upregulated in CR

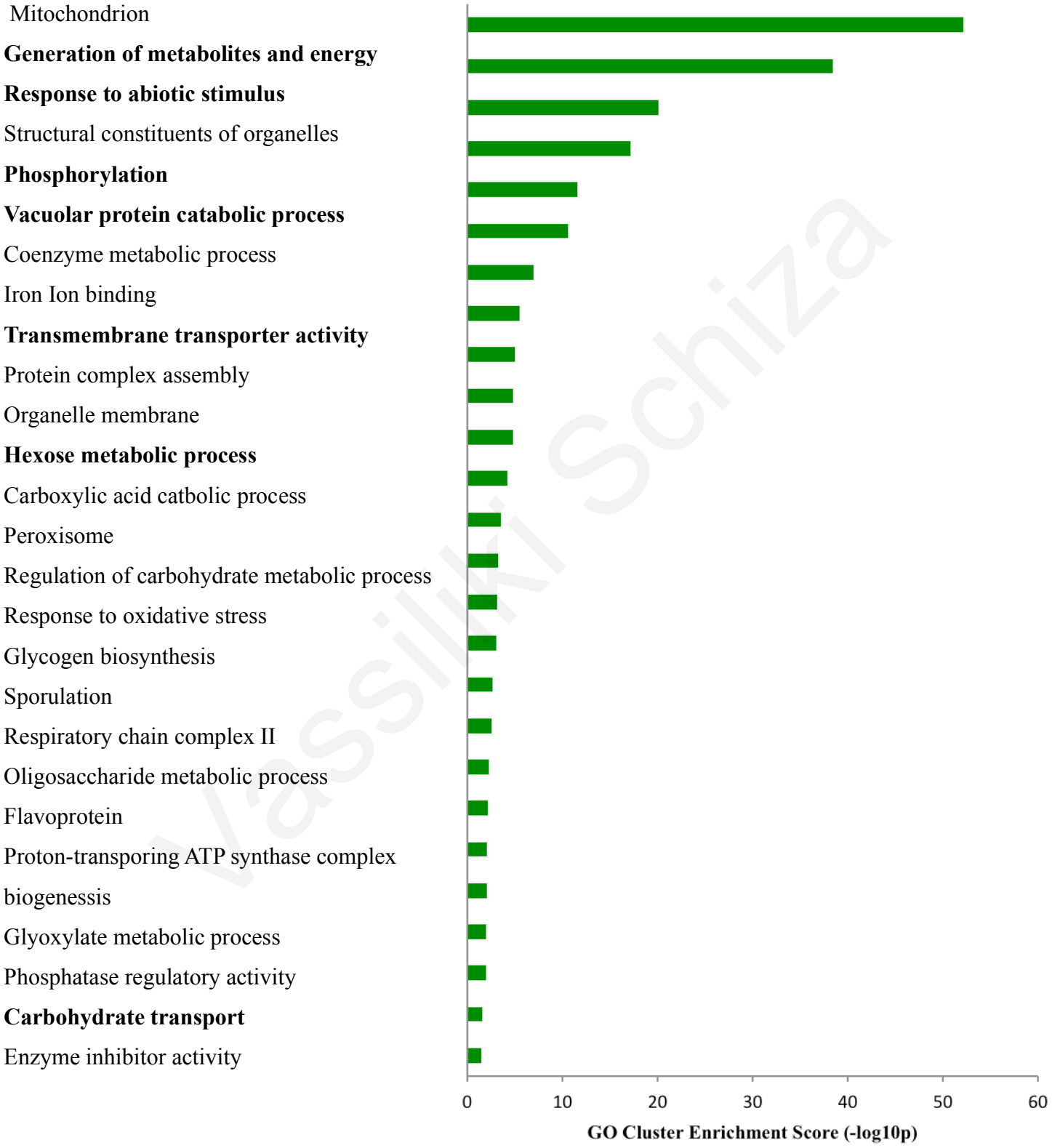

Downregulated in CR

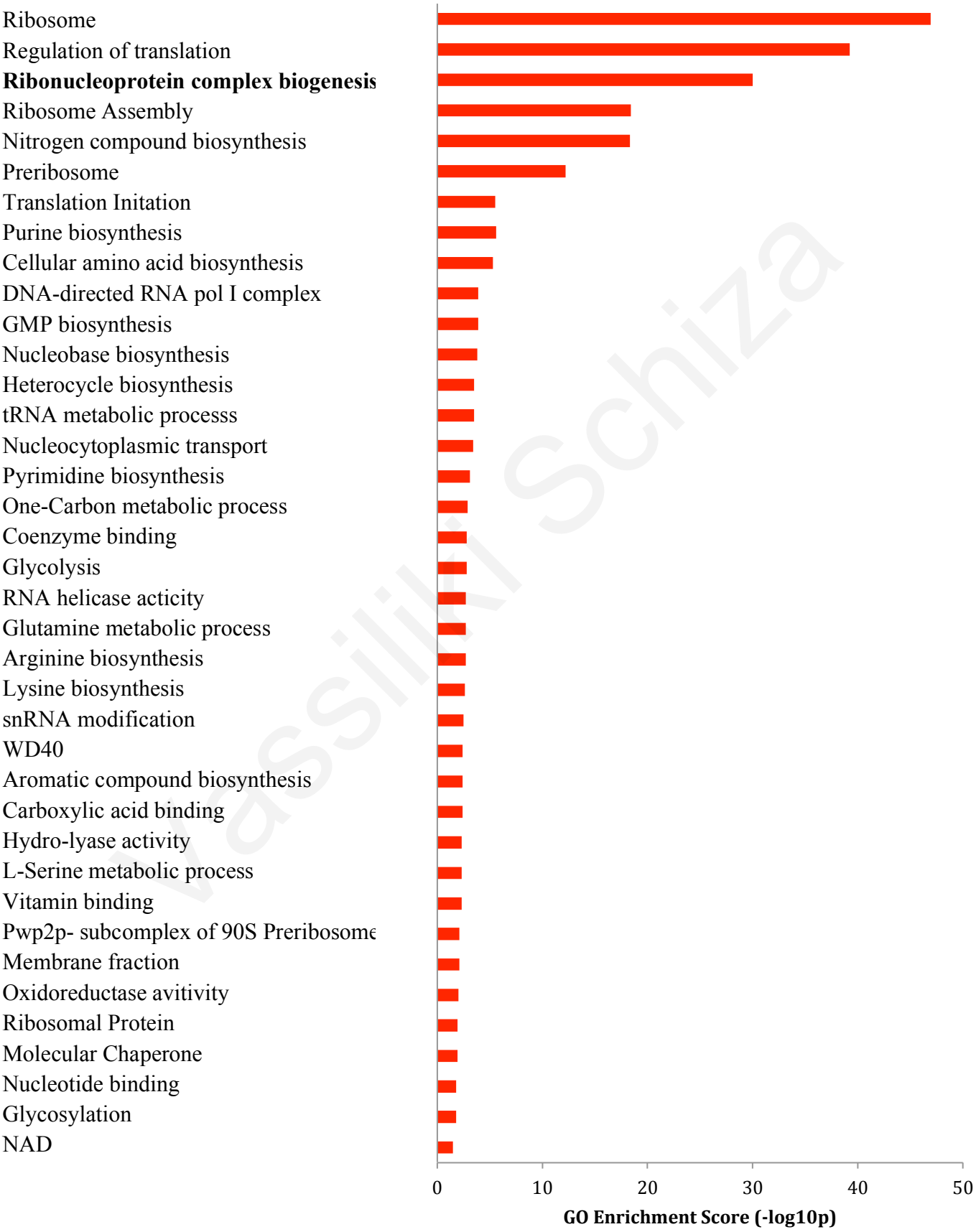

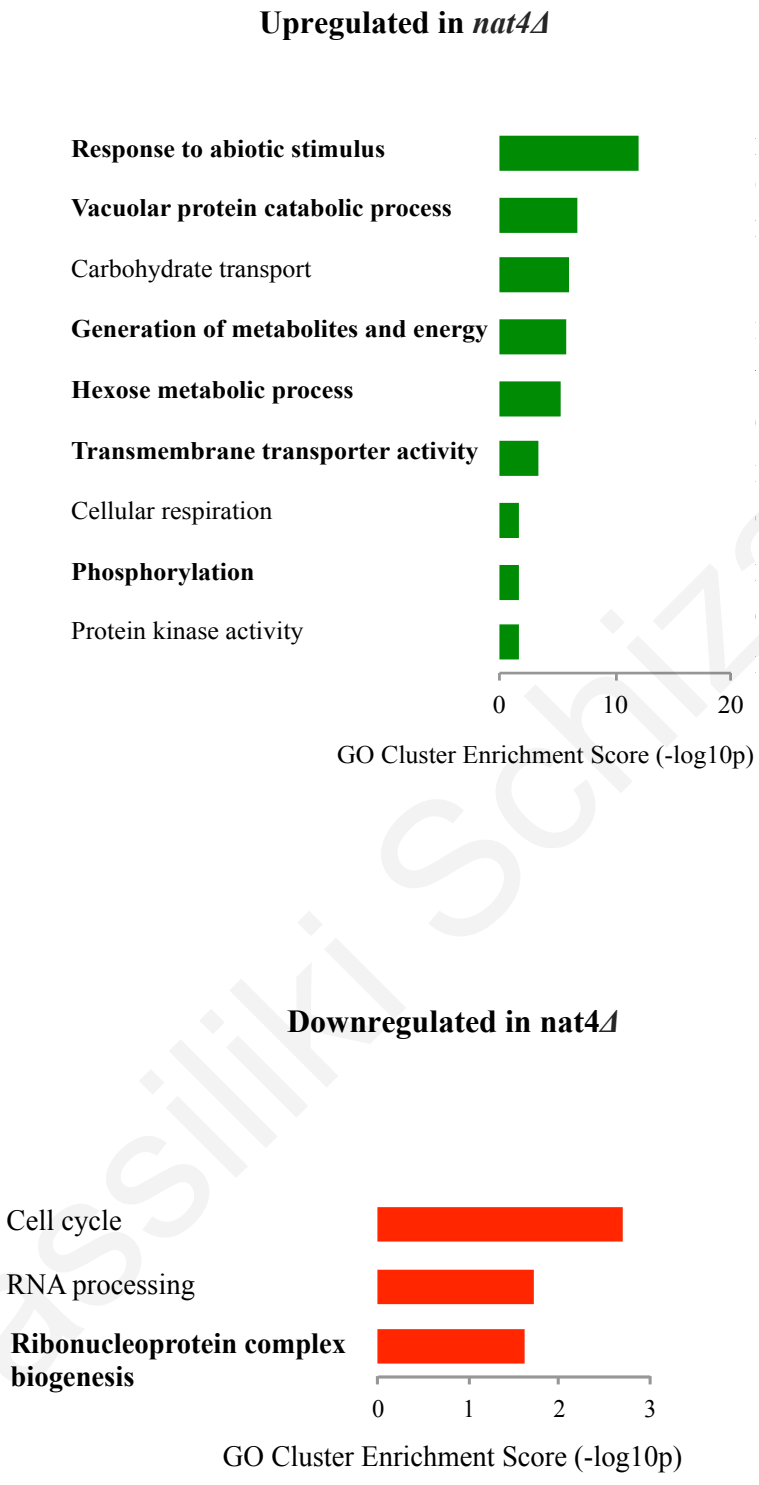

Figure 4.2. Deletion of *NAT4* exhibits gene expression changes that resemble calorie restriction effects. (A) Clustering analysis for upegulated and downregulated genes in CR (0.1%) and *nat4Δ*. Gene ontology was calculated by DAVID software (version 6). GO categories with enrichment scores of $p < 0.05$ are shown.

B

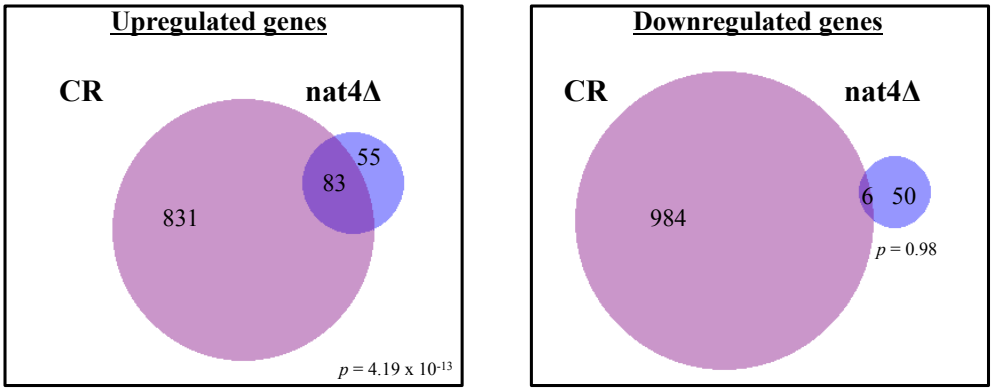

C

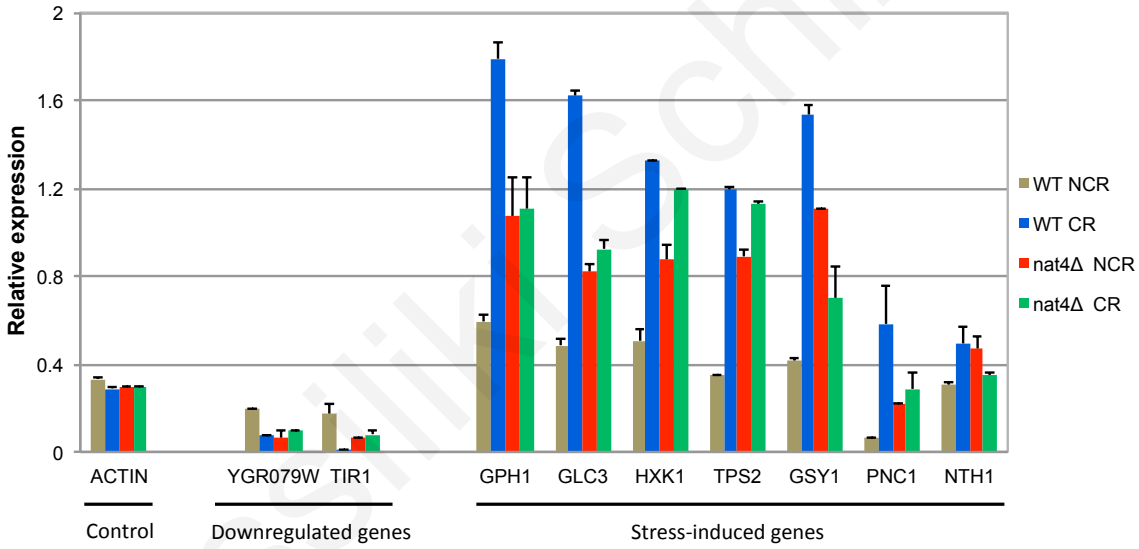

Figure 4.2. Deletion of *NAT4* exhibits gene expression changes that resemble calorie restriction effects (contd). (B) Venn diagrams showing at the left panel, statistically significant overlap (83 genes) between upregulated genes in *nat4Δ* cells (138) and in cells grown in CR conditions (914). At the right panel, venn diagram shows the overlap (6 genes) between downregulated genes in *nat4Δ* cells (56) and in cells grown in CR conditions (990). Size proportional Venn diagrams were drawn using the online software www.cmbi.ru.nl/cdd/biovenn/index.php. Significance of overlap between the two sets is shown as p=4.19 x10^{13} and p=0.98 for upregulated genes and downregulated genes respectively. Venn diagram overlap significance/enrichment was calculated by R package (C) Gene expression assay by qPCR-RT for seven stress-induced genes upregulated *(GPH1, GLC3, HXK1, TPS12, GSY1, PNC1, NTH1)* and two genes that were downregulated (*YGR079W, TIR1*) in *nat4Δ* and CR in RNA-seq data. Expression levels were measured using total RNA extracted from a wild-type strain (BY4741) grown in 2% glucose YPD (NCR) and in 0.05% glucose YPD (CR) and a *nat4Δ* strain (BY4741) grown in 2% glucose YPD (NCR) and in 0.1% glucose YPD (CR). Expression levels were normalized to *TAF10*, that acts as a housekeeping gene as its expression has previously been shown to remain stable, independent of growth conditions (Teste et al., 2009). Error bars indicate s.e.m

4.3 Loss of Nat4 extends lifespan via a CR-mediated pathway

The above results on differential gene expression profiling suggested that lack of Nat4 largely mimics CR (Figure 4.2). Numerous previous studies have shown that CR extends lifespan in several species (Skinner and Lin, 2010) including budding yeast (Lin et al., 2000; Kaeberlein et al., 2004; Smith et al., 2007; Kaeberlein et al., 2010). Therefore, we were interested to examine whether deletion of *NAT4* has an effect on longevity. We perfomed replicative lifespan assays in wild type and *nat4Δ* cells grown in rich media (2% glucose). Interestingly, we found that *nat4Δ* cells show an extended replicative lifespan of about 20% compared to isogenic BY4741 WT cells (Figure 4.3A). In order to check whether the effect we see in BY4741 is mating-type specific (*MAT*a) or not, we also tested lifespan in BY4742, which is a strain possessing the opposite mating type (*MATα*). Furthermore, to stregthen our analysis, we examined the effect of *nat4Δ* on longevity in an additional yeast strain YSC5106. Loss of Nat4 extends lifespan by 40% in the BY4742 strain and by 26% in the YSC5106 strain (Figure 4.3B) confirming our initial observation with the BY4741 strain.

The extension of lifepsan observed for *nat4Δ* cells is very similar to that demonstrated for cells grown in CR (Parrou et al., 1997; Boender et al., 2011; Choi et al., 2011). This is also consistent with the fact that these two conditions showed an epistatic effect with regards to controling the expression of stress-response genes (Fig 4.2C). Hence, we sought to examine whether *nat4Δ* and CR regulate lifespan extension through a similar pathway. To do this, we intially performed replicative lifespan assays in wild-type and *nat4Δ* cells grown under CR conditions (0.05% glucose). In agreement with previous studies, (Lin et al., 2000; Jo et al 2015) CR using 0.05% glucose extended lifespan by about 35% (Figure 4.3C). Importantly, the deletion of *NAT4* in combination with CR (*nat4Δ* 0.05%) does not have an additive effect on longevity, keeping the extension to 33% (Figure 4.3C). This suggests that *nat4Δ* and CR affect lifespan through a common pathway. To verify the above results we also performed replicative lifespan assays in a genetic mimic of CR, *tor1Δ*. The TOR1 kinase is part of the TOR signaling pathway, which is inhibited under CR conditions to prolong lifespan (Kaeberlein et al., 2005). In agreement with results above double deletion of *nat4Δtor1Δ* extended lifespan by 30%, which is not significantly increased compared to the extension of lifespan (29.3%) observed for an isogenic *nat4Δ* strain (Figure 4.3D). This result again points out that *nat4Δ* and CR control longevity through the same pathway.

The above findings raised the hypothesis that the activity of Nat4 might be regulated by CR. To explore this hypothesis, we performed gene expression assays using RT-PCR and we observed a significant decrease in the levels of *NAT4 mRNA* when glucose was diminished from 2% (NCR) to 0.05% (CR) (Figure 4.3E). This result was also found in our RNA-seq analysis where Nat4 was five-fold downregulated in CR. We next wanted to determine whether the activity of Nat4 is also reduced in CR by examing the levels of N-acH4 on chromatin. Thus we performed ChIP assays and tested the deposition of N-acH4 across the rDNA locus in wild type cells grown in CR and compared it to cells grown in NCR. As expected based on our results in Fig 3.2.3, N-acH4 levels were reduced under CR conditions across the entire rDNA locus (Figure 4.3F). Overall, these findings propose that *nat4Δ* increases longevity through a CR-mediated pathway because Nat4 activity is dimished during glucose limitation.

A

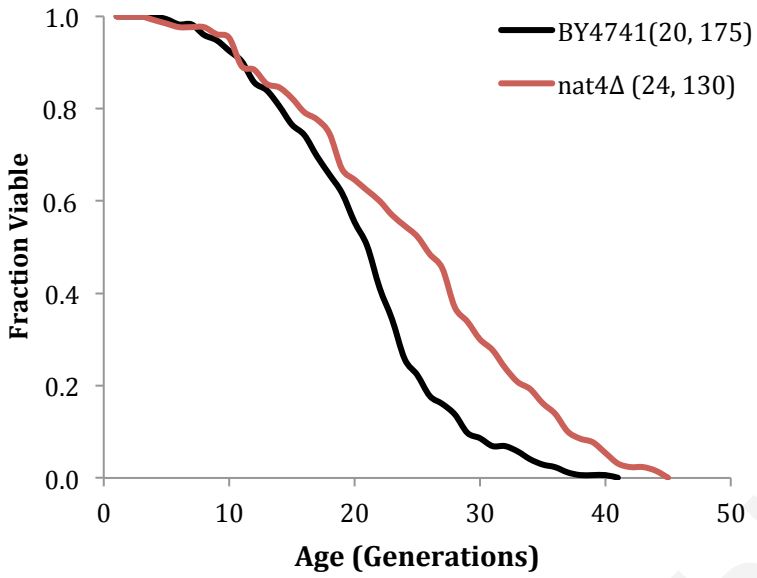

B

Yeast strain	wt	natΔ	p-value
BY4741	19.9 (175)	24 (130)	2.1E-04
BY4742	20.8 (83)	29.3 (60)	3.8E-07
YSC5106	18.3 (118)	23.1 (80)	1.25-05

C

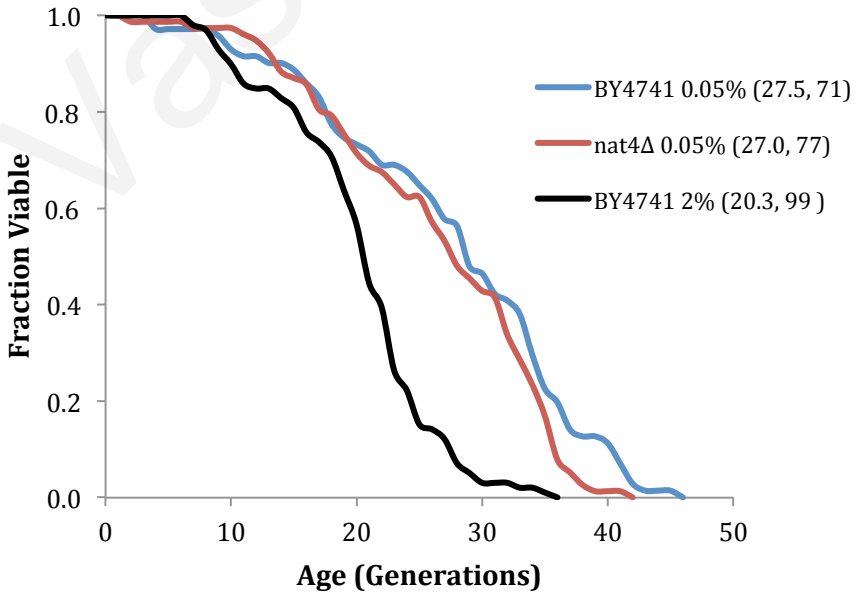

D

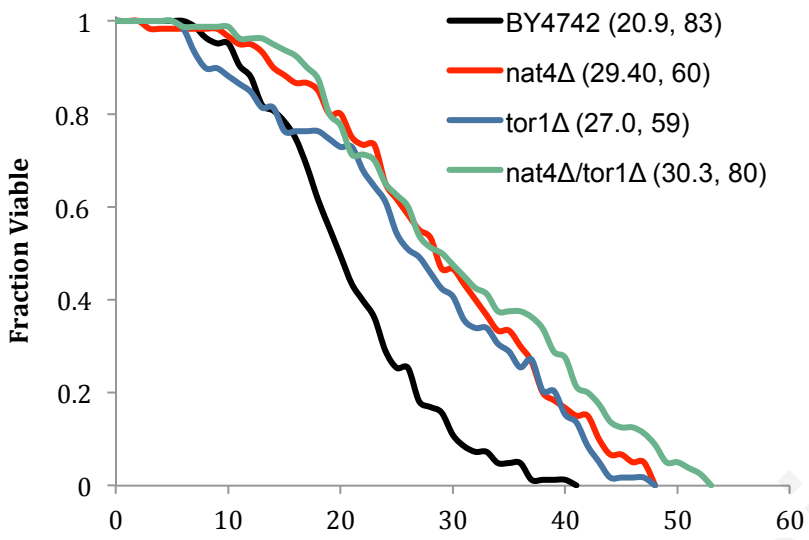

E

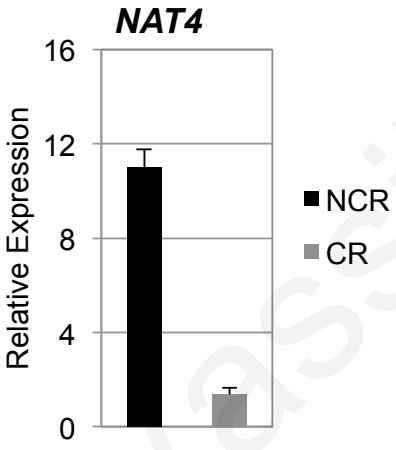

F

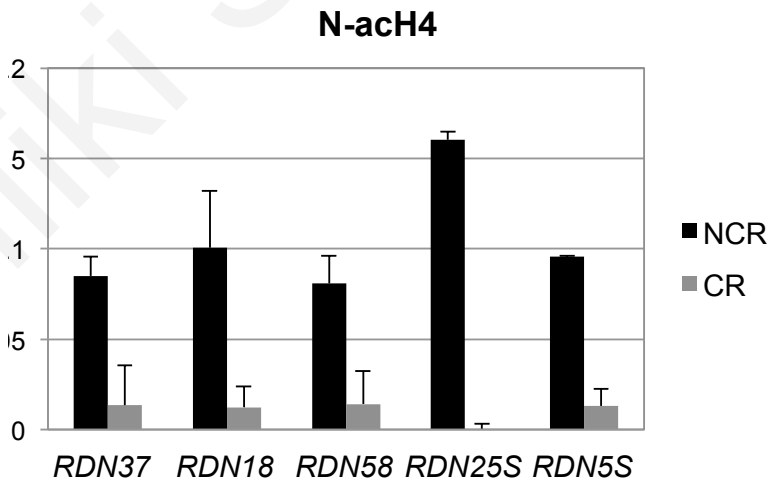

Figure 4.3. Deletion of *NAT4* extends lifespan via a CR-mediated pathway. (A) Replicative lifespan for BY4741 WT and *nat4Δ* in rich media (YPD with 2% glucose). Survival curve is obtained by plotting the fraction of mother cells still alive as a function of replicative age (number of buds produced). Values in parentheses are mean lifespan and number of cells tested.(B) Table showing extension of lifespan in three different yeast strains (BY4741, BY4742 and YSC5106) (C) Replicative lifespan for BY4741 wt and *nat4Δ* under severe CR condition (YPD with 0.05% glucose) compared to BY4741 wt (YPD with 2% glucose). Survival curve is obtained as in (A). (D) Replicative lifespan for BY4742 WT, *nat4Δ, tor1Δ, nat4Δ/tor1Δ,* in rich media (YPD with 2% glucose). Survival curve is obtained by plotting the fraction of mother cells still alive as a function of replicative age (number of buds produced). Values in parentheses are mean lifespan and number of cells tested. (E) Expression levels of *NAT4* analyzed by qRT-PCR using total RNA extracted from a wild-type strain (BY4741) grown in 2% glucose YPD (NCR) and in 0.05% glucose YPD (CR). Expression levels of *NAT4* were normalizd to *TAF10* levels. (F) ChIP experiments were performed in a wild-type strain (BY4741) grown in 2% glucose YPD (NCR) and in 0.05% glucose YPD (CR) using an antibody against N-acH4. The immunoprecpitated chromatin was analyzed by qRT-PCR using primers for the different *RDN* genes. Enrichment was normalized to the levels of histone H4. Error bars in (E) and (F) indicate s.e.m for dublicate experiments.

4.4 Nat4 regulates lifespan through N-terminal-acetylation of H4

Our data so far implied that loss of Nat4 enzymatic activity and consequently decrease in acetylation of its histone substrates (Figure 4.3F), might be responsible for the extension of lifespan observed in *nat4Δ*. To explore this implication, we developed a Nat4 catalytic mutant strain (*nat4E186A*) in which the highly conserved residue E186 was changed to alanine and this mutation was previously shown to abolish the enzymatic activity of Naa40, the human Nat4 ortholog (Magin et al., 2015). Using this catalytic mutant strain we performed replicative lifespan assays and detected an extension in lifespan by approximately 12% in the *nat4E186A* as compared to WT (Figure 4.4A), suggesting that lifespan regulation by Nat4 is dependent on its acetyltransferase activity. To further explore the possibility that Nat4 regulates lifespan through N-alpha acetylation of histone H4, we decided to examine replicative lifespan in a yeast strain in which H4 was compromised for N-terminal acetylation by mutating serine 1. For the purpose of these experiments, we used the mutant of serine 1 to aspartic acid (H4S1D) that is available from the integrated histone mutant library collection (YSC5106). We could not use our previously constructed H4S1P or H4S1A mutants because those mutants were generated in a yeast strain (JHY6) that does not survive the replicative aging assay. In line with our previous results, H4S1D results in extension of lifespan by about 33% compared to the isogenic wild-type strain (Figure 4.4B). This extension is slightly longer than the 24% increase in longevity observed for *nat4Δ* in this background strain (Figure 4.4B). Possibly mutating the Nat4 substrate (H4S1D) might be more influential on longevity as opposed to *nat4Δ* whose activity might be partially complemented by other NATs as indicated by the residual N-acH4 detected in our ChIP assays in *nat4Δ* cells (Figure 3.2.3)

Since H4S1D affects lifespan in a similar manner to *nat4Δ* we expected that it would alter the expression of genes that are also deregulated in the *nat4Δ* strain. Specifically, we examined by RT-PCR the expression of several ribosomal rRNAs (5S, 25S, 5.8S and 18S, as well as their precursor 35S), which are downregulated in *nat4Δ* (see Figure 3.2.3) and the expression of stress-response genes examined above (*GPH1, GLC3, HXK1, TPS2, GSY1, PNC1, NTH1*) whose transcription is upregulated upon deletion of Nat4 (see Figure 4.2C). In accordance to our expectations, the expression of rRNAs was decreased while the expression of stress-response genes was increased in *nat4Δ* within this strain background (Figure 4.4C). Notably, a similar deregulation of these genes was also obtained with the H4S1D mutant strain (Fig 4.4C). This further validates our previous conclusions that Nat4 controls gene expression through a mechanism that involves N-

terminal acetylation of H4. Altogether, the above results strongly suggest that the N-terminal acetyltransfease activity of Nat4 towards H4 is necessary for its role in regulating lifespan.

A

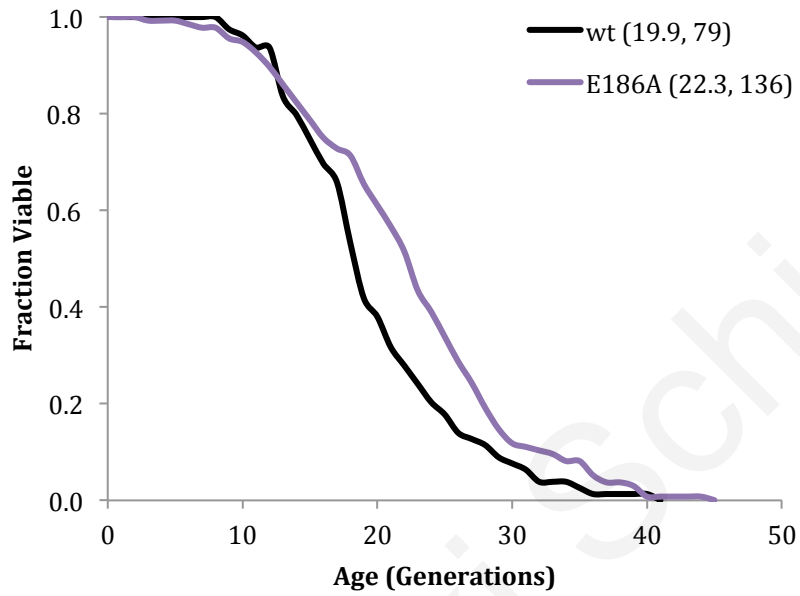

B

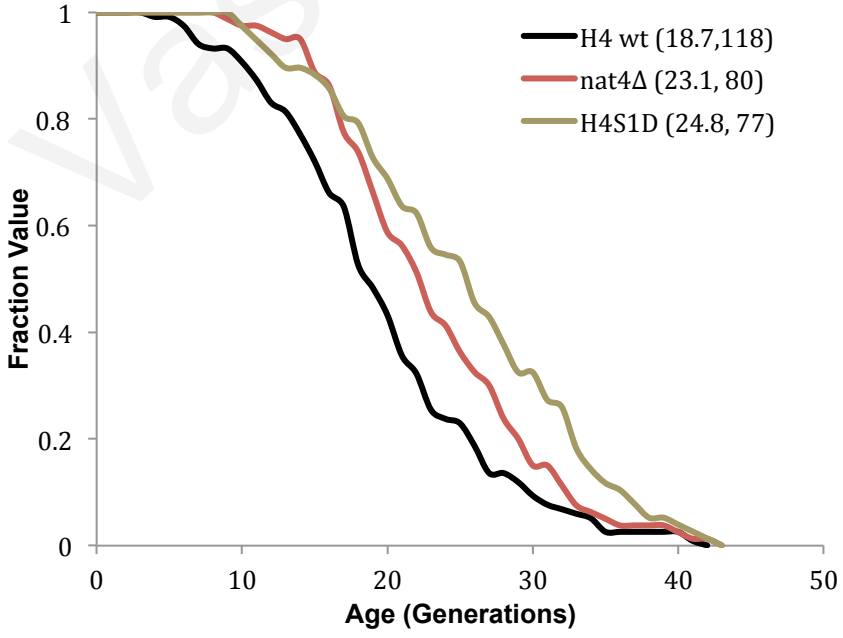

C

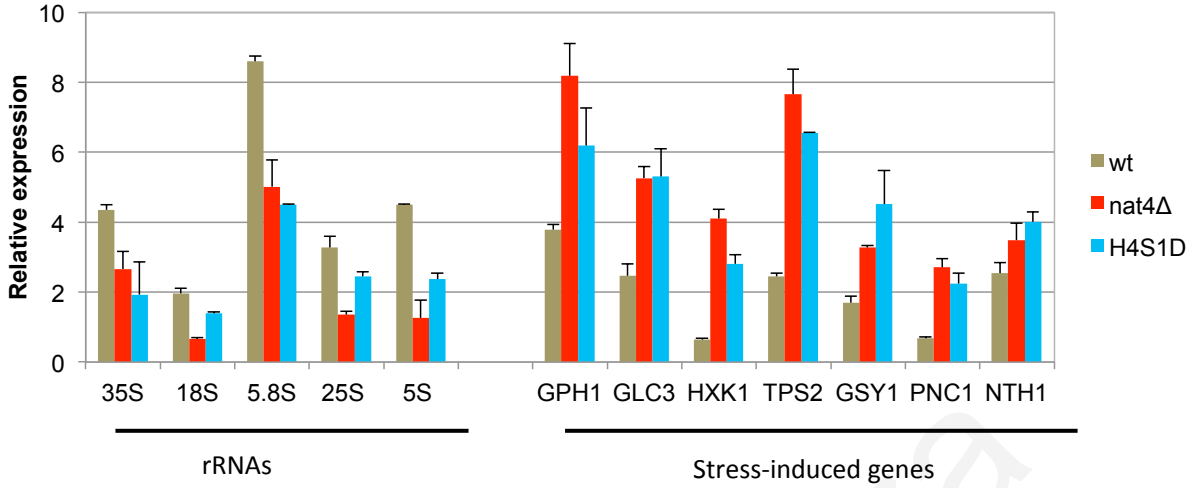

Figure 4.4. Nat4 regulates lifespan through N-terminal acetylation of H4. (A) Replicative lifespan for wild type and catalytic mutant *nat4E186A* cells in 2% glucose YPD, obtained by plotting the fraction of mother cells still alive as a function of replicative age (number of buds produced). Values in parenthesis are mean lifespan for each strain. (B) Replicative lifespan for H4 wild type (H4wt), *nat4Δ* and H4S1D mutant in 2% glucose YPD, obtained as in (A). (C) Gene expression analysis of rRNAs and the different stress-induced genes, performed using the same strains as in (B). The expression levels were normalized to *RPP0* whose expression levels remain unchanged. Error bars indicate s.e.m for triplicate experiments.

4.5 H4R3 is required for the extension of lifespan induced by Nat4 deletion

We have previously shown that H4R3me2a is antagonistic to N-acH4 in regulating rRNA expression (Figure 3.1-3.4). Furthermore, arginine 3 on histone H4 is required for the regulation of rDNA silencing by Nat4 (Figure 3.5). These facts prompted us to investigate whether H4R3 is also required for the extension of lifespan that is induced in the absence of Nat4. To determine this, we used the H4R3K mutant within the YSC5106 strain, which maintains the charge of the amino acid residue but prevents its methylation. We performed lifespan assays using H4R3K, along with a wild-type strain (wt), *nat4Δ* and the double mutant H4R3K *nat4Δ*. Interestingly, *nat4Δ* was unable to extend lifespan in the presence of H4R3K. In fact, the double mutant nat4/H4R3K decreased lifespan by 63% when compared to wt (Figure 4.5A). Additionally, a similar decrease in lifespan was also observed with the H4R3K mutant alone, suggesting this residue and perhaps its methylation act downstream of Nat4 to control replicative lifespan in yeast (Figure 4.5A). These findings demonstrate the requirement of intact H4R3 in order for Nat4 to control longevity and also indicate that this residue and possibly its methylation play an important role in controlling aging of yeast cells.

Based on the above findings we hypothesized that H4R3K should block the deregulation of genes that is observed in *nat4Δ*. To address this hypothesis we performed gene expression analysis using total RNA isolated from wt, *nat4Δ*, H4R3K and *nat4Δ*/H4R3K strains. Consitent with our previous finding on 25S rRNA (Fig 3.5B), H4R3K blocks the reduction of all rRNAs (18S, 5.8S, 5S, and their precursor 35S) that is stimulated by Nat4 deletion (Figure 4.5B, compare *nat4Δ* to *nat4Δ* H4R3K). Likewise, H4R3K blocks the upregulation of stress-response genes, which is typically induced in the absence of Nat4 (Figure 4.5B, compare *nat4Δ* to *nat4Δ* H4R3K). Notably, H4R3K does not have the opposite effect on gene expression compared to *nat4Δ* but instead maintains the expression of these genes to WT levels (Fig 4.5B, compare WT to H4R3K). Therefore, we conclude that, firstly, H4R3 is required for Nat4-mediated regulation of gene expression and, secondly, H4R3 is vital for Nat4 to control longevity.

A

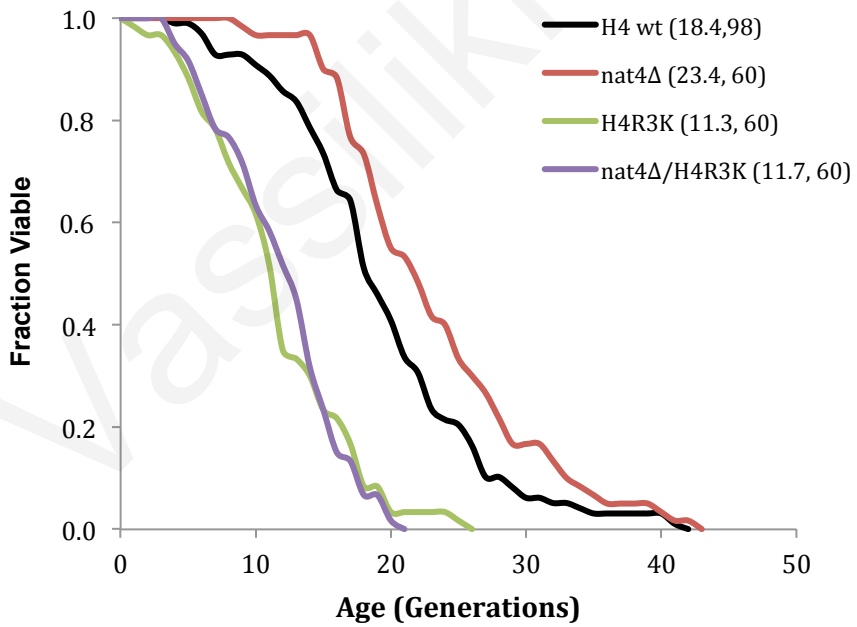

B

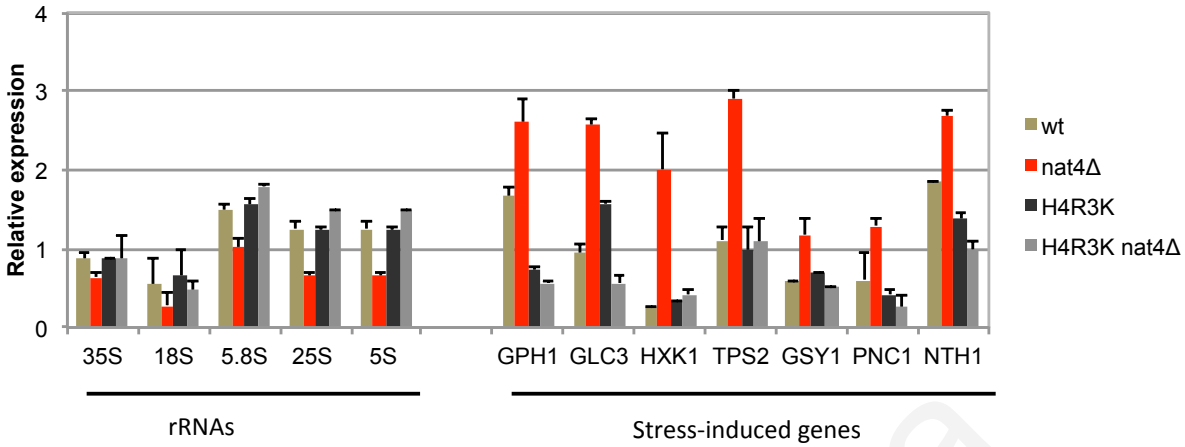

Figure 4.5. H4R3 is necessary for the extension of lifespan mediated by Nat4 deletion. (A) Replicative lifespan for H4 wt, *nat4Δ, H4R3K* and *nat4Δ/ H4R3K* in rich media (YPD with 2% glucose). Survival curve is obtained by plotting the fraction of mother cells still alive as a function of replicative age (number of buds produced). Values in parentheses are mean lifespan and number of cells tested. (B) Expression levels of rRNAs 18S, 5.8S, 25S, 5S and their precursor 35S; and of the different stress-induced genes *GPH1, GLC3, HXK1, TPS2, GSY1, PNC1, NTH1,* grown in 2% glucose YPD. Total RNA was extracted from the strains indicated in (A) and was analyzed by qRT-PCR. Expression levels were normalized to *RPP0* whose expression remains unaltered in these conditions. Error bars indicate s.e.m for triplicate experiments.

4.6 Nat4 regulates longevity through an increased resistance to stress

From our results we can conclude that Nat4 affects expression both at the rDNA locus (Figure 3.2.3) and stress response genes (Figure 4.2). In order to look more into the mechanism by which Nat4 may induce longevity, we first explored the possibility that the rDNA locus is implicated within this mechanism. Evidence from other studies raised the hypothesis that Nat4 regulates longevity either by reducing biogenesis of ribosomal subunits (Steffen et al., 2008) or by promoting rDNA instability (Kobayashi et al., 2004). Hence, to explore this hypothesis, we first analyzed by polysome profiling the abundance of ribosomal subunits and polysomes in wild type cells and cells that lack Nat4 (*nat4Δ*). By looking at the polysome profiles of the two strains we observed no change in ribosome biogenesis between wild type and *nat4Δ* cells (Figure 4.6A). Thus, we conclude that Nat4 does not regulate longevity by decreasing ribosome biogenesis or by general reduction of protein translation (Steffen et al., 2008; Smith et al., 2008; Dang et al., 2014).

A primary cause of ageing is instability of rDNA (Kobayashi et al., 2011). Such instability leads to homologous recombination between rDNA repeats leading to the

generation of toxic ERCs and ageing (see section 1.4.3.1) (Kaeberlein et al., 1999). A decrease in ERC accumulation has previously been associated with increased lifespan (Sinclair and Guarente, 1997; Kaeberlein et al., 1999). Hence, we tested whether *nat4 Δ* could reduce the accumulation of ERCs by using quantitiatve real-time PCR targeting rDNA sequences. Interestingly, we observed no change in rDNA copy number in *nat4Δ* compared to wild type cells (Figure 4.6B) suggesting that *nat4Δ* does not increase longevity by suppressing the formation of ERCs. As expected, in the *fob1Δ* the rDNA copy number decreased (Figure 4.6B) since in the absence of Fob1 rDNA recombination and ERC formation decrease (Kobayashi et al., 1998).

Moreover, it has been shown that recombination frequency (copy number instability) in the rDNA determines life span (Kobayashi et al., 2004). The recombination frequency is controlled by the Sir2 protein which represses transcription of the E-pro bidirectional promoter found within the rDNA region in order to suppress rDNA recombination and maintain the rDNA copy number to physiological levels (Kobayashi and Ganley, 2005). Hence, the expression of E-pro is indicative of high rDNA recombination and hence instability (Kobayashi and Ganley, 2005). In order to investigate whether loss of Nat4 affects through this process we examined the expression of E-pro using Northern analysis in wild type cells, *nat4Δ* cells and *sir2* cells as control. In *sir2Δ*, transcription of E-pro is increased as expected. However, we could not detect a diffference in E-pro expression between wild type and *nat4Δ* cells (Figure 4.6C), ruling out the possibility that Nat4 regulates lifespan through rDNA instability. These results suggest that the rDNA region might not be part of the underlying mechanism for Nat4's role in lifespan.

Previous papers suggested that certain genetic mutations (*tor1Δ, tPK1/2/3Δ, Sch9Δ, hxk2, pnc1Δ isw2Δ)* mimic calorie restriction effects by upregulating stress response genes (Toda et al., 1987; Lin et al., 2000; Fabrizio et al., 2001; Kaebelein et al., 2005; Powers et al., 2006). Recently, a model was proposed in which the absence of the chromatin remodelling enzyme *ISW2* regulates longevity through stress repsonse pathways and this mimics CR in extending longevity (Dang et al., 2014). Hence, we sought to examine whether *nat4Δ* regulates lifespan extension through a similar pathway. One of the genes that is highly induced in the absence of Nat4 is the nicotinamidase gene *PNC1* (Figure 4.6D), which was also shown to be induced under CR conditions as part of a stress response to nutrient limitation and its overexpression prolongs lifespan (Anderson et al.,2003; Gallo et al., 2004). Therefore, we sought to determine whether the expression of *PNC1* was required for the *nat4Δ*-mediated longevity. We constructed a mutant in which

nat4Δ was combined with the absence of *PNC1* (*nat4Δ pnc1Δ*) and performed replicative lifespan assays. Our data show an extension in lifespan by 28% in *nat4Δ* as expected but intrerestingly, *nat4Δ pnc1Δ* restores lifespan to wild type levels, indicating that *PNC1* is necessary for Nat4-mediated extension of lifespan (Figure 4.6D).

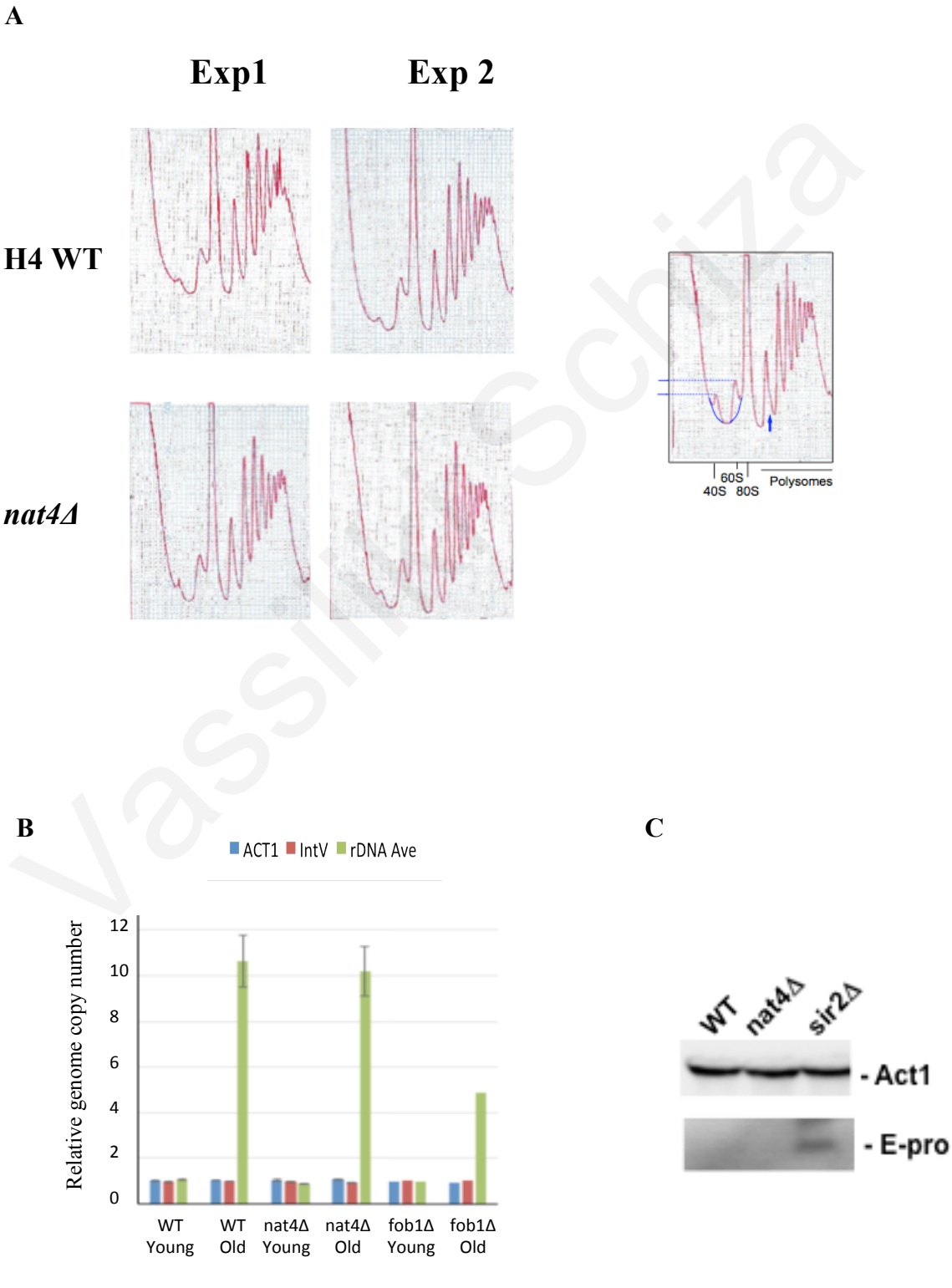

D

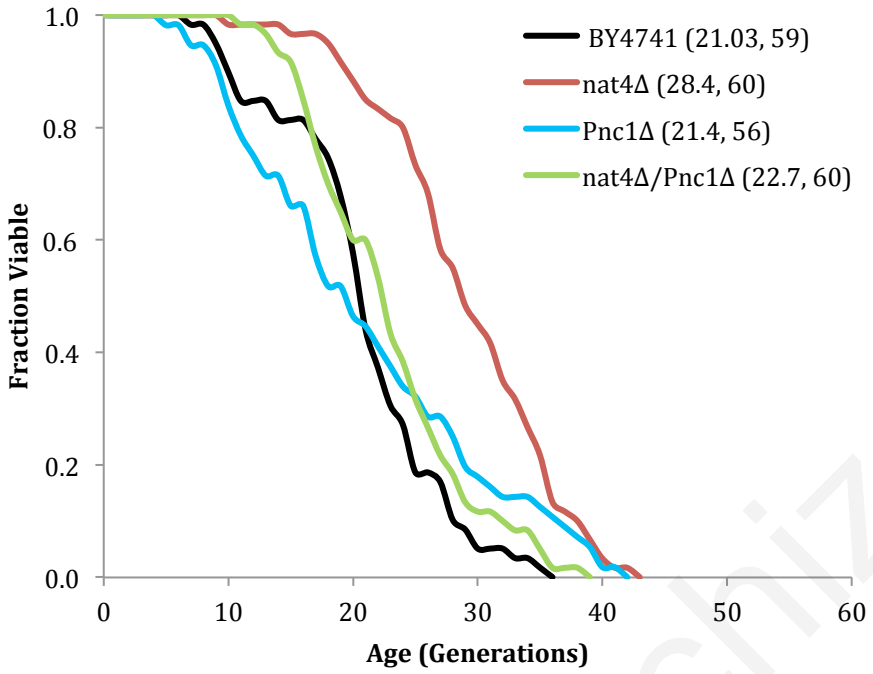

Figure 4.6. Nat4 does not regulate longevity through ribosome biogenesis or rDNA stability. (A) Polysome profiles for wt and *nat4Δ* from two different experiments (Exp1, Exp2). (B) Quantitative real-time PCR analysis of rDNA copy number for young and old WT and *nat4Δ* cells. *fob1Δ* cells were used as a positive control. Error bars indicate SEM. (C) Northern blot analysis using total RNA from wt, *nat4Δ* and *sir2Δ* cells. (D) Replicative lifespan for wild type, *nat4Δ, pnc1Δ* and double mutant *nat4Δ pnc1Δ* in 2% glucose YPD, obtained by plotting the fraction of mother cells still alive as a function of replicative age (number of buds produced). Values in parenthesis are mean lifespan for each strain.

CHAPTER 5
DISCUSSION

5. Discussion

Histone H4 N-terminal acetylation (N-acH4) is an abundant and conserved modification (Polevoda and Sherman 2003; Starheim et al., 2012). Although previous studies investigated the biological role of the yeast (Nat4) and human (Naa40) enzymes that catalyse this histone modification (Polevoda et al., 2009; Liu et al., 2009; Liu et al., 2012) the knowledge on the molecular function of histone N-terminal acetylation remained marginal. The work in this study exposes the role of histone N-terminal acetylation and its associated enzyme Nat4 in the regulation of gene expression. First, we revealed that histone H4 N-terminal controls the deposition of an adjacent histone mark (H4R3me2a) and by doing so it regulates the expression of the ribosomal DNA locus (Chapter 3). Second, we identified an important novel biological role of Nat4 and N-acH4 in regulating yeast cellular lifespan by modulating the expression of stress reponse genes (Chapter 4).

5.1 Regulation of rDNA silencing by Nat4

Our initial hypothesis that N^{α}-terminal acetyltransferase Nat4 might be involved in the regulation of gene expression is supported by a mechanistic model in which N-acH4 mediated by Nat4 strongly inhibits the activity of Hmt1 methyltransferase towards H4R3 (Figure 3.4). This inhibition leads to activation of the rDNA locus. Removal of N-acH4 by a yet unknown mechanism allows deposition of H4R3me2a and increases repression of rRNA transcription (Figure 5.1). This mechanism plays a role during nutrient deprivation in order to reduce the expression of the rDNA region in response to the limited source of energy. In the absence of N-acH4, internal lysine acetylation at K5, K8 and K12 catalysed by Esa1 (Clarke et al., 1999) or Hat1 (Poveda et al., 2009) remain unaffected (Figures 3.6.1A, compare lanes 1, 2 and 3.6.1B). These acetyl marks can fine-tune the levels of H4R3me2a because otherwise excessive methylation of H4R3 by loss of Nat4 and K5,8,12 acetylation will result in a severe growth defect (Figures 3.6.4B and 3.6.4C, Figure 5.1).

Moreover, the mechanism we propose explains the previously observed synthetic defect of the H4K5,8,12R *nat4Δ* mutant strain (Polevoda et al., 2009). Whether the growth defect observed in our experiments (Figure 3.6.4B-C) is due to deregulation of the rDNA region only or whether other genomic loci whose expression is influenced by H4R3me2a also contribute to this phenotype is still unclear. There are two possible scenarios, which are not mutually exclusive, on how H4R3me2a then mediates rDNA silencing in yeast.

First, it was proposed that H4R3me2a facilitates recruitment of Sir2 to the rDNA region (Yu et al., 2006). Sir2 is part of an rDNA silencing complex called regulator of nucleolar silencing and telophase exit (RENT) complex, which is also composed of two more subunits, Net1 and Cdc14 (Shou et al., 1999; Visintin et al, 1999). Net1 recruits Sir2 to the rDNA and is also required for rDNA silencing. Thus, we tested the binding of Net1 on the rDNA in the absence of Nat4. Interestingly, Net1 showed an increase in binding in the absence of Nat4 compared to wild type cells (data not shown). Thus, it is possible that H4R3me2a mediates rDNA silencing through binding of Net1 on the rh et al., 2009; Hole et al., 2011). However, it has been suggested that Nat4 and hNaa40 may target H4 post-translationally because a significant amount of hNaa40 localizes to the nucleus (Liu et al., 2009; Hole et al., 2011). Similarly to other acetyl marks such as H4K5ac and H4K12ac (Ai et al., 2004), N-acH4 might be catalyzed on soluble nuclear histones that are subsequently incorporated into chromatin. Intriguingly, N-alpha-terminal acetylation has already been proposed to occur post-translationally on other proteins (Helbig et al., 2010; Helsens et al., 2011; Varland et al., 2015). How N-acH4 is then removed from histones needs further examination. One possibility is through histone exchange by which unacetylated H4 replaces N-terminally acetylated H4 found in chromatin. Another scenario is through active deacetylation mediated by a deacetylase, an activity that has not been demonstrated yet for any protein N-terminal acetylation mark (Starheim et al., 2012; Varland et al., 2015).

Interestingly, Nat4 is not the only Nat that has been implicated in the regulation of heterochromatic regions in yeast. NatA has a role in chromatin silencing (Gautchi et al., 2003; Geissenhoner et al., 2004). However, NatA functions through a mechanism that is distinct from that of Nat4 for several reasons. Firstly, NatA establishes telomeric and HML silencing by acetylating Orc1 and Sir3 in order to stimulate their recruitment onto chromatin (Geissenhoner et al., 2004; Onishi et al., 2007; van Welsem et al., 2007). However, silencing at the rDNA region does not involve these proteins (Huang et al., 2003). Secondly, in our experiments, the absence of Ard1 (the catalytic subunit of NatA) has no effect on the levels of H4R3me2a (Figure 3.2.5A). Finally, in the *ard1Δ* strain, the levels of 25S rRNA are not significantly altered compared to a wild-type strain (Figure 3.2.5B). Therefore, we believe that Nat4 and NatA impact on chromatin silencing through different pathways.

5.2 Model of N-acH4 in rDNA silencing may be conserved in higher eukaryotes

The cross-talk we propose among N-acH4, internal lysine acetylation and H4R3 methylation might be conserved in mammals since the activity of Nat4 towards H4 is conserved in humans (Hole et al. 2011) and its ortholog hNaa40 can re-establish normal levels of H4R3me2a in the absence of Nat4 (Figure 3.3F–G). Furthermore, mass spectrometry analysis of mouse histone H4 revealed that N-terminal acetylation co-exists with K5, K8 and K12 acetylation, and has an inverse relationship with H4R3 methylation (Tweedie-Cullen et al., 2012). Interestingly, this anticorrelation in mouse cells does not involve asymmetric dimethylation but rather a trimethylated form of H4R3 (Tweedie-Cullen et al., 2012), whose existence is still under debate. The mutual exclusive pattern between N-terminal acetylation and H4R3 methylation becomes even more apparent on H2A peptides, (Tweedie-Cullen et al., 2012), suggesting that in mammals this modification crosstalk could also occur on histone H2A. This is consistent with the fact that mammalian H2A (Ser-Gly-Arg-Gly- Lys) has an arginine at position 3 and its N-terminal sequence is identical to H4, in contrast to yeast H2A (Ser-Gly-Gly-Lys-Gly) whose third residue is a glycine. Determining whether Naa40 utilizes a similar mechanism to control gene activation in mammalian cells is intriguing, considering that this enzyme has a pro-apoptotic function and was found significantly downregulated in hepatocellular carcinomas (Liu et al., 2012).

5.3 Regulation of Longevity by Nat4

Evidence that the proposed crosstalk between N-acH4 and H4R3me2a (Figure 5.1) might work in lifespan came from the fact that this crosstalk was functional under CR conditions (Figure 3.7). The established link between enhanced rDNA silencing with calorie restriction (Lin et al., 2002; Lamming et al., 2005) and increased lifespan (Kaeberlein et al. 2010), led us to examine whether CR affects these modifications. Consistent with the finding that CR indeed induces changes (Figure 3.7; Figure 4.3F), we were interested to determine whether these modifications and their respective enzymes are part of a mechanism that extends cellular lifespan and we uncovered a role for Nat4 in a longevity pathway that is induced by CR (Chapter 4). Accordingly, in a transcriptome analysis performed in wild type and Nat4 deleted cells, we observed a significant deregulation of metabolic and stress-induced genes that are also activated in response to

CR (Lee et al., 2008; Steffen et al., 2008; Wang et al., 2010; Sharma et al., 2011; Dang et al., 2014) (Figure 4.1- 4.2).

The above evidence prompted us to investigate the role of Nat4 in regulating longevity. Deletion of Nat4 indeed extended lifespan and this was dependent on its enzymatic activity (*nat4E186A*) and the N-terminal acetylation of its substrate histone H4 (H4S1D). This longevity extension occurs via a CR-mediated pathway (Figure 4.3A, 4.4A,B) and this is supported by various findings: a) deletion of *NAT4* in combination with CR does not have an additive effect on longevity (Figure 4.3-4.4A), b) a genetic mimetic of CR (*tor1Δ,* Kaeberlein et al., 2005) when combined with *nat4Δ* does not have an additive effect on *nat4Δ* mediated longevity (Figure 4.3D), c) CR represses Nat4 expression and the deposition of N-acH4 onto chromatin (Figure 4.3E,F) and d) deletion of *PNC1* which governs the longevity induced by CR (Anderson et al 2003; Gallo et al., 2004) also blocks the longevity that is stimulated by *nat4Δ* (Figure 4.6D).

5.4 Nat4-mediated regulation of longevity through induction of stress response

Based on our findings that linked Nat4 with a CR-mediated pathway (Chapter 3 and 4), the regulation of the rDNA region (Chapter 3) and induction of stress-response genes (Chapter 4), we predicted that Nat4 would operate through one or more of the following three reported CR-controlled mechanisms: a) loss of Nat4 would decrease rDNA stability to induce longevity (Sinclair and Guarente, 1997; Kaeberlein et al., 1999; Kobayashi et al., 2004; Kobayashi and Ganley, 2005; Kobayashi et al., 2011;), b) *nat4Δ* would increase the stress resistance of cells to prolong their lifespan (Toda et al., 1987; Lin et al., 2000; Fabrizio et al., 2001; Kaebelein et al., 2005; Powers et al., 2006; Dang et al., 2014) and/or c) deletion of Nat4 would reduce ribosome biogenesis and protein translation to stimulate cellular longevity (Smith et al., 2008; Steffen et al., 2008; Johnson et al., 2013). We report that the presence of arginine methylation on histone H4 (H4R3) is necessary in order for Nat4 to control replicative lifespan in yeast (Figure 4.5). Histone H4 acetylation (H4K16ac) has already been implicated in the regulation of lifespan in yeast through a mechanism that maintains telomeric chromatin intact (Dang et al., 2009).

We initially anticipated that N-acH4 and H4R3me2a, if involved in lifespan regulation, would be part of a pathway that controls rDNA silencing (Lin et al., 2002; Lamming et al., 2005), since our data show that deletion of *NAT4* does not affect telomeric

silencing (Figure 3.2.1). Previous studies demonstrated that Sir2 affects yeast lifespan by regulating rDNA recombination (Kaeberlein et al., 1999) and Hmt1 activity represses this process (Yu et al., 2006). Thus, we further wanted to explore if loss of N-acH4 affects rDNA recombination. From our data, however, we rule out the possibility of rDNA involvement for Na4-mediated longevity based on two facts. First, since ERC accumulation in the cell is the result of rDNA instability (Kobaysahi et al., 2005), we checked ERC levels in wild type and *nat4Δ* but did not observe any changes in ERC accumulation between the two (Figure 4.6B). Second, during rDNA recombination, the silencing protein Sir2 represses transcription of E-pro and prevents the appearance of the first rDNA circle that accumulates in mother cells by creating a silenced chromatin. We observe no change in the levels of E-pro expression as indicated by Northern blot (Figure 4.6C).

Previous studies have shown that ribosome protein production is decreased in the presence of calorie restriction conditions and through downregulation of Tor1, proposing an extension of lifespan as a result of a decrease in ribosome biogenesis (Steffen et al., 2008; Johnson et al., 2013). Our results point out that Nat4-mediated longevity is not a result of a decrease in ribosome biogenesis as shown by ribosome profliling analysis (Figure 4.6A). We estimate that downregulation of the ribosome biogenesis cluster in our gene ontology results (Figure 4.2A) is probably due to a uniform decrease in rRNA transcription for the cell to save energy by producing less ribosomes in the absence of Nat4; and not a cause of Nat4-mediated longevity.

Moreover, a hallmark of ageing is the accumulation of cellular damage. Several mechanisms are known to be activated by the cell to fight this damage encompassing a cellular stress response system (Guarente et al., 2008). By increasing resistance to different types of stress such as heat shock or oxidative damage yeast cells live longer (Sharma et al., 2011; Delaney et al., 2103). It is possible that Nat4 regulates lifespan by bypassing Sir2-dependent rDNA silencing and by activating cellular stress pathways through upregulation of metabolic and stress induced genes (Figures 4.1, 4.2, 5.2). A similar CR-mediated longevity pathway that is distinct from TOR and sirtuin pathways has been previously reported, as deletion of the chromatin remodeling complex Isw2 extends longevity through induction of genotoxic stress response (Dang et al., 2014). Our findings support the idea that upon inactivation of Nat4, an environment that mimics calorie restriction is created, which provides increased resistance to stress as yeast cells age. In addition, metabolic and stress response genes become activated, rendering cells in a stress

responsive state (Figure 5.2).

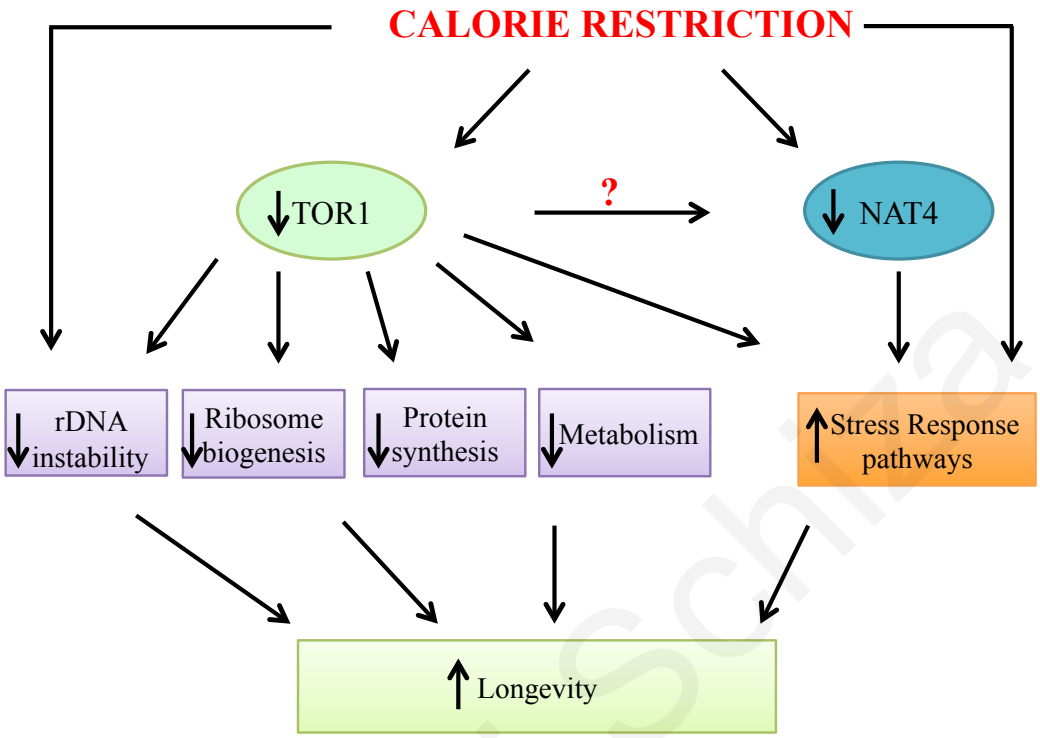

Figure 5.2: Proposed model of Nat4 mediated-longevity. Under calorie restriction conditions a decrease in rDNA instability occurs and leads to an increase in longevity. Tor1 is inhibited and this leads to several changes in the cell. In addition to rDNA instability, a decrease in ribosome biogenesis, in protein synthesis as well as metabolism takes place leading to an increase in longevity. Nat4 is downregulated and extends lifespan through a CR-mediated pathway. Polysome profiling did not show a decrease in ribosomal subunit formation in the absence of Nat4, suggesting that Nat4 does not mediate longevity through ribosome biogenesis. In addition, loss of Nat4 does not seem to affect rDNA stability or ERC formation. As a result of nutrient deprivation, Nat4 is downregulated and extends lifespan through a response to stress since a number of stress-induced genes are upregulated. Whether Tor1 activates Nat4 expression is still not known (?).

5.5 Significance of this work

Findings from this work could provide general mechanistic implications for histone N^{α}-terminal acetylation. Importantly, lack or abnormal N^{α}-terminal acetylation results in defects, preventing regular protein function. The importance of N^{α}-terminal acetylation in human cell biology and disease has been increasingly recognized (Arnesen, 2011; Starheim et al., 2012, Varland et al., 2015). Recently, studies revealed the importance of human hNaa40 in hepatic lipid metabolism and hepatocellular carcinogenesis (Liu et al.,

2009). These findings imply the role of Nat4 in carcinogenesis and suggest its application in cancer therapeutics. To date, NAT compounds have been developed that can target the NatA complex and its catalytic subunit Naa10 as well as the enzyme NatE/Naa50 (Foyn et al., 2013; Kalvik and Arnesen, 2013; Popp et al., 2015). In addition, Nat4 shows unique structural features; such as the Nat4 substrate site that is tailored only for the four first residues (Ser-Gly-Arg-Gly) of the N terminus of histone H4 and H2A as well as the presence of a unique Arg3 pocket that can be exploited to develop Nat4 inhibitors (Magin et al., 2015).

Moreover, histone modifications provide an important platform for many processes such as gene transcription. Studies have shown that misregulation of histone modifications and histone modifying enzymes is associated to human disease. Importantly, aberrant histone modification profiles are intimately linked to cancer. Hence, these modifications and their enzymes are considered to be good targets for therapy. Notably, results from this study revealed a crosstalk amongst histone N^{α}-terminal acetylation and other histone modifications. Such crosstalks might lead to certain functional outputs implicated in disease. Thus, histone N^{α}-terminal acetylation and Nat4 could be further exploited as therapeutic targets.

Furthemore, since deletion and inhibition of enzymatic activity of *NAT4* showed an extension in lifespan, Nat4 could be further explored as a candidate for novel therapeutics for delaying the onset and progression of physiological declines that characterize physiological ageing; as well as various premature age-associated diseases in humans, such as the Werner syndrome (Yu et al., 1997). Interestingly, Naa40 knockout in mice has been reported to offer protection from an age-associated disease, hepatic stetatosis. This possibly shows that the role of Nat4 in cellular longevity is maintained in mammals, pointing out the significance of our findings.

5.6 Future Directions

Strong cellular stress response capability has been associated with longevity and this is supported by the existence of the longest-lived rodent, the naked mole rat. This mammal lives approximately eight times longer than mice and despite the oxidative damage that it demonstrates at a young age, it shows much stronger resistance to various stressors (Lewis et al., 2012). To further evaluate the contribution of *nat4Δ* to the stress response specifically associated with aged cells, expression changes should be examined by qRT-PCR for stress response genes in wild type and *nat4Δ* cells in both young and old cells. We expect a higher expression of stress response genes in the aged population of *nat4Δ* compared to old wild type cells. Such experiments will confirm whether induction of stress genes that results from inactivation of Nat4 provides cells with an advantage to handle the damage induced during ageing, thus leading to longevity effects. Moreover, loss of arginine methylation (H4R3K) shortens lifespan, even when Nat4 is deleted (Figure 4.5). This shows that perhaps H4R3K does not shorten lifespan through deregulation of metabolc and stress response genes, but through a mechanism independently from Nat4. Furthermore, it would be interesting to examine whether the regulation of lifespan by Nat4 is evolutionary conserved among eukaryotes. Although deletion of *NAA40* in *Drosophila* melanogaster seems to be lethal (data not shown), it would be interesting to check for conservation of longevity in *Caenorhabditis elegans*, which has a Nat4 ortholog known as *Y38A10A.7* that contains all critical amino acids and motifs of Nat4, indicating that most likely functions like Nat4.

It is important to note that by changing our cut off from 2-fold to 1.5-fold in our *nat4Δ* transcriptome data, we observe an increase in the expression of autophagy-related genes (i.e. *ATG1*, *ATG8, ATG22*). Possibly, the autophagy response is activated in *nat4Δ* cells. Autophagy is an essential cellular process in which parts of the cytosol are encapsulated into vesicles and fuse with vacuoles (He and Klionsky, 2009). Interestingly, our gene ontology data show vacuolar protein catabolic process to be the second most upregulated group in gene ontology clustering analysis of *nat4Δ* (Figure 4.2A), which is also present in the CR transcriptomics data (Figure 4.2A). Autophagy is a major player in cellular homeostasis and an increase in autophagy is induced under calorie restriction conditions (Tsukada and Ohsumi, 1993). Furthermore, it can delay the pathogenic manifestations of ageing and age-associated disease (Gelino and Hansen, 2012; Madeo et al., 2010; Rubinsztein et al., 2011) and is linked to prolonged lifespan (Eisenberg et al., 2009). Moreover, there is an established link between autophagy and increased longevity.

Inhibition of autophagy has been shown to cause premature ageing and shortens lifespan, whereas activation delays ageing and extends lifespan in many organisms (Rubinsztein et al., 2011). Moreover, regulation of autophagy has been characterized to depend on epigenetic processes such as histone acetylation (Fullgrabe et al., 2013; Eisenberg et al., 2009). Recently, it was demonstrated that acetylation at lysine 16 of histone H4 (H4K16ac) influences the transcriptional status of autophagy (*ATG*) genes and determines the outcome of autophagy (Fullgrabe et al., 2013).

Therefore it is worth investigating in the future whether *nat4Δ* activates constitutively the autophagy pathway in order to prolong lifespan. In addition, future experiments will examine whether the loss of N-acH4 mediated by Nat4 promotes longevity through regulation of autophagy-associated genes. Initial experiments will involve the use of fluorescence microscopy and yeast autophagy measurements in wild-type and *nat4Δ* cells by monitoring the cytosol to vacuole translocation of a component of the autophagosome known as Atg8p using an *ATG8*-GFP strain (Eisenberg et al., 2009), in which Nat4 will be deleted. Notably, autophagy is a downstream regulatory target of Tor1 following treatment with rapamycin, resulting in extension of lifespan in flies (Bjedov et al., 2010). Thus, in addition to the induction of stress response, it is possible that the absence of Nat4 might regulate longevity through an increase in autophagy. Further support for this comes from a recent study that supported that loss of another acetyltransferase, NatA causes impairment of mitochondrial degradation, suggesting that NatA is crucial for mitophagy in yeast (Eiyama and Okamoto, 2015). All in all, our findings provide new leads that may help to reveal the mechanisms underlying the anti-ageing effect of CR. Future studies will establish whether Nat4-regulated longevity may be one of the anti-ageing mechanisms in mammals that can be used also as a clinical intervention in age-associated human disease.

6. Thesis Synopsis

Taken together, our aims contributed towards accomplishing the overall research goal of understanding the role of Nat4 in gene regulation. The flow diagram (Figure 6.1) below illustrates the hypothesis and specific aims along with the conclusions drawn within each aim. In summary, this study provides a novel link between protein N- terminal acetylation and the regulation of gene expression. Specifically, this regulation employs a unique mechanism by which histone N- terminal acetylation influences the deposition of another in cis modification, H4R3me2a, to control rDNA silencing. Moreover, we report a novel biological role for Nat4 and histone N-terminal acetylation, in regulating lifespan through increased cellular resistance to stress.

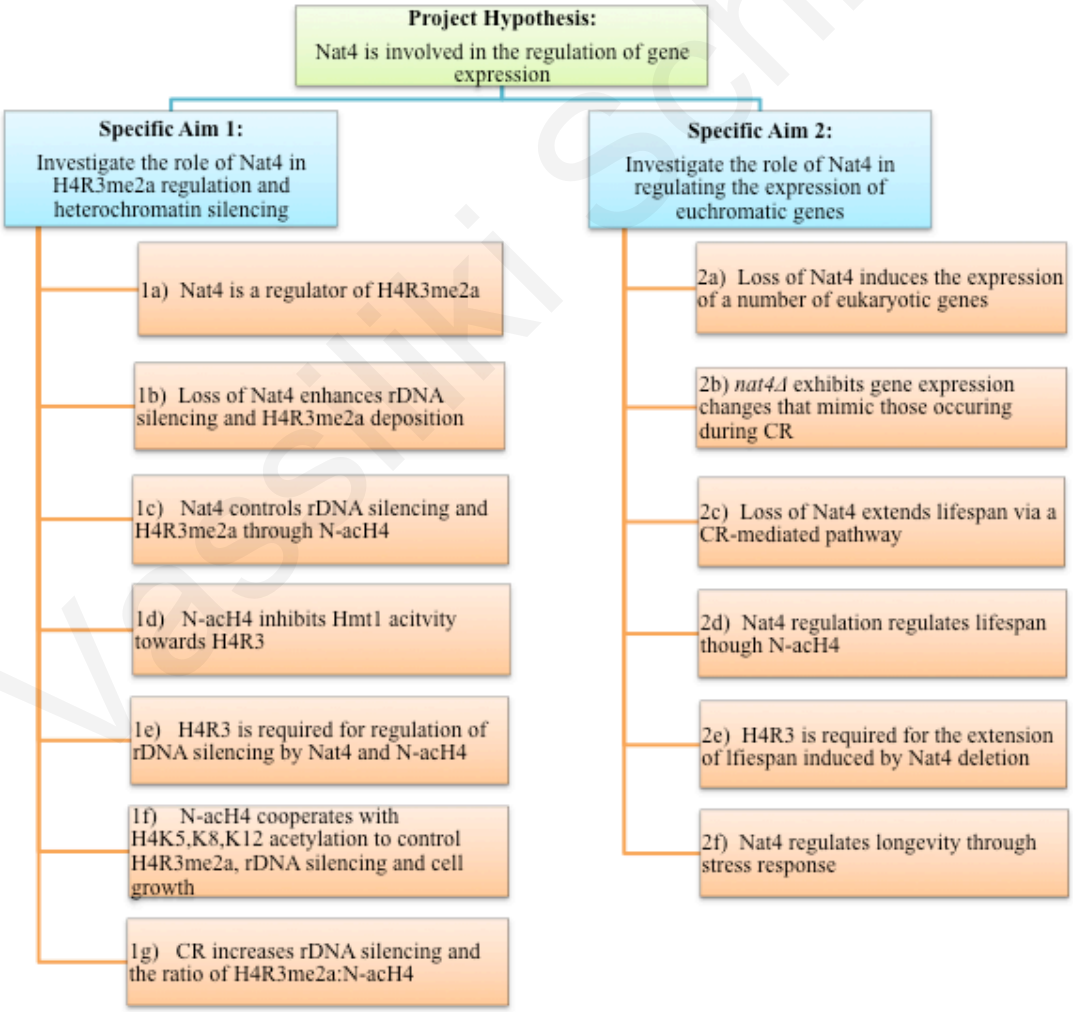

Figure 6.1. Thesis synopsis. Flow diagram illustrating the hypothesis and specific aims along with the conclusion drawn within each aim.

CHAPTER 6
REFERENCES

AI X, PARTHUN MR (2004) The nuclear Hat1p/Hat2p complex: a molecular link between type B histone acetyltransferases and chromatin assembly. *Mol Cell* 14, 195–205

ALLFREY, V.G., FAULKNER, R. and MIRSKY, A.E., 1964. Acetylation and Methylation of Histones and their Possible Role in the Regulation of Rna Synthesis. *Proceedings of the National Academy of Sciences of the United States of America,* 51, 786-794.

AN, W., KIM, J. and ROEDER, R.G., 2004. Ordered cooperative functions of PRMT1, p300, and CARM1 in transcriptional activation by p53. *Cell,* 117(6), 735-748.

ANDERSON, R.M., BITTERMAN, K.J., WOOD, J.G., MEDVEDIK, O. and SINCLAIR, D.A., 2003. Nicotinamide and PNC1 govern lifespan extension by calorie restriction in Saccharomyces cerevisiae. *Nature,* 423(6936), 181-185.

ARNESEN, T., 2011. Towards a functional understanding of protein N-terminal acetylation. *PLoS biology,* 9(5), e1001074.

ARNESEN, T., 2009. Protein N-terminal acetylation: NAT 2007-2008 Symposia. *BMC proceedings,* 3 Suppl 6, S1-6561-3-S6-S1.

ASHRAFI, K., SINCLAIR, D., GORDON, J.I. and GUARENTE, L., 1999. Passage through stationary phase advances replicative aging in Saccharomyces cerevisiae. *Proceedings of the National Academy of Sciences of the United States of America,* 96(16), 9100-9105.

BANNISTER, A.J. and KOUZARIDES, T., 2011. Regulation of chromatin by histone modifications. *Cell research,* 21(3), 381-395.

BECK, T. and HALL, M.N., 1999. The TOR signalling pathway controls nuclear localization of nutrient-regulated transcription factors. *Nature,* 402(6762), 689-692.

BEDFORD, M.T. and CLARKE, S.G., 2009. Protein arginine methylation in mammals: who, what, and why. *Molecular cell,* 33(1), 1-13.

BEDFORD, M.T. and RICHARD, S., 2005. Arginine methylation an emerging regulator of protein function. *Molecular cell,* 18(3), 263-272.

BERGER, S.L., 2007. The complex language of chromatin regulation during transcription. *Nature,* 447(7143), 407-412.

BJEDOV, I., TOIVONEN, J.M., KERR, F., SLACK, C., JACOBSON, J., FOLEY, A. and PARTRIDGE, L., 2010. Mechanisms of life span extension by rapamycin in the fruit fly Drosophila melanogaster. *Cell metabolism,* 11(1), 35-46.

BOEKE, J.D., LACROUTE, F. and FINK, G.R., 1984. A positive selection for mutants lacking orotidine-5'-phosphate decarboxylase activity in yeast: 5-fluoro-orotic acid resistance. *Molecular & general genetics : MGG,* 197(2), 345-346.

BOENDER, L.G., ALMERING, M.J., DIJK, M., VAN MARIS, A.J., DE WINDE, J.H., PRONK, J.T. and DARAN-LAPUJADE, P., 2011. Extreme calorie restriction and energy

source starvation in Saccharomyces cerevisiae represent distinct physiological states. *Biochimica et biophysica acta,* 1813(12), 2133-2144.

BROWN, J.L. and ROBERTS, W.K., 1976. Evidence that approximately eighty per cent of the soluble proteins from Ehrlich ascites cells are Nalpha-acetylated. *The Journal of biological chemistry,* 251(4), 1009-1014.

CHA, B. and JHO, E.H., 2012. Protein arginine methyltransferases (PRMTs) as therapeutic targets. *Expert opinion on therapeutic targets,* 16(7), 651-664.

CHANG, B., CHEN, Y., ZHAO, Y. and BRUICK, R.K., 2007. JMJD6 is a histone arginine demethylase. *Science (New York, N.Y.),* 318(5849), 444-447.

CHEN, D., PAN, K.Z., PALTER, J.E. and KAPAHI, P., 2007. Longevity determined by developmental arrest genes in Caenorhabditis elegans. *Aging cell,* 6(4), 525-533.

CHOI, H.R., CHO, K.A., KANG, H.T., LEE, J.B., KAEBERLEIN, M., SUH, Y., CHUNG, I.K. and PARK, S.C., 2011. Restoration of senescent human diploid fibroblasts by modulation of the extracellular matrix. *Aging cell,* 10(1), 148-157.

CLARKE, A.S., LOWELL, J.E., JACOBSON, S.J. and PILLUS, L., 1999. Esa1p is an essential histone acetyltransferase required for cell cycle progression. *Molecular and cellular biology,* 19(4), 2515-2526.

CURRAN, S.P. and RUVKUN, G., 2007. Lifespan regulation by evolutionarily conserved genes essential for viability. *PLoS genetics,* 3(4), e56.

DANG, W., STEFFEN, K.K., PERRY, R., DORSEY, J.A., JOHNSON, F.B., SHILATIFARD, A., KAEBERLEIN, M., KENNEDY, B.K. and BERGER, S.L., 2009. Histone H4 lysine 16 acetylation regulates cellular lifespan. *Nature,* 459(7248), 802-807.

DANG, W., SUTPHIN, G.L., DORSEY, J.A., OTTE, G.L., CAO, K., PERRY, R.M., WANAT, J.J., SAVIOLAKI, D., MURAKAMI, C.J., TSUCHIYAMA, S., ROBISON, B., GREGORY, B.D., VERMEULEN, M., SHIEKHATTAR, R., JOHNSON, F.B., KENNEDY, B.K., KAEBERLEIN, M. and BERGER, S.L., 2014. Inactivation of yeast Isw2 chromatin remodeling enzyme mimics longevity effect of calorie restriction via induction of genotoxic stress response. *Cell metabolism,* 19(6), 952-966.

DAWSON, M.A. and KOUZARIDES, T., 2012. Cancer epigenetics: from mechanism to therapy. *Cell,* 150(1), 12-27.

DEFOSSEZ, P.A., PRUSTY, R., KAEBERLEIN, M., LIN, S.J., FERRIGNO, P., SILVER, P.A., KEIL, R.L. and GUARENTE, L., 1999. Elimination of replication block protein Fob1 extends the life span of yeast mother cells. *Molecular cell,* 3(4), 447-455.

DHAR, S., VEMULAPALLI, V., PATANANAN, A.N., HUANG, G.L., DI LORENZO, A., RICHARD, S., COMB, M.J., GUO, A., CLARKE, S.G. and BEDFORD, M.T., 2013. Loss of the major Type I arginine methyltransferase PRMT1 causes substrate scavenging by other PRMTs. *Scientific reports,* 3, 1311.

DUPONT, C., ARMANT, D.R. and BRENNER, C.A., 2009. Epigenetics: definition, mechanisms and clinical perspective. *Seminars in reproductive medicine,* 27(5), 351-357.

EISENBERG, T., KNAUER, H., SCHAUER, A., BUTTNER, S., RUCKENSTUHL, C., CARMONA-GUTIERREZ, D., RING, J., SCHROEDER, S., MAGNES, C., ANTONACCI, L., FUSSI, H., DESZCZ, L., HARTL, R., SCHRAML, E., CRIOLLO, A., MEGALOU, E., WEISKOPF, D., LAUN, P., HEEREN, G., BREITENBACH, M., GRUBECK-LOEBENSTEIN, B., HERKER, E., FAHRENKROG, B., FROHLICH, K.U., SINNER, F., TAVERNARAKIS, N., MINOIS, N., KROEMER, G. and MADEO, F., 2009. Induction of autophagy by spermidine promotes longevity. *Nature cell biology,* 11(11), 1305-1314.

EIYAMA, A. and OKAMOTO, K., 2015. Protein N-terminal Acetylation by the NatA Complex Is Critical for Selective Mitochondrial Degradation. *The Journal of biological chemistry,* 290(41), 25034-25044.

ELGIN, S.C. and REUTER, G., 2013. Position-effect variegation, heterochromatin formation, and gene silencing in Drosophila. *Cold Spring Harbor perspectives in biology,* 5(8), a017780.

FABRIZIO, P., POZZA, F., PLETCHER, S.D., GENDRON, C.M. and LONGO, V.D., 2001. Regulation of longevity and stress resistance by Sch9 in yeast. *Science (New York, N.Y.),* 292(5515), 288-290.

FALB, M., AIVALIOTIS, M., GARCIA-RIZO, C., BISLE, B., TEBBE, A., KLEIN, C., KONSTANTINIDIS, K., SIEDLER, F., PFEIFFER, F. and OESTERHELT, D., 2006. Archaeal N-terminal protein maturation commonly involves N-terminal acetylation: a large-scale proteomics survey. *Journal of Molecular Biology,* 362(5), 915-924.

FELSENFELD, G. and GROUDINE, M., 2003. Controlling the double helix. *Nature,* 421(6921), 448-453.

FENG, Y., WANG, J., ASHER, S., HOANG, L., GUARDIANI, C., IVANOV, I. and ZHENG, Y.G., 2011. Histone H4 acetylation differentially modulates arginine methylation by an in Cis mechanism. . *J Biol Chem,* 286, 20323-20334.

FOYN, H., JONES, J.E., LEWALLEN, D., NARAWANE, R., VARHAUG, J.E., THOMPSON, P.R. and ARNESEN, T., 2013. Design, synthesis, and kinetic characterization of protein N-terminal acetyltransferase inhibitors. *ACS chemical biology,* 8(6), 1121-1127.

FULLGRABE, J., LYNCH-DAY, M.A., HELDRING, N., LI, W., STRUIJK, R.B., MA, Q., HERMANSON, O., ROSENFELD, M.G., KLIONSKY, D.J. and JOSEPH, B., 2013. The histone H4 lysine 16 acetyltransferase hMOF regulates the outcome of autophagy. *Nature,* 500(7463), 468-471.

GALDIERI, L., MEHROTRA, S., YU, S. and VANCURA, A., 2010. Transcriptional regulation in yeast during diauxic shift and stationary phase. *Omics : a journal of integrative biology,* 14(6), 629-638.

GALLO, C.M., SMITH, D.L.,JR and SMITH, J.S., 2004. Nicotinamide clearance by Pnc1 directly regulates Sir2-mediated silencing and longevity. *Molecular and cellular biology,* 24(3), 1301-1312.

GAUTSCHI, M., JUST, S., MUN, A., ROSS, S., RUCKNAGEL, P., DUBAQUIE, Y., EHRENHOFER-MURRAY, A. and ROSPERT, S., 2003. The yeast N(alpha)-acetyltransferase NatA is quantitatively anchored to the ribosome and interacts with nascent polypeptides. *Molecular and cellular biology,* 23(20), 7403-7414.

GAYATRI, S. and BEDFORD, M.T., 2014. Readers of histone methylarginine marks. *Biochimica et biophysica acta,* 1839(8), 702-710.

GEISSENHONER, A., WEISE, C. and EHRENHOFER-MURRAY, A.E., 2004. Dependence of ORC silencing function on NatA-mediated Nalpha acetylation in Saccharomyces cerevisiae. *Molecular and cellular biology,* 24(23), 10300-10312.

GELINO, S. and HANSEN, M., 2012. Autophagy - An Emerging Anti-Aging Mechanism. *Journal of clinical & experimental pathology,* Suppl 4, 006.

GELPERIN, D.M., WHITE, M.A., WILKINSON, M.L., KON, Y., KUNG, L.A., WISE, K.J., LOPEZ-HOYO, N., JIANG, L., PICCIRILLO, S., YU, H., GERSTEIN, M., DUMONT, M.E., PHIZICKY, E.M., SNYDER, M. and GRAYHACK, E.J., 2005. Biochemical and genetic analysis of the yeast proteome with a movable ORF collection. *Genes & development,* 19(23), 2816-2826.

GIAEVER, G. and NISLOW, C., 2014. The yeast deletion collection: a decade of functional genomics. *Genetics,* 197(2), 451-465.

GRAY, J.V., PETSKO, G.A., JOHNSTON, G.C., RINGE, D., SINGER, R.A. and WERNER-WASHBURNE, M., 2004. "Sleeping beauty": quiescence in Saccharomyces cerevisiae. *Microbiology and molecular biology reviews : MMBR,* 68(2), 187-206.

GREEN, E.M., MAS, G., YOUNG, N.L., GARCIA, B.A. and GOZANI, O., 2012. Methylation of H4 lysines 5, 8 and 12 by yeast Set5 calibrates chromatin stress responses. *Nature structural & molecular biology,* 19(3), 361-363.

GRUNSTEIN, M. and GASSER, S.M., 2013. Epigenetics in Saccharomyces cerevisiae. *Cold Spring Harbor perspectives in biology,* 5(7), 10.1101/cshperspect.a017491.

GUCCIONE, E., BASSI, C., CASADIO, F., MARTINATO, F., CESARONI, M., SCHUCHLAUTZ, H., LUSCHER, B. and AMATI, B., 2007. Methylation of histone H3R2 by PRMT6 and H3K4 by an MLL complex are mutually exclusive. *Nature,* 449(7164), 933-937.

HA, C.W. and HUH, W.K., 2011. Rapamycin increases rDNA stability by enhancing association of Sir2 with rDNA in Saccharomyces cerevisiae. *Nucleic acids research,* 39(4), 1336-1350.

HANSEN, M., TAUBERT, S., CRAWFORD, D., LIBINA, N., LEE, S.J. and KENYON, C., 2007. Lifespan extension by conditions that inhibit translation in Caenorhabditis elegans. *Aging cell,* 6(1), 95-110.

HARDWICK, J.S., KURUVILLA, F.G., TONG, J.K., SHAMJI, A.F. and SCHREIBER, S.L., 1999. Rapamycin-modulated transcription defines the subset of nutrient-sensitive signaling pathways directly controlled by the Tor proteins. *Proceedings of the National Academy of Sciences of the United States of America,* 96(26), 14866-14870.

HARVEY, A.C., JACKSON, S.P. and DOWNS, J.A., 2005. Saccharomyces cerevisiae histone H2A Ser122 facilitates DNA repair. *Genetics,* 170(2), 543-553.

HAZELWOOD, L.A., WALSH, M.C., LUTTIK, M.A., DARAN-LAPUJADE, P., PRONK, J.T. and DARAN, J.M., 2009. Identity of the growth-limiting nutrient strongly affects storage carbohydrate accumulation in anaerobic chemostat cultures of Saccharomyces cerevisiae. *Applied and Environmental Microbiology,* 75(21), 6876-6885.

HE, C. and KLIONSKY, D.J., 2009. Regulation mechanisms and signaling pathways of autophagy.Annu. Rev. Genet. 43, 67-93.

HELBIG, A.O., ROSATI, S., PIJNAPPEL, P.W., VAN BREUKELEN, B., TIMMERS, M.H., MOHAMMED, S., SLIJPER, M. and HECK, A.J., 2010. Perturbation of the yeast N-acetyltransferase NatB induces elevation of protein phosphorylation levels. *BMC genomics,* 11, 685-2164-11-685.

HELSENS, K., VAN DAMME, P., DEGROEVE, S., MARTENS, L., ARNESEN, T., VANDEKERCKHOVE, J. and GEVAERT, K., 2011. Bioinformatics analysis of a Saccharomyces cerevisiae N-terminal proteome provides evidence of alternative translation initiation and post-translational N-terminal acetylation. *Journal of proteome research,* 10(8), 3578-3589.

HERSKOWITZ, I., 1988. Life cycle of the budding yeast Saccharomyces cerevisiae. *Microbiological reviews,* 52(4), 536-553.

HOLE, K., VAN DAMME, P., DALVA, M., AKSNES, H., GLOMNES, N., VARHAUG, J.E., LILLEHAUG, J.R., GEVAERT, K. and ARNESEN, T., 2011. The human N-alpha-acetyltransferase 40 (hNaa40p/hNatD) is conserved from yeast and N-terminally acetylates histones H2A and H4. *PloS one,* 6(9), e24713.

HOLLIDAY, R., 1987. The inheritance of epigenetic defects. *Science (New York, N.Y.),* 238(4824), 163-170.

HOLLIDAY, R. and PUGH, J.E., 1975. DNA modification mechanisms and gene activity during development. *Science (New York, N.Y.),* 187(4173), 226-232.

HUANG, J. and MOAZED, D., 2003. Association of the RENT complex with nontranscribed and coding regions of rDNA and a regional requirement for the replication fork block protein Fob1 in rDNA silencing. . *Genes Dev,* 17, 2162-2176.

HUANG, H., MAERTENS, A.M., HYLAND, E.M., DAI, J., NORRIS, A., BOEKE, J.D. and BADER, J.S., 2009. HistoneHits: a database for histone mutations and their phenotypes. *Genome research,* 19(4), 674-681.

HUANG, S., LITT, M. and FELSENFELD, G., 2005. Methylation of histone H4 by arginine methyltransferase PRMT1 is essential in vivo for many subsequent histone modifications. *Genes & development,* 19(16), 1885-1893.

HUBERTS, D.H.E.W., GONZALEZ, H., LEE, S.S., LITSIOS, A., HUBMANN, G., WIT, E.C. and HEINEMANN, M., 2014. Calorie restriction does not elicit a robust extension of replicative lifespan in *Saccharomyces cerevisia*. *PNAS,* 11(32), pp. 11727-11731.

IZZO, A. and SCHNEIDER, R., 2010. Chatting histone modifications in mammals. *Briefings in functional genomics,* 9(5-6), 429-443.

JAHAN, S. and DAVIE, J.R., 2015. Protein arginine methyltransferases (PRMTs): role in chromatin organization. *Advances in biological regulation,* 57, 173-184.

JELINIC, P., STEHLE, J.C. and SHAW, P., 2006. The testis-specific factor CTCFL cooperates with the protein methyltransferase PRMT7 in H19 imprinting control region methylation. *PLoS biology,* 4(11), e355.

JO, M.C., LIU, W., GU, L., DANG, W. and QIN, L., 2015. High-throughput analysis of yeast replicative aging using a microfluidic system. *Proceedings of the National Academy of Sciences of the United States of America,* 112(30), 9364-9369.

JOHNSON, S.C., RABINOVITCH, P.S. and KAEBERLEIN, M., 2013. mTOR is a key modulator of ageing and age-related disease. *Nature,* 493(7432), 338-345.

KAEBERLEIN, M., 2010. Lessons on longevity from budding yeast. *Nature,* 464(7288), 513-519.

KAEBERLEIN, M., 2006. Genome-wide approaches to understanding human ageing. *Human genomics,* 2(6), 422-428.

KAEBERLEIN, M., KIRKLAND, K.T., FIELDS, S. and KENNEDY, B.K., 2004. Sir2-independent life span extension by calorie restriction in yeast. *PLoS biology,* 2(9), E296.

KAEBERLEIN, M., MCVEY, M. and GUARENTE, L., 1999. The SIR2/3/4 complex and SIR2 alone promote longevity in Saccharomyces cerevisiae by two different mechanisms. *Genes & development,* 13(19), 2570-2580.

KAEBERLEIN, M., POWERS, R.W.,3RD, STEFFEN, K.K., WESTMAN, E.A., HU, D., DANG, N., KERR, E.O., KIRKLAND, K.T., FIELDS, S. and KENNEDY, B.K., 2005. Regulation of yeast replicative life span by TOR and Sch9 in response to nutrients. *Science (New York, N.Y.),* 310(5751), 1193-1196.

KALVIK, T.V. and ARNESEN, T., 2013. Protein N-terminal acetyltransferases in cancer. *Oncogene,* 32(3), 269-276.

KAPAHI, P., ZID, B.M., HARPER, T., KOSLOVER, D., SAPIN, V. and BENZER, S., 2004. Regulation of lifespan in Drosophila by modulation of genes in the TOR signaling pathway. *Current biology : CB,* 14(10), 885-890.

KENNEDY, B.K., AUSTRIACO, N.R. and GUARENTE, L., 1994. Daughter cells of Saccharomyces cerevisiae from old mothers display a re- duced life span. *J. Cell Biol,* 127, 1985–1993.

KENNEDY, B.K., AUSTRIACO, N.R.,JR, ZHANG, J. and GUARENTE, L., 1995. Mutation in the silencing gene SIR4 can delay aging in S. cerevisiae. *Cell,* 80(3), 485-496.

KIRMIZIS, A., SANTOS-ROSA, H., PENKETT, C.J., SINGER, M.A., VERMEULEN, M., MANN, M., BAHLER, J., GREEN, R.D. and KOUZARIDES, T., 2007. Arginine

methylation at histone H3R2 controls deposition of H3K4 trimethylation. *Nature,* 449(7164), 928-932.

KIRMIZIS, A., SANTOS-ROSA, H., PENKETT, C.J., SINGER, M.A., GREEN, R.D. and KOUZARIDES, T., 2009. Distinct transcriptional outputs associated with mono- and dimethylated histone H3 arginine 2. *Nature structural & molecular biology,* 16(4), 449-451.

KOBAYASHI, T., HORIUCHI, T., TONGAONKAR, P., VU, L. and NOMURA, M., 2004. SIR2 regulates recombination between different rDNA repeats, but not recombination within individual rRNA genes in yeast. . *Cell,* 117(4), 441-53.

KOBAYASHI, T., 2011. How does genome instability affect lifespan?: roles of rDNA and telomeres. *Genes to cells : devoted to molecular & cellular mechanisms,* 16(6), 617-624.

KOBAYASHI, T., 2011. Regulation of ribosomal RNA gene copy number and its role in modulating genome integrity and evolutionary adaptability in yeast. *Cellular and molecular life sciences : CMLS,* 68(8), 1395-1403.

KOBAYASHI, T., 2003. The replication fork barrier site forms a unique structure with Fob1p and inhibits the replication fork. *Molecular and cellular biology,* 23(24), 9178-9188.

KOBAYASHI, T. and GANLEY, A.R., 2005. Recombination regulation by transcription-induced cohesin dissociation in rDNA repeats. *Science (New York, N.Y.),* 309(5740), 1581-1584.

KOBAYASHI, T., HECK, D.J., NOMURA, M. and HORIUCHI, T., 1998. Expansion and contraction of ribosomal DNA repeats in Saccharomyces cerevisiae: requirement of replication fork blocking (Fob1) protein and the role of RNA polymerase I. *Genes & development,* 12(24), 3821-3830.

KOUZARIDES, T., 2007. Chromatin modifications and their function. *Cell,* 128(4), 693-705.

KRISHNAMOORTHY, T., CHEN, X., GOVIN, J., CHEUNG, W.L., DORSEY, J., SCHINDLER, K., WINTER, E., ALLIS, C.D., GUACCI, V., KHOCHBIN, S., FULLER, M.T. and BERGER, S.L., 2006. Phosphorylation of histone H4 Ser1 regulates sporulation in yeast and is conserved in fly and mouse spermatogenesis. *Genes & development,* 20(18), 2580-2592.

LACOSTE, N., UTLEY, R.T., HUNTER, J.M., POIRIER, G.G. and COTE, J., 2002. Disruptor of telomeric silencing-1 is a chromatin-specific histone H3 methyltransferase. *The Journal of biological chemistry,* 277(34), 30421-30424.

LAEMMLI, U.K., 1970. Cleavage of structural proteins during the assembly of the head of bacteriophage T4. *Nature,* 227(5259), 680-685.

LAMMING, D.W., LATORRE-ESTEVES, M., MEDVEDIK, O., WONG, S.N., TSANG, F.A., WANG, C., LIN, S.J. and SINCLAIR, D.A., 2005. HST2 mediates SIR2-independent life-span extension by calorie restriction. *Science (New York, N.Y.),* 309(5742), 1861-1864.

LEE, Y. and LEE, C., 2008. Transcriptional response according to strength of calorie restriction in Saccharomyces cerevisiae. *Mol. Cells,* 26, 299-307.

LEE, J.S., SMITH, E. and SHILATIFARD, A., 2010. The language of histone crosstalk. *Cell,* 142(5), 682-685.

LEE, S.S., AVALOS VIZCARRA, I., HUBERTS, D.H., LEE, L.P. and HEINEMANN, M., 2012. Whole lifespan microscopic observation of budding yeast aging through a microfluidic dissection platform. *Proceedings of the National Academy of Sciences of the United States of America,* 109(13), 4916-4920.

LEWIS, K.N., MELE, J., HORNSBY, P.J. and BUFFENSTEIN, R., 2012. Stress resistance in the naked mole-rat: the bare essentials - a mini-review. *Gerontology,* 58(5), 453-462.

LI, G. and REINBERG, D., 2011. Chromatin higher-order structures and gene regulation. *Current opinion in genetics & development,* 21(2), 175-186.

LILLIE, S.H. and PRINGLE, J.R., 1980. Reserve carbohydrate metabolism in Saccharomyces cerevisiae: responses to nutrient limitation. *Journal of Bacteriology,* 143(3),1384-1394.

LIN, S.J., DEFOSSEZ, P.A. and GUARENTE, L., 2000. Requirement of NAD and SIR2 for life-span extension by calorie restriction in Saccharomyces cerevisiae. *Science (New York, N.Y.),* 289 (5487), 2126-2128.

LIN, S.J., KAEBERLEIN, M., ANDALIS, A.A., STURTZ, L.A., DEFOSSEZ, P.A., CULOTTA, V.C., FINK, G.R. and GUARENTE, L., 2002. Calorie restriction extends Saccharomyces cerevisiae lifespan by increasing respiration. *Nature,* 418 (6895), 344-348.

LINSTROM, D.L. and GOTTSCHLING, D.E., 2009. The Mother Enrichment Program: A Genetic System for Facile Replicative Life Span Analysis in *Saccharomyces cerevisiae*. *Genetics,* 183 (2), 413-422.

LIPPUNER, A.D., S JULOU, T. and BARRAL, Y., 2014. Budding yeast as a model organism to study the effects of age *FEMS Microbiology Review,* 38, 300–325.

LISZCZAK, G., ARNESEN, T. and MARMORSTEIN, R., 2011. Structure of a ternary Naa50p (NAT5/SAN) N-terminal acetyltransferase complex reveals the molecular basis for substrate-specific acetylation. *The Journal of biological chemistry,* 286(42), 37002-37010.

LISZCZAK, G., GOLDBERG, J.M., FOYN, H., PETERSSON, E.J., ARNESEN, T. and MARMORSTEIN, R., 2013. Molecular basis for N-terminal acetylation by the heterodimeric NatA complex. *Nature structural & molecular biology,* 20(9), 1098-1105.

LIU, L., JIN, G. and ZHOU, X., 2015. Modeling the relationship of epigenetic modifications to transcription factor binding. *Nucleic acids research,* 43(8), 3873-3885.

LIU, W., MA, Q., WONG, K., LI, W., OHGI, K., ZHANG, J., AGGARWAL, A.K. and ROSENFELD, M.G., 2013. Brd4 and JMJD6-associated anti-pause enhancers in regulation of transcriptional pause release. *Cell,* 155(7), 1581-1595.

LIU, Y., ZHOU, D., ZHANG, F., TU, Y., XIA, Y., WANG, H., ZHOU, B., ZHANG, Y., WU, J., GAO, X., HE, Z. and ZHAI, Q., 2012. Liver Patt1 deficiency protects male mice from age-associated but not high-fat diet-induced hepatic steatosis. *Journal of lipid research,* 53(3), 358-367.

LIU, Z., LIU, Y., WANG, H., GE, X., JIN, Q., DING, G., HU, Y., ZHOU, B., CHEN, Z., GE, X., ZHANG, B., MAN, X. and ZHAI, Q., 2009. Patt1, a novel protein acetyltransferase that is highly expressed in liver and downregulated in hepatocellular carcinoma, enhances apoptosis of hepatoma cells. *The international journal of biochemistry & cell biology,* 41(12), 2528-2537.

LONGO, V.D. and FABRIZIO, P., 2012. Chronological aging in Saccharomyces cerevisiae. *Sub-cellular biochemistry,* 57, 101-121.

LONGO, V.D., SHADEL, G.S., KAEBERLEIN, M. and KENNEDY, B., 2012. Replicative and chronological aging in Saccharomyces cerevisiae. *Cell metabolism,* 16(1), 18-31.

LOO, S. and RINE, J., 1994. Silencers and domains of generalized repression. *Science (New York, N.Y.),* 264(5166), 1768-1771.

LUSTIG, A.J., 1998. Mechanisms of silencing in Saccharomyces cerevisiae. *Current opinion in genetics & development,* 8(2), 233-239.

MACKAY, V.L., LI, X., FLORY, M.R., TURCOTT, E., LAW, G.L., SERIKAWA, K.A., XU, X.L., LEE, H., GOODLETT, D.R., AEBERSOLD, R., ZHAO, L.P. and MORRIS, D.R., 2004. Gene expression analyzed by high-resolution state array analysis and quantitative proteomics: response of yeast to mating pheromone. *Molecular & cellular proteomics : MCP,* 3(5), 478-489.

MAGIN, R.S., LISZCZAK, G.P. and MARMORSTEIN, R., 2015. The molecular basis for histone H4- and H2A-specific amino-terminal acetylation by NatD. *Structure (London, England : 1993),* 23(2), 332-341.

MARTIN, D.E. and HALL, M.N., 2005. The expanding TOR signaling network. *Current opinion in cell biology,* 17(2), 158-166.

MCCARTHY, D.J., CHEN, Y. and SMYTH, G.K., 2012. Differential expression analysis of multifactor RNA-Seq experiments with respect to biological variation. *Nucleic acids research,* 40(10), 4288-4297.

MCCAY, C.M., CROWELL, M.F. and MAYNARD, L.A.The effect of retarded growth upon the length of life span and upon the ultimate body size. 1935. *Nutrition (Burbank, Los Angeles County, Calif.),* 5(3), 155-71

MCCORMICK, M.A., TSAI, S.Y. and KENNEDY, B.K., 2011. TOR and ageing: a complex pathway for a complex process. *Philosophical transactions of the Royal Society of London.Series B, Biological sciences,* 366(1561), 17-27.

MEDVEDIK, O., LAMMING, D.W., KIM, K.D. and SINCLAIR, D.A., 2007. MSN2 and MSN4 link calorie restriction and TOR to sirtuin-mediated lifespan extension in Saccharomyces cerevisiae. *PLoS biology,* 5(10), e261.

MELUH, P.B. and BROACH, J.R., 1999. Immunological analysis of yeast chromatin. *Methods in enzymology,* 304, 414-430.

MOLINA-SERRANO, D., SCHIZA, V. and KIRMIZIS, A., 2013. Cross-talk among epigenetic modifications: lessons from histone arginine methylation. *Biochemical Society transactions,* 41(3), 751-759.

MORTIMER, R.K. and JOHNSTON, J.R., 1959. Life span of individual yeast cells. *Nature,* 183(4677), 1751-1752.

MULLEN, J.R., KAYNE, P.S., MOERSCHELL, R.P., TSUNASAWA, S., GRIBSKOV, M., COLAVITO-SHEPANSKI, M., GRUNSTEIN, M., SHERMAN, F. and STERNGLANZ, R., 1989. Identification and characterization of genes and mutants for an N-terminal acetyltransferase from yeast. *The EMBO journal,* 8(7), 2067-2075.

MURR, R., 2010. Interplay between different epigenetic modifications and mechanisms. *Advances in Genetics,* 70, 101-141.

MUSSELMAN, C.A., LALONDE, M.E., COTE, J. and KUTATELADZE, T.G., 2012. Perceiving the epigenetic landscape through histone readers. *Nature structural & molecular biology,* 19(12), 1218-1227.

MYKLEBUST, L.M., VAN DAMME, P., STOVE, S.I., DORFEL, M.J., ABBOUD, A., KALVIK, T.V., GRAUFFEL, C., JONCKHEERE, V., WU, Y., SWENSEN, J., KAASA, H., LISZCZAK, G., MARMORSTEIN, R., REUTER, N., LYON, G.J., GEVAERT, K. and ARNESEN, T., 2015. Biochemical and cellular analysis of Ogden syndrome reveals downstream Nt-acetylation defects. *Human molecular genetics,* 24(7), 1956-1976.

NAGARAJAN, S., KRUCKEBERG, A.L., SCHMIDT, K.H., KROLL, E., HAMILTON, M., MCINNERNEY, K., SUMMERS, R., TAYLOR, T. and ROSENZWEIG, F., 2014. Uncoupling reproduction from metabolism extends chronological lifespan in yeast. *Proceedings of the National Academy of Sciences of the United States of America,* 111(15), E1538-47.

NEUWALD, A.F. and LANDSMAN, D., 1997. GCN5-related histone N-acetyltransferases belong to a diverse superfamily that includes the yeast SPT10 protein. *Trends in biochemical sciences,* 22(5), 154-155.

NODA, T. and OHSUMI, Y., 1998. Tor, a phosphatidylinositol kinase homologue, controls autophagy in yeast. *The Journal of biological chemistry,* 273(7), 3963-3966.

OKANO, M., BELL, D.W., HABER, D.A. and LI, E., 1999. DNA methyltransferases Dnmt3a and Dnmt3b are essential for de novo methylation and mammalian development. *Cell,* 99(3), 247-257.

ONISHI, M., LIOU, G.G., BUCHBERGER, J.R., WALZ, T. and MOAZED, D., 2007. Role of the conserved Sir3-BAH domain in nucleosome binding and silent chromatin assembly. *Molecular cell,* 28(6), 1015-1028.

PARROU, J.L., ENJALBERT, B., PLOURDE, L., BAUCHE, A., GONZALEZ, B. and FRANCOIS, J., 1999. Dynamic responses of reserve carbohydrate metabolism under

carbon and nitrogen limitations in Saccharomyces cerevisiae. *Yeast (Chichester, England),* 15(3), 191-203.

PARROU, J.L., TESTE, M.A. and FRANCOIS, J., 1997. Effects of various types of stress on the metabolism of reserve carbohydrates in Saccharomyces cerevisiae: genetic evidence for a stress-induced recycling of glycogen and trehalose. *Microbiology (Reading, England),* 143 (Pt 6)(Pt 6), 1891-1900.

PESCHANSKY, V.J. and WAHLESTEDT, C., 2014. Non-coding RNAs as direct and indirect modulators of epigenetic regulation. *Epigenetics,* 9(1), 3-12.

PLONGTHONGKUM, N., DIEP, D.H. and ZHANG, K., 2014. Advances in the profiling of DNA modifications: cytosine methylation and beyond. *Nature reviews.Genetics,* 15(10), 647-661.

POLEVODA, B., HOSKINS, J. and SHERMAN, F., 2009. Properties of Nat4, an N (alpha) acetyltransferase of Saccharomyces cerevisiae that modifies N termini of histones H2A and H4. *Mol Cell Biol,* 29(11), 2913-24.

POLEVODA, B., CARDILLO, T.S., DOYLE, T.C., BEDI, G.S. and SHERMAN, F., 2003. Nat3p and Mdm20p are required for function of yeast NatB Nalpha-terminal acetyltransferase and of actin and tropomyosin. *The Journal of biological chemistry,* 278(33), 30686-30697.

POLEVODA, B., NORBECK, J., TAKAKURA, H., BLOMBERG, A. and SHERMAN, F., 1999. Identification and specificities of N-terminal acetyltransferases from Saccharomyces cerevisiae. *The EMBO journal,* 18(21), 6155-6168.

POLEVODA, B. and SHERMAN, F., 2003. Composition and function of the eukaryotic N-terminal acetyltransferase subunits. *Biochemical and biophysical research communications,* 308(1), 1-11.

POPP, B., STOVE, S.I., ENDELE, S., MYKLEBUST, L.M., HOYER, J., STICHT, H., AZZARELLO-BURRI, S., RAUCH, A., ARNESEN, T. and REIS, A., 2015. De novo missense mutations in the NAA10 gene cause severe non-syndromic developmental delay in males and females. *European journal of human genetics : EJHG,* 23(5), 602-609.

POWERS, R.W.,3RD, KAEBERLEIN, M., CALDWELL, S.D., KENNEDY, B.K. and FIELDS, S., 2006. Extension of chronological life span in yeast by decreased TOR pathway signaling. *Genes & development,* 20(2), 174-184.

POWERS, T. and WALTER, P., 1999. Regulation of ribosome biogenesis by the rapamycin-sensitive TOR-signaling pathway in Saccharomyces cerevisiae. *Molecular biology of the cell,* 10(4), 987-1000.

RIESEN, M. and MORGAN, A., 2009. Calorie restriction reduces rDNA recombination independently of rDNA silencing. *Aging cell,* 8(6), 624-632.

ROSSMANN, M.P., LUO, W., TSAPONINA, O., CHABES, A. and STILLMAN, B., 2011. A common telomeric gene silencing assay is affected by nucleotide metabolism. *Molecular cell,* 42(1), 127-136.

ROTHBART, S.B. and STRAHL, B.D., 2014. Interpreting the language of histone and DNA modifications. *Biochimica et biophysica acta,* 1839(8), 627-643.

RUBINSZTEIN, D.C., MARIÑO, G. and KROEMER, G., 2011. Autophagy and aging. . *Cell,* 146, 682-695.

SANDELL, L.L., GOTTSCHLING, D.E. and ZAKIAN, V.A., 1994. Transcription of a yeast telomere alleviates telomere position effect without affecting chromosome stability. *Proceedings of the National Academy of Sciences of the United States of America,* 91(25), 12061-12065.

SCHMITT, M.E., BROWN, T.A. and TRUMPOWER, B.L., 1990. A rapid and simple method for preparation of RNA from Saccharomyces cerevisiae. *Nucleic acids research,* 18(10), 3091-3092.

SCHNEIDER, J., DOVER, J., JOHNSTON, M. and SHILATIFARD, A., 2004. Global proteomic analysis of S. cerevisiae (GPS) to identify proteins required for histone modifications. *Methods in enzymology,* 377, 227-234.

SHARMA, P.K., AGRAWAL, V. and ROY, N., 2011. Mitochondria-mediated hormetic response in life span extension of calorie-restricted Saccharomyces cerevisiae. *Age (Dordrecht, Netherlands),* 33(2), 143-154.

SHERMAN, F., 2002. Getting started with yeast. *Methods in enzymology,* 350, 3-41.

SHOU, W., SAKAMOTO, K.M., KEENER, J., MORIMOTO, K.W., TRAVERSO, E.E., AZZAM, R., HOPPE, G.J., FELDMAN, R.M., DEMODENA, J., MOAZED, D., CHARBONNEAU, H., NOMURA, M. and DESHAIES, R.J., 2001. Net1 stimulates RNA polymerase I transcription and regulates nucleolar structure independently of controlling mitotic exit. *Molecular cell,* 8(1), 45-55.

SHOU, W., SEOL, J.H., SHEVCHENKO, A., BASKERVILLE, C., MOAZED, D., CHEN, Z.W., JANG, J., SHEVCHENKO, A., CHARBONNEAU, H. and DESHAIES, R.J., 1999. Exit from mitosis is triggered by Tem1-dependent release of the protein phosphatase Cdc14 from nucleolar RENT complex. *Cell,* 97(2), 233-244.

SILLJE, H.H., PAALMAN, J.W., TER SCHURE, E.G., OLSTHOORN, S.Q., VERKLEIJ, A.J., BOONSTRA, J. and VERRIPS, C.T., 1999. Function of trehalose and glycogen in cell cycle progression and cell viability in Saccharomyces cerevisiae. *Journal of Bacteriology,* 181(2), 396-400.

SINCLAIR, D.A., GUARENTE, L (1997). Extrachromosomal rDNA circles-a cause of aging in yeast. *Cell,* 91 (7): 1033-1042

SINCLAIR, D.A., MILLS, K. and GUARENTE, L., 1997. Accelerated aging and nucleolar fragmentation in yeast sgs1 mutants. *Science (New York, N.Y.),* 277(5330), 1313-1316.

SKINNER, C. and LIN, S.J., 2010. Effects of calorie restriction on life span of microorganisms. *Applied Microbiology and Biotechnology,* 88(4), 817-828.

SMITH, D.L.,JR, LI, C., MATECIC, M., MAQANI, N., BRYK, M. and SMITH, J.S., 2009. Calorie restriction effects on silencing and recombination at the yeast rDNA. *Aging cell,* 8(6), 633-642.

SMITH, E.D., KENNEDY, B.K. and KAEBERLEIN, M., 2007. Genome-wide identification of conserved longevity genes in yeast and worms. *Mechanisms of ageing and development,* 128(1), 106-111.

SMITH, E.D., TSUCHIYA, M., FOX, L.A., DANG, N., HU, D., KERR, E.O., JOHNSTON, E.D., TCHAO, B.N., PAK, D.N., WELTON, K.L., PROMISLOW, D.E., THOMAS, J.H., KAEBERLEIN, M. and KENNEDY, B.K., 2008. Quantitative evidence for conserved longevity pathways between divergent eukaryotic species. *Genome research,* 18(4), 564-570.

SMITH, J.S. and BOEKE, J.D., 1997. An unusual form of transcriptional silencing in yeast ribosomal DNA. *Genes & development,* 11(2), 241-254.

SOLDI, M., CUOMO, A., BREMANG, M. and BONALDI, T., 2013. Mass spectrometry-based proteomics for the analysis of chromatin structure and dynamics. *International journal of molecular sciences,* 14(3), 5402-5431.

SONG, O.K., WANG, X., WATERBORG, J.H. and STERNGLANZ, R., 2003. An Nalpha-acetyltransferase responsible for acetylation of the N-terminal residues of histones H4 and H2A. *The Journal of biological chemistry,* 278(40), 38109-38112.

STARHEIM, K.K., GEVAERT, K. and ARNESEN, T., 2012. Protein N-terminal acetyltransferases: when the start matters. *Trends in biochemical sciences,* 37(4), 152-161.

STEFFEN, K.K., MACKAY, V.L. and KERR, E.O., 2008. Yeast life span extension by depletion of 60s ribosomal subunits is mediated by Gcn4. *Cell,* 133, 292-302.

STEFFEN, K.K., KENNEDY, B.K. and KAEBERLEIN, M., 2009. Measuring replicative life span in the budding yeast. *Journal of visualized experiments : JoVE,* (28). pii: 1209. doi(28), 10.3791/1209.

STRAHL, B.D., BRIGGS, S.D., BRAME, C.J., CALDWELL, J.A., KOH, S.S., MA, H., COOK, R.G., SHABANOWITZ, J., HUNT, D.F., STALLCUP, M.R. and ALLIS, C.D., 2001. Methylation of histone H4 at arginine 3 occurs in vivo and is mediated by the nuclear receptor coactivator PRMT1. *Current biology : CB,* 11(12), 996-1000.

SUGANUMA, T. and WORKMAN, J.L., 2008. Crosstalk among Histone Modifications. *Cell,* 135(4), 604-607.

SYNTICHAKI, P. and TAVERNARAKIS, N., 2006. Signaling pathways regulating protein synthesis during ageing. *Experimental gerontology,* 41(10), 1020-1025.

TAHARA, E.B., CUNHA, F.M., BASSO, T.O., DELLA BIANCA, B.E., GOMBERT, A.K. and KOWALTOWSKI, A.J., 2013. Calorie restriction hysteretically primes aging Saccharomyces cerevisiae toward more effective oxidative metabolism. *PloS one,* 8(2), e56388.

TESTE, M.A., DUQUENNE, M., FRANCOIS, J.M. and PARROU, J.L., 2009. Validation of reference genes for quantitative expression analysis by real-time RT-PCR in Saccharomyces cerevisiae. *BMC molecular biology,* **10**, 99-2199-10-99.

THOMAS, G. and HALL, M.N., 1997. TOR signalling and control of cell growth. *Current opinion in cell biology,* 9(6), 782-787.

TODA, T., CAMERON, S., SASS, P. and WIGLER, M., 1988. SCH9, a gene of Saccharomyces cerevisiae that encodes a protein distinct from, but functionally and structurally related to, cAMP-dependent protein kinase catalytic subunits. *Genes & development,* 2(5), pp. 517-527.

TSUKADA, M. and OHSUMI, Y., 1993. Isolation and characterization of autophagy-defective mutants of Saccharomyces cerevisiae. *FEBS letters,* 333(1-2), 169-174.

TWEEDIE-CULLEN, R.Y., BRUNNER, A.M., GROSSMANN, J., MOHANNA, S., SICHAU, D., NANNI, P., PANSE, C. and MANSUY, I.M., 2012. Identification of combinatorial patterns of post-translational modifications on individual histones in the mouse brain. *PloS one,* 7(5), e36980.

VAN DAMME, P., HOLE, K., PIMENTA-MARQUES, A., HELSENS, K., VANDEKERCKHOVE, J., MARTINHO, R.G., GEVAERT, K. and ARNESEN, T., 2011. NatF contributes to an evolutionary shift in protein N-terminal acetylation and is important for normal chromosome segregation. *PLoS Genet,* 7(7), e1002169.

VAN DAMME, P., ARNESEN, T. and GEVAERT, K., 2011. Protein alpha-N-acetylation studied by N-terminomics. *The FEBS journal,* 278(20), 3822-3834.

VAN DAMME, P., LASA, M., POLEVODA, B., GAZQUEZ, C., ELOSEGUI-ARTOLA, A., KIM, D.S., DE JUAN-PARDO, E., DEMEYER, K., HOLE, K., LARREA, E., TIMMERMAN, E., PRIETO, J., ARNESEN, T., SHERMAN, F., GEVAERT, K. and ALDABE, R., 2012. N-terminal acetylome analyses and functional insights of the N-terminal acetyltransferase NatB. *Proceedings of the National Academy of Sciences of the United States of America,* 109(31), 12449-12454.

VAN DAMME, P., STOVE, S.I., GLOMNES, N., GEVAERT, K. and ARNESEN, T., 2014. A Saccharomyces cerevisiae model reveals in vivo functional impairment of the Ogden syndrome N-terminal acetyltransferase NAA10 Ser37Pro mutant. *Molecular & cellular proteomics : MCP,* 13(8), 2031-2041.

VAN WELSEM, T., FREDERIKS, F., VERZIJLBERGEN, K.F., FABER, A.W., NELSON, Z.W., EGAN, D.A., GOTTSCHLING, D.E. and VAN LEEUWEN, F., 2008. Synthetic lethal screens identify gene silencing processes in yeast and implicate the acetylated amino terminus of Sir3 in recognition of the nucleosome core. *Molecular and cellular biology,* 28(11), 3861-3872.

VAQUERO, A. and REINBERG, D., 2009. Calorie restriction and the exercise of chromatin. *Genes & development,* 23(16), 1849-1869.

VARLAND, S., OSBERG, C. and ARNESEN, T., 2015. N-terminal modifications of cellular proteins: The enzymes involved, their substrate specificities and biological effects. *Proteomics,* 15(14), 2385-401.

VELLAI, T., TAKACS-VELLAI, K., ZHANG, Y., KOVACS, A.L., OROSZ, L. and MULLER, F., 2003. Genetics: influence of TOR kinase on lifespan in C. elegans. *Nature,* 426(6967), 620.

VENEMA, J. and TOLLERVEY, D., 1999. Ribosome synthesis in Saccharomyces cerevisiae. *Annual Review of Genetics,* 33, 261-311.

VISINTIN, R., HWANG, E.S. and AMON, A., 1999. Cfi1 prevents premature exit from mitosis by anchoring Cdc14 phosphatase in the nucleolus. *Nature,* 398(6730), 818-823.

WANG, H., HUANG, Z.Q., XIA, L., FENG, Q., ERDJUMENT-BROMAGE, H., STRAHL, B.D., BRIGGS, S.D., ALLIS, C.D., WONG, J., TEMPST, P. and ZHANG, Y., 2001. Methylation of histone H4 at arginine 3 facilitating transcriptional activation by nuclear hormone receptor. *Science (New York, N.Y.),* 293(5531), 853-857.

WANG, J., JIANG, J.C. and JAZWINSKI, S.M., 2010. Gene regulatory changes in yeast during life extension by nutrient limitation. *Experimental gerontology,* 45(7-8), 621-631.

WARNER, J.R., 1999. The economics of ribosome biosynthesis in yeast. *Trends in biochemical sciences,* 24(11), 437-440.

WEBBY, C.J., WOLF, A., GROMAK, N., DREGER, M., KRAMER, H., KESSLER, B., NIELSEN, M.L., SCHMITZ, C., BUTLER, D.S., YATES, J.R.,3RD, DELAHUNTY, C.M., HAHN, P., LENGELING, A., MANN, M., PROUDFOOT, N.J., SCHOFIELD, C.J. and BOTTGER, A., 2009. Jmjd6 catalyses lysyl-hydroxylation of U2AF65, a protein associated with RNA splicing. *Science (New York, N.Y.),* 325(5936), 90-93.

WEI, M., FABRIZIO, P., HU, J., GE, H., CHENG, C., LI, L. and LONGO, V.D., 2008. Life span extension by calorie restriction depends on Rim15 and transcription factors downstream of Ras/PKA, Tor, and Sch9. *PLoS genetics,* 4(1), e13.

WOODCOCK, C.L. and GHOSH, R.P., 2010. Chromatin higher-order structure and dynamics. *Cold Spring Harbor perspectives in biology,* 2(5), a000596.

WOOLFORD, J.L.,JR and BASERGA, S.J., 2013. Ribosome biogenesis in the yeast Saccharomyces cerevisiae. *Genetics,* 195(3), 643-681.

WU, C. and MORRIS, J.R., 2001. Genes, genetics, and epigenetics: a correspondence. *Science,* 293(5532), 1103-1105.

XIE, Z., ZHANG, Y., ZOU, K., BRANDMAN, O., LUO, C., OUYANG, Q. and LI, H., 2012. Molecular phenotyping of aging in single yeast cells using a novel microfluidic device. *Aging cell,* 11(4), pp. 599-606.

YANG, Y. and BEDFORD, M.T., 2013. Protein arginine methyltransferases and cancer. *Nature reviews.Cancer,* 13(1), 37-50.

YU, C.E., OSHIMA, J., WIJSMAN, E.M., NAKURA, J., MIKI, T., PIUSSAN, C., MATTHEWS, S., FU, Y.H., MULLIGAN, J., MARTIN, G.M. and SCHELLENBERG, G.D., 1997. Mutations in the consensus helicase domains of the Werner syndrome gene.

Werner's Syndrome Collaborative Group. *American Journal of Human Genetics,* 60(2), 330-341.

YU, M.C., LAMMING, D.W., ESKIN, J.A., SINCLAIR, D.A. and SILVER, P.A., 2006. The role of protein arginine methylation in the formation of silent chromatin. *Genes & development,* 20(23), 3249-3254.

ZARAGOZA, D., GHAVIDEL, A., HEITMAN, J. and SCHULTZ, M.C., 1998. Rapamycin induces the G0 program of transcriptional repression in yeast by interfering with the TOR signaling pathway. *Molecular and cellular biology,* 18(8), 4463-4470.

ZHANG, T., COOPER, S. and BROCKDORFF, N., 2015. The interplay of histone modifications - writers that read. *EMBO reports,* doi 10.15252/embr.201540945

OPEN ACCESS Freely available online

PLOS | GENETICS

N-alpha-terminal Acetylation of Histone H4 Regulates Arginine Methylation and Ribosomal DNA Silencing

Vassia Schiza[☯], **Diego Molina-Serrano**[☯], **Dimitris Kyriakou, Antonia Hadjiantoniou, Antonis Kirmizis***

Department of Biological Sciences, University of Cyprus, Nicosia, Cyprus

Abstract

Post-translational modifications of histones play a key role in DNA-based processes, like transcription, by modulating chromatin structure. N-terminal acetylation is unique among the numerous histone modifications because it is deposited on the N-alpha amino group of the first residue instead of the side-chain of amino acids. The function of this modification and its interplay with other internal histone marks has not been previously addressed. Here, we identified N-terminal acetylation of H4 (N-acH4) as a novel regulator of arginine methylation and chromatin silencing in *Saccharomyces cerevisiae*. Lack of the H4 N-alpha acetyltransferase (Nat4) activity results specifically in increased deposition of asymmetric dimethylation of histone H4 arginine 3 (H4R3me2a) and in enhanced ribosomal-DNA silencing. Consistent with this, H4 N-terminal acetylation impairs the activity of the Hmt1 methyltransferase towards H4R3 *in vitro*. Furthermore, combinatorial loss of N-acH4 with internal histone acetylation at lysines 5, 8 and 12 has a synergistic induction of H4R3me2a deposition and rDNA silencing that leads to a severe growth defect. This defect is completely rescued by mutating arginine 3 to lysine (H4R3K), suggesting that abnormal deposition of a single histone modification, H4R3me2a, can impact on cell growth. Notably, the cross-talk between N-acH4 and H4R3me2a, which regulates rDNA silencing, is induced under calorie restriction conditions. Collectively, these findings unveil a molecular and biological function for H4 N-terminal acetylation, identify its interplay with internal histone modifications, and provide general mechanistic implications for N-alpha-terminal acetylation, one of the most common protein modifications in eukaryotes.

Citation: Schiza V, Molina-Serrano D, Kyriakou D, Hadjiantoniou A, Kirmizis A (2013) N-alpha-terminal Acetylation of Histone H4 Regulates Arginine Methylation and Ribosomal DNA Silencing. PLoS Genet 9(9): e1003805. doi:10.1371/journal.pgen.1003805

Editor: Wendy A. Bickmore, Medical Research Council Human Genetics Unit, United Kingdom

Received April 17, 2013; **Accepted** August 3, 2013; **Published** September 19, 2013

Funding: This work was supported by grants from the European Research Council (ERC-2010-Stg, N.260797, ChromatinModWeb) and the Cyprus Research Promotion Foundation (Health/Bio/0609(BE)/09). The funders had no role in study design, data collection and analysis, decision to publish, or preparation of the manuscript.

Competing Interests: The authors have declared that no competing interests exist.

* E-mail: kirmizis@ucy.ac.cy

☯ These authors contributed equally to this work.

Introduction

The nucleosome is the basic unit of chromatin and comprises 147 base pairs of DNA wrapped around a histone octamer, which contains two copies of each of the four histones H2A, H2B, H3 and H4. These histones are subjected to a variety of post-translational modifications, such as methylation, acetylation and phosphorylation, mediated by specific modifying enzymes [1]. Histone modifications often function by recruiting effector molecules to alter the structure of chromatin in order to regulate DNA-based processes such as transcription, replication and DNA repair [1]. An additional property of these modifications is the fact that they cross-talk to each other, whereby one modification influences the establishment or maintenance of a second modification [2].

N-alpha-terminal acetylation is a type of modification occurring on histones. In fact, it is one of the most common protein modifications, present on 80–90% of soluble mammalian proteins and 50–70% of yeast proteins [3,4]. This mark, which is deposited on the first amino acid residue of the protein has a range of molecular and biological roles, including regulation of protein degradation, protein translocation, protein complex formation, membrane attachment, apoptosis and cellular metabolism [5]. All four core histones [6–8] and the linker histone H1 [9] possess N-terminal acetylation, but this modification is more abundant on histones H2A and H4 [8]. N-terminal acetylation of these two histones is mediated by the N-alpha terminal acetyltransferase Nat4 (also known as NatD or Naa40). This enzyme was originally identified in the budding yeast *S. cerevisiae* [7], but also the human ortholog hNaa40 (also designated as hNatD, Nat11 or Patt1) has been recently characterized [10,11]. Both yeast Nat4 and hNaa40 target only histones H2A and H4, and this specificity differentiates them from all other described N-alpha acetyltransferases, which can target numerous substrates [5].

Previous studies have attempted to determine the biological role of yeast and human Nat4. Deletion of *NAT4* in yeast showed growth sensitivity when cells were cultured in media containing various chemicals such as 3-aminotriazole (3-AT), an inhibitor of transcription [12]. This sensitivity is enhanced when the *NAT4* deletion is combined with mutations in histone H4 where lysines 5, 8 and 12 have been replaced by arginines (K5,8,12R) [12], suggesting that modifications at these residues and N-terminal acetylation are linked through a mechanism that remains elusive. In humans, hNaa40 has been identified as a pro-apoptotic factor and has been implicated in hepatocellular carcinogenesis [11]. Furthermore, a recent study demonstrated that in mice this N-terminal acetyltransferase plays a role in hepatic lipid metabolism [13]. Although some studies have already uncovered phenotypes

Author Summary

The genome of eukaryotic cells is packaged into nucleosomes consisting of an octamer of histone proteins that is wrapped around by DNA. Histone proteins are often modified with chemical groups that can influence the arrangement of nucleosomes and thereby affect DNA-based processes like transcription. Histone N-terminal acetylation, which comprises the addition of a chemical group at the tip of the histone tail, is an abundant modification whose function is unknown. In this work, we show that N-terminal acetylation of histone H4 can strongly inhibit the occurrence of a neighboring modification, namely dimethylation at the third arginine. To do this, N-terminal acetylation cooperates with other internal lysine acetylation marks. We find that the communication amongst these histone modifications is necessary for controlling the expression of ribosomal RNA genes that are required for protein synthesis and cell growth. Our experiments show that in the absence of both N-terminal acetylation and lysine acetylation there is a strong increase in H4 arginine 3 dimethylation levels leading to cell lethality. This growth defect can be rescued by a point mutation on H4 that blocks methylation at position 3. Together, our results unveil a molecular and biological function for the previously uncharacterized N-terminal acetylation of histones.

related to the loss of Nat4 and have provided insights about the biological role of its human ortholog, the molecular function of histone N-terminal acetylation still remains unknown.

Arginine methylation is another histone modification that has attracted much attention in recent years. This is because of its involvement in various cellular processes and the identification of a family of enzymes that catalyze it. These enzymes are called protein arginine methyltransferases (PRMTs) and have already been associated with cancer pathogenesis [14]. PRMTs deposit one or two methyl groups to the guanidino groups of arginine residues resulting in monomethylated (Rme1), asymmetrically dimethylated (Rme2a) or symmetrically dimethylated (Rme2s) states. Others and we have previously shown that arginine methylation cross-talks with adjacent histone modifications by controlling their deposition [15–21]. It is, however, also important to discover the mechanisms that regulate PRMT activity and the deposition of histone arginine methylation.

Histone H4 arginine 3 (H4R3) is one of the residues that can possess any of the methylation states [20]. In particular, its asymmetrically dimethylated form is mediated by PRMT1 and it is associated with active transcription in mammals [22,23]. In yeast, however, the functional homolog of PRMT1 (known as Hmt1) that catalyzes H4R3me2a *in vitro* [24], has been linked to transcriptional repression. Specifically, Hmt1 and its associated H4R3me2a modification have been implicated in the formation of silent chromatin at yeast heterochromatin-like loci, including the rDNA repeat region [25]. This region contains an array of approximately 150 tandem repeats covering approximately 1–2 megabases of chromosome 12 [26]. Within each 9.1 kb rDNA repeat there are two transcriptional units known as *RDN5* and *RDN37* which, respectively, encode for the 5S and 35S rRNAs. The 35S transcript is quickly processed after transcription to generate the 18S, 5.8S and 25S rRNAs [27,28], which together with 5S are components of a eukaryotic ribosome. Whether the link between H4R3me2a and rDNA silencing relate to the transcriptional levels of these rRNAs is unclear [25].

A previous study has shown that neighboring histone acetylation at lysines 5, 8 and 12 regulates the activity of PRMT1 towards H4R3 *in vitro* [29]. A similar crosstalk among these adjacent modifications has also been proposed to occur in yeast histones [30], but in general the regulation of H4R3me2a *in vivo* remains largely unexplored. Here, we sought to identify factors that control the occurrence of this mark by employing a GPS (Global proteomic screen in *S. cerevisiae*) approach [31]. Using an antibody that specifically detects H4R3me2a we identified Nat4 as an inhibitor of this modification in yeast. Consistent with a role of H4R3me2a in promoting silencing at the rDNA region [25], we find that deletion or inactivation of Nat4 results in enhanced silencing of ribosomal DNA genes. Importantly, we demonstrate that this regulation is mediated through N-terminal acetylation of H4 (N-acH4), but not of H2A. Additionally, we show by using *in vitro* methylation assays that H4 N-terminal acetylation inhibits the activity of the Hmt1 arginine methyltransferase towards H4R3. Interestingly, we find that combinatorial loss of H4 N-terminal and internal K5, 8, and 12 acetylation can induce H4R3me2a deposition even more. Excessive H4R3me2a leads to a severe growth defect, which is rescued by preventing arginine 3 methylation by mutating this residue to lysine. Finally, we provide evidence that the interplay between N-acH4 and H4R3me2a functions under conditions of calorie restriction, which induce rDNA silencing. Altogether, our results reveal the function of H4 N-terminal acetylation in gene regulation, and elucidate the underlying molecular mechanism that links this N-terminal acetylation to other internal histone modifications.

Results

Nat4 is a novel regulator of H4R3me2a

We sought to identify proteins that regulate the deposition of asymmetrically dimethylated arginine 3 on histone H4 (H4R3me2a). To do this we developed an antibody that recognizes specifically methylated H4R3 (Figures S1A and S1B) when it is asymmetrically dimethylated (Figure S1C) and performed a GPS screen using the yeast deletion collection. We found that deletion of the N-alpha acetyltransferase 4 (*nat4Δ*) results in robust induction of the H4R3me2a levels (Figure 1A, lane 6). None of the other four yeast N-terminal acetyltransferases (NatA, NatB, NatC or NatE) showed an effect on H4R3me2a when they were deleted (Figure S2A). This effect was specific to the asymmetrically dimethylated form at H4R3, as specific antibodies (Figure S1C) towards monomethylated (H4R3me1) or symmetrically dimethylated (H4R3me2s) states of this residue detected similar levels for these marks between wild-type and *nat4Δ* strains (Figure 1B, compare lane 1 to 2). To determine whether Nat4 regulation towards H4R3me2a was dependent on its N-terminal acetyltransferase activity we constructed a catalytically inactive version of this enzyme. Mutation of four highly conserved residues (Figure 1C) found within the two motifs of its acetyltransferase domain [7] result in increased signal of H4R3me2a, phenocopying *nat4Δ* (Figure 1D, compare lane 2 and lane 6). Notably, the increase of H4R3me2a in Nat4 deficient cells is not due to epitope preference of the H4R3me2a antibody, as it recognizes equally well H4R3me2a peptides that are either N-terminally acetylated or unacetylated (Figure S1C, compare rows 5 and 6). Together, these findings show that Nat4 regulates the levels of H4R3me2a through its N-terminal acetyltransferase activity.

Loss of Nat4 activity enhances rDNA silencing and H4R3me2a deposition

Since a previous study has linked H4R3me2a with the establishment of silencing at the four heterochromatin-like regions

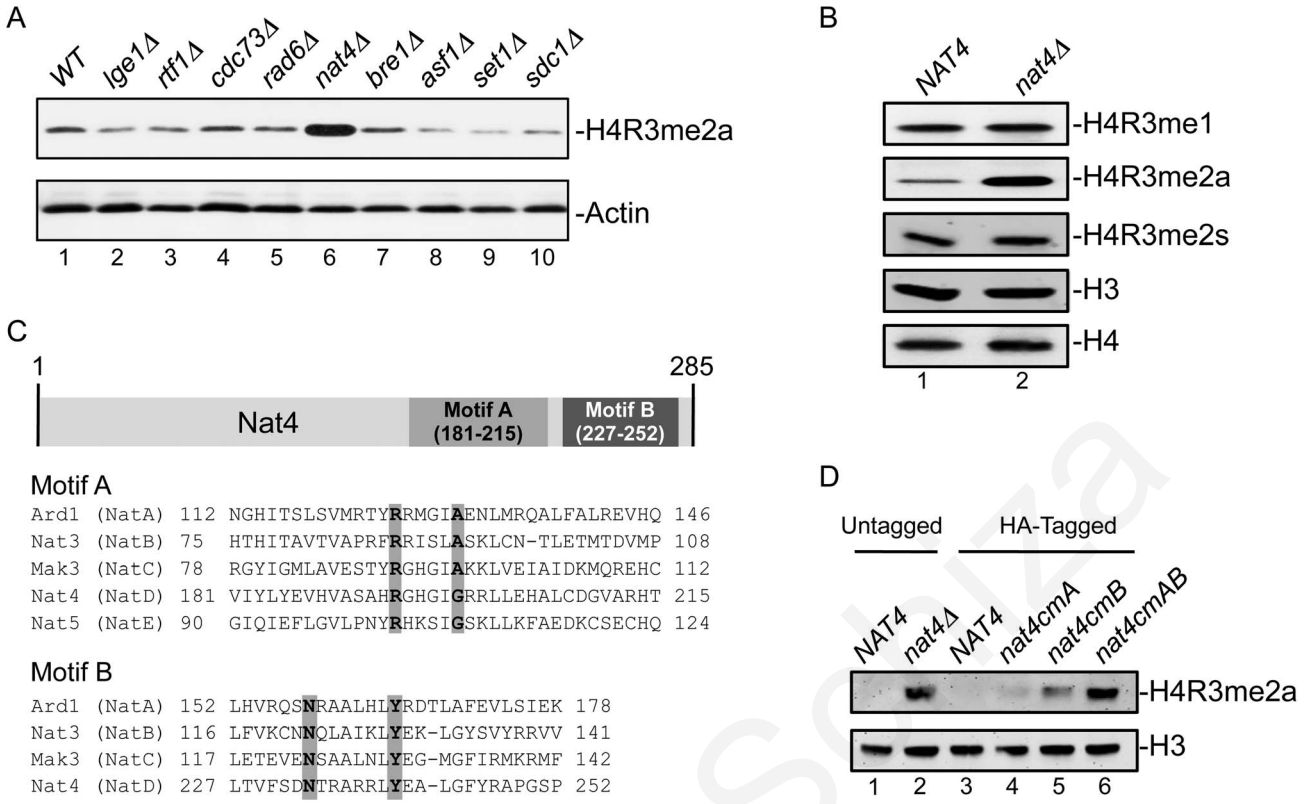

Figure 1. Deletion or inactivation of *NAT4* increases the levels of H4R3me2a. *(A)* Whole cell extracts from the indicated deletion strains were analyzed by western blotting with an antibody against H4R3me2a (top panel). Equal loading was monitored using an antibody against actin (bottom panel). *(B)* Whole cell extracts from a wild-type strain (*NAT4*, lane1) and another one carrying a *NAT4* deletion (*nat4Δ*, lane 2) were analyzed using antibodies against various H4R3 methylation states. Equal loading was monitored with H3 and H4 antibodies. *(C)* Sequence alignment of the catalytic motifs A and B of the five *S. cerevisiae* N-alpha acetyltransferases (NATs). The residues that were mutated within each motif to generate the Nat4 catalytic mutants are highlighted in grey. *(D)* Whole cell extracts from strains containing wild-type *NAT4* (lanes 1 and 3)) and different *NAT4* mutants (lanes 2, 4, 5 and 6) were analyzed by western blotting using antibodies against H4R3me2a (top panel) and H3 (bottom panel). The strain in lane 2 represents a Nat4 deletion strain. All catalytic mutant strains (lanes 4–6) have a C-terminal hemagglutinin (HA) tag. The strain containing the mutations within motif A is designated as *nat4cmA* (lane 4), the one with mutations in motif B is *nat4cmB* (lane 5) and the one with mutations in both motifs is noted as *nat4cmAB* (lane 6). Their equivalent wild-type strain contains only the C-terminal HA-tag (lane 3).
doi:10.1371/journal.pgen.1003805.g001

in yeast (rDNA, *HML*, *HMR* and telomeres) [25], we sought to determine whether deficiency of Nat4 activity will affect expression at these loci. We found that deletion of *NAT4* did not affect greatly the expression at *HMR*, *HML* and *TEL-VII-L* (Figure S3), but strongly enhances silencing at the rDNA locus (Figure 2A). Due to recent concerns in using FOA-sensitivity assays to assess chromatin silencing [32,33], we tried to validate the above result by testing the expression of the endogenous rDNA transcripts (Figure 2B). Examining the levels of the different ribosomal RNAs (5S, 25S, 5.8S and 18S, as well as their precursor 35S) by real time-PCR we confirmed the above result, as deletion of *NAT4* significantly reduced the amount of all rRNAs (Figure 2B). It is worth mentioning that because the 35S primary transcript is quickly processed [27,28], the observed changes in the levels of rRNAs are most likely caused by a decrease in transcription. Interestingly, the deletion of *NAT4* does not affect the mRNA levels of the ribosomal protein Rpp0 (Figure 2B, rightmost panel). A similar result was obtained when the Nat4 catalytic mutant strain (*nat4cmAB-HA*) was used to examine the levels of 25S (Figure S4A), suggesting that rDNA expression is dependent on the Nat4 acetyltransferase activity.

According to these findings, we anticipated that the reduced expression of all rRNAs would correlate with increased deposition of H4R3me2a at the rDNA genes. Indeed, ChIP analysis confirmed that there is higher nucleosomal deposition of H4R3me2a across the entire rDNA locus when Nat4 is absent (Figure 2C, top panel). Consistent with this, an induction of H4R3me2a deposition was also observed at *RDN25* in the strain expressing a catalytically inactivated Nat4 (Figure S4B). As expected, based on the results in figure 1B we did not see changes in the occupancy of H4R3me1 at *RDN25* in the *nat4Δ* strain (Figure S4C). Importantly, the lack of N-terminal acetyltransferase activity in the *nat4Δ* and Nat4 catalytic mutant (*nat4cmAB-HA*) strains was confirmed by an antibody against N-terminally acetylated H4 (N-acH4), which showed that this modification was reduced throughout the rDNA region (Figure 2C, bottom panel and figures S4B–C).

Nat4 controls rDNA silencing and H4R3me2a through N-alpha-acetylation of H4

Although our data above demonstrate that Nat4 suppresses rDNA silencing and prevents H4R3me2a deposition, they do not show which one of its two targets, histone H4 or H2A, is implicated in this regulation. To determine this, we constructed yeast strains in which either H4 or H2A were compromised for N-terminal acetylation. Endogenous H4 or H2A were expressed with

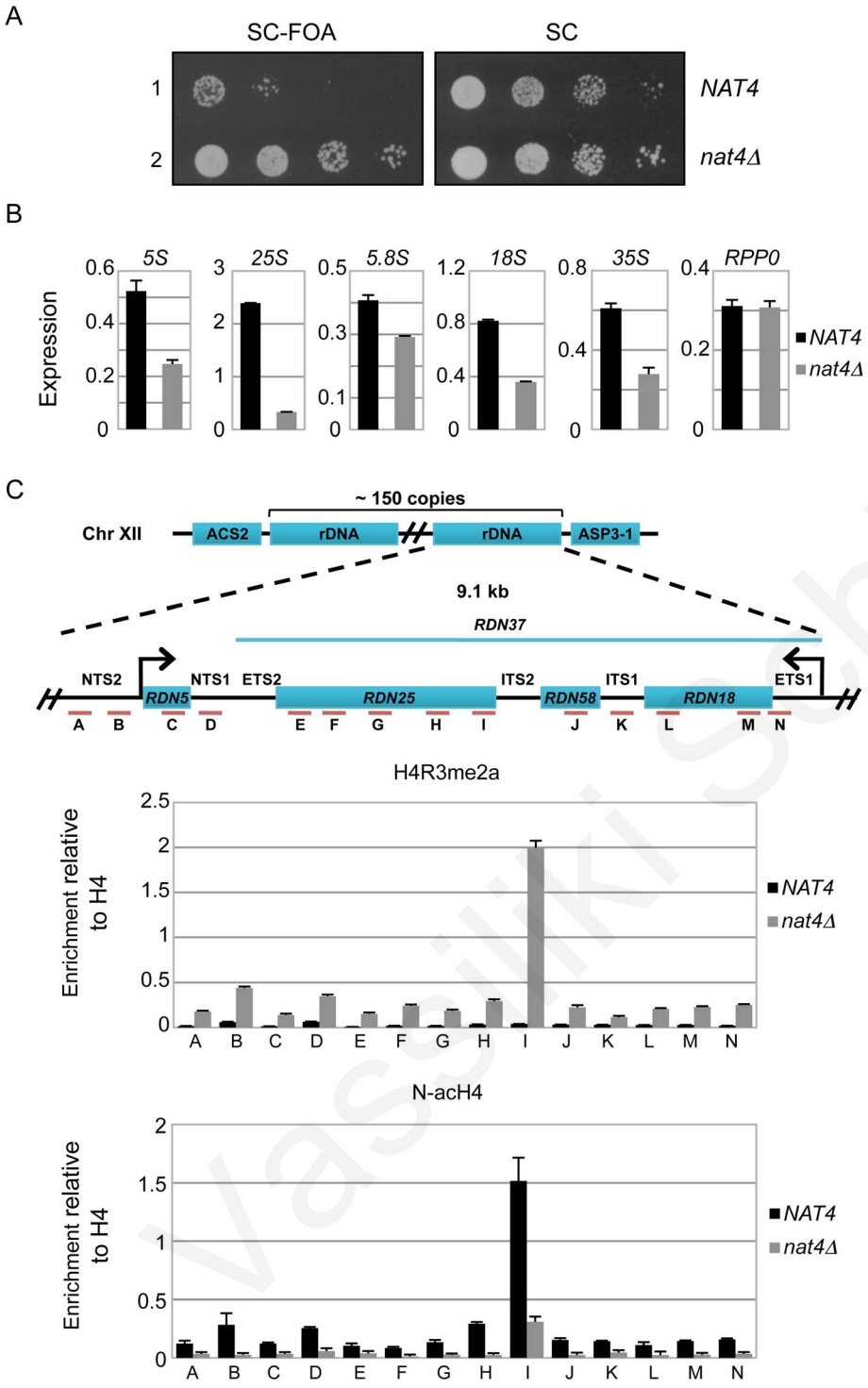

Figure 2. Deletion of *NAT4* enhances silencing and H4R3me2a deposition across the *rDNA* locus. *(A)* Silencing assays for the *rDNA* region were performed with wild-type (row 1) or *nat4Δ* (row 2) strains. Both strains (*NAT4* and *nat4Δ*) carry a copy of the *URA3* gene, that encodes for an essential enzyme in the Uracil metabolic pathway, inserted in the rDNA locus (*RDN1::URA3*). This enzyme metabolizes 5′-Fluoroorotic acid (FOA) into a toxic compound, and the ability of the cell to survive in the presence of FOA depends on the degree of silencing in the rDNA region, such that stronger silencing coincides with more cell growth. The cells were spotted in 10-fold dilutions on SC medium (right panel) or SC+FOA (left panel) and grown for 48 h at 30°C. *(B)* Expression levels of rRNAs 5S, 25S, 5.8S, 18S, 35S and the *RPP0* gene were analyzed by qRT-PCR using total RNA extracted from *NAT4* and *nat4Δ* strains. *(C)* Schematic of the budding yeast rDNA locus on chromosome XII. The rDNA region represents an array consisting of ~150 tandem copies of a 9.1 kb repeating unit. Each repeat contains the genes *RDN5* and *RDN37* (encodes the 35S primary transcript) as well as two non-transcribed spacers (*NTS1*, *NTS2*), two external transcribed spacers (*ETS1*, *ETS2*) and two internal transcribed spacers (*ITS1*, *ITS2*). Primers were designed along the rDNA locus as indicated by the red lines and letters A–N. ChIP experiments were performed in the *NAT4* and *nat4Δ* strains using antibodies against H4R3me2a (top panel) and N-acH4 (bottom panel). The immunoprecipitated chromatin was analyzed by qRT-PCR using the primers A–N. (see Table S2 for their sequence). The enrichment from each antibody was normalized to the levels of histone H4. Error bars in *(B)* and *(C)* indicate s.e.m for duplicate experiments.
doi:10.1371/journal.pgen.1003805.g002

an alanine instead of a serine (H4S1A or H2AS1A) at the first residue because for both histones, the sequence of their first 30 amino acids is absolutely required for efficient acetylation by Nat4 [7,12]. Figure 3A shows that mutation of H4 serine 1 to alanine induces H4R3me2a deposition (compare lanes 1 and 2), but the same mutation in H2A has no effect on this methylation (compare lanes 3 and 4). Furthermore, in the H4S1A mutant strain we detected higher amounts of H4R3me2a deposited at the *RDN25* gene compared to an isogenic wild-type (H4WT) strain (Figure 3B). On the other hand, the H2AS1A mutant did not show significant difference in H4R3me2a levels compared to H2AWT strain (Figure 3B). We also like to note that the results of the H4S1A haploid mutant strain are not affected by the fact that H4S1 is also phosphorylated because this modification is only induced under sporulation conditions in diploid cells [34].

To validate that Nat4 regulation of rDNA silencing is mediated through H4, we then examined the expression of this locus in the H4S1A strain (Figure 3C and 3D). Both, analysis of 25S rRNA expression levels and silencing spot assays demonstrate that the H4S1A mutation enhances repression of this locus similarly to *nat4Δ* (compare Figure 3C and 3D to Figure 2B and 2A, respectively), albeit to a lesser extent. This result is in agreement with the increased H4R3me2a levels shown above (Figure 3B). In contrast, H2AS1A mutation does not alter the levels of 25S rRNA (Figure 3C). Additional evidence that rDNA silencing is mediated through N-terminal acetylation of H4 comes from using a strain expressing a H4S1P mutant. The presence of proline at position 1 blocks N-terminal acetylation completely as shown by mass-spectrometry analysis of proteins extracted from yeast, *Drosophila melanogaster* and human cells [3,35]. As expected, we observed a significant decrease in the levels of 25S rRNA in the H4S1P mutant strain, similarly to the effect observed in the *nat4Δ* strain (Figure S5). Altogether, these results suggest that Nat4 regulates rDNA silencing and H4R3me2a deposition via H4 N-terminal acetylation, but not through N-acH2A.

Finally, to verify the link of N-acH4 within this mechanism, we have also monitored the levels of H4R3me2a in a *nat4Δ* strain that expresses ectopically the human ortholog of Nat4 (hNaa40). It was previously shown that expression of hNaa40 in yeast results in N-terminal acetylation of H4 but not of H2A [10]. In agreement with

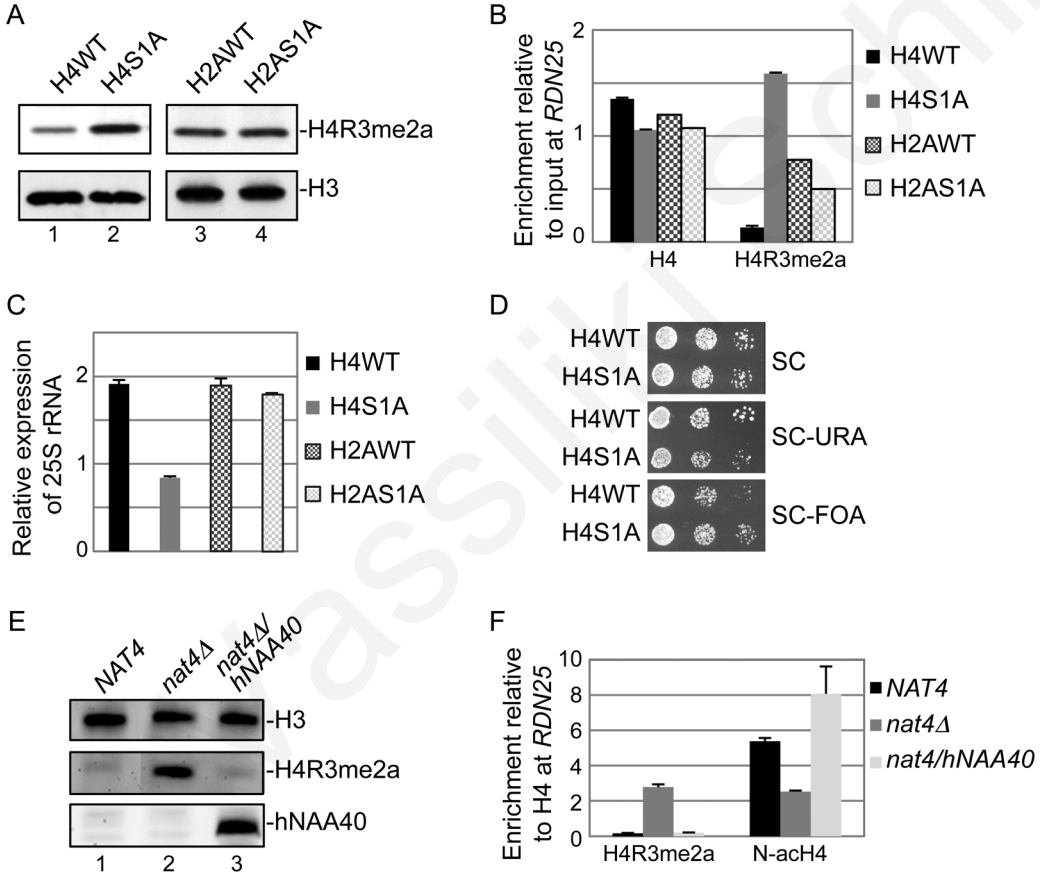

Figure 3. Nat4 inhibits rDNA silencing and H4R3me2a through N-terminal acetylation of H4. *(A)* Whole cell extracts prepared from the wild-type strains (H4WT and H2AWT) and their correspondent Serine-to-Alanine mutants in position 1 (H4S1A and H2AS1A) were analyzed by western blotting using antibodies against H4R3me2a (top panel) and H3 as control (bottom panel). *(B)* ChIP experiments were performed in the same strains as in *(A)* using the H4 and H4R3me2a antibodies. The immunoprecipitated chromatin was analyzed by qRT-PCR using primer I specific to the *RDN25* gene (shown in figure 2C). The enrichment from each antibody was normalized to 1% of the total input DNA. *(C)* Gene expression analysis of 25S rRNA performed using the same strains as in *(A)*. The expression levels of the 25S rRNA were normalized to the levels of *RPP0*. *(D)* Silencing assays for the *rDNA* locus were performed with a wild-type (H4WT) or a H4S1A mutant strain as described in (*2A*). *(E)* Whole yeast cell extracts prepared from the wild-type strains *NAT4* (lane 1), and the mutant strains *nat4Δ* (lane 2) and *nat4Δ/hNAA40* (that carries a *NAT4* deletion and a plasmid that expresses ectopically *hNAA40*, lane 3) were analyzed by western blotting using the indicated antibodies. Equal loading was monitored by an H3 antibody (top panel). *(F)* ChIP experiments performed in the indicated strains as in *(E)* using antibodies against H4R3me2a and N-acH4. The enrichment of each antibody was normalized to the levels of H4 occupancy. Error bars in *(B)*, *(C)* and *(F)* indicate s.e.m for duplicate experiments.
doi:10.1371/journal.pgen.1003805.g003

our data above, we found by western blotting that expression of hNaa40 in a *nat4Δ* strain reduces H4R3me2a back to wild-type levels (Figure 3E, compare lane 3 to lane 1). ChIP analysis also showed that expression of hNaa40 in a *nat4Δ* strain fully restores the N-acH4 levels at *RDN25* (Figure 3F), confirming that histone H4 is the main substrate through which Nat4 regulates H4R3me2a.

N-acH4 inhibits the Hmt1 methylase activity towards H4R3

The above results suggest that N-acH4 regulates the deposition of H4R3me2a. To explore this further, we wanted to determine whether the activity of the yeast arginine methyltransferase Hmt1, which was previously shown to target H4R3 *in vitro* [24], is inhibited by N-acH4. We performed methyltransferase assays using Hmt1 purified from yeast cells (Figure S6) and synthetic peptides corresponding to the first twenty amino acids of H4. Immunoblotting for H4R3me2a showed that Hmt1 dimethylates much more efficiently H4R3me1 peptides that are not N-terminally acetylated as opposed to those that possess N-acH4 (Figure 4A, compare lanes 13 and 14). Overall, these findings show that N-acH4 represses the deposition of H4R3me2a by blocking the activity of the associated arginine methyltransferase.

H4R3 is required for the regulation of rDNA silencing by Nat4 and N-acH4

The previous results link Nat4 with rDNA silencing and H4R3me2a. However, they do not demonstrate whether methylation at H4R3 is necessary and sufficient for the effect of Nat4 towards rDNA expression. To determine this, we investigated the effect of *NAT4* deletion on 25S rRNA expression when arginine 3 was mutated to lysine (H4R3K) in order to prevent its methylation (Figure S1A). Despite the loss of N-acH4 in a H4R3K *nat4Δ* double mutant strain (Figure 4B), the expression levels of 25S rRNA are not reduced compared to the *nat4Δ* only strain (Figure 4C). ChIP analysis at *RDN25* confirms that H4R3me2a is induced in the *nat4Δ* strain, and is undetected in the H4R3K *nat4Δ* strain (Figure 4B). This finding indicates that H4R3 and most likely its methylation are absolutely required for the control of rDNA silencing by Nat4 and N-acH4.

N-acH4 cooperates with H4K5,-K8,-K12 acetylation to control H4R3me2a, rDNA silencing and cell growth

Evidence from two previous studies have raised the hypothesis that N-acH4 works together with acetylation of H4K5, H4K8 and H4K12 to control the deposition of H4R3me2a. The first study showed that asymmetric dimethylation of H4R3 mediated by PRMT1 is inhibited *in vitro* by acetylation of lysines 5, 8 and 12 of H4 [29]. The second one demonstrated a synthetic defect in yeast containing *nat4Δ* and a triple lysine to arginine mutant (H4K5,8,12R) [12]. Hence, to explore this hypothesis, we combined *nat4Δ* with the H4K5,8,12R mutant because deletion of Esa1, that acetylates these three lysines is inviable [36]. Interestingly, we found that concurrent loss of N-acH4 and acetylation of H4K5, 8, 12 (H4K5,8,12R *nat4Δ*) results in robust induction of H4R3me2a (Figure 5A, compare lanes 2 and 4), suggesting that these H4 residues collaborate to regulate H4R3me2a. This result is not due to an antibody artifact, as the H4R3me2a antibody recognizes slightly better methylated peptides in which positions 5, 8, and 12 are lysines than when these residues are arginines (Figure S7, compare rows 2 and 3). Because it was recently shown that H4K5, K8 and K12 could also be methylated by Set5 [37], we wanted to investigate the possibility

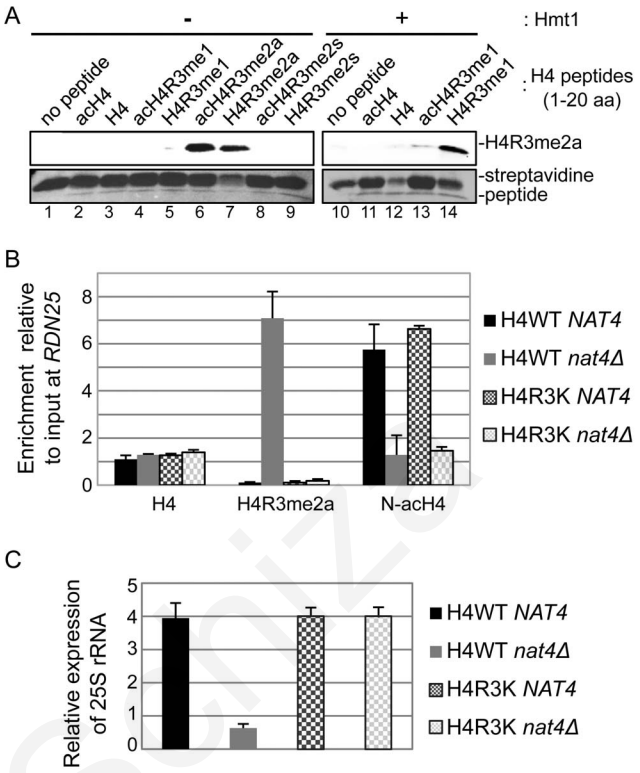

Figure 4. N-acH4 inhibits the Hmt1 methyltransferase activity towards H4R3. *(A) In vitro* methylation assays were performed with synthetic biotinylated peptides representing the first 20 amino acids of histone H4 in the absence (lanes 1 to 9) or presence (lanes 10 to 14) of purified yeast Hmt1. The methyltransferase activity was monitored by western blotting using an antibody against H4R3me2a. Peptide loading was controlled by ponceau staining. *(B)* ChIP experiments were performed in the wild-type (H4WT *NAT4*) and the mutant strains carrying a *NAT4* deletion (H4WT *nat4Δ*), an H4 Arginine-to-Lysine mutation in position 3 (H4R3K *NAT4*) or both (H4R3K *nat4Δ*), using antibodies against H4, H4R3me2a and N-acH4. The enrichment at *RDN25* was analyzed as in (*3B*). *(C)* 25S rRNA expression level analysis was performed in the same strains as in *(B)*. The qRT-PCR analysis was performed as in *(3C)*. Error bars in *(B)* and *(C)* indicate s.e.m for duplicate experiments.
doi:10.1371/journal.pgen.1003805.g004

that methylation of these lysines could act synergistically with N-acH4 to control H4R3me2a. Double *nat4Δ set5Δ* deletion did not enhance H4R3me2a levels compared to the *nat4Δ* single mutant (Figure S8, compare lanes 2 and 4), indicating that it is acetylation, and not methylation of H4K5, 8, 12 that cooperates with N-acH4. Notably, N-acH4 is the major regulator of H4R3me2a, as the H4K5,8,12R mutant alone does not increase the levels of H4R3me2a to the same extent as *nat4Δ* (Figure 5A, compare lanes 2 and 3).

To further validate the above results, we also examined the effect of the combination of *nat4Δ* with H4K5,8,12R on the deposition of H4R3me2a and 25S rRNA expression. Consistent with the previous findings we observed a significant enrichment in H4R3me2a at the *RDN25* gene when *NAT4* is deleted together with the H4K5,8,12R mutant as opposed to the *nat4Δ* single mutant (Figure 5B). Moreover, the higher presence of H4R3me2a in the H4K5,8,12R *nat4Δ* double mutant strain results in further reduction of 25S rRNA levels when compared to the *nat4Δ* alone (Figure 5C). Taken together, these results indicate that, both N-acH4 (Figure 4A) and internal lysine acetylation [29] can impede

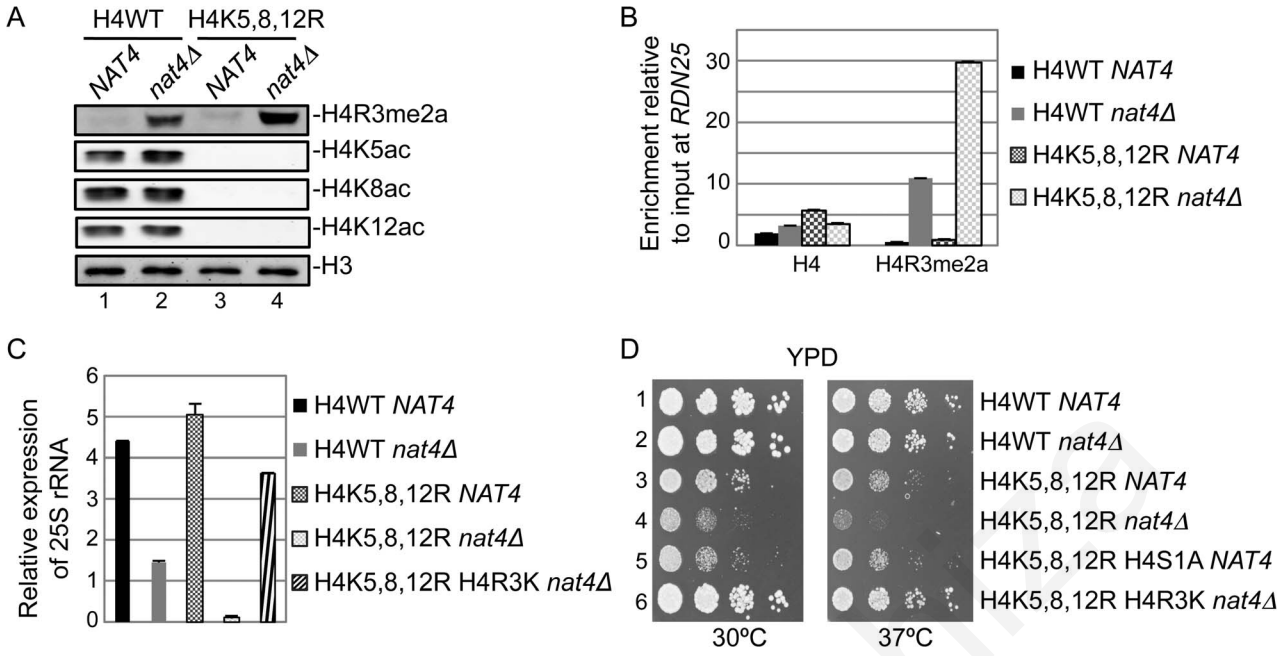

Figure 5. N-acH4 acts synergistically with H4K5, 8, 12 acetylation to control rDNA silencing, H4R3me2a and cell growth. *(A)* Whole yeast cell extracts were prepared from the wild-type (H4WT *NAT4*) and the mutant strains carrying a *NAT4* deletion (H4WT *nat4Δ*), a triple Lysine-to-Arginine mutation in H4 in positions 5, 8 and 12 (H4K5,8,12R *NAT4*) or both (H4K5,8,12R *nat4Δ*) and then analyzed by western blotting using the H4 modification antibodies are shown. Equal loading was monitored with an H3 antibody (bottom panel). *(B)* ChIP experiments were performed in the same strains as in (*A*) using the antibodies against H4 and H4R3me2a. The enrichment of each antibody was analyzed as in *(3B). (C)* 25S rRNA expression level analysis was performed in the wild-type (H4WT *NAT4*) and the mutant strains carrying a *NAT4* deletion (H4WT *nat4Δ*), a triple H4 Lysine-to-Arginine mutation in positions 5, 8 and 12 (H4K5,8,12R *NAT4*) both (H4K5,8,12R *nat4Δ*), and a multiple H4 mutant with a triple Lysine-to-Arginine substitution in positions 5, 8 and 12, an Arginine-to-Lysine mutation in position 3, and a *NAT4* deletion (*H4K5,8,12R H4R3K nat4Δ*). The analysis was performed as in (*3C*). Error bars in *(B)* and *(C)* indicate s.e.m for duplicate experiments. *(D)* Growth assay of the same yeast strains as in *(C)* plus a multiple H4 mutant with a triple Lysine-to-Arginine substitution in positions 5, 8 and 12, and Serine-to-Alanine mutation in position 1 (H4K5,8,12R H4S1A *NAT4*). Cells were spotted in 10-fold dilutions on YPAD medium plates. Cell growth was examined at 30°C (left panel) or 37°C (right panel).
doi:10.1371/journal.pgen.1003805.g005

on the methylase activity that targets H4R3, but according to our findings N-acH4 is the predominant regulator of H4R3me2a and rDNA silencing (Figure 5A–C).

Considering that the double mutant of *nat4Δ* with H4K5,8,12R results in robust reduction of 25S rRNA levels (Figure 5C), we then examined the growth rate of this strain using serial dilution spotting assays (Figure 5D) and by measuring its doubling time (Figure S9). Notably, the double mutant strain (H4K5,8,12R *nat4Δ*) has a severe growth defect in comparison to the corresponding single mutants (Figures 5D and S9, left panels). This growth defect becomes lethal when cells are grown at a higher (37°C) temperature (Figures 5D and S9, right panels). Moreover, when H4S1A is combined with the H4K5,8,12R mutant a growth defect is also observed, albeit less severe (Figures 5D and S9, left panels), consistent with the milder deregulation of H4R3me2a and rDNA expression in the H4S1A mutant as opposed to *nat4Δ* (compare Figures 2 and 3). This synthetic defect supports the synergistic effect between N-acH4 and internal H4 lysine acetylation in controlling H4R3me2a and rDNA expression. Based on the previous experiments which showed that arginine 3 is necessary and sufficient for the regulation of rDNA silencing by Nat4 (Figure 4), we then examined whether H4R3K can rescue the growth defect caused by the combination of *nat4Δ* and the H4K5,8,12R mutant. Interestingly, H4R3K rescues entirely the growth defect of the double H4K5,8,12R *nat4Δ* mutant grown at an ambient (30°C) or even at a higher (37°C) temperature (Figures 5D and S9). Additionally, H4R3K restores the rRNA expression levels to almost near wild-type in the double H4K5,8,12R-*nat4Δ* mutant strain (Figure 5C). All together, these results reveal that excessive H4R3 asymmetric dimethylation caused by lack of N-acH4 and internal lysine acetylation impairs cell growth.

Calorie restriction increases rDNA silencing and the ratio of H4R3me2a to N-acH4

The expression of the rRNA transcripts is modulated by various environmental and intracellular stress conditions. One such condition is calorie restriction, which is studied in yeast by diminishing the levels of glucose in the media. Previous studies have shown that reduction of glucose levels from 2% to 0.5% can enhance rDNA silencing [38,39]. Hence, we sought to determine whether the crosstalk of N-acH4 and H4R3me2a is induced under these conditions in a wild-type yeast strain. In agreement with previous studies, we found that lowering the glucose availability decreases the levels of 25S rRNA, and this reduction is greater under severe (0.1% and 0.05% glucose) calorie restriction (Figure 6A). Most importantly, the decrease in the amount of 25S rRNA correlates with an increase in the H4R3me2a:N-acH4 enrichment ratio at the *RDN25* gene. The increase in the enrichment of H4R3me2a against N-acH4 is evident under severe calorie restriction, in line with the lower levels of 25S rRNA (Figure 6B, see 0.1% and 0.05% glucose). These findings suggest that the interplay between H4 N-terminal acetylation and H4R3me2a controls rDNA silencing in response to environmental stimuli such as nutrient deficiency.

Discussion

The molecular function of histone H4 N-terminal acetylation was unknown until now, even though this is an abundant and conserved modification that was reported several decades ago [40]. In this study, we describe an important role of N-acH4 in the regulation of histone arginine methylation and rDNA silencing. Taken together, our data support a model in which N-acH4 mediated by Nat4 strongly inhibits the activity of the Hmt1 methyltransferase towards H4R3. This inhibition leads to activation of the rDNA loci. Removal of N-acH4 by a yet unknown mechanism, allows deposition of H4R3me2a and results in repression of rRNA transcription (Figure 7). This mechanism is activated during calorie restriction in order to reduce the expression of the rDNA region in response to the limited source of energy. In the absence of N-acH4, internal lysine acetylation at K5, K8 and K12 catalysed by Esa1 [36] or Hat1 [41] remain unaffected (Figure 5A, compare lanes 1–2 and Figure S10). These acetyl marks can fine-tune the levels of H4R3me2a because otherwise excessive methylation of H4R3 will result in a severe growth defect (Figures 5D and S9). The proposed mechanism also provides an explanation for the previously observed synthetic defect of the double H4K5,8,12R *nat4Δ* mutant strain [12]. Whether the growth defect observed in our experiments is due to deregulation of the rDNA region only or whether other genomic loci whose expression is influenced by H4R3me2a also contribute to this phenotype is still unclear. There are two possible scenarios, which are not mutually exclusive, on how H4R3me2a then mediates rDNA silencing in yeast. First, it was proposed earlier that H4R3me2a facilitates recruitment of Sir2 to the rDNA region [25]. Second, based on previous findings that arginine methylation occludes recruitment of effectors to adjacent modifications [16–18,20,42], it is possible that H4R3me2a prevents the binding of an activator at the neighboring N-terminal or lysine acetylation marks.

Previous studies suggested that Nat4 and hNaa40 acetylate H4 co-translationally as they were found associated with the ribosomes [10,12]. However, it remains possible that Nat4 and hNaa40 target H4 post-translationally because a significant amount of hNaa40 localizes to the nucleus [10,11]. Similarly to other acetyl marks such as H4K5ac and H4K12ac [43], N-acH4 might be catalyzed on soluble nuclear histones that are subsequently incorporated into chromatin. In support of this, N-alpha-terminal acetylation has been proposed to occur post-translationally on other proteins [44,45]. How N-acH4 is then removed from histones is another pending question. One possibility is through histone exchange by which unacetylated H4 replaces N-terminally acetylated H4 found in chromatin. Another scenario is through active deacetylation mediated by a deacetylase, an activity that has not been demonstrated yet for any protein N-terminal acetylation mark [5].

Interestingly, Nat4 is not the only Nat that has been implicated in the regulation of heterochromatic regions in yeast. NatA has also an active role in chromatin silencing but possibly functions through a mechanism that is distinct from that of Nat4 for three main reasons. Firstly, NatA establishes telomeric and HML silencing by acetylating Orc1 and Sir3 in order to stimulate their recruitment onto chromatin [46–48]. However, silencing at the rDNA region does not involve these proteins [49]. Secondly, in our experiments the absence of Ard1 (the catalytic subunit of NatA) has no effect on the levels of H4R3me2a (Figure S2A). Finally, in the *ard1Δ* strain, the levels of 25S rRNA are not significantly altered compared to a wild-type strain (Figure S2B). Therefore, we believe that Nat4 and NatA impact on chromatin silencing through different pathways.

A link between calorie restriction and increased lifespan in yeast and other organisms has already been established [50]. Considering that changes in the levels of N-acH4 and H4R3me2a are associated with calorie restriction (Figure 6), it would be interesting to determine in future studies whether these modifications and their respective enzymes are part of a mechanism that extends cellular lifespan. Another histone H4 acetylation (H4K16ac) has already been implicated in the regulation of lifespan in yeast through a mechanism that maintains telomeric chromatin intact [51]. In contrast, we anticipate that N-acH4 and H4R3me2a, if involved in lifespan regulation, would be part of a pathway that controls rDNA silencing [38,39], since our data show that deletion of *NAT4* does not affect telomeric silencing (Figure S3). Alternatively, N-acH4, H4R3me2a and their associated enzymes could influence longevity by regulating rDNA recombination, given that Hmt1 activity represses this process [25]. Two recent studies support this idea because they show that calorie restriction suppresses rDNA recombination independently of rDNA silencing in order to extend lifespan [52,53].

Although this study was performed entirely in yeast, there is evidence suggesting that the cross-talk among N-acH4, internal

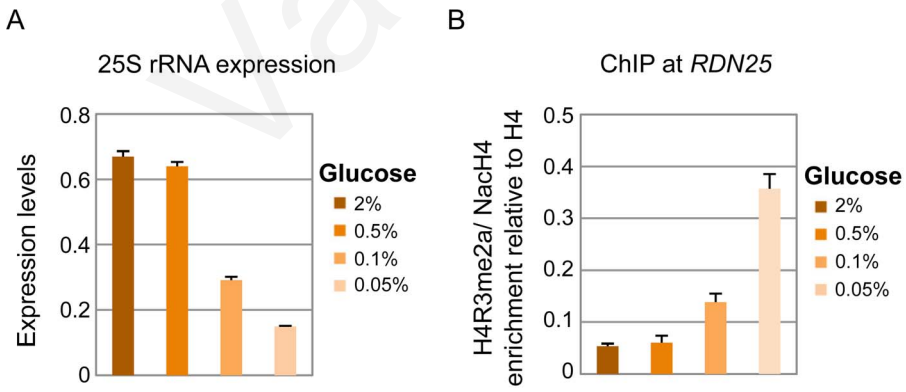

Figure 6. Calorie restriction increases *RDN25* silencing and the H4R3me2a: NacH4 enrichment ratio. *(A)* The levels of 25S rRNA were analyzed by qRT-PCR using total RNA extracted from a wild-type strain (BY4741) grown in minimal media containing different glucose concentrations (2%, 0.5%, 0.1% and 0.05%). *(B)* ChIP experiments were performed in a wild-type BY4741 strain grown in the same conditions as in *(A)*, using antibodies against H4R3me2a and N-acH4. Their enrichment is normalized to histone H4 and represented as ratio of H4R3me2a to N-acH4. Error bars in *(A)* and *(B)* indicate s.e.m for duplicate experiments.
doi:10.1371/journal.pgen.1003805.g006

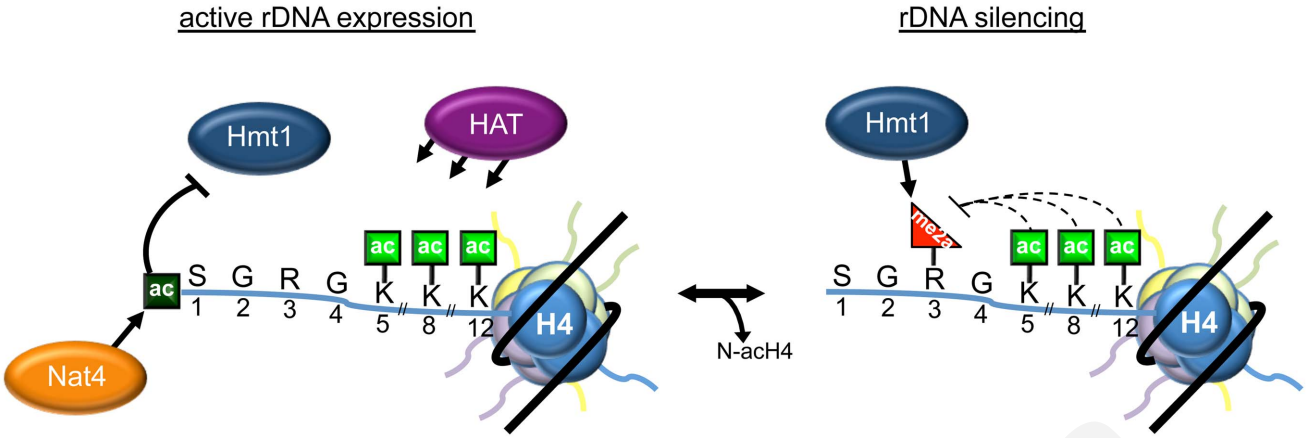

Figure 7. Model depicting the role of N-acH4 in rDNA silencing. When rDNA expression is required, Nat4-catalyzed H4 N-terminal acetylation inhibits Hmt1-mediated H4R3me2a. Under conditions where rDNA expression needs to be repressed, as in an environment with low glucose concentration, N-terminal acetylation decreases by a mechanism still unknown. This mechanism, that can be active (by an enzyme) or passive (by histone dilution) reduces the levels of N-acH4 and allows Hmt1 to asymmetrically dimethylate H4R3, triggering rDNA silencing. Lysine acetylation on residues 5, 8 and 12 fine-tunes the levels of H4R3me2a, as excessive deposition of this mark leads to a severe growth defect at 30°C or even cell lethality at a higher temperature (37°C).
doi:10.1371/journal.pgen.1003805.g007

lysine acetylation and H4R3 methylation may be conserved in mammals. For instance, the activity of Nat4 towards H4 is conserved in humans [10], and its ortholog hNaa40 can re-establish normal levels of H4R3me2a in the absence of Nat4 (Figure 3E–F). Furthermore, mass spectrometry analysis of mouse histone H4 revealed that N-terminal acetylation co-exists with K5, K8 and K12 acetylation and has an inverse relationship with H4R3 methylation [54]. Interestingly, this anticorrelation in mouse cells does not involve asymmetric dimethylation but rather a trimethylated form of H4R3 [54], whose existence is still under debate. The mutual exclusive pattern between N-terminal acetylation and H4R3 methylation becomes even more apparent on H2A peptides [54], suggesting that in mammals this modification crosstalk could also occur on histone H2A. This is consistent with the fact that mammalian H2A (Ser-Gly-Arg-Gly-Lys) has an arginine at position 3 and its N-terminal sequence is identical to H4, in contrast to yeast H2A (Ser-Gly-Gly-Lys-Gly) whose third residue is a glycine. Determining whether Naa40 utilizes a similar mechanism to control gene activation in mammalian cells is intriguing, considering that this enzyme has a pro-apoptotic function and was found significantly downregulated in hepatocellular carcinomas [11].

In summary, this study provides a novel link between protein N-terminal acetylation and the regulation of gene expression. This regulation employs a unique mechanism by which histone N-terminal acetylation influences the deposition of another *in cis* modification. Since N-terminal acetylation occurs on the majority of soluble eukaryotic proteins [3,4], we propose that its crosstalk with internal post-translational modifications might be a common mechanism for controlling protein function.

Materials and Methods

Yeast strains

All strains used in this study are listed in Table S1 and described in Protocol S1.

Antibodies

Rabbit polyclonal antibodies were raised against H4R3me2a and N-acH4 by Eurogentec (Belgium). Additional details are provided in Protocol S1. Other antibodies used were: H4K5ac (ab51997; Abcam), H4K12ac (ab46983; Abcam), H4K8ac (ab15823; Abcam), H4R3me1 (ab17339; Abcam), H4R3me2s (ab5823; Abcam), H3 (ab1791; Abcam), H4 (62-141-13; Millipore), Naa40 (ab106408; Abcam), b-Actin (ab8226; Abcam) and His-tag (2365; Cell Signalling).

Growth and silencing assays

Overnight cultures were diluted to OD ~0.1 and grown to mid-log phase. Approximately 1.2×10^4 cells were serially diluted 10-fold, and spotted onto the right media plates (YPAD, SC or SC+5′-Fluoroorotic acid). The plates were incubated at 30°C or 37°C for 2 days. Doubling time of cell growth was measured as indicated on http://www.doubling-time.com/compute.php.

Gene expression analysis

Total RNA from logarithmically grown (OD 0.8) yeast cells was isolated using the hot phenol extraction method [55] and was then treated with the TURBO DNA-free DNase kit (Ambion). Isolated total RNA (0.5 µg) from each sample was mixed with 1 µl dNTP mix (10 mM) and 1 µl of primer cocktail that consists of 0.5 µl oligo-(dT)20 primer (50 µM) and 0.5 µl random hexamers (50 µM) (Invitrogen). DNase RNase-free water was added up to a final volume of 13 µl. The mixture was incubated at 65°C for 5 min for first strand cDNA synthesis. After addition of 4 µl 1× first strand buffer, 1 µl DTT (0.1M), 1 µl RNase inhibitor (RNaseOut 40 U/ µl) and 1 µl Superscript III reverse transcriptase (200 U/µl) (all Invitrogen), the mixture was incubated for 5 min at 25°C, 60 min at 50°C and 15 min at 70°C. A negative control reaction was carried out with 1 µl of DNase RNase-free water instead of the SSIII enzyme. 50 µl of DNase RNAse-free water was added to the final cDNA before analyzing with real-time PCR. SYBR Green (Kapa SYBR Fast Master Mix # KK4602) was used to quantify the level of expression. Relative quantification took place using the reference gene *RPP0* for normalization. Real-time PCR (10 µl reactions) included 1 µl of cDNA, 0.2 µl of forward primer (50 µM), 0.2 µl of reverse primer (50 µM), 5 µl of SYBR Green and 3.6 µl DNase RNase free water. Reactions were incubated in a Biorad CFX96 Real-Time PCR system in 96-well plates using the primers listed in table S2.

ChIP

ChIP assays were performed as described previously [18].

Methyltransferase assay

Purified yeast Hmt1 (5 µg) and 22.5 µg of biotinylated histone H4 peptides (Cambridge Peptides, UK) were incubated with 40 µl of MyOne Dynal Streptavidine beads T1 (Invitrogen, #65601) in 100 µl total Reaction Buffer (20 mM Tris-Hcl pH 8, 50 mM NaCl, 1 mM EDTA pH 8, 5% Glycerol, 1 mM DTT, 2 mM S-adenosylmethionine and protease inhibitors) for 20 hours at 30°C with shaking. The beads were then precipitated using a magnetic rack (Invitrogen) and resuspended in 10 µl SDS-loading buffer. The peptides were eluted by alternately boiling, cooling and vortexing the beads three times. The eluted samples were then analyzed by Western blotting and ponceau staining.

SDS-PAGE and western blotting

Yeast cells were grown to mid-exponential phase in a 30°C shaker. Total yeast extracts were prepared by first resuspending cell pellets in a tenfold volume of SDS loading buffer (50 mM Tris-HCl pH 6.8, 2% SDS, 10% glycerol, 1% β-mercaptoethanol, 12.5 mM EDTA and 0.02% bromophenol blue). The samples were then alternately boiled and chilled three times to rupture cell membranes. Proteins were separated in a 7 cm long, 17% SDS-PAGE (Laemmli 1970) at 200 V for 1 h. The proteins were wet transferred into a PVDF membrane (GE Healthcare life sciences) with 20% Methanol transfer buffer (25 mM Tris, 192 mM glycine, pH 8.3), at 100 V for 1 h. Before incubation with the appropriate antibody, the membrane was blocked in 5% BSA, 0.1% Tween-20 TBS buffer (25 mM Tris, 150 mM NaCl, 2 mM KCl, pH 8).

Dot blot analysis

Synthesized peptides with at least 90% purity (Cambridge Peptides, UK) were dissolved in water, and drops containing 250, 50, or 10 pmol were deposited on a PVDF membrane, and allowed to air-dry for 1 h. The membrane was then submerged in 100% Methanol for a minute, water for another minute and then stained with Ponceau S or blocked as described above before probing with the appropriate antibody.

Supporting Information

Figure S1 Specificity of the H4R3me antibodies. *(A)* Whole cell extracts from the indicated wild-type and mutant strains were analyzed by western blotting using an antibody against H4R3me2a. Equal loading was monitored with an H3 antibody. *(B)* Western blot analysis of whole yeast cell extract or recombinant histones H4 and H2A expressed and purified from bacteria. The samples were analyzed with antibodies against H4R3me2a, H4 and H2A. The H4R3me2a antibody recognizes a band in yeast extract that is equivalent to the size of histone H4. *(C)* Dot-blot analysis using synthetic peptides representing the first 20 amino acids of histone H4 and possessing various combinations of R3 methylation and S1 N-alpha-amine acetylation. The peptides were spotted on a PVDF membrane at the indicated concentrations and then probed with antibodies against H4R3me1, H4R3me2a and H4R3me2s. Equal loading of peptides was monitored by Ponceau staining (left panel).
(TIF)

Figure S2 The yeast N-acetyltransferases A, B, C or E do not regulate H4R3me2a. Whole cell extracts prepared from the indicated wild-type and single deletion (*ard1Δ*, *nat3Δ*, *mak3Δ*, *nat4Δ*, *nat5Δ*) strains were analyzed by western blotting using an antibody against H4R3me2a (top panel). The H3 antibody was used as a loading control (bottom panel). *(B)* 25S rRNA expression level analysis was performed with wild-type and the indicated deletion (*nat4Δ* or *ard1Δ*) strains as in *(3C)*. Error bars indicate s.e.m for duplicate experiments.
(TIF)

Figure S3 Deletion of *NAT4* does not affect telomeric, *HMR* or *HML* silencing. Silencing assays were performed as in *(2A)* using *NAT4* and *nat4Δ* strains containing the *URA3* reporter gene integrated at telomere-VIIL, *HMR* or *HML* (*adh4::URA3-TelVII-L*, *hmr::URA3*, or *hml::URA3*). The cells were spotted in 10-fold dilutions on SC medium (right panel) or SC+5′-Fluoroorotic acid (left panel) and then grown for 48 h at 30°C.
(TIF)

Figure S4 The catalytic activity of Nat4 is required to control *RDN25* silencing and H4R3me2a deposition. *(A)* The expression levels of 25S rRNA were analyzed by qRT-PCR as in *(3C)* using total RNA that was extracted from *NAT4-HA* and *nat4cmAB-HA* (for more information about these strains, see *(1C)* and *(1D)*. *(B)* ChIP experiments performed in the strains indicated in *(A)* using H4R3me2a and N-acH4 antibodies and analyzed as in *(3B)*. *(C)* ChIP experiments were performed in *NAT4* and *nat4Δ* strains using antibodies against H4, H4R3me2a, H4R3me1 and N-acH4. The immunoprecipitated chromatin was analyzed as indicated in *(3B)*. Error bars in *(A)* *(B)* and *(C)* indicate s.e.m for duplicate experiments.
(TIF)

Figure S5 The H4S1P mutant mimics the effect of *nat4Δ*. Gene expression analysis of the 25S rRNA was performed in wild-type (H4WT *NAT4*) and in mutant strains containing a *NAT4* deletion (H4WT *nat4Δ*) or a serine to proline substitution at position 1 of H4 (H4S1P *NAT4*). The expression levels of 25S were normalized to the levels of *RPP0*. Error bars indicate s.e.m for duplicate experiments.
(TIF)

Figure S6 Purification of yeast Hmt1. Immunoblot analysis of purified Hmt1-6His-Ha-ZZ protein using an antibody against the His-tag (right panel). Crude extract (input) prepared from the strain expressing Hmt1-6His-Ha-ZZ was used as a positive control and post-purification extract (depleted) were used to examine the efficiency of the protein purification. Coomassie staining (left panel) was used to monitor protein loading.
(TIF)

Figure S7 The H4K5,8,12R mutation does not enhance recognition by the H4R3me2a antibody. Dot-blot analysis using the indicated synthetic peptides containing the first 20 amino acids of histone H4. The peptides were spotted on a PVDF membrane at the indicated concentrations, and then probed with a H4R3m2a antibody (right panel). Equal loading of peptides was monitored with Ponceau S staining (left panel).
(TIF)

Figure S8 Methylation of H4K5, 8 and 12 by SET5 does not act synergistically with N-acH4 in regulating H4R3me2a. Whole cell extracts prepared from the wild-type (*NAT4 SET5*) and the mutant strains carrying a *NAT4* deletion (*nat4Δ SET5*), a *SET5* deletion (*NAT4 set5Δ*) or both (*nat4Δ set5Δ*) were analyzed by western blotting as in (*S1A*).
(TIF)

Figure S9 The growth defect observed in the H4K5, 8,12R *nat4Δ* strain is rescued by the H4R3K mutation. Cell growth

analysis was performed at 30 and 37°C. The strains used are described in *(5D)*. The OD at 600 nm was measured at 0, 1, 2, 4, 6, 8, 10, 20, 24 and 30 h after inoculation of the culture.
(TIF)

Figure S10 Deletion of *NAT4* does not affect the levels of H4K5, 8 or 12 acetylation. ChIP experiments were performed in the indicated strains using antibodies against H4K5ac, H4K8ac and H4K12ac. The immunoprecipitated chromatin was analyzed by quantitative RT-PCR using primers specific to the *RDN25* gene. The enrichment from each antibody was normalized to the occupancy of H4. Errors bars indicate s.e.m for duplicate experiments.
(TIF)

Protocol S1 Additional materials and methods used to construct yeast strains generate antibodies and purify Hmt1.
(DOCX)

Table S1 List of yeast strains used in this study.
(DOCX)

Table S2 List of primer sequences used for qRT-PCR.
(DOCX)

Acknowledgments

We thank Charlie Boone for providing the yeast deletion collection and Brenda Andrews for plasmids; Thomas Arnesen, Shelley Berger, Daniel Gottschling and Jessica Downs for making their strains available; Helena Santos-Rosa and Ann E. Ehrenhofer-Murray for critical reading of the manuscript; and Christis Demosthenous for excellent technical assistance.

Author Contributions

Conceived and designed the experiments: VS DMS AK. Performed the experiments: VS DMS DK AH AK. Analyzed the data: VS DMS AK. Wrote the paper: AK.

References

1. Bannister AJ, Kouzarides T (2011) Regulation of chromatin by histone modifications. Cell Res 21: 381–395.
2. Lee JS, Smith E, Shilatifard A (2010) The language of histone crosstalk. Cell 142: 682–685.
3. Arnesen T, Van Damme P, Polevoda B, Helsens K, Evjenth R, et al. (2009) Proteomics analyses reveal the evolutionary conservation and divergence of N-terminal acetyltransferases from yeast and humans. Proc Natl Acad Sci U S A 106: 8157–8162.
4. Brown JL, Roberts WK (1976) Evidence that approximately eighty per cent of the soluble proteins from Ehrlich ascites cells are Nalpha-acetylated. J Biol Chem 251: 1009–1014.
5. Starheim KK, Gevaert K, Arnesen T (2012) Protein N-terminal acetyltransferases: when the start matters. Trends Biochem Sci 37: 152–161.
6. Mullen JR, Kayne PS, Moerschell RP, Tsunasawa S, Gribskov M, et al. (1989) Identification and characterization of genes and mutants for an N-terminal acetyltransferase from yeast. EMBO J 8: 2067–2075.
7. Song OK, Wang X, Waterborg JH, Sternglanz R (2003) An Nalpha-acetyltransferase responsible for acetylation of the N-terminal residues of histones H4 and H2A. J Biol Chem 278: 38109–38112.
8. Tran JC, Zamdborg L, Ahlf DR, Lee JE, Catherman AD, et al. (2011) Mapping intact protein isoforms in discovery mode using top-down proteomics. Nature 480: 254–258.
9. Snijders AP, Pongdam S, Lambert SJ, Wood CM, Baldwin JP, et al. (2008) Characterization of post-translational modifications of the linker histones H1 and H5 from chicken erythrocytes using mass spectrometry. J Proteome Res 7: 4326–4335.
10. Hole K, Van Damme P, Dalva M, Aksnes H, Glomnes N, et al. (2011) The human N-alpha-acetyltransferase 40 (hNaa40p/hNatD) is conserved from yeast and N-terminally acetylates histones H2A and H4. PLoS One 6: e24713.
11. Liu Z, Liu Y, Wang H, Ge X, Jin Q, et al. (2009) Patt1, a novel protein acetyltransferase that is highly expressed in liver and downregulated in hepatocellular carcinoma, enhances apoptosis of hepatoma cells. Int J Biochem Cell Biol 41: 2528–2537.
12. Polevoda B, Hoskins J, Sherman F (2009) Properties of Nat4, an N(alpha)-acetyltransferase of Saccharomyces cerevisiae that modifies N termini of histones H2A and H4. Mol Cell Biol 29: 2913–2924.
13. Liu Y, Zhou D, Zhang F, Tu Y, Xia Y, et al. (2012) Liver Patt1 deficiency protects male mice from age-associated but not high-fat diet-induced hepatic steatosis. J Lipid Res 53: 358–367.
14. Yang Y, Bedford MT (2013) Protein arginine methyltransferases and cancer. Nat Rev Cancer 13: 37–50.
15. Dhar SS, Lee SH, Kan PY, Voigt P, Ma L, et al. (2012) Trans-tail regulation of MLL4-catalyzed H3K4 methylation by H4R3 symmetric dimethylation is mediated by a tandem PHD of MLL4. Genes Dev 26: 2749–2762.
16. Guccione E, Bassi C, Casadio F, Martinato F, Cesaroni M, et al. (2007) Methylation of histone H3R2 by PRMT6 and H3K4 by an MLL complex are mutually exclusive. Nature 449: 933–937.
17. Iberg AN, Espejo A, Cheng D, Kim D, Michaud-Levesque J, et al. (2008) Arginine methylation of the histone H3 tail impedes effector binding. J Biol Chem 283: 3006–3010.
18. Kirmizis A, Santos-Rosa H, Penkett CJ, Singer MA, Vermeulen M, et al. (2007) Arginine methylation at histone H3R2 controls deposition of H3K4 trimethylation. Nature 449: 928–932.
19. Migliori V, Muller J, Phalke S, Low D, Bezzi M, et al. (2012) Symmetric dimethylation of H3R2 is a newly identified histone mark that supports euchromatin maintenance. Nat Struct Mol Biol 19: 136–144.
20. Molina-Serrano D, Schiza V, Kirmizis A (2013) Cross-talk among epigenetic modifications: lessons from histone arginine methylation. Biochem Soc Trans 41: 751–759.
21. Yuan CC, Matthews AG, Jin Y, Chen CF, Chapman BA, et al. (2012) Histone H3R2 symmetric dimethylation and histone H3K4 trimethylation are tightly correlated in eukaryotic genomes. Cell Rep 1: 83–90.
22. Strahl BD, Briggs SD, Brame CJ, Caldwell JA, Koh SS, et al. (2001) Methylation of histone H4 at arginine 3 occurs in vivo and is mediated by the nuclear receptor coactivator PRMT1. Curr Biol 11: 996–1000.
23. Wang H, Huang ZQ, Xia L, Feng Q, Erdjument-Bromage H, et al. (2001) Methylation of histone H4 at arginine 3 facilitating transcriptional activation by nuclear hormone receptor. Science 293: 853–857.
24. Lacoste N, Utley RT, Hunter JM, Poirier GG, Cote J (2002) Disruptor of telomeric silencing-1 is a chromatin-specific histone H3 methyltransferase. J Biol Chem 277: 30421–30424.
25. Yu MC, Lamming DW, Eskin JA, Sinclair DA, Silver PA (2006) The role of protein arginine methylation in the formation of silent chromatin. Genes Dev 20: 3249–3254.
26. Venema J, Tollervey D (1999) Ribosome synthesis in Saccharomyces cerevisiae. Annu Rev Genet 33: 261–311.
27. Kos M, Tollervey D (2010) Yeast pre-rRNA processing and modification occur cotranscriptionally. Mol Cell 37: 809–820.
28. Veinot-Drebot LM, Singer RA, Johnston GC (1988) Rapid initial cleavage of nascent pre-rRNA transcripts in yeast. J Mol Biol 199: 107–113.
29. Feng Y, Wang J, Asher S, Hoang L, Guardiani C, et al. (2011) Histone H4 acetylation differentially modulates arginine methylation by an in Cis mechanism. J Biol Chem 286: 20323–20334.
30. Kuo MH, Xu XJ, Bolck HA, Guo D (2009) Functional connection between histone acetyltransferase Gcn5p and methyltransferase Hmt1p. Biochim Biophys Acta 1789: 395–402.
31. Schneider J, Dover J, Johnston M, Shilatifard A (2004) Global proteomic analysis of S. cerevisiae (GPS) to identify proteins required for histone modifications. Methods Enzymol 377: 227–234.
32. Rossmann MP, Luo W, Tsaponina O, Chabes A, Stillman B (2011) A common telomeric gene silencing assay is affected by nucleotide metabolism. Mol Cell 42: 127–136.
33. Takahashi YH, Schulze JM, Jackson J, Hentrich T, Seidel C, et al. (2011) Dot1 and histone H3K79 methylation in natural telomeric and HM silencing. Mol Cell 42: 118–126.
34. Krishnamoorthy T, Chen X, Govin J, Cheung WL, Dorsey J, et al. (2006) Phosphorylation of histone H4 Ser1 regulates sporulation in yeast and is conserved in fly and mouse spermatogenesis. Genes Dev 20: 2580–2592.
35. Goetze S, Qeli E, Mosimann C, Staes A, Gerrits B, et al. (2009) Identification and functional characterization of N-terminally acetylated proteins in Drosophila melanogaster. PLoS Biol 7: e1000236.
36. Clarke AS, Lowell JE, Jacobson SJ, Pillus L (1999) Esa1p is an essential histone acetyltransferase required for cell cycle progression. Mol Cell Biol 19: 2515–2526.
37. Green EM, Mas G, Young NL, Garcia BA, Gozani O (2012) Methylation of H4 lysines 5, 8 and 12 by yeast Set5 calibrates chromatin stress responses. Nat Struct Mol Biol 19: 361–363.
38. Lamming DW, Latorre-Esteves M, Medvedik O, Wong SN, Tsang FA, et al. (2005) HST2 mediates SIR2-independent life-span extension by calorie restriction. Science 309: 1861–1864.
39. Lin SJ, Kaeberlein M, Andalis AA, Sturtz LA, Defossez PA, et al. (2002) Calorie restriction extends Saccharomyces cerevisiae lifespan by increasing respiration. Nature 418: 344–348.

40. DeLange RJ, Fambrough DM, Smith EL, Bonner J (1969) Calf and pea histone IV. II. The complete amino acid sequence of calf thymus histone IV; presence of epsilon-N-acetyllysine. J Biol Chem 244: 319–334.
41. Poveda A, Sendra R (2008) Site specificity of yeast histone acetyltransferase B complex in vivo. FEBS J 275: 2122–2136.
42. Migliori V, Phalke S, Bezzi M, Guccione E (2010) Arginine/lysine-methyl/methyl switches: biochemical role of histone arginine methylation in transcriptional regulation. Epigenomics 2: 119–137.
43. Ai X, Parthun MR (2004) The nuclear Hat1p/Hat2p complex: a molecular link between type B histone acetyltransferases and chromatin assembly. Mol Cell 14: 195–205.
44. Helbig AO, Rosati S, Pijnappel PW, van Breukelen B, Timmers MH, et al. (2010) Perturbation of the yeast N-acetyltransferase NatB induces elevation of protein phosphorylation levels. BMC Genomics 11: 685.
45. Helsens K, Van Damme P, Degroeve S, Martens L, Arnesen T, et al. (2011) Bioinformatics analysis of a Saccharomyces cerevisiae N-terminal proteome provides evidence of alternative translation initiation and post-translational N-terminal acetylation. J Proteome Res 10: 3578–3589.
46. Geissenhoner A, Weise C, Ehrenhofer-Murray AE (2004) Dependence of ORC silencing function on NatA-mediated Nalpha acetylation in Saccharomyces cerevisiae. Mol Cell Biol 24: 10300–10312.
47. Onishi M, Liou GG, Buchberger JR, Walz T, Moazed D (2007) Role of the conserved Sir3-BAH domain in nucleosome binding and silent chromatin assembly. Mol Cell 28: 1015–1028.
48. van Welsem T, Frederiks F, Verzijlbergen KF, Faber AW, Nelson ZW, et al. (2008) Synthetic lethal screens identify gene silencing processes in yeast and implicate the acetylated amino terminus of Sir3 in recognition of the nucleosome core. Mol Cell Biol 28: 3861–3872.
49. Huang J, Moazed D (2003) Association of the RENT complex with nontranscribed and coding regions of rDNA and a regional requirement for the replication fork block protein Fob1 in rDNA silencing. Genes Dev 17: 2162–2176.
50. Kaeberlein M (2010) Lessons on longevity from budding yeast. Nature 464: 513–519.
51. Dang W, Steffen KK, Perry R, Dorsey JA, Johnson FB, et al. (2009) Histone H4 lysine 16 acetylation regulates cellular lifespan. Nature 459: 802–807.
52. Riesen M, Morgan A (2009) Calorie restriction reduces rDNA recombination independently of rDNA silencing. Aging Cell 8: 624–632.
53. Smith DL, Jr., Li C, Matecic M, Maqani N, Bryk M, et al. (2009) Calorie restriction effects on silencing and recombination at the yeast rDNA. Aging Cell 8: 633–642.
54. Tweedie-Cullen RY, Brunner AM, Grossmann J, Mohanna S, Sichau D, et al. (2012) Identification of combinatorial patterns of post-translational modifications on individual histones in the mouse brain. PLoS One 7: e36980.
55. Schmitt ME, Brown TA, Trumpower BL (1990) A rapid and simple method for preparation of RNA from Saccharomyces cerevisiae. Nucleic Acids Res 18: 3091–3092.

Biochemical Society Annual Symposium No. 80

Cross-talk among epigenetic modifications: lessons from histone arginine methylation

Diego Molina-Serrano, Vassia Schiza and Antonis Kirmizis[1]
Department of Biological Sciences, University of Cyprus, 1678 Nicosia, Cyprus

Abstract

Epigenetic modifications, including those occurring on DNA and on histone proteins, control gene expression by establishing and maintaining different chromatin states. In recent years, it has become apparent that epigenetic modifications do not function alone, but work together in various combinations, and cross-regulate each other in a manner that diversifies their functional states. Arginine methylation is one of the numerous PTMs (post-translational modifications) occurring on histones, catalysed by a family of PRMTs (protein arginine methyltransferases). This modification is involved in the regulation of the epigenome largely by controlling the recruitment of effector molecules to chromatin. Histone arginine methylation associates with both active and repressed chromatin states depending on the residue involved and the configuration of the deposited methyl groups. The present review focuses on the increasing number of cross-talks between histone arginine methylation and other epigenetic modifications, and describe how these cross-talks influence factor binding to regulate transcription. Furthermore, we present models of general cross-talk mechanisms that emerge from the examples of histone arginine methylation and allude to various techniques that help decipher the interplay among epigenetic modifications.

Introduction

The genomic DNA of eukaryotes was once thought to be the ultimate template of inheritance. This view has been challenged in recent years, with epigenetics supporting the idea that heritable changes which influence gene expression may not have anything to do with changes in the DNA sequence [1]. DNA is wrapped around an octamer of proteins that comprises two copies of each of the core histones: H2A, H2B, H3 and H4. This dynamic structure is known as the nucleosome and is the basic unit of chromatin. Euchromatin refers to the decondensed form of chromatin that can be active or inactive, whereas heterochromatin is defined as the compacted silenced state. Hence chromatin is dynamically modulated between transcriptionally repressed and active states in order to regulate gene expression. These states can be altered by PTMs (post-translational modifications) deposited on either the DNA or histones, thus affecting the readout of the underlying DNA sequence [2].

Histones are susceptible to various PTMs including phosphorylation, methylation, acetylation and ubiquitination [3]. The numerous histone modifications identified to date communicate among themselves by influencing the presence of each other or by collaborating to bring about a functional outcome. These communications, referred to as cross-talks, happen in a context-dependent manner revealing that the once-thought strict histone code is actually a complex histone language [4]. Cross-talks can occur on the same histone (*cis*) or between different histones (*trans*), and it has been proposed that *trans* mechanisms could even involve more than one nucleosome [2,3]. The study of these cross-talks has received great attention because the reading of these modifications by different effectors influences gene expression [2], and misinterpretation of these cross-talks by readers may trigger various diseases, including cancer [5–7].

Lately, arginine methylation has attracted much interest owing to its involvement in several cellular processes such as transcription, RNA processing, signal transduction and

Key words: epigenetics, histone arginine methylation, modification cross-talk, post-translational modification, protein arginine methyltransferase.

Abbreviations used: AIRE, autoimmune regulator protein; BPTF, bromodomain PHD finger transcription factor; ChIP, chromatin immunoprecipitation; COMPASS, complex proteins associated with Set1; HP1, heterochromatin protein 1; ING, inhibitor of growth; JMJD6, Jumonji domain-containing 6; MLL, mixed-lineage leukaemia; PADI, peptidyl arginine deiminase; PHD, plant homeodomain; PRMT, protein arginine methyltransferase; PTM, post-translational modification; RAG2, recombination activating gene 2; SILAC, stable isotope labelling by amino acids in cell culture; TFIID, transcription factor IID; UHRF1, ubiquitin-like with PHD and ring finger domains 1.

[1]To whom correspondence should be addressed (email kirmizis@ucy.ac.cy).

Figure 1 | Protein arginine methylation catalysed by PRMTs

The mammalian family of PRMTs is shown, consisting of nine members, classified into the three types. All three types of PRMT (I, II and III) can monomethylate arginine (Rme1) on one of the terminal guanidino nitrogen atoms. Type I PRMTs generate asymmetric dimethylation (Rme2a), whereas type II PRMTs generate symmetric dimethylation (Rme2s).

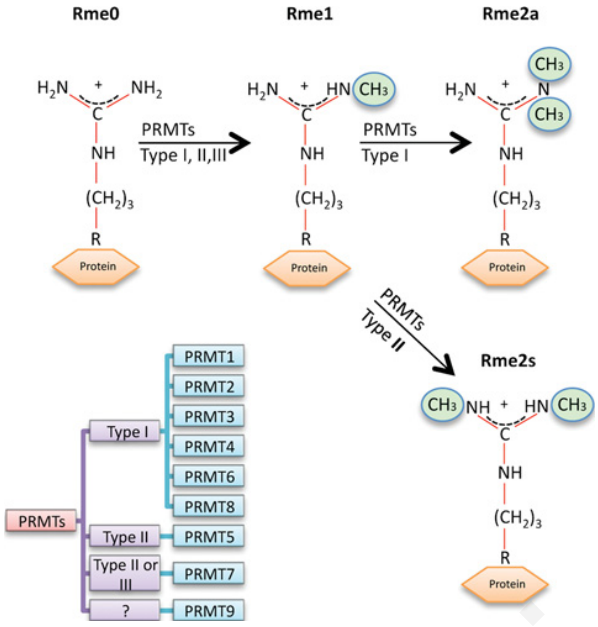

DNA repair. This PTM involves the addition of one or two methyl groups to the guanidino groups of arginine residues resulting in three different methylation states: monomethylated (Rme1), asymmetrically dimethylated (Rme2a) or symmetrically dimethylated (Rme2s) arginine (Figure 1). The methyl groups are deposited by PRMTs (protein arginine methyltransferases). The mammalian family of PRMTs includes nine members which are classified into three types: type I (PRMTs 1, 2, 3, 4, 6 and 8) catalyse the formation of Rme2a, and type II (PRMTs 5 and 7) catalyse the formation of Rme2s. Both types are also able to mediate the formation of Rme1. PRMT7 can only monomethylate some substrates, thus it is also referred to as a type III PRMT. To date, PRMT9 has not been shown to possess enzymatic activity [7]. Histone arginine methylation associates with both active and repressed chromatin states depending on the residue involved and the status of methylation. For example, asymmetric dimethylation of histone H3 Arg^2 (H3R2me2a) is associated with transcriptional repression [8–10], whereas symmetric dimethylation or monomethylation of the same residue (H3R2me2s and H3R2me1 respectively) have been linked to gene activation [11–13].

Whether or not arginine methylation can be enzymatically reversed is still under investigation. An enzyme, JMJD6 (Jumonji domain-containing 6), was reported to demethylate both H3R2me2 and H4R3me2 [14]. This finding, however, was disputed by another study which showed that JMJD6 is a lysine hydroxylase [15]. Although it is not clear whether or not arginine methylation can be reversed, methylation of this residue can be blocked by deimination, a reaction catalysed by a family of enzymes called PADs or PADIs (peptidyl arginine deiminases). This modification converts an arginine residue into citrulline by the removal of one of the two terminal amino groups and, as a result, the new residue can no longer be targeted by PRMTs. To date, two different PADIs have been shown to exert this activity on histones. PADI4 can remove the amino group from Arg^2, Arg^8, Arg^{17} and Arg^{26} in histone H3, and also Arg^3 in histones H4 and H2A [16,17]. Recently, it was shown that PADI2 could also convert Arg^{26} of histone H3 into citrulline *in vivo* [18].

In the present review, we discuss the interplay between histone arginine methylation and other epigenetic modifications. We describe the different cross-talk mechanisms identified to date, focusing on histones H3 and H4, and then, define general models for these mechanisms. How deregulation of the mechanisms employed by histone arginine methylation and PRMTs may lead to diseases such as cancer has been recently reviewed elsewhere [7].

Interplay between histone arginine methylation and other epigenetic modifications

Histone H3 arginine residues

On histone 3, Arg^2 is the most characterized arginine residue to date, and its dimethylation states have been shown to participate in several cross-talks. One of the most studied cross-talks is between H3R2me2a and H3K4me3 (trimethylation of histone H3 Lys^4). These two modifications are catalysed in humans by PRMT6 [8,9,19] and the COMPASS (complex proteins associated with Set1) complex [20] respectively. Experiments from different groups have shown that H3K4 can be trimethylated only in the absence of H3R2me2a [8–10,21]. ChIP (chromatin immunoprecipitation) analysis both in humans and yeast (*Saccharomyces cerevisiae*) showed that H3R2me2a and H3K4me3 are mutually exclusive. H3R2me2a is present in heterochromatic regions in yeast and within the middle and 3′-ends of euchromatic genes, whereas H3K4me3 is abundant at the 5′-end of active genes [8,10].

H3R2me2a interferes with the binding of the WD40-domain-containing protein WDR5 (a subunit of the methyltransferase COMPASS complex) to the H3 tail. The prevention of WDR5 binding in turn disrupts the activity of the catalytic component of the complex, MLL (mixed-lineage leukaemia) 1 protein, necessary to trimethylate H3K4 [9,22]. The same mechanism has been observed in *S. cerevisiae*, where H3R2me2a regulates the activity of Set1 (yeast orthologue of human MLL1) by modulating the binding of the COMPASS subunit Spp1 [10]. Spp1 recognizes H3K4me2 (dimethylation of H3K4) through its PHD (plant homeodomain) finger only when H3R2me2a is absent, in order to stimulate H3K4me3 by Set1.

Although H3R2me2a by PRMT6 and H3K4me3 by MLL1 inhibit the deposition of each other [8,9,19], it is reasonable that both modifications coexist within cells [19], perhaps for a short period of time. Structural and crystallographic analysis of many H3K4me3-binding proteins showed that, when H3K4me3 and H3R2me2a coexist on the same peptide, the latter modification blocks the recognition of H3K4me3 by many proteins. The double chromodomain-containing CHD1 (chromodomain helicase DNA-binding protein 1) [23,24], the Tudor-domain-containing JMD2A, the aforementioned WD40-containing WDR5 and several PHD-containing proteins PHF2 (PHD finger protein 2), ING (inhibitor of growth) 2, BPTF (bromodomain PHD finger transcription factor), DATF1 (death-associated transcription factor 1) [9,19,25], TFIID (transcription factor IID) subunit TAF3 [26,27] and ING4 [28] all show a marked decrease or total loss of H3K4me3 recognition when H3R2me2a is present. However, the effect of H3R2me2a on the binding of ING2 and BPTF to H3K4me3 has not been clearly established; some authors showed a decrease in the binding [19,25], whereas others did not observe any inhibition [26]. Furthermore, the recruitment of some proteins by this part of histone H3 is insensitive to this cross-talk, for instance RAG2 (recombination activating gene 2) [19,29] and Pygo [30]. These findings suggest that H3R2me2a blocks the recruitment of H3K4me3 readers selectively and hence regulates specific downstream events on chromatin.

More recent studies showed that H3R2 can also be symmetrically dimethylated *in vivo*, a reaction catalysed in mammals by PRMT5 and PRMT7 [12,13]. Using ChIP-seq analysis, Yuan et al. [13] showed that H3R2me2s co-localizes with H3K4me3 throughout the mouse genome and this overlap is conserved in many eukaryotes. Another study showed that in human cells H3R2me2s, unlike its asymmetric form, is present specifically at the -1 nucleosome in gene promoters together with H3K4me3 [12]. The apparent co-localization between H3R2me2s and H3K4me3 raised the hypothesis that these two modifications might influence the deposition of each other. Indeed, yeast Set1 and other COMPASS subunits are required for H3R2me2s, in a way that seems to be dependent on H3K4me3. Consistent with this result, mutation of H3K4 to alanine impairs the deposition of H3R2me2s, suggesting that COMPASS regulates simultaneously methylation of Arg^2 and at Lys^4 [13]. Additionally, the presence of H3R2me2s enhances H3K4 methylation by facilitating the recruitment of the human COMPASS core subunit WDR5 [12]. This recruitment is PRMT5-dependent, and both PRMT5 and WDR5 co-immunoprecipitate [31]. Once both modifications are deposited, further evidence proposes that these two marks function together to influence the recruitment of effector molecules to chromatin. Ramon-Maiques et al. [29] and Yuan et al. [13] showed that, *in vitro*, the PHD-containing protein RAG2 binds with higher affinity to peptides that are concurrently modified with H3R2me2s and H3K4me3 than to peptides carrying single modifications [13,29]. Hence, the cross-talk between H3R2me2s and H3K4me3 constitutes one of the rare examples in which two modifications first influence the deposition of each other and then together control downstream factor-binding events.

Interestingly, H3R2me2s is also found at locations distant to the transcription start sites, where it overlaps with high levels of H3K4me1 and H3K4me2 [12]. A similar overlap has also been observed between H3R2me2a and these two Lys^4-methyl marks, but this co-localization occurs within the body of genes [10]. Therefore it would be of interest to determine whether cross-talk exists between the two H3R2 dimethyl states and H3K4me1/H3K4me2 that is dependent on the genomic location of nucleosomes.

Methylation of H3R2 is also involved in a cross-talk with the unmodified version of Lys^4 (H3K4me0). H3K4me0 is recognized by the AIRE (autoimmune regulator protein) through its PHD domain to activate gene expression [32]. Addition of one methyl group to H3R2 inhibits severely the binding of AIRE to the H3 tail, while dimethylation of H3R2 abrogates it completely [25,33–35]. The same effect is observed when Arg^2 is mutated to alanine or lysine, which is consistent with the fact that an unmodified arginine residue is required for this interaction [32,34,35]. In line with the above observations, overexpression of PRMT6 reduced activation of AIRE target genes [34].

Another well-documented cross-talk of Arg^2 is the one involving its non-methylated state (H3R2me0) and DNA methylation. UHRF1 (ubiquitin-like with PHD and ring finger domains 1), a PHD and tandem Tudor-domain-containing protein, recognizes H3R2me0. This protein acts as a transcriptional repressor by maintaining CpG methylation and heterochromatin formation [36–38]. H3R2me1 decreases UHRF1 binding to the histone tail, an effect amplified by dimethylation of H3R2, as shown by structural analysis [36,38,39] and *in vitro* binding assays [37]. ChIP experiments also showed that promoters of UHRF1 target genes are devoid of H3R2me2s [37]. UHFR1 can also bind H3K9me3 through its Tudor domain [36,37,40], and the binding is stronger when both H3K9me3 and H3R2me0 are present [40].

The above work describes well-characterized cross-talk mechanisms of H3R2, but recent evidence indicates that H3R2 methylation may be involved in additional cross-talks. For example, a recent report linked dNTMT (*Drosophila* N-terminal methyltransferase), an enzyme involved in histone H2B N-terminal methylation, to an H3R2me2a-mediating PRMT [dART8 (*Drosophila* arginine methyltransferase 8)] in *Drosophila melanogaster* [41]. The authors suggest that H3R2me2a inhibits histone H2B N-terminal methylation, but the precise mechanism of this possible cross-talk needs to be elucidated. Another potential cross-talk is the one between H3R2 methylation and H3T3ph (histone H3 Thr^3 phosphorylation). This is proposed on the basis of the fact that H3T3ph disrupts UHRF1 binding to H3R2me0 [37,40] and influences the recognition of H3K4me3 by some binding factors, similarly to dimethylated H3R2 [25,33,34,37].

Apart from Arg^2, histone H3 can also be methylated at Arg^8, Arg^{17} and Arg^{26}, and all three residues are involved

in modification cross-talks. However, in general, their cross-talk mechanisms are less studied in comparison with those involving H3R2. Pal et al. [42] showed that H3R8me2s is catalysed by PRMT5, and this methylation is inhibited by the presence of H3K9ac and H3K14ac (acetylation of histone H3 Lys^{9} and Lys^{14} respectively) [42]. Reciprocally, H3R8me2s decreases the deposition of H3K9ac [42]. Methylation on this same lysine residue by the histone methyltransferase G9a is almost completely disrupted by the presence of H3R8me2 (both symmetric and asymmetric), as shown by *in vitro* experiments [43]. H3R8me2a also inhibits HP1 (heterochromatin protein 1) γ binding to H3K9me2 and me3 [44]. Additionally, Southall et al. [21] found that H3R8me2s reduces MLL1 activity towards H3K4 by 30 %, but the precise mechanism underlying this cross-talk remains to be determined.

Regarding H3R17, Daujat et al. [45] showed that H3K18ac and, to a lesser extent, H3K23ac promotes methylation of this arginine residue by PRMT4 [45], a result confirmed later by two other studies [46,47]. More recently, Wu and Xu [48] have indirectly linked H3R17me2a to H3K4me3. During this cross-talk, PAF1c (RNA polymerase-associated factor 1 complex) acts as a methyl arginine reader by binding to methylated Arg^{17} and subsequently recruits MLL1 through an interaction with Ash2L in order to trigger H3K4me3 deposition. Another study showed that R17me2a and R26me2a, together with pan-H3ac, reduce the binding of the NuRD (nucleosome remodelling and deacetylase complex) and TIF1 (translation initiation factor 1) co-repressors to histone H3 [49]. On the basis of the above findings, a reasonable sequence of events would be that H3K18ac and H3K23ac are deposited first to stimulate Arg^{17} methylation (and probably R26me2a), which then inhibits the recruitment of co-repressors to chromatin and enhances trimethylation of H3K4 to activate gene expression.

A rather unique cross-talk of histone arginine methylation is the one with citrullination because this mechanism involves the same amino acid residue. For example, deiminated arginine residues can no longer be methylated by PRMTs, whereas arginine methylation blocks its own citrullination. More specifically, PADI4 binds to the promoter of the oestrogen-responsive gene *pS2* leading to citrullination of Arg^{17} of H3 (H3Cit17) and Arg^{3} of H4 (H4Cit3). This citrullination is followed by disengagement of RNA polymerase II from the promoter and transcriptional repression [16,17]. In contrast, oestrogen-induced citrullination of H3R26 by PADI2 facilitates oestrogen-receptor-mediated gene transactivation [18]. H3Cit26 strongly co-localizes with H3K27ac in MCF-7 cells, raising the possibility for a cross-talk between these two modifications [18].

The cross-talk between arginine methylation and citrullination influences downstream chromatin events [6]. The authors showed that H3R8 methylation reduces slightly the binding of HP1α to H3K9me3, whereas deimination of the same residue upon oestrogen stimulation of PADI4 completely abrogates HP1α recruitment. It was proposed that the difference in HP1α-binding affinity to H3K9me3 in the context of H3R8me or H3Cit8 may allow for a gradual activation of the genes targeted by the HP1α repressor during oestrogen induction [6].

Histone H4 arginine residues

All known cross-talk mechanisms described for arginine methylation on H4 involve Arg^{3}, and specifically its dimethylated (asymmetric or symmetric) forms (Table 1). Earlier studies have shown by *in vitro* and *in vivo* work that H4R3me2a by PRMT1 facilitates p300-mediated histone H4 acetylation, leading to nuclear-receptor-dependent transcription [50,51]. More recent work validated this cross-talk by demonstrating that the tumour-suppressor gene p53 recruits PRMT1, p300 and PRMT4 to activate transcription in a stepwise manner. During this p53-mediated activation, H4R3me2a is initially deposited and then stimulates the acetylase activity of p300 towards H4 Lys^{5}, Lys^{8} and Lys^{12} [46]. Additionally, ChIP analysis in chicken erythroleukaemia 6C2 cells in which PRMT1 was knocked down showed that loss of H4R3me2a across the β-globin locus is accompanied by a vast reduction in the levels of H4K5ac, H4K8ac and H4K12ac [52]. The reverse relationship between these two modifications differs because H4 acetylation inhibits PRMT1-mediated methylation of H4R3 [51,53]. An *in vitro* study, however, showed that H4 acetylation of any of Lys^{5}, Lys^{8}, Lys^{12} or Lys^{16} stimulates the methylase activity of the yeast PRMT1 orthologue (Hmt1p) towards H4R3. Despite this discrepancy, it was shown that mutation at Arg^{3} or Lys^{8} results in a similar phenotype in yeast, suggesting that modifications at these two residues function within the same pathway [54].

Two studies showed that H4R3me2a is also involved in an arginine methylation *trans*-histone cross-talk. Li et al. [55] demonstrated that H4R3me2a catalysed by PRMT1 facilitates subsequent acetylation of H3K9 and H3K14, and recruitment of the transcriptional machinery to activate expression of the globin genes. *In vitro* experiments provide a direct link for this cross-talk, as H4R3me2a is a binding surface for the co-activator PCAF (p300/CREB [cAMP-response-element-binding protein)-binding protein-associated factor], which possesses H3K9/H3K14 acetyltransferase activity. In the second study, Huang et al. [52] showed that loss of H4R3me2a by PRMT1 knockdown leads to localized induction of H3K9me2 and global increase of H3K27me3 over the β-globin locus. Whether the interplay between H4R3me2a and methylated H3K9/H3K27 is direct remains to be determined.

The symmetrically dimethylated form of H4R3 is mediated by PRMT5 and PRTM7, and is implicated in transcriptional repression. A recent study demonstrated a *trans*-histone cross-talk involving H4R3me2s and H3K4me. MLL4, a methyltransferase related to MLL1, which can also trimethylate H3K4, binds to unmodified or asymmetrically modified H4R3 through a tandem PHD domain. However, H4R3me2s strongly impairs MLL4 recruitment and downstream H3K4 methylation, inhibiting neuronal differentiation [56]. In another study, Feng et al. [53] tested whether H4 acetylation affects PRMT5-mediated H4R3me2s in a manner similar

Table 1 | **Cross-talks of histone arginine methylation**

Mod, modification; Rme, arginine methylation; → and ←, promotes; –| and |–, blocks, (?), not determined. *G. gallus*, *Gallus gallus*; *H. sapiens*, *Homo sapiens*; *M. musculus*, *Mus musculus*; *S. cerevisiae*, *Saccharomyces cerevisiae*.

Mod1 (Rme)	Mod2	Mechanism	Function	System	PRMT(s)	Reference(s)
Histone 3						
H3R2me0	H3K9me3	Combinatorial synergistic	DNA methylation maintenance	*In vitro*	–	[38,42]
H3R2me0	DNA methylation	Mod1→Mod2	Transcriptional repression, DNA methylation maintenance	*In vitro* *H. sapiens*	–	[39]
H3R2me2a	H3K4me3	Mod1–|Mod2; Mod1|–Mod2	Transcriptional regulation	*S. cerevisiae*; *H. sapiens*; *in vitro*	PRMT6	[9–11,24]
H3R2me2a	H3K4me3	Combinatorial antagonistic	Transcriptional regulation	*In vitro*	PRMT6	[20,25–30]
H3R2me1, H3R2me2a, H3R2me2s	H3K4me0	Combinatorial antagonistic	Transcriptional repression	*H. sapiens*; *in vitro*	PRMT5(?); PRMT6; PRMT7(?)	[35,36]
H3R2me2s	H3K4me3	Mod1→Mod2; Mod1←Mod2	Transcriptional activation	*H. sapiens*	PRMT5; PRMT7	[13,14]
H3R2me2s	H3K4me3	Combinatorial synergistic	Transcriptional activation	*In vitro*	PRMT5(?); PRMT7(?)	[14,31]
H3R8me	H3K9me3	Combinatorial antagonistic	Transcriptional activation	*In vitro*	(?)	[7]
H3R8me2a	H3K9me2, H3K9me3	Combinatorial antagonistic	(?)	*In vitro*	(?)	[46]
H3R8me2a, H3R8me2s	H3K9me	Mod1–|Mod2	Transcriptional repression	*In vitro*	PRMT5(?)	[45]
H3R8me2s	H3K4me3	Mod1–|Mod2	Transcriptional repression	*In vitro*	PRMT5(?)	[23]
H3R8me2s	H3K9ac H3K9ac, H3K14ac	Mod1–|Mod2 Mod1|–Mod2	Transcriptional repression	*M. musculus*	PRMT5	[44]
H3R17me2a, H3R17me2s	H3Cit17	Mod1–|Mod2	Transcriptional activation	*H. sapiens*; *in vitro*	PRMT4	[17,18]
H3R17me2a	H3K18ac, H3K23ac	Mod1←Mod2	Transcriptional activation	*H. sapiens*	PRMT4	[47–49]
H3R17me2a	H3K4me3	Mod1→Mod2	Transcriptional activation	*H. sapiens*	PRMT4	[50]
H3R17me2a, H3R26me2a	H3K9ac, H3K14ac, H3K18ac, H3K23ac	Combinatorial synergistic	Transcriptional activation	*In vitro*; *H. sapiens*	PRMT4	[51]
H3R26me	H3Cit26	Mod1–|Mod2	Transcriptional repression	*In vitro*; *M. musculus*	(?)	[19]
Histone 4						
H4R3me2a, H4R3me2s	H4Cit3	Mod1–|Mod2	Transcriptional regulation	*In vitro*	PRMT1	[18]
H4R3me2a	H4K5ac, H4K8ac, H4K12ac	Mod1→Mod2; Mod1|–Mod2	Transcriptional activation	*H. sapiens*; *G. gallus*; *M. musculus*; *in vitro*	PRMT1	[48,53–55]
H4R3me2a	H3K9ac, H3K14ac	Mod1→Mod2	Transcriptional activation	*M. musculus*; *G. gallus*	PRMT1	[54,57]
H4R3me2a	H3K9me2, H3K27me3	Mod1–|Mod2	Transcriptional activation	*G. gallus*	PRMT1	[54]
H4R3me2s	H4K5ac, H4K8ac, H4K12ac	Mod1←Mod2	Transcriptional regulation	*In vitro*	PRMT5	[55]
H4R3me2s	H3K4me3	Mod1–|Mod2	Transcriptional repression	*H. sapiens*	PRMT7	[58]
H4R3me2s	DNA methylation	Mod1→Mod2; Mod1←Mod2	Transcriptional repression	*H. sapiens*; *X. laevis*; *in vitro*; *M. musculus*	PRMT5; PRMT7	[59,60,62]
H4R3me2s	H4K20me3	Mod1→Mod2	Transcriptional repression	*H. sapiens*	PRMT5	[61]

Figure 2 | Mechanisms of cross-talk involving arginine methylation

(**A**) A sequential positive interaction, where a lysine methyltransferase (KMT) binds the histone tail through recognition of the Rme2s mark, and deposits a second PTM (Kme3). (**B**) A sequential negative interaction, where the same KMT cannot bind to the histone tail because of the Rme2a mark, thus blocking downstream PTM deposition. (**C**) A combinatorial synergistic cross-talk, where after the deposition of both PTMs by their respective enzymes, a reader can bind to the histone tail to exert its function. (**D**) A combinatorial antagonistic mechanism where a reader can recognize one PTM on the histone tail, but the deposition of a second mark (Rme2a) impairs this recognition.

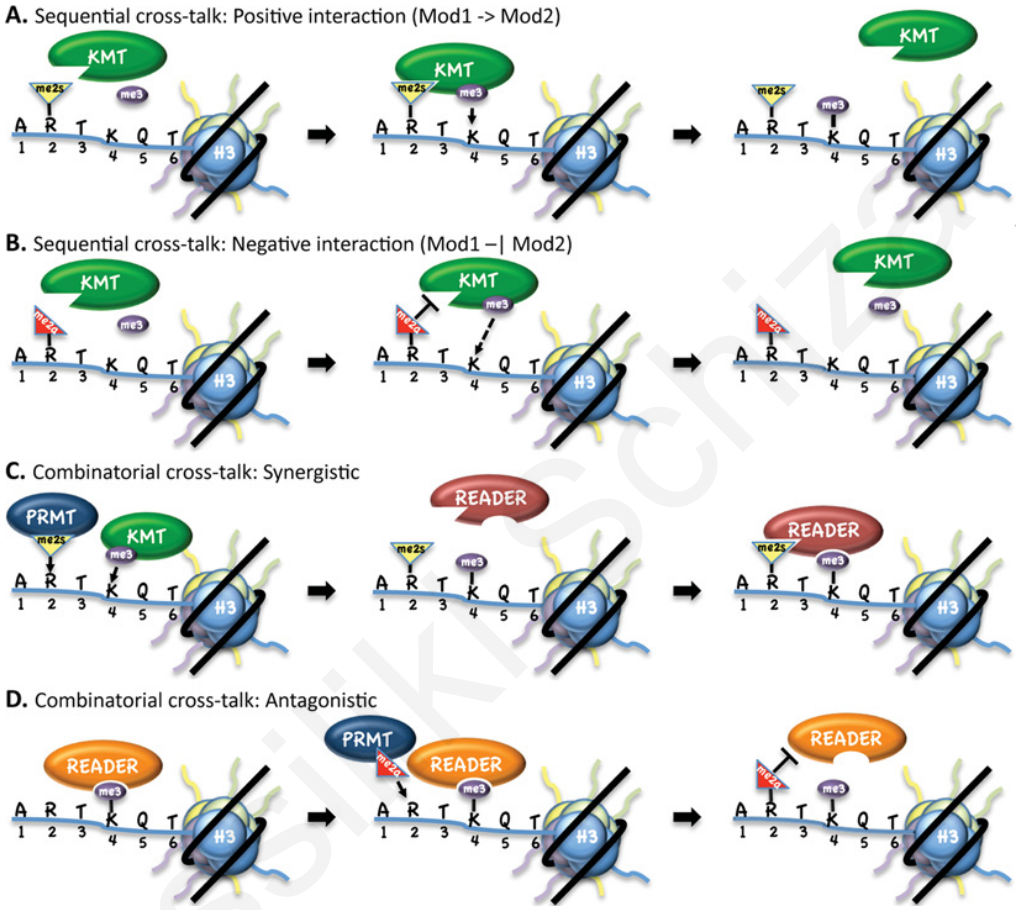

to PRMT1-mediated H4R3me2a. In contrast with their findings for PRMT1, the authors show using *in vitro* methylation assays that PRMT5 activity is stimulated by H4K5ac, H4K8ac and H4K12ac and is inhibited by H4K16ac [53].

The cross-talk mechanisms relating to H4R3 methylation expand beyond histone modifications as H4R3me2s was directly associated with DNA methylation. Evidence for this cross-talk was initially provided by a study which showed that PRMT7-mediated deposition of H4R3me2s at the ICR (imprinting control region) of the *Igf2/H19* locus was necessary for subsequent DNA methylation [57]. A direct link between H4R3me2s and DNA methylation was revealed by Zhao et al. [58], who observed that the *de novo* DNA methyltransferase DNMT3a binds directly to H4R3me2s through its ADD domain to methylate DNA and silence gene expression. More recently, the same group showed that H4R3me2s, apart from DNMT3a, recruits an additional complex containing the histone-modifying enzyme SUV4–20h1 to lay down H4K20me3 and reinforce the silencing of globin genes [59]. The above findings raise the question as to whether there is also a reverse relationship between H4R3me2s and DNA methylation. Le Guezennec et al. [60] have shown previously that DNA methylation promotes H4R3me2s by recruitment of PRMT5 through interaction with MBD2 (methyl CpG-binding domain 2). Hence DNA methylation may occur both upstream and downstream of histone arginine methylation.

Mechanisms of modification cross-talk

General themes emerge from the cross-talks of histone arginine methylation reviewed above, which are applicable across all epigenetic modifications. Cross-talks among

modifications employ mechanisms that can be divided into two major categories, each comprising two subcategories. The first category includes histone modifications that take part in a sequential cross-talk, during which one modification either promotes (sequential positive) or inhibits (sequential negative) the deposition of another modification (Figures 2A and 2B respectively). The second category of mechanisms comprises modifications that function in a combinatorial manner during which two or more modifications existing simultaneously regulate together the binding of effector molecules. These epigenetic modifications can work synergistically, for example by recruiting together a specific reader (Figure 2C), or antagonistically, where one modification blocks reader binding to the other modification (Figure 2D). These two general mechanisms appear to apply for all modification cross-talks regardless of whether they occur within the same histone (*cis*) or between histones (*trans*).

H3R2 is one of the few histone residues whose dimethylation states employ all four mechanisms of cross-talk. For example, H3R2me2s is involved in a sequential positive mechanism because it recruits the co-activator WDR5 through its WD40 domain, which subsequently enhances H3K4me3 deposition [12,13] (Figure 2A). In contrast, the alternative dimethylated form of this residue, H3R2me2a, is involved in a sequential negative mechanism because it inhibits the recruitment of Set1/MLL1 complex components and, as a result, blocks H3K4me3 [8–10,22] (Figure 2B). H3R2 methylations are also involved in cross-talks utilizing combinatorial mechanisms. H3R2me2s together with H3K4me3 enhances the recruitment of the PHD finger of RAG2 leading to V(D)J recombination and transcriptional activation [29] (Figure 2C). H3R2me2s is a unique methylation because it first uses a sequential cross-talk to lay down H3K4me3 and then together with H3K4me3 affect factor binding via a combinatorial mechanism. Finally, a combinatorial antagonistic cross-talk is observed between H3R2me2a and H3K4me3 (Figure 2D). For example, TFIID is recruited by H3K4me3 to initiate transcription, but when H3R2me2a is deposited on the same tail, this prevents the binding of TFIID to chromatin [26].

All cross-talks involving histone arginine methylation described to date can be classified in one of these categories (Table 1). These mechanisms could also apply to non-histone proteins (i.e. p53) that possess numerous modifications including arginine methylation. In addition, these mechanisms could also be relevant for cross-talks that may occur between histone modifications and modification on other chromatin-bound proteins such as polymerases, transcription factors, modifying enzymes and remodellers [4].

Concluding remarks

Determining how epigenetic modifications cross-talk with each other has attracted much interest in recent years because of the increasing evidence that deregulation of PTM deposition is key for the appearance of several diseases including cancer [5–7]. Recent developments in sequencing and MS techniques make the discovery and characterization of modification cross-talks more achievable. Methods that involve next-generation sequencing (i.e. ChIP-seq and bisulfite-seq) provide genome-wide profiles of histone and DNA modifications [61,62]. Such genome-wide profiles can infer the interplay among epigenetic modifications on the basis of the overlap of their distributions [10,12,13]. In addition, ETD (electron transfer dissociation) and ECD (electron capture dissociation) allow the analysis of long peptides (middle-down MS) or full histones (top-down MS), helping to discover PTMs co-occurring on individual histone molecules [63]. Coupling MS to SILAC (stable isotope labelling by amino acids in cell culture) leads to the analysis of PTM deposition kinetics [64], which could point towards possible cross-talks. Moreover, SNAP (SILAC nucleosome affinity purification) identifies cross-talks among histone modifications and DNA methylation occurring in the context of the nucleosome [65]. All of these MS methodologies provide unambiguous detection of amino acid modifications and offer hypotheses about their interactions. However, other biochemical techniques are also useful and utilized to elucidate modification cross-talks. Immunoassay-based methodologies such as GPS (Global Proteomic Screen in *S. cerevisiae*) can decipher histone modification cross-talks in budding yeast relying on the use of the recently developed histone point-mutant collections [66]. Protein arrays can also be used to detect cross-talks employing a combinatorial mechanism in a high-throughput manner [67].

So far, most of the efforts for elucidating cross-talks involving histone arginine methylation have been placed on two histones, H3 and H4. However, methylated arginine residues have been detected on other histones including Arg^{11} and Arg^{29} on H2A [68], and Arg^{37} on CenH3, the non-canonical histone present at centromeric chromatin [69]. Hence, it can be predicted that cross-talks involving arginine residues of histones other than H3 and H4 will be exposed after further investigation. Furthermore, cross-talks involving arginine monomethylation are not as well characterized as the ones involving dimethylated states. It is not clear whether this is due to monomethylation being mainly a transient state or because this modification has not been studied extensively. *Trans*-histone cross-talks involving arginine methylation are also scarcely reported [52,55,56]. However, the recent methodology established by Reinberg and colleagues to demonstrate that the two copies of the same histone found within one nucleosome can possess different modifications [70] creates new prospects for discovering *trans*-histone cross-talks. It might not be surprising that future studies employing this methodology will show that current cross-talks thought to be occurring *in cis* within the same histone molecule, are actually occurring *in trans* between the two sister histones.

Finally, it remains unclear whether arginine methylation can be actively removed by a demethylase. However, several independent studies demonstrated that arginine methylation levels change quickly under certain conditions, pointing towards the existence of an enzyme involved in this task

[7]. Identification of such a demethylase, which will prove the dynamic nature of this modification, will open new questions for the cross-talk mechanisms involving arginine methylation.

Acknowledgements

We thank Dr Aaron Plys for a critical reading of the paper and his helpful suggestions before submission. We apologize to those researchers whose original work could not be cited owing to limitations on the number of references.

Funding

This work was supported by the European Research Council [ERC-2010 starting grant number 260797, ChromatinModWeb] and the Cyprus Research Promotion Foundation [grant number Health/Bio/0609(BE)/09].

References

1 Holliday, R. (1987) The inheritance of epigenetic defects. Science **238**, 163–170
2 Musselman, C.A., Lalonde, M.E., Cote, J. and Kutateladze, T.G. (2012) Perceiving the epigenetic landscape through histone readers. Nat. Struct. Mol. Biol. **19**, 1218–1227
3 Murr, R. (2010) Interplay between different epigenetic modifications and mechanisms. Adv. Genet. **70**, 101–141
4 Lee, J.S., Smith, E. and Shilatifard, A. (2010) The language of histone crosstalk. Cell **142**, 682–685
5 Dawson, M.A. and Kouzarides, T. (2012) Cancer epigenetics: from mechanism to therapy. Cell **150**, 12–27
6 Sharma, P., Azebi, S., England, P., Christensen, T., Moller-Larsen, A., Petersen, T., Batsche, E. and Muchardt, C. (2012) Citrullination of histone H3 interferes with HP1-mediated transcriptional repression. PLoS Genet. **8**, e1002934
7 Yang, Y. and Bedford, M.T. (2013) Protein arginine methyltransferases and cancer. Nat. Rev. Cancer **13**, 37–50
8 Guccione, E., Bassi, C., Casadio, F., Martinato, F., Cesaroni, M., Schuchlautz, H., Luscher, B. and Amati, B. (2007) Methylation of histone H3R2 by PRMT6 and H3K4 by an MLL complex are mutually exclusive. Nature **449**, 933–937
9 Hyllus, D., Stein, C., Schnabel, K., Schiltz, E., Imhof, A., Dou, Y., Hsieh, J. and Bauer, U.M. (2007) PRMT6-mediated methylation of R2 in histone H3 antagonizes H3 K4 trimethylation. Genes Dev. **21**, 3369–3380
10 Kirmizis, A., Santos-Rosa, H., Penkett, C.J., Singer, M.A., Vermeulen, M., Mann, M., Bahler, J., Green, R.D. and Kouzarides, T. (2007) Arginine methylation at histone H3R2 controls deposition of H3K4 trimethylation. Nature **449**, 928–932
11 Kirmizis, A., Santos-Rosa, H., Penkett, C.J., Singer, M.A., Green, R.D. and Kouzarides, T. (2009) Distinct transcriptional outputs associated with mono- and dimethylated histone H3 arginine 2. Nat. Struct. Mol. Biol. **16**, 449–451
12 Migliori, V., Muller, J., Phalke, S., Low, D., Bezzi, M., Mok, W.C., Sahu, S.K., Gunaratne, J., Capasso, P., Bassi, C. et al. (2012) Symmetric dimethylation of H3R2 is a newly identified histone mark that supports euchromatin maintenance. Nat. Struct. Mol. Biol. **19**, 136–144
13 Yuan, C.C., Matthews, A.G., Jin, Y., Chen, C.F., Chapman, B.A., Ohsumi, T.K., Glass, K.C., Kutateladze, T.G., Borowsky, M.L., Struhl, K. and Oettinger, M.A. (2012) Histone H3R2 symmetric dimethylation and histone H3K4 trimethylation are tightly correlated in eukaryotic genomes. Cell Rep. **1**, 83–90
14 Chang, B., Chen, Y., Zhao, Y. and Bruick, R.K. (2007) JMJD6 is a histone arginine demethylase. Science **318**, 444–447
15 Webby, C.J., Wolf, A., Gromak, N., Dreger, M., Kramer, H., Kessler, B., Nielsen, M.L., Schmitz, C., Butler, D.S., Yates, 3rd, J.R. et al. (2009) Jmjd6 catalyses lysyl-hydroxylation of U2AF65, a protein associated with RNA splicing. Science **325**, 90–93
16 Cuthbert, G.L., Daujat, S., Snowden, A.W., Erdjument-Bromage, H., Hagiwara, T., Yamada, M., Schneider, R., Gregory, P.D., Tempst, P., Bannister, A.J. and Kouzarides, T. (2004) Histone deimination antagonizes arginine methylation. Cell **118**, 545–553
17 Wang, Y., Wysocka, J., Sayegh, J., Lee, Y.H., Perlin, J.R., Leonelli, L., Sonbuchner, L.S., McDonald, C.H., Cook, R.G., Dou, Y. et al. (2004) Human PAD4 regulates histone arginine methylation levels via demethylimination. Science **306**, 279–283
18 Zhang, X., Bolt, M., Guertin, M.J., Chen, W., Zhang, S., Cherrington, B.D., Slade, D.J., Dreyton, C.J., Subramanian, V., Bicker, K.L. et al. (2012) Peptidylarginine deiminase 2-catalyzed histone H3 arginine 26 citrullination facilitates estrogen receptor α target gene activation. Proc. Natl. Acad. Sci. U.S.A. **109**, 13331–13336
19 Iberg, A.N., Espejo, A., Cheng, D., Kim, D., Michaud-Levesque, J., Richard, S. and Bedford, M.T. (2008) Arginine methylation of the histone H3 tail impedes effector binding. J. Biol. Chem. **283**, 3006–3010
20 Shilatifard, A. (2008) Molecular implementation and physiological roles for histone H3 lysine 4 (H3K4) methylation. Curr. Opin. Cell Biol. **20**, 341–348
21 Southall, S.M., Wong, P.S., Odho, Z., Roe, S.M. and Wilson, J.R. (2009) Structural basis for the requirement of additional factors for MLL1 SET domain activity and recognition of epigenetic marks. Mol. Cell **33**, 181–191
22 Couture, J.F., Collazo, E. and Trievel, R.C. (2006) Molecular recognition of histone H3 by the WD40 protein WDR5. Nat. Struct. Mol. Biol. **13**, 698–703
23 Flanagan, J.F., Mi, L.Z., Chruszcz, M., Cymborowski, M., Clines, K.L., Kim, Y., Minor, W., Rastinejad, F. and Khorasanizadeh, S. (2005) Double chromodomains cooperate to recognize the methylated histone H3 tail. Nature **438**, 1181–1185
24 Stein, R.S. and Wang, W. (2011) The recognition specificity of the CHD1 chromodomain with modified histone H3 peptides. J. Mol. Biol. **406**, 527–541
25 Garske, A.L., Oliver, S.S., Wagner, E.K., Musselman, C.A., LeRoy, G., Garcia, B.A., Kutateladze, T.G. and Denu, J.M. (2010) Combinatorial profiling of chromatin binding modules reveals multisite discrimination. Nat. Chem. Biol. **6**, 283–290
26 Vermeulen, M., Mulder, K.W., Denissov, S., Pijnappel, W.W., van Schaik, F.M., Varier, R.A., Baltissen, M.P., Stunnenberg, H.G., Mann, M. and Timmers, H.T. (2007) Selective anchoring of TFIID to nucleosomes by trimethylation of histone H3 lysine 4. Cell **131**, 58–69
27 van Ingen, H., van Schaik, F.M., Wienk, H., Ballering, J., Rehmann, H., Dechesne, A.C., Kruijzer, J.A., Liskamp, R.M., Timmers, H.T. and Boelens, R. (2008) Structural insight into the recognition of the H3K4me3 mark by the TFIID subunit TAF3. Structure **16**, 1245–1256
28 Palacios, A., Munoz, I.G., Pantoja-Uceda, D., Marcaida, M.J., Torres, D., Martin-Garcia, J.M., Luque, I., Montoya, G. and Blanco, F.J. (2008) Molecular basis of histone H3K4me3 recognition by ING4. J. Biol. Chem. **283**, 15956–15964
29 Ramon-Maiques, S., Kuo, A.J., Carney, D., Matthews, A.G., Oettinger, M.A., Gozani, O. and Yang, W. (2007) The plant homeodomain finger of RAG2 recognizes histone H3 methylated at both lysine-4 and arginine-2. Proc. Natl. Acad. Sci. U.S.A. **104**, 18993–18998
30 Fiedler, M., Sanchez-Barrena, M.J., Nekrasov, M., Mieszczanek, J., Rybin, V., Muller, J., Evans, P. and Bienz, M. (2008) Decoding of methylated histone H3 tail by the Pygo–BCL9 Wnt signaling complex. Mol. Cell **30**, 507–518
31 Xu, Z., He, Y., Ju, J., Rank, G., Cerruti, L., Ma, C., Simpson, R.J., Moritz, R.L., Jane, S.M. and Zhao, Q. (2012) The role of WDR5 in silencing human fetal globin gene expression. Haematologica **97**, 1632–1640
32 Org, T., Chignola, F., Hetenyi, C., Gaetani, M., Rebane, A., Liiv, I., Maran, U., Mollica, L., Bottomley, M.J., Musco, G. and Peterson, P. (2008) The autoimmune regulator PHD finger binds to non-methylated histone H3K4 to activate gene expression. EMBO Rep. **9**, 370–376
33 Koh, A.S., Kuo, A.J., Park, S.Y., Cheung, P., Abramson, J., Bua, D., Carney, D., Shoelson, S.E., Gozani, O., Kingston, R.E. et al. (2008) Aire employs a histone-binding module to mediate immunological tolerance, linking chromatin regulation with organ-specific autoimmunity. Proc. Natl. Acad. Sci. U.S.A. **105**, 15878–15883
34 Chignola, F., Gaetani, M., Rebane, A., Org, T., Mollica, L., Zucchelli, C., Spitaleri, A., Mannella, V., Peterson, P. and Musco, G. (2009) The solution structure of the first PHD finger of autoimmune regulator in complex with non-modified histone H3 tail reveals the antagonistic role of H3R2 methylation. Nucleic Acids Res. **37**, 2951–2961
35 Chakravarty, S., Zeng, L. and Zhou, M.M. (2009) Structure and site-specific recognition of histone H3 by the PHD finger of human autoimmune regulator. Structure **17**, 670–679

36 Hu, L., Li, Z., Wang, P., Lin, Y. and Xu, Y. (2011) Crystal structure of PHD domain of UHRF1 and insights into recognition of unmodified histone H3 arginine residue 2. Cell Res. **21**, 1374–1378
37 Rajakumara, E., Wang, Z., Ma, H., Hu, L., Chen, H., Lin, Y., Guo, R., Wu, F., Li, H., Lan, F. et al. (2011) PHD finger recognition of unmodified histone H3R2 links UHRF1 to regulation of euchromatic gene expression. Mol. Cell **43**, 275–284
38 Wang, C., Shen, J., Yang, Z., Chen, P., Zhao, B., Hu, W., Lan, W., Tong, X., Wu, H., Li, G. and Cao, C. (2011) Structural basis for site-specific reading of unmodified R2 of histone H3 tail by UHRF1 PHD finger. Cell Res. **21**, 1379–1382
39 Lallous, N., Legrand, P., McEwen, A.G., Ramon-Maiques, S., Samama, J.P. and Birck, C. (2011) The PHD finger of human UHRF1 reveals a new subgroup of unmethylated histone H3 tail readers. PLoS ONE **6**, e27599
40 Arita, K., Isogai, S., Oda, T., Unoki, M., Sugita, K., Sekiyama, N., Kuwata, K., Hamamoto, R., Tochio, H., Sato, M. et al. (2012) Recognition of modification status on a histone H3 tail by linked histone reader modules of the epigenetic regulator UHRF1. Proc. Natl. Acad. Sci. U.S.A. **109**, 12950–12955
41 Villar-Garea, A., Forne, I., Vetter, I., Kremmer, E., Thomae, A. and Imhof, A. (2012) Developmental regulation of N-terminal H2B methylation in *Drosophila melanogaster*. Nucleic Acids Res. **40**, 1536–1549
42 Pal, S., Vishwanath, S.N., Erdjument-Bromage, H., Tempst, P. and Sif, S. (2004) Human SWI/SNF-associated PRMT5 methylates histone H3 arginine 8 and negatively regulates expression of ST7 and NM23 tumor suppressor genes. Mol. Cell. Biol. **24**, 9630–9645
43 Rathert, P., Dhayalan, A., Murakami, M., Zhang, X., Tamas, R., Jurkowska, R., Komatsu, Y., Shinkai, Y., Cheng, X. and Jeltsch, A. (2008) Protein lysine methyltransferase G9a acts on non-histone targets. Nat. Chem. Biol. **4**, 344–346
44 Rothbart, S.B., Krajewski, K., Nady, N., Tempel, W., Xue, S., Badeaux, A.I., Barsyte-Lovejoy, D., Martinez, J.Y., Bedford, M.T., Fuchs, S.M. et al. (2012) Association of UHRF1 with methylated H3K9 directs the maintenance of DNA methylation. Nat. Struct. Mol. Biol. **19**, 1155–1160
45 Daujat, S., Bauer, U.M., Shah, V., Turner, B., Berger, S. and Kouzarides, T. (2002) Crosstalk between CARM1 methylation and CBP acetylation on histone H3. Curr. Biol. **12**, 2090–2097
46 An, W., Kim, J. and Roeder, R.G. (2004) Ordered cooperative functions of PRMT1, p300, and CARM1 in transcriptional activation by p53. Cell **117**, 735–748
47 Yue, W.W., Hassler, M., Roe, S.M., Thompson-Vale, V. and Pearl, L.H. (2007) Insights into histone code syntax from structural and biochemical studies of CARM1 methyltransferase. EMBO J. **26**, 4402–4412
48 Wu, J. and Xu, W. (2012) Histone H3R17me2a mark recruits human RNA polymerase-associated factor 1 complex to activate transcription. Proc. Natl. Acad. Sci. U.S.A. **109**, 5675–5680
49 Wu, J., Cui, N., Wang, R., Li, J. and Wong, J. (2012) A role for CARM1-mediated histone H3 arginine methylation in protecting histone acetylation by releasing corepressors from chromatin. PLoS ONE **7**, e34692
50 Strahl, B.D., Briggs, S.D., Brame, C.J., Caldwell, J.A., Koh, S.S., Ma, H., Cook, R.G., Shabanowitz, J., Hunt, D.F., Stallcup, M.R. and Allis, C.D. (2001) Methylation of histone H4 at arginine 3 occurs *in vivo* and is mediated by the nuclear receptor coactivator PRMT1. Curr. Biol. **11**, 996–1000
51 Wang, H., Huang, Z.Q., Xia, L., Feng, Q., Erdjument-Bromage, H., Strahl, B.D., Briggs, S.D., Allis, C.D., Wong, J., Tempst, P. and Zhang, Y. (2001) Methylation of histone H4 at arginine 3 facilitating transcriptional activation by nuclear hormone receptor. Science **293**, 853–857
52 Huang, S., Litt, M. and Felsenfeld, G. (2005) Methylation of histone H4 by arginine methyltransferase PRMT1 is essential *in vivo* for many subsequent histone modifications. Genes Dev. **19**, 1885–1893
53 Feng, Y., Wang, J., Asher, S., Hoang, L., Guardiani, C., Ivanov, I. and Zheng, Y.G. (2011) Histone H4 acetylation differentially modulates arginine methylation by an *in cis* mechanism. J. Biol. Chem. **286**, 20323–20334
54 Kuo, M.H., Xu, X.J., Bolck, H.A. and Guo, D. (2009) Functional connection between histone acetyltransferase Gcn5p and methyltransferase Hmt1p. Biochim. Biophys. Acta **1789**, 395–402
55 Li, X., Hu, X., Patel, B., Zhou, Z., Liang, S., Ybarra, R., Qiu, Y., Felsenfeld, G., Bungert, J. and Huang, S. (2010) H4R3 methylation facilitates β-globin transcription by regulating histone acetyltransferase binding and H3 acetylation. Blood **115**, 2028–2037
56 Dhar, S.S., Lee, S.H., Kan, P.Y., Voigt, P., Ma, L., Shi, X., Reinberg, D. and Lee, M.G. (2012) Trans-tail regulation of MLL4-catalyzed H3K4 methylation by H4R3 symmetric dimethylation is mediated by a tandem PHD of MLL4. Genes Dev. **26**, 2749–2762
57 Jelinic, P., Stehle, J.C. and Shaw, P. (2006) The testis-specific factor CTCFL cooperates with the protein methyltransferase PRMT7 in H19 imprinting control region methylation. PLoS Biol. **4**, e355
58 Zhao, Q., Rank, G., Tan, Y.T., Li, H., Moritz, R.L., Simpson, R.J., Cerruti, L., Curtis, D.J., Patel, D.J., Allis, C.D. et al. (2009) PRMT5-mediated methylation of histone H4R3 recruits DNMT3A, coupling histone and DNA methylation in gene silencing. Nat. Struct. Mol. Biol. **16**, 304–311
59 Rank, G., Cerruti, L., Simpson, R.J., Moritz, R.L., Jane, S.M. and Zhao, Q. (2010) Identification of a PRMT5-dependent repressor complex linked to silencing of human fetal globin gene expression. Blood **116**, 1585–1592
60 Le Guezennec, X., Vermeulen, M., Brinkman, A.B., Hoeijmakers, W.A., Cohen, A., Lasonder, E. and Stunnenberg, H.G. (2006) MBD2/NuRD and MBD3/NuRD, two distinct complexes with different biochemical and functional properties. Mol. Cell. Biol. **26**, 843–851
61 Booth, M.J., Branco, M.R., Ficz, G., Oxley, D., Krueger, F., Reik, W. and Balasubramanian, S. (2012) Quantitative sequencing of 5-methylcytosine and 5-hydroxymethylcytosine at single-base resolution. Science **336**, 934–937
62 Ku, C.S., Naidoo, N., Wu, M. and Soong, R. (2011) Studying the epigenome using next generation sequencing. J. Med. Genet. **48**, 721–730
63 Garcia, B.A., Shabanowitz, J. and Hunt, D.F. (2007) Characterization of histones and their post-translational modifications by mass spectrometry. Curr. Opin. Chem. Biol. **11**, 66–73
64 Zee, B.M., Levin, R.S., Xu, B., LeRoy, G., Wingreen, N.S. and Garcia, B.A. (2010) *In vivo* residue-specific histone methylation dynamics. J. Biol. Chem. **285**, 3341–3350
65 Bartke, T., Vermeulen, M., Xhemalce, B., Robson, S.C., Mann, M. and Kouzarides, T. (2010) Nucleosome-interacting proteins regulated by DNA and histone methylation. Cell **143**, 470–484
66 Huang, H., Maertens, A.M., Hyland, E.M., Dai, J., Norris, A., Boeke, J.D. and Bader, J.S. (2009) HistoneHits: a database for histone mutations and their phenotypes. Genome Res. **19**, 674–681
67 Rothbart, S.B., Krajewski, K., Strahl, B.D. and Fuchs, S.M. (2012) Peptide microarrays to interrogate the "histone code". Methods Enzymol. **512**, 107–135
68 Waldmann, T., Izzo, A., Kamieniarz, K., Richter, F., Vogler, C., Sarg, B., Lindner, H., Young, N.L., Mittler, G., Garcia, B.A. and Schneider, R. (2011) Methylation of H2AR29 is a novel repressive PRMT6 target. Epigenet. Chromatin **4**, 11
69 Samel, A., Cuomo, A., Bonaldi, T. and Ehrenhofer-Murray, A.E. (2012) Methylation of CenH3 arginine 37 regulates kinetochore integrity and chromosome segregation. Proc. Natl. Acad. Sci. U.S.A. **109**, 9029–9034
70 Voigt, P., LeRoy, G., Drury, 3rd, W.J., Zee, B.M., Son, J., Beck, D.B., Young, N.L., Garcia, B.A. and Reinberg, D. (2012) Asymmetrically modified nucleosomes. Cell **151**, 181–193

Received 15 January 2013
doi:10.1042/BST20130003